IMPROVEMENT OF ASPHALT PERFORMANCE USING INDUSTRIAL WASTES

BY
MOHAMMAD ANWAR PARVEZ

A Dissertation Presented to the
FACULTY OF THE COLLEGE OF GRADUATE STUDIES
KING FAHD UNIVERSITY OF PETROLEUM & MINERALS
DHAHRAN, SAUDI ARABIA

In Partial Fulfillment of the
Requirements for the Degree of

DOCTOR OF PHILOSOPHY
In
CHEMICAL ENGINEERING

MAY 2013

KING FAHD UNIVERSITY OF PETROLEUM & MINERALS

DHAHRAN- 31261, SAUDI ARABIA

DEANSHIP OF GRADUATE STUDIES

This thesis, written by **MOHAMMAD ANWAR PARVEZ** under the direction his thesis advisor and approved by his thesis committee, has been presented and accepted by the Dean of Graduate Studies, in partial fulfillment of the requirements for the degree of **DOCTOR OF PHILOSOPHY IN CHEMICAL ENGINEERING.**

Dr. Ibnelwaleed A. Hussein
(Advisor)

Dr. Usamah A. Al-Mubaiyedh
Department Chairman

Dr. Hamad I. Abdul Wahhab
(Co-Advisor)

Dr. Salam A. Zummo
Dean of Graduate Studies

Dr. Reyad A. Shawabkeh
(Member)

17/7/13
Date

Dr. Mohamed B. Amin
(Member)

Dr. S. U. Rahman
(Member)

Dedicated

To

My Parents

ACKNOWLEDGEMENTS

In the name of Allah, the most Beneficent, the most Merciful.

All praises be to Allah and the peace and blessings of Allah upon his prophet, Muhammad (S.A.W). First I would like to thank King Fahd University of Petroleum & Minerals (KFUPM) for offering me the opportunity to pursue my Ph.D. degree in the department of Chemical Engineering.

This research was conducted under the supervision of Professor Ibnelwaleed A. Hussein, to whom I deeply express my gratitude for his guidance, patience, assistance, and inspiration throughout my studies at KFUPM. Thanks also go to my Co-supervisor Professor Hamad I. Al-Abdul Wahhab for giving expert advice and time to this project. Most of the work done in this thesis was performed in the highway laboratory. I would like to offer my special thanks to my thesis committee members: Professor Riyad A. Shawabkeh, Professor Mohamed B. Amin, and Professor S. U. Rahman for their review and comments.

This research was made possible by the financial assistance from King Abdul Aziz City for Science and Technology (KACST), and Saudi Aramco. My special thanks go to these organizations.

I am thankful to the chairman of the Chemical Engineering Department, Dr. Usama A. Al-Mubaiyedh for his help and cooperation. I am also thankful to Dr. Anwar Ul

Hamid of Research Institute, KFUPM for his help with characterizing ash samples. Moreover, I would like to thank Mr. M. G. Baig, Mr. Mofizul Islam, Mr. Nasser and Mr. Fathi for their assistance in the experimental work.

Sincere appreciations go to my parents, brothers and sister for their love, patience, prayers and words of encouragement throughout my academic career. Finally, I would like to thank my wife for her patience, thoughtfulness, prayers, moral and emotional support throughout the duration of this work.

TABLE OF CONTENTS

LIST OF FIGURES

LIST OF TABLES

THESIS ABSTRACT

Full Name : MOHAMMAD ANWAR PARVEZ

Thesis Title : IMPROVEMENT OF ASPHALT PERFORMANCE USING INDUSTRIAL WASTES

Major Field : CHEMICAL ENGINEERING

Date of Degree: MAY, 2013

Asphalt demand and price are increasing day by day due to construction of massive highway worldwide. Use of waste materials in asphalt modification can reduce the price of asphalt as well as solve waste disposal problems. Also, variation in seasonal climate demands asphalt modification to prevent stress cracking and rutting of asphalt pavement structure. The following industrial wastes were used to modify and improve the performance of asphalt wastes: sulfur from oil and gas processing plants, crumb rubber from used tires, polyethylene wax from polymer industry and oil fly ash (OFA) from power generation plants. Standard tests on asphalt binder and asphalt concrete mixes were performed with focus on rheological and thermorheological performance. Polyethylene wax and crumb rubber were used to modify sulfur-asphalt. The main problems of sulfur in asphalt are cracking due to lack of flexibility of the sulfur-asphalt mix. Use of polyethylene wax and crumb rubber with sulfur-asphalt showed improvement in elasticity and flexibility of asphalt-sulfur binder. Polyethylene wax and crumb rubber modified sulfur-asphalt concrete mixes showed improved performance grading, resilient modulus, stability, indirect tensile stress and durability and rutting resistance. On the other hand, OFA was treated by physical and chemical methods to improve its surface properties which lead to better compatibility and reactivity of modified OFA and asphalt. Use of treated OFA in asphalt concrete mixes showed improvement in resilient modulus, indirect tensile stress and stability. It also improved rutting resistance and fatigue life of asphalt concrete mixes. All wastes showed a potential for application in asphalt pavement.

DOCTOR OF PHILOSOPHY

KING FAHD UNIVERSITY OF PETROLEUM & MINERALS

DHAHRAN, SAUDI ARABIA.

ملخص الرسالة

الإســـــم : محمد أنور برويز

عنوان الرسالة : تطوير أداء ألاسفلت باستخدام المخلفات الصناعية

تاريخ التخرج : مايو 2013م

يزداد الطلب على الاسفلت و يزداد سعره يوما بعد يوم نتيجة لبناء شبكات الطرق السريعة الضخمه في جميع أنحاء العالم. ان استخدام مواد النفايات في تعديل الأسفلت يمكن أن تقلل من أسعار الإسفلت وكذلك حل مشاكل التخلص من النفايات. كما أن التباين في المناخ الموسمي يتطلب تحسين الأسفلت لمنع اجهاد الكلال والتخدد للرصفات الأسفلتيه. تم استخدام النفايات الصناعية التالية لتعديل وتحسين الأداء للاسفلت: الكبريت من مصانع معالجة النفط و الغاز، فتات المطاط من الإطارات المستعملة، شمع البولي ايثيلين من صناعة البوليمرات ورماد النفط المتطاير من محطات توليد الطاقة. وأجريت الاختبارات القياسية على الرابط الاسفلتي وخلطات الخرسانة الإسفلتية مع التركيز على أداء الانسيابية و الانسيابية الحراريه. استخدم شمع البولي ايثيلين و فتات المطاط لتعديل الأسفلت الكبريتي.و كانت المشاكل الرئيسية للكبريت في الأسفلت هو تكسر الكلال بسبب عدم وجود مرونة كافية في مزيج الأسفلت الكبريتي. أظهر استخدام شمع البولي ايثلين و فتات المطاط مع الأسفلت الكبريتي تحسنا في مرونة الأسفلت الكبريتي. كما أظهر مزيج الأسفلت الكبريتي وشمع البولي ايثيلين وفتات المطاط تحسن في درجة الأداء، ومعامل المرونة والثبات وإجهاد الشد غير المباشرة والديمومه ومقاومة التخدد. من ناحية أخرى، تمت معالجة رماد النفط المتطاير بواسطة الطرق الفيزيائية والكيميائية لتحسين خصائص سطحها مما يؤدي إلى تحسين التوافق والتفاعل بين رماد النفط المتطاير المعدل والأسفلت. و أظهر استخدام رماد النفط المتطاير المعدل في خلطات الخرسانة الإسفلتية تحسنا في معامل المرونة، وإجهاد الشد غير المباشرة والثبات. كما تحسنت أيضا مقاومة التخدد و الكلال لخلطات الخرسانة الأسفلتية. كما أظهرت جميع النفايات إمكانية استخدامها لتحسين الرصفات الأسفلتيه.

دكتوراه الفلسفة

قسم الهندسة الكيميائية

جامعة الملك فهد للبترول والمعادن

الظهران – المملكة العربية السعودية

CHAPTER 1

INTRODUCTION

Asphalt binder is a thermoplastic material that behaves as an elastic solid at low service temperatures or during rapid loading, and as a viscous liquid at high temperatures or slow loading. This double behavior creates a need to improve the performance of the asphalt binder to minimize stress cracking, which occurs at low temperatures, and permanent deformation, which occurs at high service temperatures. The daily and seasonal temperature variations plus the growth in truck traffic volume, tire pressure, and axle loading have increased stresses on asphalt pavements. The local asphalt pavement temperature in Saudi Arabia ranges between -10^{o}C in winter and 76^{o}C in summer. This increases the demand to modify asphalt binders (to reduce cracking and deformation). Different methods have been used to upgrade the properties of asphalt binders (Iqbal, et al., 2006; Hussein, et al., 2005; Hussein, et al., 2006; Polacco, et al., 2004). In this study several industrial wastes namely: sulfur, polyethylene wax, crumb rubber and oil fly ash (OFA) have been used to modify asphalt to improve its performance.

The rate of elemental sulfur production is increasing day by day due to increased oil and gas production. Total elemental production in 2010 was 57 million ton and consumption of the same was 55.6 million ton indifferent section including

production of fertilizers and sulfuric acid. The balance 1.4 million ton was unused. The early study on the use of sulfur in asphalt mixes showed better properties than the conventional asphalt mixes (Benzowitz & Boe, 1938). But due to high prices of sulfur, the product sulfur asphalt was uneconomical. In view of the increase in asphalt price since the beginning of the 1970s, the product was studied again by the US Bureau of Mines and Federal Highways. However, significant problems with storing hot sulfur at asphalt mix plants as well as pre-blending the sulfur with the bitumen were encountered. In many oil and gas producing countries, such as the Arabian Gulf countries, there is high production of elemental sulfur from processing plants. Therefore, and for several reasons, there is a renewed interest to seek new and efficient utilization of sulfur. First, sulfur is a valuable natural resource. Second, the income realized from the beneficial use of sulfur can help offset the cost of pollution control and ease a potential disposal problem. Finally, the stockpiling of sulfur in built-up areas without concurrent utilization could create additional pollution problems. Of the several potential uses for sulfur, a sulfur/asphalt combination for highway pavements seems to have the greatest potential for increasing the beneficial consumption of this element. This sulfur asphalt pavement material could utilize much of the elemental sulfur which will be recovered from fossil fuels.

Sulfur asphalt with high amounts of sulfur is brittle. Therefore, it is necessary to add rheology modifiers to sulfur asphalt to improve its rheological properties. No previous work was done to examine the effect of crumb rubber on the rheological

properties of sulfur asphalt binder. In this study polyethylene wax and crumb rubber have been used to improve sulfur asphalt binder performance.

Oil fly ash (OFA) is typically a black powder type waste material that results from the use of crude and residual oil in power generation. OFA is collected in the electrostatic precipitators which are installed on boilers burning residual oil for air pollution control. According to a survey of American Coal Ash Association, 69.30 million tons of coal fly ash produced in 2011 in the United States by coal fired plants and 38% of this quantity was reused in different applications (American Coal Ash Association, 2011). In Saudi Arabia, there are 70 power plants consuming 22 million metric tons of oil and the total amount of disposed OFA in 2008 was about 240,000 cubic meters. This amount is expected to increase to 400,000 cubic meters in 2014. These quantities must be disposed off in an environment friendly way. OFA is mainly used as a replacement of Portland cement; as a filler in polymers, asphalt and cementitious materials; stabilizing agent and also for adsorption of solutes and, solidification for waste and sludge (Sinha, et al., 2010; Shawabkeh & Harahsheh, 2007; Shawabkeh, et al., 2004; Woo-Teck, et al., 2005).

Additive or filler materials can be used in asphalt binders to design against or to repair pavement due to the following problems: surface defects (raveling and stripping), structural defects (rutting, shoving and distortion) and cracking (fatigue and thermal).Many authors have studied the effects of mineral fillers, which are materials passing a sieve size of 0.075mm, on the behavior of asphalt mix (Anani &

Al-Abdul Wahhab, 1982; Asi & Assa'ad, 2005; Kandhal, et al., 1998; Karasahin & Terzi, 2007). Different filler materials may have different mechanical properties in the asphalt mixture.

In a recent patent untreated OFA (3-10%) was used in asphalt binder and asphalt concrete mix (Al-Amethel, et al., 2011). Addition of untreated OFA improved rutting resistance, stability and modulus. However, the fatigue properties of the mix were poor due to poor dispersion of ash which is likely due to the inert nature of the OFA surface. Surface modification and grafting are widely used in the polymer literature to improve the bonding between different polymers or between polymers and asphalt. Recently, surface modification of carbon nanotubes (CNT), which resembles OFA in composition, has improved the dispersion in polymers and improved the bonding between the polymer and CNT (Abbasi, et al., 2013). The proven success of surface modification in polymers, polymer nanocomposites and polymer-modified asphalt in improving the interfacial bonding suggests the potential of chemical modification of OFA in improving the dispersion and bonding with asphalt. Therefore, as-received OFA has been treated chemically to incorporate different functional groups (carboxylic, 1-Ocatdecanoate, amine) to OFA surface to enhance OFA surface properties. This study focused on the surface modification of OFA and the influence of treated OFA on asphalt binder and asphalt concrete mixes properties.

CHAPTER 2

LITERATURE REVIEW

2.1 Sulfur in Asphalt

Sulfur has been used as a modifier for asphalt, by itself or with polymers, for vulcanization properties. Forrest (1915) describes a refining process for natural asphalts, which prevents loss of naturally occurring sulfur found in crude oils, which are refined to produce asphalt compositions. Hydrogen sulfide liberation is minimized by utilizing fixed oils to absorb sulfur. White (1920) describes acid and alkali resistant coatings containing coal tar pitch and crystallized sulfur, which are prepared at low temperatures in order to prevent reaction of the pitch with sulfur. The sulfur is added to increase viscosity and reduce the melting point of the pitch.

Burris (1981) used a stockpile asphalt emulsion of 50-98% paving grade asphalt, 1-10% added sulfur, and 1-35% liquid hydrocarbon, added as a softening agent. Sulfur is melted and sulfur and asphalt mixed, then oil is "preferably mixed with the material after the asphalt and sulfur have been combined."

Ott (1988) reported the preparation of high quality asphalts by adding sulfur into asphalt or oil feedstocks and heating until asphaltenes formed. Chaverot (1994) discloses an asphalt/polymer composition produced by mixing polymer, e.g., styrene

and butadiene co-polymer, with asphalt and then incorporating at 100°C to 230°C a sulfur-donating coupling agent in an amount suitable for providing an amount of elemental or radical sulfur representing 0.5 to 10% of the weight of the polymer.

When added to bitumen at 140^{o}C, sulfur is finely dispersed in bitumen as uniformly small particles; coagulation and settlement of sulfur particles become noticeable after three hours. (Kennepohl et. al, 1975). Therefore, the sulfur-asphalt mixtures (SEA) had to be produced directly in the mixing plant just before the laying of the asphalt mixture. One major concern in handling sulfur–asphalt mix is the fear of the evolution of hydrogen sulfide during production and laying. Literature reports that H_2S evolution only start at temperatures higher than 150^{o}C (Kennepohl et al., 1975; Fromm & Kennephol, 1979; Fromm et al., 1981; Bocca et al., 1973), so that the application at temperatures up to 150°C should not cause pollution and safety problems. However, early experiments carried out with the help of thermoanalytical techniques have shown that H_2S evolution starts well below 150^{o}C, i.e. about 130^{o}C (Giavarini, 1975; Giavarini & Rinaldi, 1979; De Filippis et al., 1997).

2.2 Crumb Rubber in Asphalt

Scrap tire rubber has been used in hot mix asphalt (HMA) for several decades in the United States and other countries. In 1960, Charles McDonald became the first engineer to use scrap tire rubber in asphalt mixtures to improve pavements in Phoenix, Arizona. Since then, many experimental studies and field test sections have been constructed and tested. The mixing of crumb rubber with conventional binders

results in an improvement in the binder's resistance to rutting, fatigue cracking and thermal cracking (Dantas Neto et al., 2003; Way, 2003). Over the past several years, researchers have concluded that rubberized asphalt mixes can be helpful in reducing the thickness of asphalt overlays and reflective cracking potential (Amirkhanian, 2003; Holleran and Van, 2000; Cano et al., 1989; Esch, 1982; Choubane et al., 1999; Sousa et al., 2002), in addition to protecting the environment and saving resources (e.g., landfill space). Rubber, one type of polymer, is known to absorb liquids and swell. The extent of swelling is dependent on the nature, temperature and viscosity of the liquid (or solvent) and the type of polymers (Treloar, 1975). The bulk of the rubber absorbs the solvent, which increases the dimensions of the rubber network until the concentration of liquid is uniform and equilibrium swelling is achieved (Airey et al., 2003). The amount of solvent diffused into the rubber depends on the shape and number of cross-links in the rubber and the compatibility of the solvent. The greater the number of cross-links in the rubber, the shorter the average lengths of rubber chains between cross-links and the lower the rate of diffusion (McCrum et al., 1999).

Most of the rubberized asphalt projects conducted in the United States use the "wet" process; which entails adding the crumb rubber to the binder before mixing it with aggregate. The research conducted and reported by McCrum et al. (1999) used the wet process to blend the crumb rubber with the virgin binder. Previous research has indicated that the crumb rubber particles reacting with asphalt binder swell and form a viscous gel due to absorption of some of the lighter fractions in the asphalt

binder (Green and Tolonen, 1997; Heitzman, 1992; Bahia and Davies, 1994; Zanzotto and Kennepohl, 1996; Kim et al., 2001; Airey et al., 2003). Furthermore, Mathias Leite et al. (2003) discovered that the proportion of the crumb rubber in the mixture changes significantly since a rubber particle can swell to 3 to 5 times its original size when blended with an asphalt binder. To measure the swelling of crumb rubber particles, researchers have developed several useful methods (Airey et al., 2003; Gaulliard and Leblanc, 2004).

2.3 Polyethylene Wax in Asphalt

A study by Edwards et al. (2006), investigated the effect of commercial wax on the rheological properties of bitumen 160/220-grade penetration at low temperature. Their study considered low temperature effects, which can influence the thermal cracking resistance of the asphalt concrete. In a second study, the effect of commercial wax on the rheological properties of bitumen 60/220-grade penetration at high and medium temperature was investigated by Edwards et al. (2006). Their study considered high and medium temperature effects, which can influence the rutting resistance of the asphalt concrete. The study indicated that the magnitude and type of effect on the bitumen rheology depends on the bitumen type as well as the type and quantity of the additive used, as adding polyethylene wax to the binder has showed considerable changes on the rheological properties of the binder at medium and high temperatures.

A study to investigate the potentials of warm mix asphalt additives was conducted by Kanitpong et al. (2008). They examine the effect of Sasobit^{TM} (long-chain aliphatic hydrocarbon) when used as an asphalt modifier, on the rheological properties, viscosity, rutting resistance and fatigue resistance. They also investigated the compatibility of the binder with sulfur at low temperature and also the effect of sulfur on the performance of the binder mixtures produced at low temperatures.

Meor et al. (2010), investigated the potential of Sasobit^{TM} to reduce heat energy and CO_2 emission in the asphalt industry. They quantified the reduction in fuel consumption due to the reduction in mixing and compaction temperatures in the production of asphalt concrete using Sasobit^{TM} modified binder.

2.4 Waste Oil fly ash

Fly ash is a finely divided residue that results from the combustion of coal or oil-fired power generators. Based on the type of fuel used, it is divided into "Coal Fly Ash" (CFA) and "Oil Fly Ash" (OFA). The generated fly ash consists of very small individual particles that are carried up and out of the boiler with the flow of exhaust gases, leaving the boiler after the coal and/or oil is consumed. The combustion process may also result in the enrichment of trace elements in the ash, most often adhered to the surface of the ash particles. The quantity and characteristics of fly ash depend primarily on the fuel characteristics and the burning process [NCASI, 2003]. The fly ash generated from combustion of fuel oil is the unburned residue found in the fuel and the additives used. It contains the organometallics from crude oil,

inorganic contaminants or metallic catalyst fines used in the refining process. In addition to carbon, the major elements in fuel oil fly ash include magnesium, vanadium, nickel and sulfur. On the other hand, coal fly ash particles are enriched with arsenic and selenium. Heavy fuel oil ash and coal ash particles have unique elemental compositions which distinguish them from each other.

Although the fundamental particle formation processes during the combustion of heavy fuel oils are the same as those for pulverized coal, there are distinct differences between the two fuels. In contrast to coals, oils do not typically contain significant mineral matter. The metals in heavy fuel oils are generally inherently bound within the organic molecule, which may be the case for only a small portion of the metals in higher rank coals. Unlike coal, interactions between volatile metal species and nonvolatile minerals within the heavy fuel oil droplets are much less likely in heavy fuel oils.

According to a 2009 survey of the American Chemical Society, more than 71 million tons of fly ash is produced annually in USA by coal-fired plants and 45% of this quantity is reused in different applications [Chemical & Engineering News, 2009a]. It is mainly used as a replacement of Portland cement; as a filler in polymers, asphalt and cementitious materials; stabilizing agent and also for solidification of wastage and sludge. It is estimated by a report of C&EN in December 2009 that 7% of global carbon dioxide and greenhouse gases are emitted by cement production which can be reduced by the use of fly ash [Gregg and Sing,

1982; Shawabkeh, 2004, 2006; Shawabkeh et al., 2006; Shawabkeh and Harahsheh, 2007; Al-Harahsheh et al., 2009; Chemical & Engineering News, 2009b; Bhagiyalakshmi et al., 2010; Guo et al., 2010; Sinha et al., 2010; Visa et al., 2010; Zeng et al., 2010]. Fly ash is a finely grained, black powdery particulate type material. OFA is mainly composed of more than 70% unburned carbon with some inorganic substances such as SiO_2, Fe_2O_3, Al_2O_3 and CaO and traces of heavy metals [Riu et al., 1996; Woo-Teck et al., 2005; National Research Council, 2006; U.S. Environmental Protection Agency, 2007].

Hersh et al. [1979], Piper and Nazimowitz [1985], and Walsh et al. [1991] showed that, in contrast to pulverized coal, the majority of the sampled fly ash masses from residual fuel oil combustion in power plants is likely to lie below 1.0 μm in diameter, although larger particles can form with poor carbon burnout. Furthermore, Walsh et al. [1991] have demonstrated that Fe, Mg, and Ni are concentrated at the center of the submicron particles, while Na and V are associated with a "halo of sulfate residue". Bacci et al. [1983] found substantial enrichment of both Ni and V in the submicron particle size fraction of samples collected at a large oil-fired power plant.

2.5 Fly Ash Characteristics

Oil fly ash (OFA) is typically a black powder type waste material that results from the use of crude and residual oil for power generation. Abu-Rizaiza [2004] and Daous [2004] have studied fly ash resulting from combustion of heavy fuel oil in the

power generation plant of the Saudi Electricity Company in Rabigh, using chemical analysis of oil fly ash as shown in Table 2.1. Samples were analyzed to characterize the physical and chemical content of the fly ash and its morphology. The result obtained using Atomic Adsorption Spectrophotometer (AAS) and Inductive Coupled Plasma (ICP) indicates high content of metals and heavy metals. Vanadium, nickel, and lead are among the metals of high concentration. Other elements with elevated concentration include sodium and chromium. Scanning Electron Microscopy (SEM) was used to assess the morphology of the fly ash. The ash particles are amorphous and spherical in shape. High concentrations of carbon and sulfur were also identified when the SEM was combined with Energy Dispersive X-ray Spectrometry (EDX). The fly ash sample and a sample of clear graphite were analyzed using X-ray Diffraction (XRD).

Table 2. 1: Heavy fuel oil fly ash analysis

Parameter	Quantity	
pH @ 18°C	2.8	
Moisture	0.33	wt %
Unburned Carbon @ 700°C	90.18	wt %
Ash Content	9.82	wt %
SO_3	3.06	wt %
Vanadium as V	4007	ppm
Nickel as Ni	1021	ppm
Iron as Fe	559.4	ppm
Magnesium as Mg	1800	ppm

The chemical characteristics of the fuel oil fly ash generated at a power plant differ significantly from that of coal fly ash. The carbon content of heavy fuel oil fly ash is about 95% while that of coal fly ash generally ranges between 20% and 50%. Toxic heavy metals, such as vanadium (2.08% as V_2O_5) and nickel (0.37% as NiO) are also present in the heavy fuel oil fly ash. The high carbon content and presence of toxic heavy metals suggested that this fuel oil fly ash can be considered as a hazardous respirable dust that demands careful handling and safe disposal to ensure proper environmental protection.

2.6 Production

Fly ash is produced from the combustion of coal in electric utility or industrial boilers. There are four basic types of coal-fired boilers: pulverized coal (PC), stoker-fired or traveling grate, cyclone, and fluidized-bed combustion (FBC) boilers. The PC boiler is the most widely used, especially for large electric generating units. The other boilers are more common at industrial or cogeneration facilities. Fly ashes produced by FBC boilers are not considered in this document. Fly ash is captured from the flue gases using electrostatic precipitators (ESP) or in-filter fabric collectors, commonly referred to as baghouses. The physical and chemical characteristics of fly ash vary among combustion methods, coal source, and particle shape.

In 2001, out of the 62 million metric tons (68 million tons) of fly ash produced in the United States, only 20 million metric tons (22 million tons), or 32 percent of total production, was used. Table 2.2 is a breakdown of fly ash uses in USA [EPA, 2005],

much of which are used in the transportation industry. In Saudi Arabia, the total amount of disposed OFA in 2008 was about 240,000 cubic meters. The amount was expected to increase to 340,000 cubic meters in 2012.

2.7 Ash Disposal alternatives

Fly ash is produced in large quantities as a by-product of the combustion of coal, gas, crude and fuel oil in power plants. It is collected from flue gases mainly through air pollution control devices. A very small fraction of the collected coal fly ash is utilized currently as a supplementary cementing material for cement, concrete industries, and other purposes. The remaining large fraction adds to the major waste disposal problem for the industries [Yazici, 2007]. A number of disposal alternatives are practiced for different types of wastes. The disposal alternatives that are most commonly used for fly ashes are briefly discussed below [American Coal Ash Association, 2003; EPA, 2005].

2.8 Wet Settling Basins

Wet basins have been historically the most widely used method for ash disposal due to their relatively low cost and simplicity of operation. Where topography is suitable and space is available, the use of lagoons is a standard practice to dispose huge amount of fly ash. Lagoons are ponds or lakes typically located near the power plants. In USA, the majority of lagoons located around the country have no liners or

groundwater monitoring option despite the concentrated levels of heavy metals and many other contaminants [http://www.hecweb.org/ccw/CCWdoc.html].

Ash from boilers and collectors is carried by a hose system to the disposal area. The ash settles in the lagoon. The overflow, which is usually alkaline, is discharged into the nearest watercourse. With properly designed lagoons and appropriate skimmer devices to prevent discharge of any floating ash, this system of ash disposal from power plants is satisfactory, particularly from the stand point of stream and groundwater pollution control [http://www.hecweb.org/ccw/ CCWdoc.html].

Table 2. 2: Details of coal combustion products uses, short tons

Uses of Coal Combustion Products	Fly Ash	Bottom Ash	Boiler Slag	Flue Gas Desulfurization Material
Concrete/concrete products/grout	12,265,169	298,181	15,907	99,877
Structural fills/embankments	5,496,948	2,443,206	11,074	236,241
Cement/raw feed for cement clinker	3,024,930	493,765	15,766	422,512
Road base/subbase/pavement	493,487	1,138,101	29,800	0
Snow and ice control	1,928	683,556	102,700	0
Aggregate	137,171	512,769	31,600	6,299
Flowable fill	136,618	20,327	0	9,184
Mineral filler in asphalt	52,608	0	31,402	0
Wall board	0	0	0	7,780,906
Waste stabilization/solidification	3,919,898	30,508	0	0
Mining applications	683,925	1,184,927	59,800	390,331
Blasting grit/roofing granules	0	42,604	1,455,140	0
Soil modification/stabilization	515,552	67,998	0	818
Miscellaneous/other	408,290	1,331,331	2,815	34,813
Total	27,136,524	8,247,273	1,756,004	8,980,981

Wen and Chung [2004] indicated that the addition of 7.0 vol % carbon black to asphalt (with sand) resulted in an increase of the softening temperature from 44 to 81°C and an increase of the storage modulus (under flexure at 0.2 Hz) from 1.3 to 2.1 kPa. All these effects were due to the increase in carbon black content. The percolation threshold was probably between 5.4 and 7.0 vol % carbon black in the mix.

2.9 Incineration

Another possible alternative method for ash disposal is to burn fly ash in incinerators with the help of auxiliary fuel. The carbon content of fly ash generated at power plants that burn heavy fuel oil is significant (i.e. above 90%). The high carbon content and the volume of such fly ashes could be reduced significantly after incineration. The residual ash obtained after incineration could be rich in heavy metal contents that could encourage recovery of heavy metals. However, because of the presence of toxic metals in fuel oil fly ash, there exists a high possibility of emission of harmful gaseous pollutants and particulate matter into the atmosphere during improper incineration of the fly ash [Seggiani et al., 2007]. Relevant literature on this subject is currently not available. Therefore, this alternative method should be carefully investigated, particularly in terms of potential environmental pollution from toxic emission before its application.

2.10 Recycling of Fly ash

Potential uses of fly ash as a resource material for different purposes have been explored by various research agencies, scientists and institutes [Dermatas and Meng, 2003; Prabakar et al., 2004; Sezer et al., 2006; Yazici, 2007]. Most of the studies have addressed fly ash generated from burning coals. Literature on reuse and/or recycling of fly ash generated from combustion of heavy fuel oil (HFO) is very scarce because of the limited use of heavy fuel oil for power generation. Therefore, specific research programs should be initiated to identify possible uses for fuel oil fly ashes. Experience indicates that coal fly ash has a potential for reuse, particularly in the following civil engineering and related applications [American Coal Ash Association, 2003; Dermatas and Meng, 2003; EPA, 2005]:

- As an admixture in Portland cement concrete.
- As raw material for cement manufacturing.
- Highway construction.
- Waste management.
- Agriculture.
- Stabilized base course.
- Flowable fill.
- Structural fills/embankments.
- Soil improvements.
- Asphalt pavements.
- Grouts for pavement sub-sealing.

Most of the fly ash reuses that are reported in the literature are related to ash generated from coal. Other potential uses include re-burning for full utilization of the energy of unburned carbon in the fly ash. The proper reuse and/or recycling of fly ash is desired over the conventional disposal practices not only for its economic benefits but also for ecological advantages. Therefore, fly ash generated from combustion of heavy fuel oil, which has not been significantly used for beneficial applications similar to those reported for other fossil fuel ashes [EPA, 1999], should be studied for consideration of reuse.

Anani and Al-Abdul Wahhab [1982] carried out a research to determine the effects of baghouse fines and diesel fuel ash rich dust on asphalt mixes. The analysis included Marshall tests on mixes that had various ratios of filler to baghouse fines. Other tests to study these effects included stability loss, viscosity, penetration, shear-modulus, and softening point. The results of the study indicated that baghouse fines can greatly affect the properties of the mix, such as the optimum asphalt content, stability, and stability loss. Asphalt mortars that used different ratios of filler to baghouse fines exhibited varied viscosity and penetration. Stability loss, which is a main factor in the design of local mixes, was decreased drastically by the inclusion of baghouse fines. One factor that controls the effect of baghouse fines on asphalt mixes was the percentage of carbon. The addition of baghouse fines greatly helps in the improvement of mix properties.

Al-Suhaibani [1986] investigated the feasibility of using fly ash to replace part of asphalt cement in asphalt concrete mixes. An important aspect of this research was to study the effect of fly ash particle size. From the resilient modulus results before and after water immersion, it was found that changing fly ash size did not affect the resistance of various mixes to water damage. Livingston [1989] reported an experimental section of asphalt concrete pavement overlay which contained the additive carbon black funded by Washington DOT. Preliminary laboratory results indicated that the viscosity/temperature curve for the carbon black asphalt binder has been altered in a way that the temperature susceptibility of the pavement is decreased. Jones [1990] has carried out a research to identify the most promising types of asphalt modifiers for reducing pavement deformation (rutting) in flexible airfield pavements. A series of binder and mixture tests were performed to evaluate the effect of modifier before and after aging. Test results indicated that all additives improved rut resistance. Carbon black ranked the second best in terms of performance.

Woo-Teck et al. [2005] studied the physical and chemical properties of fly ash generated from heavy oil (HOFA). HOFA was analyzed and compared to those of carbon black to investigate the possibility of reutilizing it as a black pigment for secondary cementitious materials. They indicated that HOFA is mainly composed of carbon, sulfur and residue ash, whereas carbon is a dominant content of carbon black. Compared with carbon black sample, heavy oil fly ash contains lower carbon content and higher amount of sulfur and residue ash. Lower carbon content in heavy oil fly ash is attributed to higher combustion rate of heavy oil. The particle size ranged from

10 to 120 μm, and XRD data confirms that it is composed of amorphous carbon. The characteristic color property of fly ash was similar to carbon black. According to the SEM result (Figure 3.1), heavy oil fly ash has spherical shape. The result of the mortar test shows stable compressive strength with increasing heavy oil fly ash additions. They concluded that glass-state inorganic substances such as SiO_2, Fe_2O_3, Al_2O_3 and CaO in heavy oil fly ash contribute to the formation of hydrate cementitious material that enhances its compressive strength. According to the results achieved from this study, heavy oil fly ash has good physical and chemical properties. There is a possibility of finding ways to substitute carbon black with heavy oil fly ash for secondary cementitious materials through several additional experiments.

Asphalt pavements are constructed depending on the thermo-plasticity of the asphalt, which is the property of softening by heating and hardening by cooling. However, these effective properties become a disadvantage for in-service periods, as rutting of pavements occurs in a hot summer and cracking in a cold winter. These phenomena are the main modes of failure of asphalt pavements. A pilot study was carried out in the Civil Engineering highway laboratory at KFUPM to explore the effect of unmodified OFA on the performance of asphalt concrete mixes. Results indicated that unmodified OFA has adverse effect on the fatigue resistance of asphalt concrete mixes.

2.11 OFA Rheology and Modification

The following literature review will mainly search the melt rheology, increased interfacial interaction and improvement of the dispersion of nanomaterial into the matrix of nanocomposites. This literature review shows the success of organic modification of nanomaterials in improving the compatibility of polymer nanocomposites. This is what is aimed for when modifying the surface of the ash. Improvement in the dispersion of ash and the elasticity of the composite will have a significant impact on the fatigue life of OFA modified asphalt concrete mixes.

Here, some of the rheological concepts are introduced that will explain the improvement in the interfacial bonding, hence, the elasticity of the composite. Small amplitude oscillatory shear measurements in strain controlled rheometer) are generally performed by applying a time dependent strain of $\gamma(t) = \gamma_o \sin(\omega t)$ and measuring the resultant shear stress $\tau(t) = \tau_o [G' \sin(\omega t) + G'' \cos(\omega t)]$, where G' and G'' are the storage and loss moduli, respectively. Generally, the dynamic rheology of melts depends strongly on the temperature and frequency at which the measurement is carried out.

Buffa et al. [2005] functionalized single wall carbon nanotube with 4-hydroxymethylaniline (HMA) via the diazonium salt. Thermal analysis indicated that 1 out of every 33 C atoms remained functionalized. Raman, FTIR, and optical absorption spectroscopy confirmed the side-wall functionalization and show that it can be reversed by thermolysis. The OH group that was generated from the

functionalization could be used to start the ring-opening polymerization of ε-caprolactone. The polymer produced remained grafted to the nanotube and was demonstrated by FTIR.

Al-Ostaz et al. [2008] used molecular dynamic simulation to study single-wall carbon nanotube (SWCNT) embedded in polyethylene matrix. They also compared the elastic properties of bundles with 7, 9, and 19 SWCNTs. The results they obtained were in good agreement with experimental data. They found out that the interface is an important constituent of CNT-PE composites. They were able to model it with reasonable success.

Several studies were performed for the surface modification of fly ash. Yang et al. [2006] investigated the surface modification of fly ash by using isothermal heating and examined its impact on the properties of polymer composites. The authors observed an increase in surface area and whiteness of fly ash particles was observed as a result of thermal treatment. Also, improvement in interfacial loading between polypropylene and fly ash was reported. Kishore et al. [2002] studied the effect of surface treatment of fly ash by adhesion-increasing and adhesion-decreasing on impact behavior of polymer composite. The adhesion-increasing modification (silane-acetone treatment) showed greater absorption of energy and maximum load while adhesion-reducing modification increased the ductility index. The effect of chemical treatment of fly ash on the properties of natural rubber/fly ash composite was investigated by Sombatsompop et al. [2004]. Researchers used various contents

of bis-(triethoxysilylpropyl) tetrasulfane for surface modification. The mechanical properties of composites increased up to 4% loading of filler, while NaOH treatment showed no improvement in properties.

In carbon nanotubes literature, the attachment of carboxylic group to the nanotubes not only enhanced the interface linking property of CNT/polymer but also provided reactive sites to attach a variety of functional groups [Chen et al., 1998, 2001; Ya-Ping et al., 2002]. The composition of OFA contains more than 90% carbon which makes it similar to carbon nanotubes. So, the authors used similar techniques for surface modification of OFA to improve the properties of OFA. Therefore, the synthesis of fly ash particle functionalized by carboxylic group was carried out using acid treatment methods.

The optimization of different parameters such as acid ratio and oxidation was performed. The experimental study used elemental analysis, functional and morphological characterization by FTIR, SEM, XRD and BET methods. Reaction parameters were investigated with the objective of increasing the surface area. The chemical modification of carbon nanotubes (CNTs) resulted in major improvements of CNT/polymer blends [Yang et al., 2007; Bing-Xing et al., 2008,]. Similarly, the chemical modification of waste OFA can lead to improved OFA/polymer properties [Khan, 2010]. Further, the inherent problem of ash such as the incompatibility of ash as a filler and agglomeration can be altered by surface modification. Furthermore, the

increase in surface area of ash as a result of chemical modification is expected to further support the use of modified ash in adsorption related applications.

Baek and Lee [2007] indicated that OFA is an industrial waste that is obtainable without payment with high carbon and sulfur contents and sufficient surface area by CO_2 activation that has potential for Hg sorbent by chemical modification. Three methods were used to modify OFA:

- Activation with CO_2
- Treatment with aqueous HNO_3, H_2SO_4, and HCl solutions
- Impregnation with sulfur

They indicated that HCl and H_2SO_4-treated OFA and S-impregnated OFA showed maximum initial mercury removal efficiencies similar to those of commercial ACs in spite of much smaller surface area. Active mercury sorption sites like sulfur and chloride can be created on the surface of OFA by chemical treatment and the existence of those sites is much more important than large surface area to obtain higher mercury removal. Among the chemicals used in this work, HCl and S were most preferable in both sides of mercury removal efficiency and physical properties of the resultant sorbents. Results of their work suggested that chemically modified heavy oil fly ash could be one of the candidates as a novel sorbent to remove vapor-phase Hg from coal-fired flue gases.

In summary, the above literature review shows that the organic modification of the CNTs has improved the compatibility and interfacial properties of the composite.

It was also observed that surface modified CNT resulted in good dispersion in polymers. The aim of this research is to achieve in OFA-asphalt blends what was achieved in CNT or clay-polymer blends. The physics of the two systems are very similar. CNT is mainly carbon and OFA is more than 80% carbon. The success of carbon black which possesses high surface area/unit volume in comparison with OFA, as a filler for asphalt, is another indicator of the potential success of physical modification of OFA. On the other hand, the authors will modify the surface of OFA by some functional groups that proved to work with polymer/asphalt systems. This literature review suggests the high potential of modified OFA in improving local binders and asphalt mixes, which will result in better pavement performance, increasing pavement life, and reducing pavement cost.

CHAPTER 3

EXPERIMENTAL WORK

3.1 Introduction

All works have been divided into two phases. In the first phase, different waste materials were subjected to different physical and chemical treatments and blended with asphalt binder. Improvement of modified asphalt binder performance was determined by comparing with base asphalt. In the second phase, base asphalt as well as selected modified asphalt binder was mixed with aggregate to produce asphalt concrete mixes to evaluate marshal mix properties, spite tensile strength, Resilient modulus, rutting and fatigue performance.

3.2 Materials

Polyethylene wax was collected from Tasnee Petrochemicals Complex, Jubail, Saudi Arabia. It has melting point of ~ 70^{o}C. It is a byproduct resulting from incomplete polymerization of polyethylene. Crumb rubber was collected from a local supplier. The source of the used rubber was waste car tires. Rubber was ground to fine powder to increase the surface area. Elemental sulfur (99.9% purity) was collected from Saudi Aramco. It is a waste product from oil and gas processing plant. Asphalt cement was purchased from a local refinery.

3.3 OFA treatment

OFA was subjected to different physical and chemical modification processes to activate its surface. The following three modification methods were used:

1. Introduction of carboxyl groups onto OFA surface
2. Functionalization with amine group
3. Functionalization with 1-Octadecanol ($C_{18}H_{38}O$)

Treatment procedure and characterization has been described in chapter four.

3.4 Asphalt Modification

3.4.1 Sample Preparation

Treated wastes and pure asphalt were blended in a high shear blender. In the case sulfur asphalt, elemental sulfur and crumb rubber was grounded to powder (size less than 1 mm). The blender acts as a batch stirred tank with a constant temperature bath. Typical mixing procedure was as follows: steel cans of approximately 1000 mL were filled with 250–260 g of asphalt and put in a thermoelectric heater. When the temperature of asphalt reached 145°C, a high shear mixer was dipped into the can and set to about 2500 rpm. Calculated amount of treated wastes added gradually with asphalt. The bath temperature was maintained at 145 ± 1°C. Samples were blended for 10 minutes at high shear to confirm uniform distribution of sulfur and rubber in the asphalt matrix. Asphalt samples were poured into rubberized molds before being

used for rheological testing. The samples specimens were stored in a refrigerator at 5°C. Figure 3.1 shows the schematic diagram of the blending machine and its accessories.

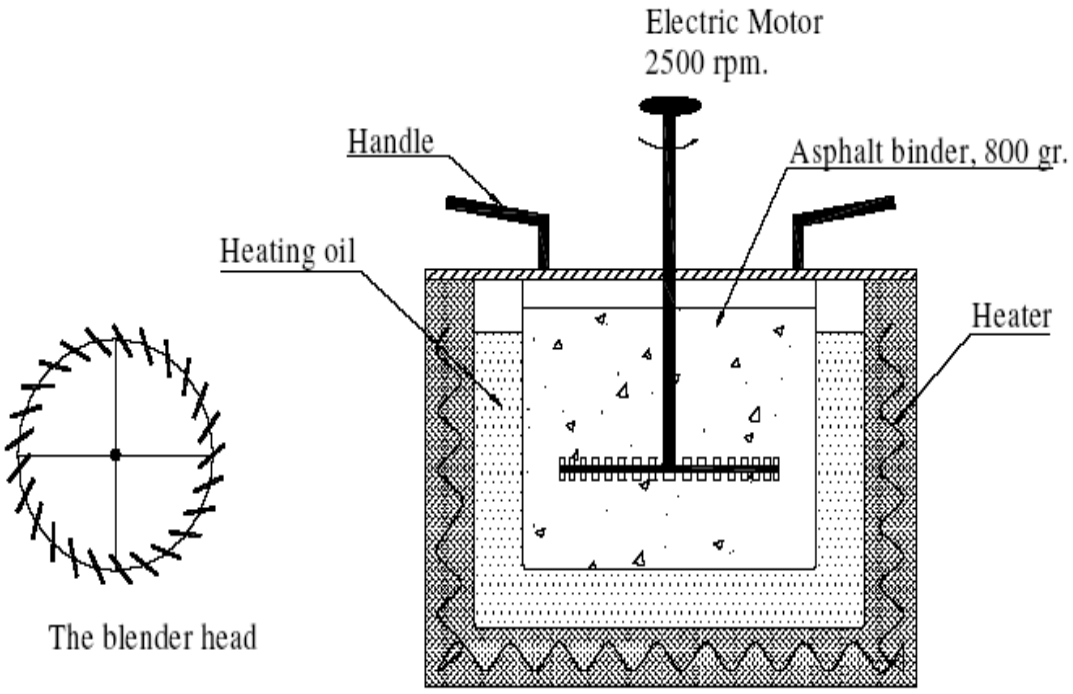

Figure 3. 1: Schematic representation of blending machines

3.4.2 DSC measurements

The thermal behaviors of the pure and modified asphalt binder as well as the compositions of the asphalt binder were determined by means of a TA Q1000 DSC. Samples of 7-10 mg were weighed and sealed in aluminum pans. Melting temperature measurements were performed by heating samples from room temperature to 150^{o}C. A heating rate of 5^{o}C/min was applied and nitrogen was used as the purge gas at a flow rate of 50 ml/min.

3.4.3 FTIR Characterization

Fourier transform infrared spectroscopy (FTIR) technique was used to determine the chemical bond changes of pure and modified asphalt binder. FTIR measurement was carried using a Nicolet 6700 spectrometer from Thermo Electron™. All the FTIR spectra were taken in the absorbance mode and in the range 600–4000 cm^{-1} at room temperature. FTIR spectra were obtained using a spectral resolution of 4 cm^{-1} and 30 co-added scans.

3.4.4 Rolling thin film oven (RTFO) test

Rolling thin film oven test (RTFO) was used to perform ageing of asphalt binders according to ASTM D 2872 procedure. This test simulates the ageing process that takes place during the production and up to the first year of the service life of the pavement. Base asphalt as well as modified asphalt was poured into cylindrical bottles. 35 grams of asphalt sample was poured in each cylindrical bottle. Then the bottles were placed horizontally in a convection oven, which was rotated at 163^{o}C for 85 min. Air was supplied into the bottle to accelerate ageing. This process created a thin film of asphalt on the inside of the bottles. After completing the run, samples were collected for rheological testing in ARES. Figure 3.2 represents RTFO machine and RTFO bottles before and after RTFO test.

(a) (b)

Figure 3. 2: (a) Rolling Thin Film Oven (RTFO) machine, (b) RTFO bottles, bottle at left is after the RTFO test, the bottle in the middle is before the test.

3.4.5 Dynamic Shear Rheometer (DSR)

The dynamic temperature step measurements for the samples were performed in an ARES rheometer. This is a constant strain rheometer equipped with a heavy transducer (range 2-2000 g for normal force; 2-2000 g-cm for torque). Figure 3.3 shows the ARES rheometer. All tests were carried out in a range of 64^{o}C-100^{o}C using a parallel plate set of diameter is 25 mm. With the sample in position, the oven was closed and the sample heated at 64^{o}C for about 10 minutes, thereafter the gap between the plate platen was adjusted to 1 mm by lowering the upper platen force transducer assembly at a constant load of 500 g. The melt that extruded beyond the platen rim by this procedure was cleaned off. Strain in the linear viscoelastic range

(strain amplitude, γ^o of 12.5 %) and frequency of 10 rad/s was used for all the tests. In all the experiments, nitrogen gas was continuously used for heating the samples during testing to avoid oxidation during testing. A holding period of 5 min. was allowed before beginning measurements to allow the temperature to reach steady state. Orchestrator software was used to calculate the dynamic shear viscosity, storage modulus and PG grading for all samples. Fresh asphalt and RTFO residue was run in ARES rheometer with plate diameter 25 mm. Asphalt samples tested after PAV were harder than that of fresh asphalt. Therefore, asphalt submersion cell with 8 mm diameter plate was used for PAV residue sample.

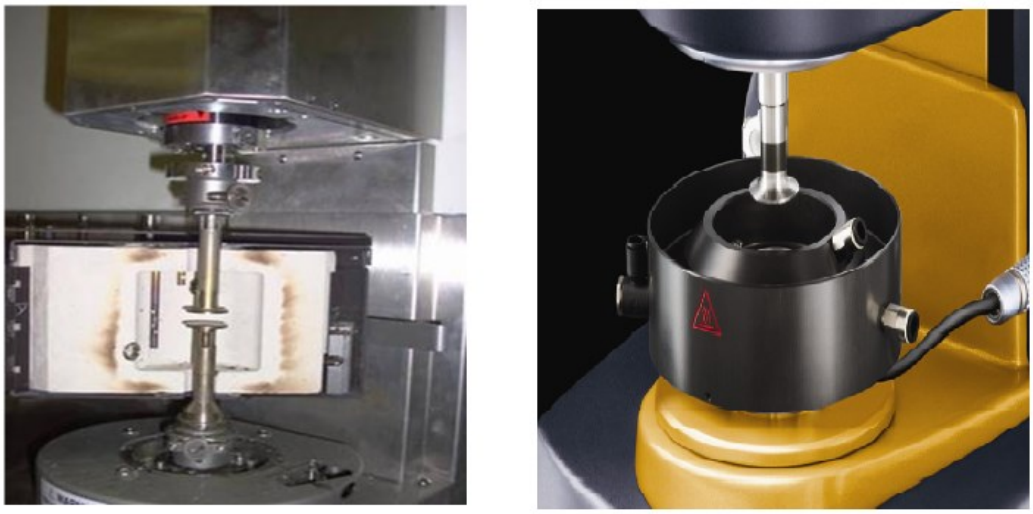

(a) (b)

Figure 3. 3: Advanced Rheometrics Expansion System (ARES) Rheometer, (b) Asphalt submersion cell

3.5 Marshall Mix Design

Superpave mix design method was used to design asphalt concrete mixes following the Ministry of Transport (MOT) specifications for typical Superpave wearing course (WC) layer and modified asphalt binder. The optimum asphalt content was obtained through Superpave mix design for different sulfur-asphalt combinations. Sulfur and pure asphalt were blended in a high shear blender. The elemental sulfur pellets were ground to fine powder before feeding the sulfur to the blender. The blender acts as a batch stirred tank with a constant temperature bath. Five levels of sulfur (including the pure asphalt or zero sulfur) were used to determine the optimal asphalt content using standard Marshall Mix design procedure.

3.5.1 Specimen Preparation

Approximately 1200 gm of aggregates and filler were heated to a temperature of 160^{o}C. Plain and sulfur modified asphalt binders were mixed with aggregate at 145^{o}Cin a large temperature-controlled mixer. Figure 3.4 represents the asphalt and aggregate mixer. Five different percentages of asphalt contents were used to prepare the sample specimens. Asphalt binders and heated aggregates were thoroughly mixed at temperatures of 154^{o}C to 160^{o}C. The mix was placed in a preheated mold and compacted by a rammer with 75 blows on either side at a temperature of 138^{o}C to 149^{o}C. Five specimens of 63.5-mm height by 101.6-mm diameter were prepared for testing. Figure 3.5 shows the equipment for the Marshall Compactor and compacted specimens.

3.5.2 Properties of the Asphalt Concrete Mix

The properties that are of interest include the theoretical or bulk specific gravity (G_{mb}), maximum specific gravity (G_{mm}), and air voids percent (V_v) in the mix. All of these physical properties were measured for each specimen before conducting the destructive Marshall Stability test.

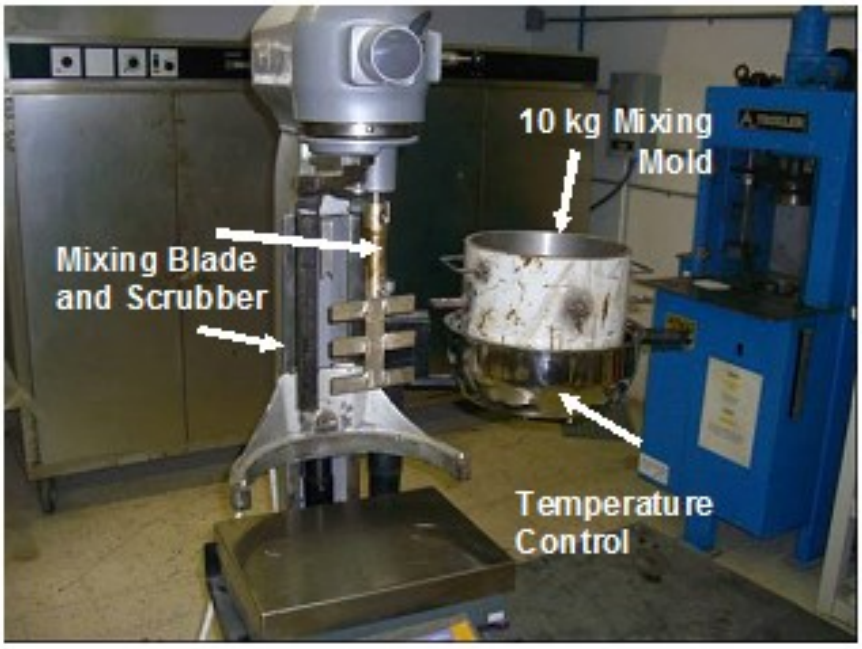

Figure 3. 4: Large capacity temperature controlled mixer

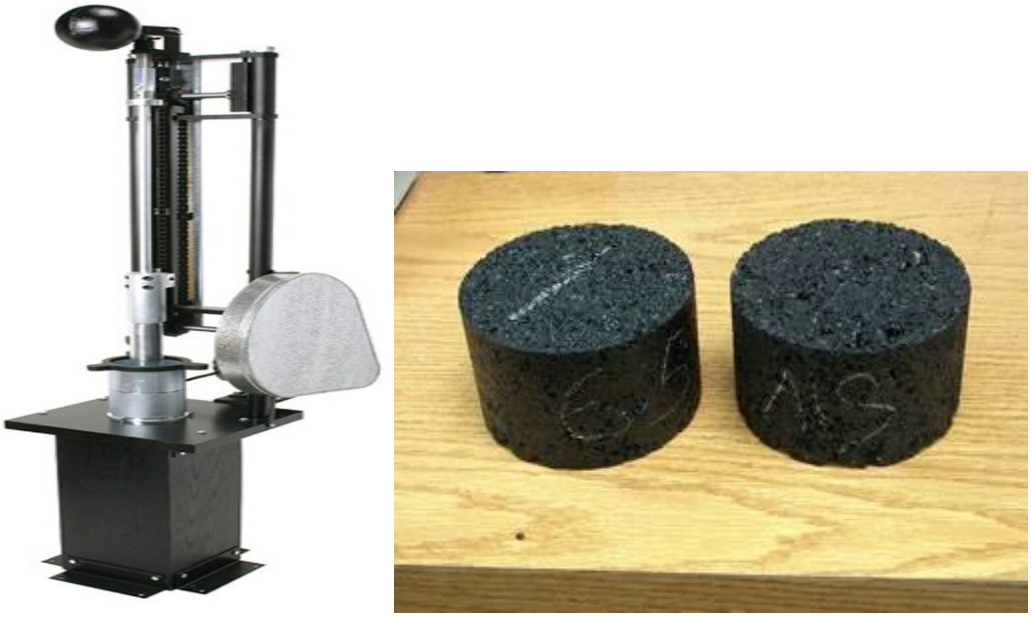

Figure 3. 5: Marshall compactor and compacted specimens

3.5.3 Marshall Stability and Flow

In conducting the stability test, the specimens were immersed in a bath of water at a temperature of 60°±1°C for a period of 35 minutes. They then were placed in the Marshall Stability testing machine and loaded at a constant rate of deformation of 5 cm per minute until failure. The maximum load in kN (that causes failure of the specimen) was taken as Marshall Stability. The stability value so obtained was corrected for the height of the specimen. The total amount of deformation is recorded as flow value. One unit of deformation is 0.25 mm.

3.5.4 Optimum Asphalt Binder Content

The optimum asphalt binder content was determined for pure asphalt and sulfur modified asphalt using Marshall Method. Three separate smooth curves were drawn with percent of asphalt on x-axis and the following on y-axis:

- Bulk specific gravity (G_{mb})
- Percent air voids
- Marshall Stability

The optimal asphalt content was determined as the average binder content for the maximum specific gravity, maximum stability and specified percent air void in the mix. So, the optimal binder content was calculated using the formula:

$$B_o = \frac{B_1 + B_2 + B_3}{3} \qquad (3.1)$$

Where,

B_0 = Optimal binder content.

B_1 = % Binder content at maximum specific gravity.

B_2 = % Binder content at maximum Marshall Stability.

B_3 = % Binder content at specific air voids (4-6%) in the total mix.

Table 3.1 represents the optimum binder content for different asphalt concrete mixes.

Table 3. 1: Optimal binder content

Serial #	Binder composition	Optimal binder content, %
1	Pure Asphalt	5%
2	20% sulfur + 80% asphalt	5.25%
3	30% sulfur + 70% asphalt	5.7%
4	40% sulfur + 60% asphalt	6%
5	50% sulfur + 50% asphalt	6.2%
6	OFA modified asphalt	4.7%

CHAPTER 4

RESULTS AND DISCUSSION

4.1 Utilization of waste sulfur and crumb rubber in asphalt modification

4.1.1 Abstract

In this study, waste crumb rubber and sulfur were utilized to enhance the performance of asphalt binder for pavement applications. 20-50% of sulfur and 1-6% crumb rubber were used. Melt properties were investigated using thermal analysis, dynamic and steady shear rheology and artificial ageing. Rheological tests were carried out in ARES rheometer. Both steady and dynamic shear rheology showed that crumb rubber improved the viscoelastic properties of the sulfur extended asphalt binder. Crumb rubber modification reduced temperature susceptibility of sulfur/asphalt, and increased the upper grading (performance) temperature of sulfur asphalt. The combined effect of sulfur and crumb rubber reduced the activation energy compared to that of pure asphalt. Zero shear viscosity and SHRP rutting parameter ($G^*/\sin\delta$) improved by crumb rubber incorporation into the sulfur extended asphalt binders. Short term ageing improved $G^*/\sin\delta$ with slight increase

in activation energy. The addition of sulfur to asphalt matrix increased the viscoelastic properties (G′ and G″) of sulfur asphalt. The addition of crumb rubber to sulfur asphalt enhanced the temperature resistance of the binder. Utilization of waste crumb rubber and sulfur in asphalt modification proved to enhance the asphalt pavement life. In addition, utilization of such wastes can help in meeting the extra demand for asphalt, reduce the pavement cost and improve solve a waste disposal problem.

4.1.2 Introduction

Asphalt cement is used to construct asphaltic surfaces and produce several products such as waterproofing membranes and emulsified asphalts. It is a strategic commodity that is in huge demand due to massive roads and highways construction plans in many countries. Asphalt binder is a thermoplastic material that behaves as an elastic solid at low service temperatures or during rapid loading, and as a viscous liquid at high temperatures or slow loading. This double behavior creates a need to improve the performance of the asphalt binder to minimize stress cracking, which occurs at low temperatures, and permanent deformation, which occurs at high service temperatures. The daily and seasonal temperature variations plus the growth in truck traffic volume, tire pressure, and axle loading have increased stresses on asphalt pavements. The local asphalt pavement temperature in Saudi Arabia ranges between -10^{o}C in winter and 76^{o}C in summer. This increases the demand to modify asphalt binders (to reduce cracking and deformation). Different methods have been used to

upgrade the properties of asphalt binders (Iqbal, et al., 2006; Hussein, et al., 2005; Hussein, et al., 2006; Polacco, et al., 2004).

Most of the previous work focused on polymer modification of base asphalt. Also, most of the previous work was performed in cold climates (Canada and Sweden) where improvement of the low temperature performance of polymer modified asphalt (PMA) was of great concern. For hot climates, such as Saudi Arabia, the high-temperature performance is important for modified asphalt binders. Limited number of publications used sulfur to modify asphalt with SBS polymer and the amount of sulfur was limited to 5-10% (Zhang, et al., 2011; Zhang, et al., 2010). The function of sulfur in asphalt paving mixture depends on the sulfur concentration and the sulfur-asphalt ratio. At low sulfur content, where sulfur/asphalt ratio is less than 0.2, sulfur modifies the chemical and rheological properties of asphalt through chemical reactions. At high sulfur/asphalt ratio (> l), sulfur acts as filler and "structuring agent", improving the workability of the sulfur-asphalt aggregate mixture at processing temperatures (130°-160°C) and the mechanical strength of the mixture at service temperatures (Lee, 1975).

Meanwhile, the rate of production of elemental sulfur is increasing due to increased oil and gas production. For example, Saudi Aramco produces approximately 6,000 tons/day of elemental sulfur. The rate of production is expected to increase to 10,000 tons/day in a few years. Although sulfur is a vital raw material to manufacture a myriad of products, its abundance has reduced its price worldwide. Meanwhile, the

storage of sulfur poses an environmental hazard and usages of this abundant sulfur in a useful, economical, and environmentally-friendly way are needed. Sulfur asphalt concrete is one such uses.

The early study on the use of sulfur in asphalt mixes showed better properties than the conventional asphalt mixes (Benzowitz & Boe, 1938). But due to high prices of sulfur, the product sulfur asphalt was uneconomical. In view of the increase in asphalt price since the beginning of the 1970s, the product was studied again by the US Bureau of Mines and Federal Highways. However, significant problems with storing hot sulfur at asphalt mix plants as well as pre-blending the sulfur with the bitumen were encountered. In many oil and gas producing countries, such as the Arabian Gulf countries, there is high production of elemental sulfur from processing plants. Therefore, and for several reasons, there is a renewed interest to seek new and efficient utilization of sulfur. First, sulfur is a valuable natural resource. Second, the income realized from the beneficial use of sulfur can help offset the cost of pollution control and ease a potential disposal problem. Finally, the stockpiling of sulfur in built-up areas without concurrent utilization could create additional pollution problems. Of the several potential uses for sulfur, a sulfur/asphalt combination for highway pavements seems to have the greatest potential for increasing the beneficial consumption of this element. This sulfur asphalt pavement material could utilize much of the elemental sulfur which will be recovered from fossil fuels.

On the other hand, waste tires discarded every year reach 10 million worldwide (Qingxi, 2010). Discarding waste rubber is a huge waste of energy and causes environmental problems because the waste rubber will not degrade. Using waste crumb rubber as dispersant in asphalt is a smart way to solve the waste disposal problem caused by waste tires and to improve the quality of road pavements, such as extending road service life. Waste crumb rubber used in pavement not only can help to solve the waste tire problem, but also can save petroleum resources. The previous use of crumb rubber was limited to modify base asphalt. Some US Patent (Liang, 1998; Syvester, 2006; Benko, 2002; Bernard, 1999) where crumb rubber was used to make bituminous pavement, but none of them used sulfur in their embodiments.

The objective of this study is to maximize the utilization of two wastes namely sulfur and crumb rubber in asphalt modification. Here, we used sulfur in the range 20-50% to produce sulfur asphalt binder while rubber was used at 1-6%. Sulfur asphalt with such high amounts of sulfur is brittle. Therefore, it was proposed to add rubber to sulfur asphalt to improve its rheological properties. No previous work was done to examine the effect of crumb rubber on the rheological properties of sulfur asphalt binder. In this paper, we will try to explore the use of crumb rubber to improve sulfur asphalt binder performance and possible correlation between crumb rubber content and rheological properties of sulfur asphalt binder at medium and high temperatures of application.

4.1.3 Experimental

Materials

Crumb rubber was collected from a local supplier. The source of the used rubber was waste car tires. Rubber was ground to fine powder to increase the surface area. The crumb rubber gradation was determined using ASTM D5644 procedure. The maximum size of the crumb rubber fines is 1 mm. Figure 4.1.1 represents the sieving results of the crumb rubber fines. Elemental sulfur (99.9% purity) was collected from Saudi Aramco. It is a waste product from oil and gas processing plants. Asphalt cement was obtained from a local refinery. The results of the differential scanning calorimetry (DSC) of these samples are presented in Figure 4.1.2.

Sample Preparation

Sulfur and pure asphalt were blended in a high shear blender. The elemental sulfur pellets were ground to fine powder before feeding to the blender. The blender acts as a batch stirred tank with a constant temperature bath. Typical mixing procedure was as follows: steel cans of approximately 1000 mL were filled with 250–260 g of asphalt and put in a thermoelectric heater. Crumb rubber was mixed with base asphalt at a temperature of 180^{o}C in the blender for 2 minutes. The can with the sample was sealed from the top to prevent extra air oxidation. The sealed can was then put in an oven of the same temperature for 2 hours for swelling of rubber in asphalt. After 2 hours of conditioning, the can with the sample was dipped into oil bath having a

temperature controlled at 145 ± 1°C. When the temperature of the rubber mixed asphalt reached 145°C, a high shear mixer was dipped into the can and set to about 2500 rpm. Calculated amount of elemental sulfur powder was added gradually with asphalt/rubber. The bath temperature was maintained at 145 ± 1°C. Samples were blended for 20 minutes at high shear to confirm uniform distribution of sulfur and rubber in the asphalt matrix. Asphalt samples were poured into rubberized molds before being used for rheological testing. The samples specimens were stored in a refrigerator at 5°C. Twenty samples of sulfur modified asphalt binders and pure asphalt binder were prepared and tested. Detailed samples information is presented in Table 4.1.1.

DSC measurements

The thermal behaviors of the pure and modified asphalt binder as well as the compositions of the asphalt binder were determined by means of a TA Q1000 DSC. Samples of 7-10 mg were weighed and sealed in aluminum pans. Melting temperature measurements were performed by heating samples from room temperature to 150^{o}C. A heating rate of 5^{o}C/min was applied and nitrogen was used as the purge gas at a flow rate of 50 ml/min.

Table 4.1. 1: Percentage compositions of sulfur modified asphalt binder

Sample #	Percentages of different components		
	Sulfur%	Asphalt%	Crumb rubber%
1	0	100	0
2	20	80	0
3	20	79	1
4	20	78	2
5	20	76	4
6	20	74	6
7	30	70	0
8	30	68	1
9	30	66	2
10	30	64	4
11	30	62	6
12	40	60	0
13	40	58	1
14	40	56	2
15	40	54	4
16	40	52	6
17	50	50	0
18	50	49	1
19	50	48	2
20	50	46	4
21	50	44	6

FTIR Characterization

Fourier transform infrared spectroscopy (FTIR) technique was used to determine the chemical bond changes of pure and modified asphalt binder. FTIR measurement was carried using a Nicolet 6700 spectrometer from Thermo Electron™. All the FTIR

spectra were taken in the absorbance mode and in the range 600–4000 cm^{-1} at room temperature. FTIR spectra were obtained using a spectral resolution of 4 cm^{-1} and 30 co-added scans.

Rolling thin film oven (RTFO) test

Rolling thin film oven test (RTFO) was used to perform ageing of asphalt binders according to ASTM D 2872 procedure. This test simulates the ageing process that takes place during the production and up to the first year of the service life of the pavement. The base asphalt as well as modified asphalt was poured into cylindrical bottles. 35 grams of asphalt sample was poured in each cylindrical bottle. Then the bottles were placed horizontally in a convection oven, which was rotated at 163^{o}C for 85 min. Air was supplied into the bottle to accelerate ageing. This process created a thin film of asphalt on the inside of the bottles. After completing the run, samples were collected for rheological testing in ARES.

Rheological tests

Dynamic and steady rheological tests were carried out to investigate the effect of polyethylene wax on the rheology of sulfur modified asphalt. The dynamic temperature step measurements for the samples were performed in ARES rheometer. This is a constant strain rheometer equipped with a heavy transducer (range 2-2000 g for normal force; 2-2000 g-cm for torque). All tests were carried out in the range 64°-85°C using a parallel plate set of diameter is 25 mm. With the sample in position, the oven was closed and the sample heated at 64^{o}C for about 5 minutes, thereafter the

gap between the plate platen was adjusted to 1.5 mm by lowering the upper platen force transducer assembly at a constant load of 500 g. The melt that extruded beyond the platen rim by this procedure was cleaned off. Strain in the linear viscoelastic range (strain amplitude, γ^o of 12.5 %) and frequency of 10 rad/s was used for all the tests. In all the experiments, nitrogen gas was continuously used for heating the samples during testing to avoid oxidation during testing. A holding period of 5 min was allowed before beginning measurements when the temperature reaches steady state. The Orchestrator software was used to calculate the dynamic shear viscosity, storage modulus, complex modulus and phase angle for all samples.

Dynamic frequency sweep tests were conducted at 50^{o}C and frequency ranges of 100-0.1 rad/s and the constant strain of 10%. Different linear viscoelastic variables were calculated using TA Orchestrator software. Dynamic temperature step frequency sweep test was performed to get the master curve for selected asphalt binders. Steady shear rheological tests were conducted at 50^{o}C and shear rate ranges of 0.01-10 s^{-1}.

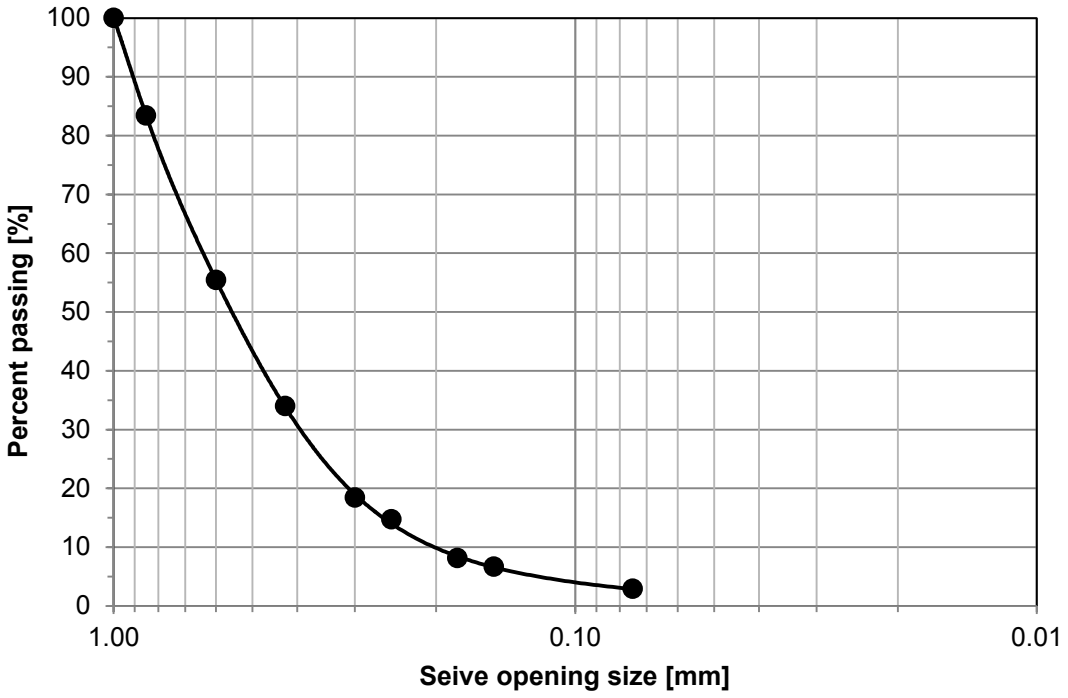

Figure 4.1. 1: Crumb rubber particles size distribution

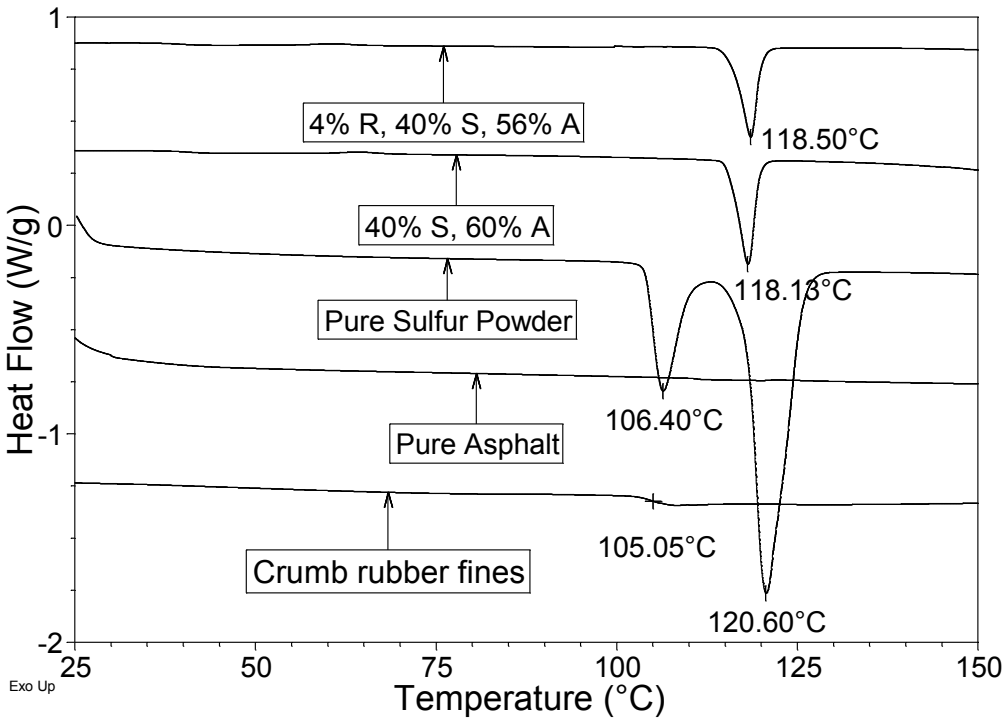

Figure 4.1. 2: DSC scans of the modified asphalt binder and its compositions

4.1.4 Results and Discussion

Thermal characterization

DSC results of the pure sulfur, crumb rubber, pure asphalt and two sulfur modified asphalt binder are shown in Figure 4.1.2. There is no peak in the DSC thermogram of pure asphalt. So, the asphalt used in this study is pure virgin asphalt. Crumb rubber has no melting point; rather it has a glass transition at ~105.5^{o}C. The DSC scan of pure elemental sulfur shows that it has two melting peaks in the range of temperature studied. The first melting peak is at 106.40^{o}C which corresponds to rhombic sulfur. The second peak is at 120.6^{o}C and it corresponds to monoclinic form of sulfur. The literature values are also in the same range (Zupancic & Zumer, 2002). The modified

asphalt binder has three different constituents namely: crumb rubber, sulfur and asphalt with different weight percentages. One interesting observation in the DSC scan of sulfur modified asphalt binder is that it has only one melting point which is around 118^{o}C. It ensures that rhombic sulfur has been converted to monoclinic sulfur in the modification process. DSC scan of 40/60 sulfur/asphalt shows that it has a melting point at 118.13^{o}C which is very close to the melting point of monoclinic sulfur. So, the blending process of sulfur with asphalt has shifted the melting point to the left side. The modified asphalt binder with 40% sulfur, 52% asphalt and 4% rubber has a melting point of ~ 118.5^{o}C. So, rubber modification has increased the melting slightly in comparison to the 40/60 sulfur/asphalt binder. The blending temperature used in the study is 145^{o}C.

FTIR results of asphalt binders

Figure 3 represents the FTIR spectra of pure asphalt binder and Table 4.1.2 listed the main bonds present in asphalt. Similar results were also mentioned in literature (Larsen, et al., 2009) . The bonding of sulfur modified asphalt binders are also similar to the one presented in Figure 4.1.3 but with different intensities.

Figure 4.1.4 represents the FTIR spectra for pure and 30% sulfur modified asphalt binders. The main differences between pure and sulfur modified asphalt binders are in the range 600-1250 cm^{-1}. The FTIR spectra of other sulfur modified binders are also similar to that presented in figure 4. It is noticed that the intensities of the bonds

has changed in modified binders. The relative change of bonding is calculated using the following equations:

$$I_{S=O} = \frac{\text{Area of the sulfoxide band centered around 1030 cm}^{-1}\text{for modifed binder}}{\text{Area of the sulfoxide band centered around 1030 cm}^{-1}\text{for pure asphalt}} \quad (4.1.1)$$

$$I_{C\text{-}S} = \frac{\text{Area of the C-S band centered around 720 cm}^{-1}\text{for modified asphalt}}{\text{Area of the C-S band centered around 720 cm}^{-1}\text{for pure asphalt}} \quad (4.1.2)$$

Based on the above equations the ratios of the areas are calculated and the results are shown in Figure 4.1.5. The relative intensities of the C-S and S=O bonds increases in comparison with pure asphalt binders. This confirms the chemical cross-linking in modified asphalt binders. It was also mentioned in the literature that part of the sulfur added reacts chemically with asphalt to form carbon-sulfur bond and polysulfide bond (Kennepohl & Miller, 1978). Figure 5 shows that the intensity of C-S in asphalt has increased by ~30% in 30/70 sulfur/asphalt binder. Further increase in crumb rubber concentration had little influence on the intensity of C-S bond. However, the intensity of S=O bond increases significantly with the addition of crumb rubber. So, it can be concluded that the increase in C-S bond is due to addition of sulfur to asphalt whereas the increase in S=O bond resulted from crumb rubber addition. Sulfur is expected to cross-link with unsaturated non-ring compounds in asphalt.

Table 4.1. 2: Assignations of the main bands of the FTIR spectra

Webnumbers [cm^{-1}]	Assigned bands
2920, 2850	υC-H aliphatic
1636	υC=C aromatic
1456	δC-H of $–(CH_2)_n$- (aliphatic index)
1376	δC-H of CH_3 (aliphatic branched)
1031	υS=O sulfoxide
808, 864	υC=C of alkenes
721	δC-H or δC-S

Note: υ = Stretching, and δ = Bending

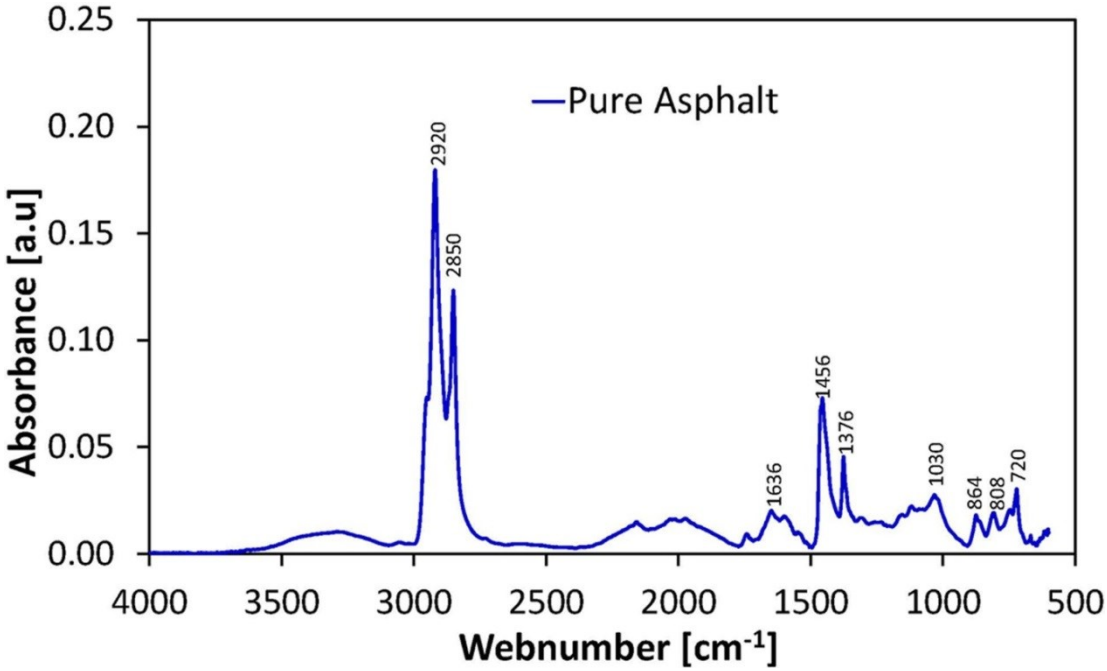

Figure 4.1. 3: FTIR spectra of pure asphalt binder

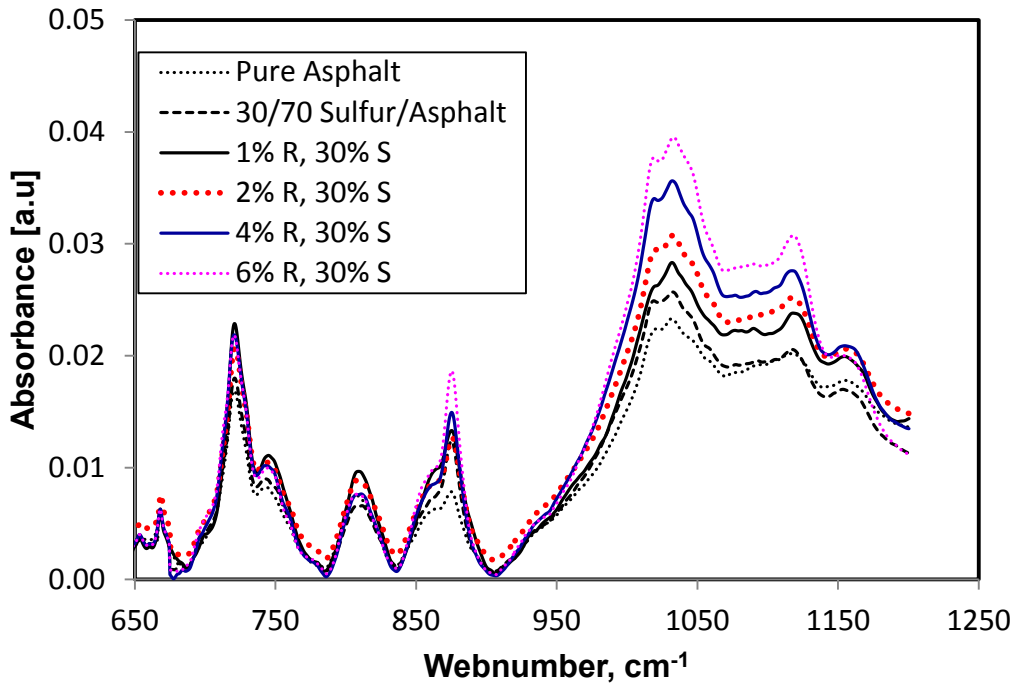

Figure 4.1. 4: FTIR spectra of pure and modified asphalt binders

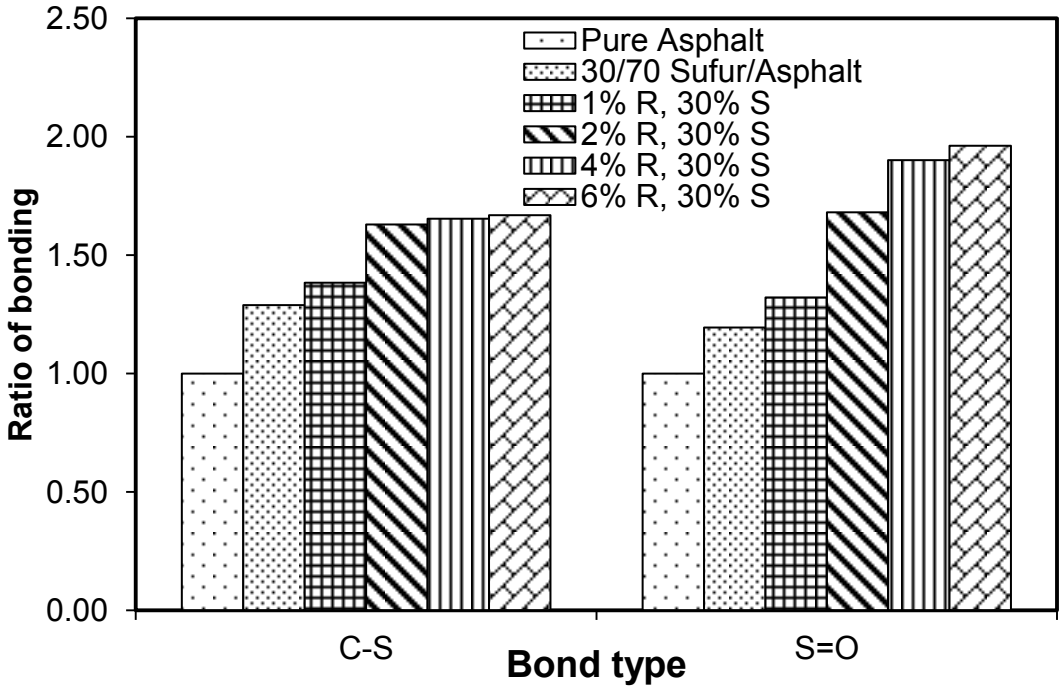

Figure 4.1. 5: The intensity of bonding in pure and modified asphalt binders

Rheological Characterization

Dynamic frequency sweep test

Dynamic frequency sweep test for all the binders were conducted at 50^{o}C and 100-0.1 rad/s at small deformation (10% strain) in the linear viscoelastic range. Typical linear viscoelastic properties of sulfur modified asphalt binders with various amounts of crumb rubber and sulfur are displayed in Figure 4.1.6 to 4.6.7. Figures 4.1.6 and 4.1.7 show the dynamic storage modulus, G′, as function of frequency, ω, for 30% and 50% sulfur modified asphalt binders. The results are shown for 0%, 1%, 2%, 4% and 6% crumb rubber by weight. The results for 20% and 40% sulfur modified binders are not shown here as the trends are very similar to the presented figures.

Sulfur modified asphalt binders have improved, G' as compared to the base asphalt for the whole ω range. The increases in G' values are higher for higher concentration of crumb rubber. The storage modulus, G', is highly sensitive to the morphological state of a heterogeneous system (Cho et al., 2009). The value of G' is an indication of how much elasticity can be boosted by asphalt modification. The relative increment in G' can be well understood by the modification index as defined by the following equation:

$$I_{G'} = \frac{G' \text{of crumb rubber modifed binder}}{G' \text{of sulfur asphalt binder}} \tag{4.1.3}$$

Here, the definition of $I_{G'}$ is applicable for the binders that contain sulfur as well as crumb rubber. For example, $I_{G'}$ for 30% sulfur modified binders is the ratio of G' of rubber modified binders to the G' of 30/70 sulfur/asphalt binder. So, the significance of this index is to calculate the relative influence of replacing the portion of asphalt by the same amount of crumb rubber. $I_{G'}$ values are calculated for ω=1 rad/s at 50°C and shown in Table 4.1.3 for different binders.

Table 4.1.3 shows that $I_{G'}$ values increase with respect to both sulfur and crumb rubber concentration. According to time temperature superposition principle low frequency data corresponds to high temperature properties. So, High values of G′ at lower frequency provide more flexibility of asphalt binder at higher temperature.

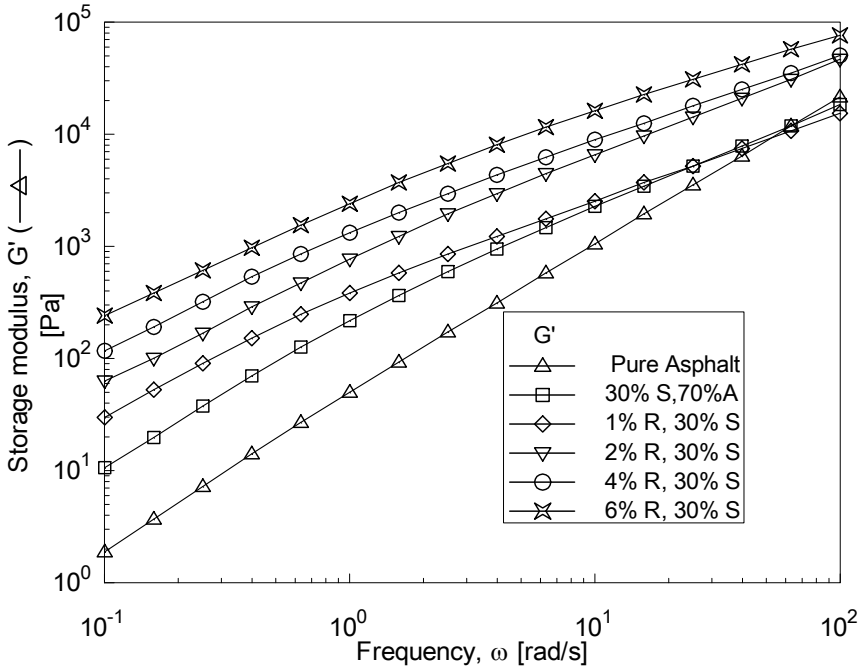

Figure 4.1. 6: *G′(ω)* for 30% sulfur modified asphalt binders at 50°C

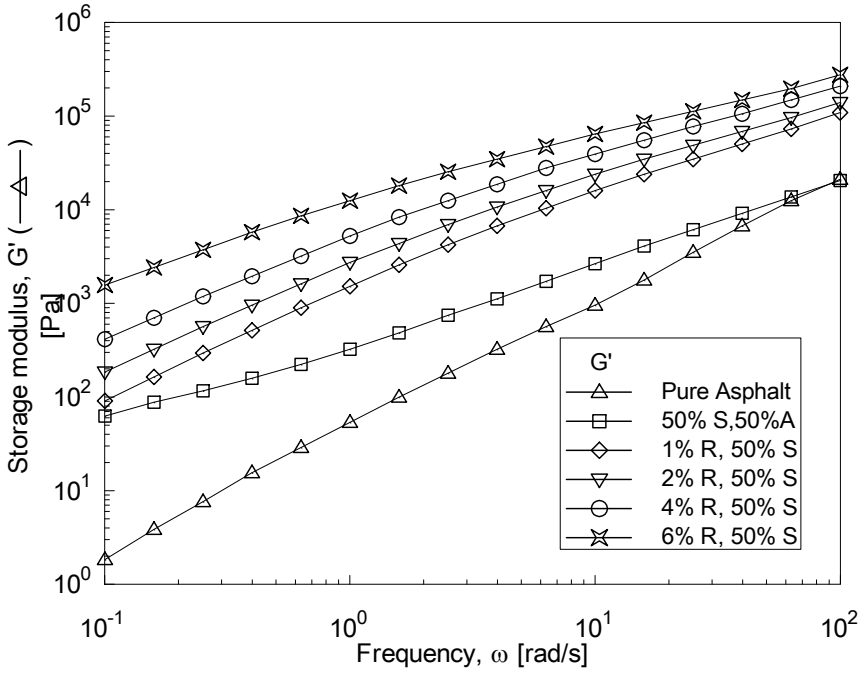

Figure 4.1. 7: *G′(ω)* for 50% sulfur modified asphalt binders at 50°C

Table 4.1. 3: Modification indexes for crumb rubber modified sulfur asphalt binders

Crumb Rubber content [%]	$I_{G'}$ for 20% Sulfur	$I_{G'}$ for 30% Sulfur	$I_{G'}$ for 40% Sulfur	$I_{G'}$ for 50% Sulfur
1	2.17	1.67	2.04	2.92
2	2.53	2.05	3.30	5.14
4	3.09	3.07	6.31	10.31
6	4.57	5.34	8.93	23.61

Further analysis of the frequency sweep data were carried out to check the relationship of viscoelastic variable, G′, with crumb rubber and sulfur concentration. Figure 4.1.8 shows the variation of G′ with crumb rubber concentration. The data are well fitted to the equation given below:

$$G' = aC_R + bC_S \tag{4.1.4}$$

where, C_R and C_S are the percentage of crumb rubber and sulfur in the asphalt matrix. Table 4.1.4 listed two parameters (a, b) and fit quality R^2. It shows that storage modulus, G′ increases linearly with crumb rubber for all sulfur/asphalt binders. Adjusted constant *a* increases with sulfur content whereas *b* decreases with sulfur content. The straight line slope increases with the increase in sulfur content suggesting that the amount of sulfur also contributes to the increase in G′. Another observation from the linear viscoelastic results is that the increment of G′ at high ω is lower than that at low ω. The high ω corresponds to low temperature behavior of asphalt binders. So, comparatively lower values of G′ at high frequency are favorable for asphalt pavement.

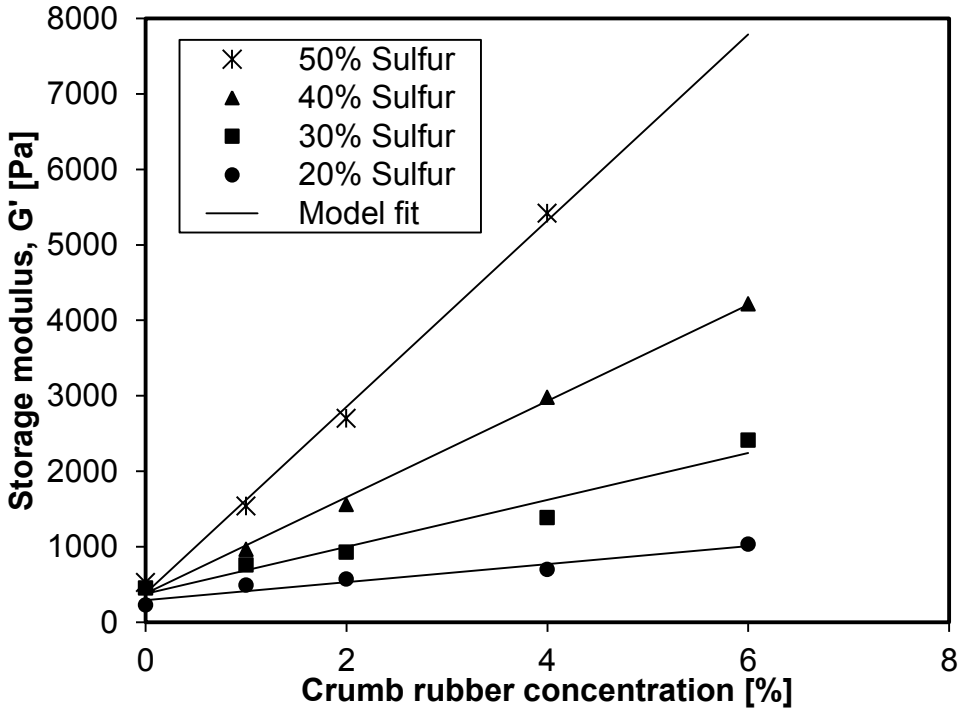

Figure 4.1. 8: G′ as function of sulfur and crumb rubber concentration (ω=1 rad/s at 50^{o}C)

Table 4.1. 4: Model parameters for equation (4.1.4)

Sulfur content [%]	Model parameters		
	a	b	R^2
20	119.60	14.65	0.948
30	310.47	12.62	0.958
40	637.80	9.49	0.998
50	1233.40	7.72	0.996

Figures 4.1.9 and 4.1.10 represent the well-known Black diagram (phase angle versus G*) representation for 30% and 50% sulfur binders at 50^{o}C. The reduction of phase angle is related to the presence of elastic networks or entanglements in the modified binder (Airey, 2003). It is noticed that incorporation of crumb rubber in sulfur/asphalt binder decreases the phase angle which means improvement in elastic behavior. This improvement can be due to the degree of crosslinking and entanglement produced by the additives crumb rubber and sulfur with asphalt matrix. The combined effect of shear and heat in the blender could result in several phenomena in the modified asphalt matrix. Some of them can be as: (1) Polymerization of sulfur to form longer chain, (2) Increase in crumb rubber particle size due to swelling effect in the asphalt matrix, (3) Change in compositions of asphalt by thermal and mechanical degradation (Miguel Rodrıguez, et al., 2006). The combination of these phenomena can lead to crosslinking/entanglement and enhance the viscoelastic properties of modified asphalt binders. The reaction and crosslinking of sulfur asphalt were discussed earlier in the FTIR section.

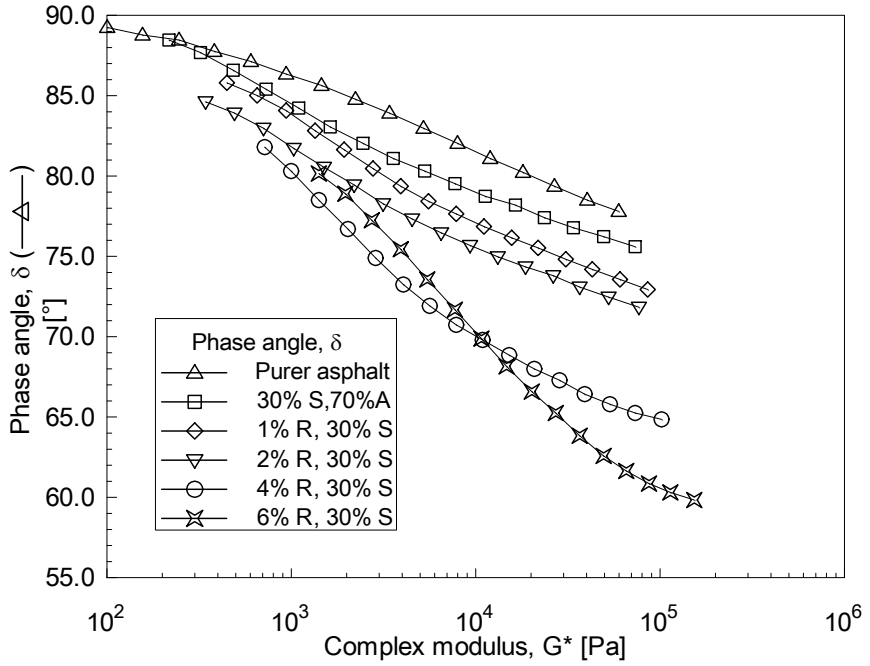

Figure 4.1. 9: Black diagram representation of 30% sulfur binders at 50°C

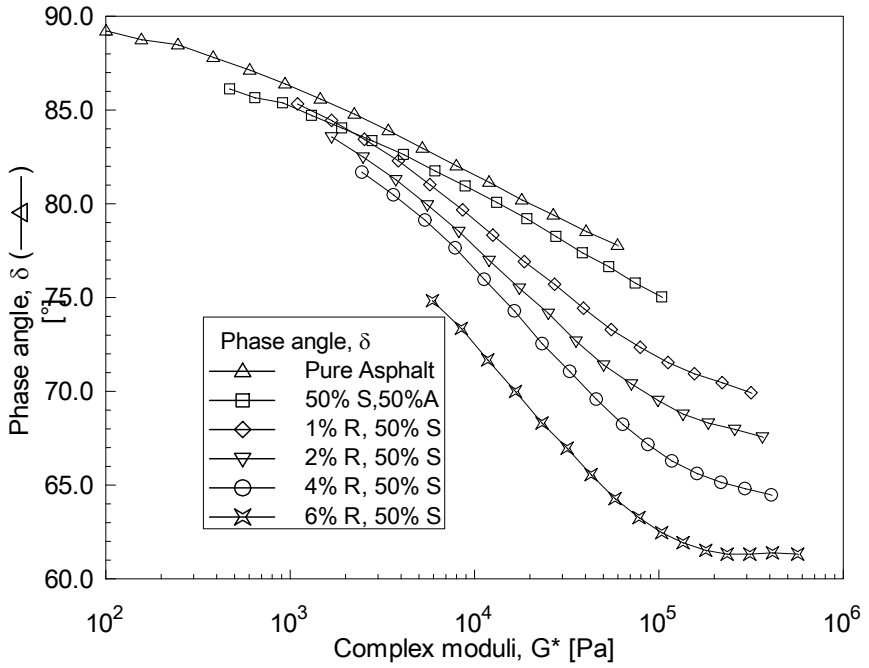

Figure 4.1. 10: Black diagram representation of 50% sulfur binders at 50°C.

Temperature sweep measurements

Temperature sweep test was conducted for all binders to extract the values of complex moduli, G^*, and phase angle, δ, as function of temperature. According to the strategic highway research program (SHRP), the stiffness parameter $G^*/\sin\delta$ is a factor used to estimate the rutting resistance of asphalt binder (The Asphalt Institute, 2003). It should be larger than 1 kPa at the maximum pavement design temperature for unaged original asphalt, when measured at 10 rad/s to simulate traffic loading. Higher values of $G^*/\sin\delta$ are expected to give a high resistance to permanent deformation. Figure 4.1.11 shows $G^*/\sin\delta$ versus temperature for all the sulfur modified asphalt binders as function of crumb content at 76^{o}C. This temperature was chosen on the basis that the maximum local pavement temperature for Saudi Arabia is 76^{o}C for hot summer season (Al-Abdul Wahhab, et al., 1997). It shows that sulfur modified asphalt binders without crumb rubber modification cannot fulfill SHRP criteria as the value of $G^*/\sin\delta$ is less than 1 for all the samples. So, there is a necessity of modification of these binders to increase $G^*/\sin\delta$ to improve rutting resistance. It is noticed that $G^*/\sin\delta$ values for the 20% sulfur modified asphalt are less than 1 for even when 6% crumb rubber was used. In the case of 30% sulfur modified binders, 4% crumb rubber is required to reach $G^*/\sin\delta \geq 1$, whereas for 40% and 50% sulfur modified binders, 1% crumb rubber is enough to reach $G^*/\sin\delta \geq 1$.

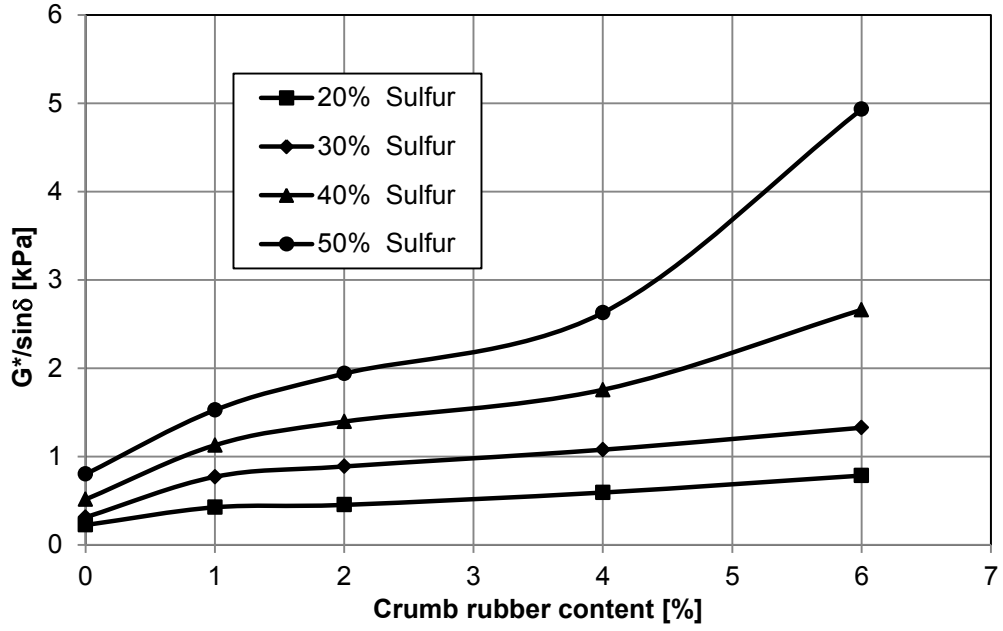

Figure 4.1. 11: G*/sinδ versus crumb rubber content for unaged modified binders at 76°C

Table 4.1. 5: Maximum temperature at which G*/sinδ is equal to 1 for sulfur modified binders

Crumb Rubber content [%]	Max. Temperature attained, °C @ $G^*/\sin\delta$=1 kPa			
	20% Sulfur	30% Sulfur	40% Sulfur	50% Sulfur
0	64	65	67	73
1	67	73	77	79
2	68	75	79	82
4	71	77	81.5	85
6	73.5	80	85	89

It is noticeable that addition of crumb rubber to sulfur/asphalt binders increases the maximum attainable temperature for all the binders. The value of $G^*/\sin\delta$ for pure asphalt is 1 at 68°C which means that pure asphalt needs modification for local pavement application. The maximum temperature of all the sulfur modified asphalt binders without crumb (zero crumb content) is less than 76°C. However, additions of crumb rubber to those binders improve it significantly. So, crumb rubber improved rutting resistance of sulfur modified asphalt. Another observation is that for the same percentage of rubber, increase in sulfur content increases the $G^*/\sin\delta$ [see Fig. 4.1.11], which leads to stiff binders. Addition of crumb rubber is expected to add toughness to the binders and make the binders flexible.

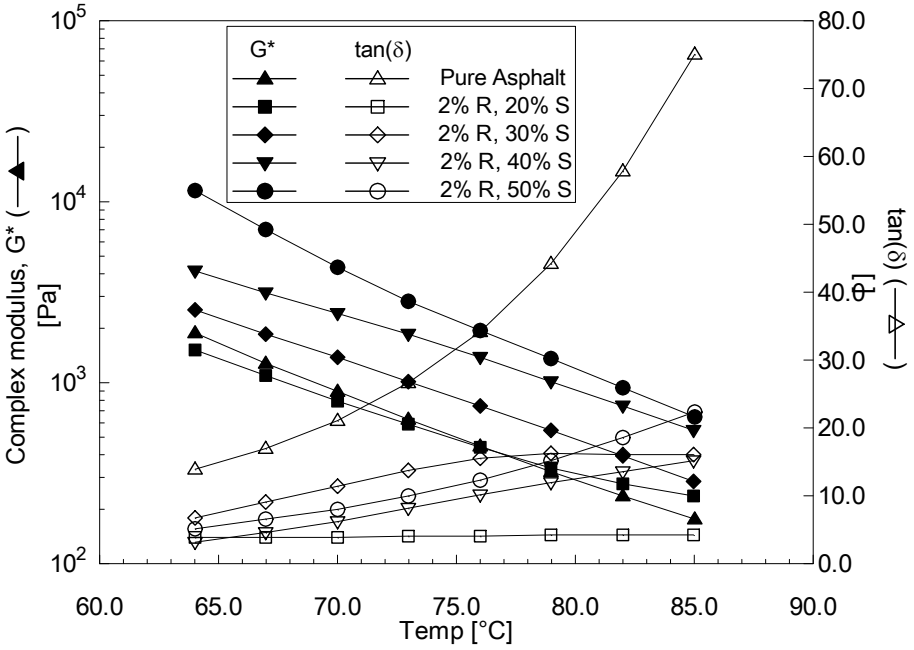

Figure 4.1. 12: Complex moduli and tanδ versus temperature for selected binders

The effect of temperature on pure and modified asphalt binders is shown in Figure 4.1.12. It shows that with increasing temperature *tanδ* increases and complex modulus, *G** decrease for pure asphalt binder. The varying trend of *tanδ* and *G** slowed down for the sulfur modified asphalt binders. A similar phenomenon has been reported in an early publication (Lu & Isacsson, 1997) for polymer modified asphalt binder. The addition of sulfur led to the increase in *G** more significantly at elevated temperatures, and *tanδ* curve became flatter over a wide range of tested temperatures. It indicates that the elasticity of the modified binder had been improved effectively with the addition of sulfur due to the formation of a chemically cross-linked network in the modified binders as described in the FTIR results.

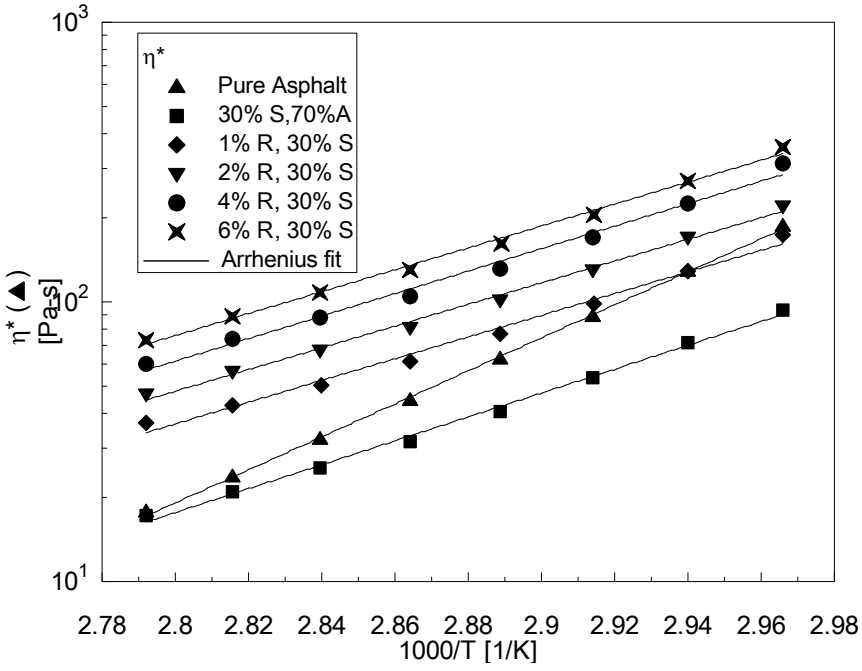

Figure 4.1. 13: Effect of temperature on complex viscosity (30% sulfur modified binders)

Temperature sweep data was further analyzed to check the effect of temperature on asphalt viscosity. Viscosity-temperature relationships of asphalt binder can be expressed by the well-known Arrhenius equation as follow:

$$\frac{G^*}{\omega} = \eta^* = Ae^{\left(E_a/RT\right)} \tag{4.1.5}$$

where E_a is the flow activation energy, A is the pre-exponential term, and R is the universal gas constant. E_a is an important factor that strongly influences the viscosity. Figure 4.1.13 shows complex viscosity versus 1/T for the 30% sulfur modified asphalt binders. As the trend is very similar for other binders, only one Figure is shown here. The data given in Figure 4.1.13 showed good fit to Arrhenius model. E_a was calculated using equation (5) and the values for different binders are given in Table 6. Activation energy for pure asphalt was tabulated to be 113.07 kJ/mol.

It is observed that addition of sulfur to asphalt reduces the activation energy of sulfur/asphalt binder as compared to pure asphalt. The crumb rubber modified asphalt binders showed lower activation energy than pure asphalt except for the 50% sulfur modified binders. Activation energy, E_a is related to the binder thermal susceptibility (García-Morales, et al., 2004). The lower activation energy of asphalt binders means lower temperature susceptibility. So, from Table 4.1.5 it can be concluded that the 20%, 30% and 40% sulfur modified asphalt binders would be less temperature susceptible than pure asphalt. However, the 50% sulfur modified asphalt binder showed higher E_a, consequently the binders will be more temperature susceptible.

Table 4.1. 6: Activation energy of crumb rubber modified sulfur/asphalt binders

Crumb Rubber content [%]	E_a for 20% sulfur modified binders, kJ/mol	E_a for 30% sulfur modified binders, kJ/mol	E_a for 40% sulfur modified binders, kJ/mol	E_a for 50% sulfur modified binders, kJ/mol	E_a for Pure Asphalt, kJ/mol
0	99.98	81.90	72.89	93.79	113.07
1	86.21	74.31	85.84	133.71	
2	91.10	76.09	95.90	135.95	
4	97.64	77.03	99.64	133.94	
6	99.34	77.91	103.22	130.85	

Rheological data of sulfur modified asphalt binders can be now quantitatively appreciated by introducing a modification index I_M (Airy, 2011). A simple modification index can be obtained from temperature sweep data using the following equation:

$$I_M = \frac{G_R^{'}}{G_S^{'}} \tag{4.1.6}$$

where $G_S^{'}$ is the storage modulus of sulfur modified asphalt binder with zero rubber content and $G_R^{'}$ is the storage modulus of the corresponding sulfur/asphalt binders with rubber content 1%-6% for ω = 1 rad/s. Equation (4.1.6) above shows the effect of rubber modification on sulfur/asphalt binders. The modification index was calculated from temperature sweep test.

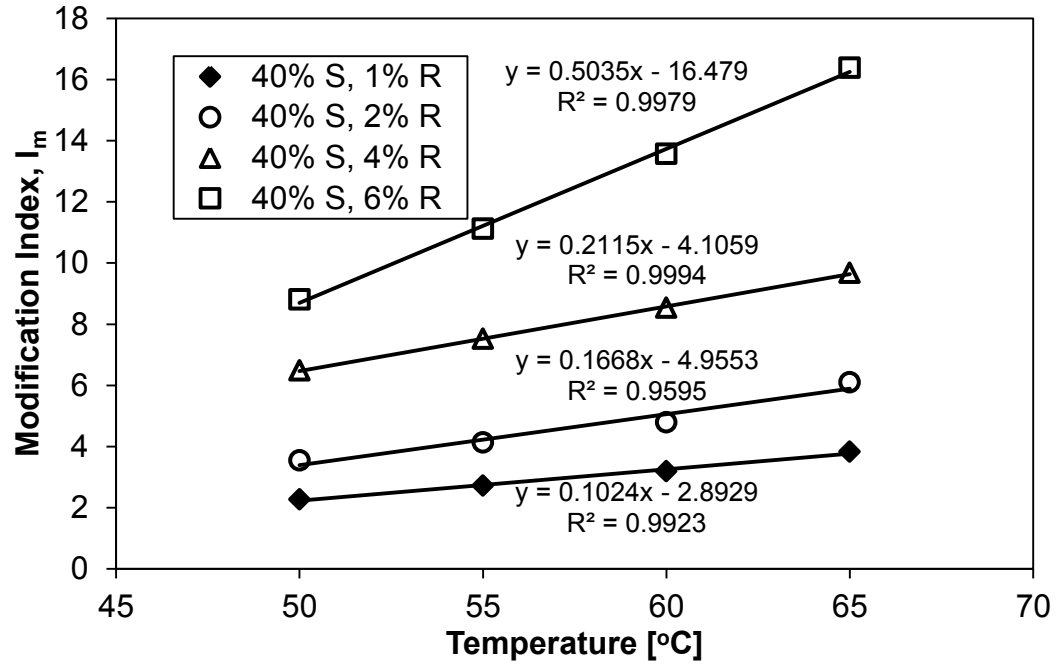

Figure 4.1. 14: Modification index for 40% sulfur modified binders for 1%-6% rubber content

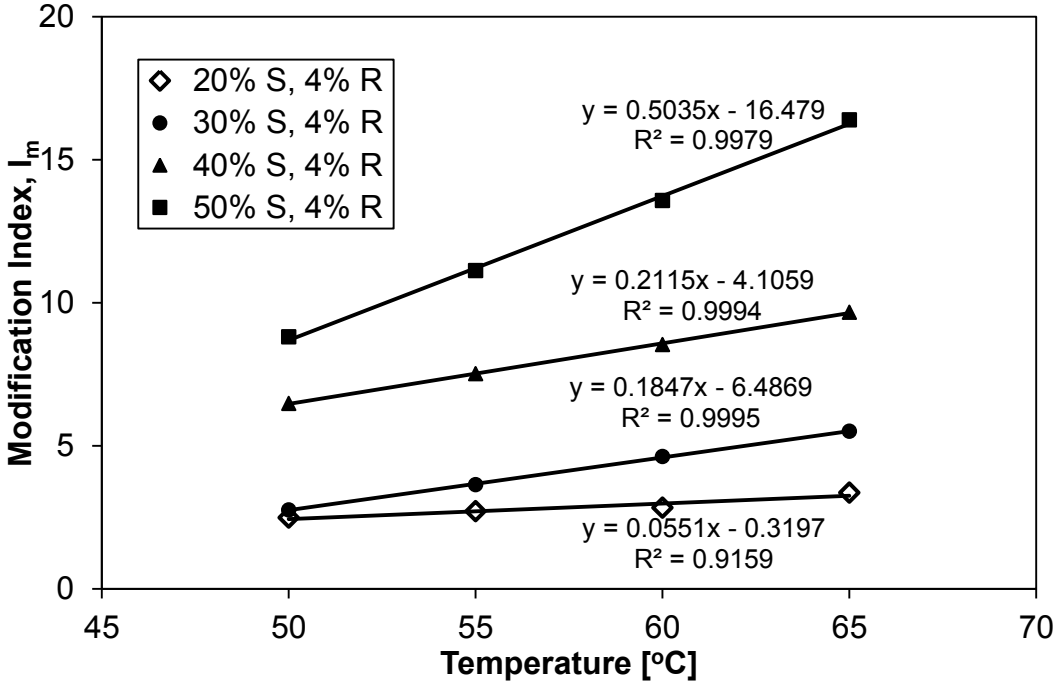

Figure 4.1. 15: Modification index for 4% crumb rubber content for 20%-50% sulfur binders

Figures 4.1.14 and 4.1.15 depicted that the viscoelastic properties of rubber modified sulfur asphalt binder increases with respect temperature as the crumb rubber content increases. The effect is minimum for the case of 20% sulfur binders and significant for other binders (30%-50% sulfur). Figure 4.1.14 shows the effect of crumb rubber content whereas Figure 4.1.15 shows the effect of sulfur content. Both of the additives have positive effect on the modification index. The slope of the straight line increase as the amount of additives increases. It is also interesting to observe that the variation of the modification index within a certain temperature interval is controlled by the material sensitivity to temperature variation. In this way, the slope of the I_M values is an indirect indicator of the thermal sensitivity and can be used to describe the influence of temperature on the rheological properties. However, higher I_M values also indicate that the corresponding sample will be stiff at lower temperature and can crack easily at low pavement temperature. So, there should be an optimum amount of the additives (sulfur and crumb rubber) to be used to suite for both high and low temperature range application. The improvement of the elastic properties with temperature can be due to the crosslinking of sulfur with asphalt. The reason for the increase in the elastic properties with temperature is due to the swelling of crumb rubber and filling of the free volume in asphalt created by thermal expansion.

The dynamic shear data analysis showed that addition of sulfur to asphalt matrix increases the viscoelastic properties (G' and G'') of the modified binder. The addition of crumb rubber to sulfur asphalt enhanced the temperature resistance of the binder.

Steady shear rheology

Steady rate sweep tests were conducted for all binders at 50^{o}C and shear rate of 0.01-10 s^{-1}. Steady shear viscosity as function of shear rate is plotted in Figure 4.1.16 for 40% sulfur modified binders. As the behaviors of the other binders are also very similar, only one Figure is provided to show the general trend. Pure asphalt samples displayed long Newtonian plateau up to a shear rate of ~ $2s^{-1}$. The crumb rubber modified binders showed very small width of Newtonian plateau followed by shear thinning behavior at high shear rate. Similar behavior was also reported for polymer modified asphalt binders (Polacco, et al., 2006). These types of shear viscosity data can be well modeled by Carreau model which is given by the following equation:

$$\eta = \frac{\eta_0}{\left[1+\left(\frac{\dot{\gamma}}{\dot{\gamma}_c}\right)^{a}\right]^{\frac{n-1}{a}}} \qquad (4.1.7)$$

where, η_0 is the zero shear viscosity, $\dot{\gamma}_c$ is the critical shear rate at the onset of shear thinning region and *a* is a parameter related to the slope of shear thinning region. The shear rate viscosity data were well fitted by the model as can be seen from the Figure 4.1.16. Crumb rubbers decrease the Newtonian plateau and broaden the shear thinning region. This shear thinning behavior can be attributed to the crosslinking of sulfur and asphalt molecules as well as the heterogeneity in molecular weight caused by the addition of rubber. As shear rate increases it destroys the crosslinking and thereby reduces viscosity sharply.

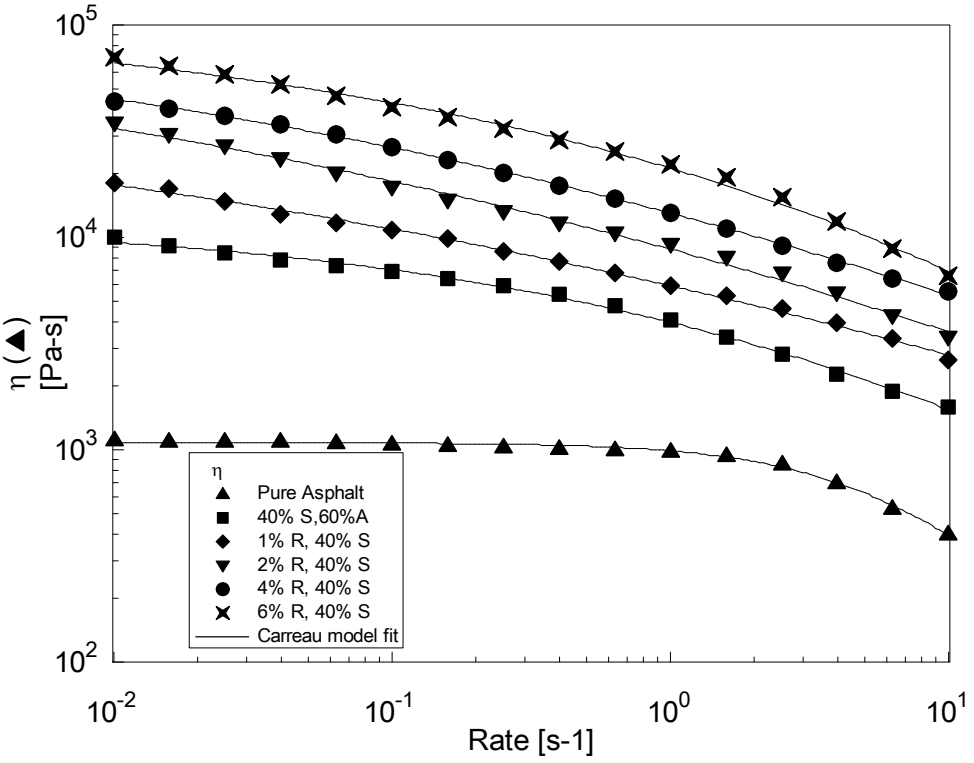

Figure 4.1. 16: Steady shear viscosity of 40% sulfur/asphalt binders at 50°C

In the last decade, researchers have observed that the SHRP rutting parameter $G^*/\sin\delta$ is not very effective in predicting the rutting performance of binders, especially in case of modified binders are (Shenoy, 2002; Bahia, et al., 1999). For such case a new parameter zero shear viscosity, η_o has been suggested by many researchers as a possible measure for the rutting resistance of modified asphalt binders (Binard, et al., 2004; Phillips & Robertus, 1996). η_o and ; were calculated for all binders using the equation (4.1.7) and the values are shown in Table 4.1.7. It is observed that η_o increases with the increase in sulfur and crumb rubber content which

supports the previous results from dynamic shear rheology. The increment in η_o is more pronounced in binders with high sulfur content (40% and 50%). The onset of shear thinning (;) decreases with the increase in sulfur and crumb in the binders.

The steady shear data analysis showed that both sulfur and crumb rubber modification added non-Newtonian behavior to modified asphalt binder. Also, the increase in η_o for rubber modified sulfur asphalts suggests improved rutting resistance. So, the steady shear data analysis supports our previous findings through dynamic shear measurements.

Table 4.1. 7: Carreau model parameters for crumb rubber modified sulfur/asphalt binders at 50°C

Crumb Rubber content [%]	η_o [Pa-s]				$\dot{\gamma}_c$ [s^{-1}]			
	20%	30%	40%	50% S	20%	30%	40%	50%
0	2672	7324	12053	22054	2.512	2.100	1.527	1.262
1	3548	7679	18526	33489	0.441	0.020	0.015	0.012
2	4455	8551	25640	45685	0.067	0.010	0.007	0.006
4	5354	14236	52497	78452	0.033	0.007	0.005	0.004
6	6129	36600	95175	202411	0.022	0.006	0.004	0.003

Rolling thin film oven (RTFO) test

Figures 4.1.17 and 4.1.18 show the effect of short term ageing on selective crumb rubber modified sulfur/asphalt binders. It is clear that ageing increases SHRP rutting parameter $G^*/\sin\delta$ as well as complex viscosity, η^* for the whole temperature range covered in this study. Table 8 listed the values of $G^*/\sin\delta$ at 76^{o}C and activation energy E_a extracted from Figures 14a and 14b. According to SHRP the values of G*/sinδ should be ≥1kPa before RTFO and ≥2.2 kPa after RTFO. So, all the binders (see Table 4.1.8) meet short term ageing criteria for Superpave binder's requirement. It is also observed that ageing increases the activation energy of the selected binders. The increase in activation energies for the selected RTFO samples was in the range 6-25% than those of unaged samples.

The improvement in rheological properties after ageing can be attributed to three major factors. Firstly, ageing has changed chemical compositions of asphalt. A modification of both the quantity and quality of asphaltenes and resins is likely to occur. The increase in asphaltenes and resins contents is a consequence of the effect that ageing has on the elastic properties of asphalt. Secondly, polymerization of sulfur and its crosslink with asphalt composition which is accelerated by high temperature (163^{o}C) and air oxidation. Also, crosslinking and entanglement of crumb rubber with asphalt and sulfur could happen through ageing.

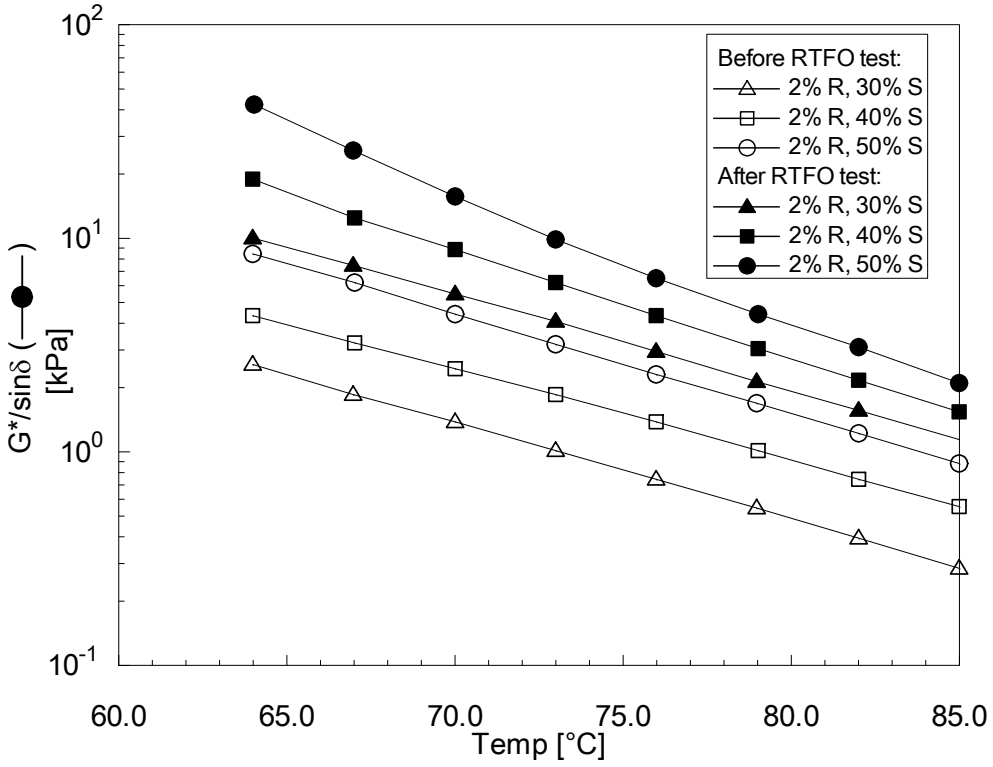

Figure 4.1. 17: Effect ageing on G*/sinδ for selective modified binders

Table 4.1. 8: Effect of short term ageing on the selective binders

Sample	G*/sinδ [kPa] @ T = 76°C		E_a [kJ/mol]	
	Before RTFO	After RTFO	Before RTFO	After RTFO
30% S, 2%	0.75	2.96	76.09	97.25
40% S, 2%	1.38	4.32	95.90	118.23
50% S, 2%	2.30	6.53	135.95	144.55

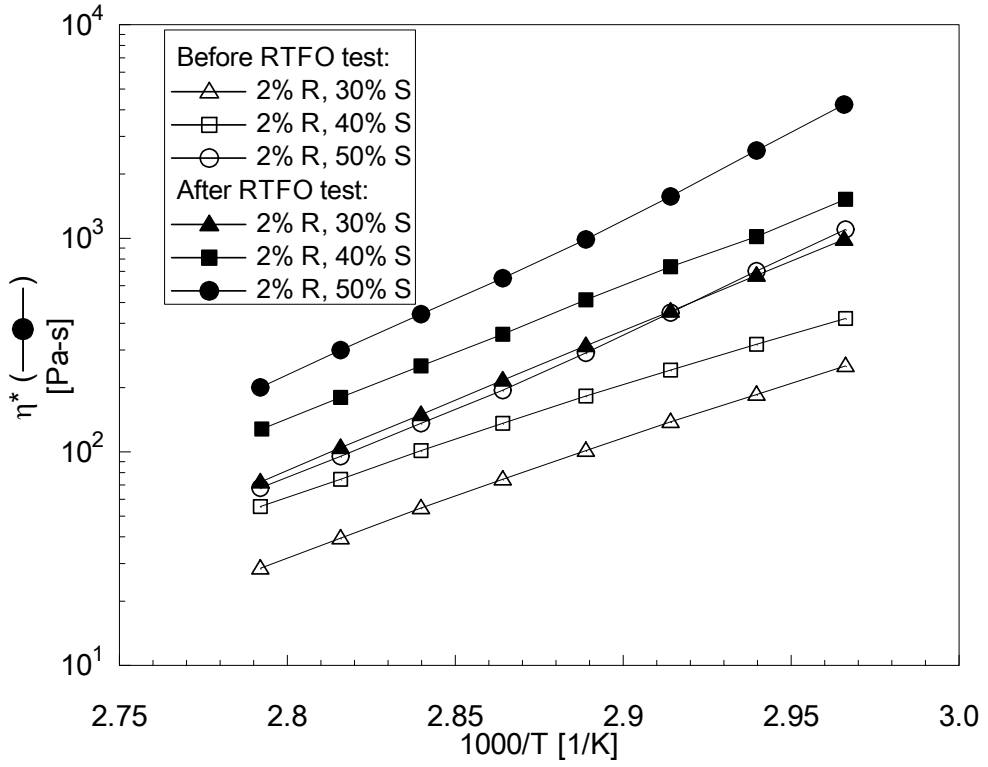

Figure 4.1. 18: Effect of ageing on complex viscosity, η^* for selective modified binders

4.1.5 Conclusion

Utilization of waste sulfur and rubber in asphalt modification was investigated. The influence of crumb rubber on the rheology of sulfur modified asphalt binders were investigated by FTIR, rheological and thermal characterization techniques. The following conclusions are drawn on the basis of this investigation:

1. FTIR results showed increase in C-S bond due to sulfur incorporation and S=O bond increased due to crumb rubber addition to sulfur asphalt binder.

2. The addition of crumb rubber has significantly increased the viscoelastic properties of the sulfur modified asphalt binders. The linear relationship was obtained for the low frequency (ω = 1 rad/s) dynamic shear data. It was shown that crumb rubber increases both viscous and elastic properties linearly. This improvement was higher for higher concentration of sulfur and crumb rubber.
3. SHRP rutting parameter ($G^*/\sin\delta$) as well as zero shear viscosity increases with increase in crumb rubber percentages for all sulfur extended asphalt binders, which suggests that crumb rubber modification increases rutting resistant at high temperature.
4. A modification index (I_M) was defined to quantify the improvement of viscoelastic properties of crumb rubber modified sulfur extended asphalt binders. It was shown that crumb rubber improved the high temperature viscoelastic properties.
5. Steady shear rheology indicated that crumb modification of sulfur extended asphalt binders increases the steady shear viscosity. Addition of crumb rubber to sulfur extended asphalt decreases the Newtonian plateau and increases the shear thinning behavior.
6. Short term ageing through RTFO improved the rheological properties of the modified binders by crosslinking and entanglement of sulfur and crumb rubber asphalt compositions.

The crumb rubber modified sulfur asphalt showed better properties compared to the conventional asphalt binder. Utilization of these two industrial wastes in asphalt modification can meet the extra demand for asphalt, reduce the price and improve asphalt pavement life. Application of this process will help to solve the waste disposal problem and keep environment clean.

4.1.6 References

1. The Asphalt Institute, 2003. *Performance Graded Asphalt Binder Specification and Testing, SP-1,* Lexington, KY: The Asphalt Institute.
2. Airey, G., 2003. Rheological properties of styrene butadiene styrene polymer modified road bitumens. *Fuel,* Volume 82, pp. 1709-1719.
3. Airy, G., 2011. *Factors affecting the rheology of polymer modified bitumen. In: Polymer Modified Bitumen – Properties and Characterization.*Tony McNally Editor. Woodhead Publishing in Materials.
4. Al-Abdul Wahhab, H., Asi, I. & M.F, A., 1997. Development of Performance-Based Bitumen Specifications for the Gulf Countries. *Construction and Building Materials Journal,* 11(1), pp. 15-22.
5. Bahia, H., Zeng, M., Zhai, H. & Khatr, 1999. *Superpave protocols for modified asphalt binders, 15th Quarterly Progess Report for NCHRP Project 9–10.,* Washington: DC: National Cooperative Highway Research Program.
6. Benko, 2002. USA, Patent No. US 6387965B1.

7. Benzowitz, J. & Boe, E., 1938. *Effect of sulfur upon some of the properties of asphalt. Proceedings of ASTM.*
8. Bernard, 1999. USA, Patent No. US 5936015.
9. Binard, C., Anderson, D., Lapalu, L. & Planche, J., 2004. *Zero shear viscosity of modified and unmodified binders.* Vienna.
10. García-Morales, M. et al., 2004. Viscous properties and microstructure of recycled EVA modified bitumen. *Fuel,* 83(1), pp. 31-38.
11. Hussein, I. A., Iqbal, M. H. & Al-Abdul Wahhab, H. I., 2005. Influence of Mw of LDPE and vinyl acetate content of EVA on the Rheology of Polymer Modified Asphalt. *Rheologica Acta, 2005,* 45(1), pp. 92-104.
12. Hussein, I. A., Wahhab, H. I. A.-A. & Iqbal, M. H., 2006. Influence of Polymer Type and Structure on Polymer Modified Asphalt Concrete Mix. *Canadian Journal of Chemical Engineering,* 84(4), pp. 480-487.
13. Iqbal, M. H., Hussein, I. A., Al-Abdul Wahhab, H. I. & Amin, B., 2006. Influence of Mw of LDPE and vinyl acetate content of EVA on the rheology of polymer modified asphalt. *Journal of Applied Polymer Science,* 102(4), pp. 3446-3456.
14. Kennepohl, G. & Miller, L., 1978. Sulfur-Asphalt Binder Technology for Pavements-New uses of sulfur II. In: *Advances in Chemistry.* Ontario, Canada: American Chemical society , pp. 113-134.

15. Larsen, D., Alessandrini, J., Bosch, A. & Cortizo, M., 2009. Micro-structural and rheological characteristics of SBS-asphalt blends during their manufacturing. *Constr Build Mater,* 23(8), pp. 2769-2774.

16. Lee, D.Y., 1975. *Ind. Eng. Chem., Prod. Res. Dev,* 14(3).

17. Liang, 1998. Canada, Patent No. US 5719215.

18. Lu, X. & Isacsson, U., 1997. Rheological characterization of styrene–butadiene-styrine copolymer modified bitumines. *Contruction and Building Materials,* 11(23).

19. Phillips, M. & Robertus, C., 1996. *Binder rheology and asphalt pavement permanent deformation; the zero shear viscosity.1996.*. Strasbourg.

20. Polacco, G, Giovanni, Stastna, Jiri, Biondi, Dario, Antonelli, Federico, Vlachovicova, Zora, Zanzotto, Ludovit, 2004. *Journal of Colloid and Interface Science 280 (2004) 366–373.,* Volume 280, pp. 366-373.

21. Polacco, G., Stastna, J., Biondi, D. & Zanzotto, L., 2006. Relation between polymer architecture and nonlinea rviscoelastic behavior of modified asphalts. *Current Opinion in Colloid & Interface Science,* Volume 11, pp. 230-245.

22. Qingxi, Y., 2010. The recycling and reuse of waste tire worldwide. *World Rubber Ind,* 37(2).

23. Shenoy, A., 2002. Model-fitting the master curves of the dynamic shear rheometer data to extract a rut-controlling term for asphalt pavements. *ASTM J Test Eval,* 30(2), pp. 95-102.

24. Syvester, 2006. USA, Patent No. US 7074846B2.

25. Zhang, F., Yu, J. & Han, J., 2011. Effects of thermal oxidative ageing on dynamic viscosity, TG/DTG, DTA and FTIR. *Construction and Building Materials,* pp. 129-137.

26. Zhang, F., Yu, J. & Wu, S., 2010. Effect of ageing on rheological properties of storage-stable SBS/sulfur-modified asphalt. *Journal of Hazardous Materials,* Volume 182, pp. 507-517.

27. Zupancic, A. & Zumer, M., 2002. Rheological examination of temperature dependence of conventional and polymer-modified road bitumens. *Can J Chem Eng,* Volume 82, pp. 253-263.

4.2 Use of Polyethylene Wax as a Rheology modifier for Sulfur Asphalt Binders

4.2.1 Abstract

The use of waste polyethylene (PE) wax to modify the rheology of sulfur asphalt binders was investigated. PE wax content was varied from 2 to 8% and sulfur up to 40% was used in asphalt binder. Pure and modified asphalt binders were characterized using Fourier transform infrared spectra (FTIR) characterization. Melt state rheology was investigated using dynamic frequency sweep, temperature sweep and artificial ageing technique. Asphalt binders with different amounts of sulfur and wax content were prepared using high shear blender and rheological tests were carried out in ARES rheometer. Melt state rheology showed improvement in the viscoelastic properties (G′ and G″) of the sulfur asphalt binders due to the addition of PE wax. PE wax modification reduced temperature susceptibility of sulfur asphalt and increased the upper performance temperature of sulfur asphalt. In addition, this modification has increased the activation energy and the zero shear viscosity of sulfur asphalt. Optimum sulfur and PE wax contents of the asphalt binder were recommended. Utilization of PE wax and sulfur wastes in asphalt modification proved to enhance asphalt pavement life.

4.2.2 Introduction

The rate of elemental sulfur production is increasing day by day due to increased oil and gas production. Total elemental production in 2010 was 57 million ton and consumption of the same was 55.6 million ton indifferent section including production of fertilizers and sulfuric acid. The balance 1.4 million ton was unused. For several reasons, there is a renewed interest to seek the new efficient utilization of sulfur due to high production of elemental sulfur from oil and gas processing plant. First, sulfur is a valuable natural resource. Second, the income realized from the beneficial use of abatement sulfur can help offset the cost of pollution control and ease a potential disposal problem. Finally, the stockpiling of sulfur in built-up areas without concurrent utilization could create additional pollution problems. Of the several potential uses for sulfur, a sulfur/asphalt combination for highway pavements seems to have a greatest potential for increasing the beneficial consumption of this element. This sulfur asphalt pavement material could utilize much of the elemental sulfur which will be recovered from fossil fuels.

Asphalt binder is a thermoplastic material that behaves as an elastic solid at low service temperatures or during rapid loading, and as a viscous liquid at high temperatures or slow loading. This double behavior creates a need to improve the performance of the asphalt binder to minimize stress cracking, which occurs at low temperatures, and permanent deformation, which occurs at high service temperatures. The daily and seasonal temperature variations plus the growth in truck traffic volume,

tire pressure, and axle loading have increased stresses on asphalt pavements. The local asphalt pavement temperature in Saudi Arabia ranges between –10^{o}C in winter and 76^{o}C in summer (Al-Abdul Wahhab, et al., 1997). This increases the demand to modify asphalt binders (to reduce cracking and deformation). Different methods have been used to upgrade the properties of asphalt binders (Iqbal, et al., 2006; Hussein, et al., 2005; Hussein, et al., 2006; Polacco, et al., 2004).

Most of the previous work focused on polymer modification of base asphalt. Also, most of the previous work was performed in cold climates (Canada and Sweden) where improvement of the low temperature performance of polymer modified asphalt (PMA) was of great concern. For hot climates, the high-temperature performance is important for modified asphalt binders. Limited number of publications used sulfur to modify asphalt with SBS polymer and the amount of sulfur was limited to 5-10% (Zhang, et al., 2011; Zhang, et al., 2010). The function of sulfur in asphalt paving mixture depends on the sulfur concentration and the sulfur-asphalt ratio. At low sulfur content, where sulfur/asphalt ratio is less than 0.2, sulfur modifies the chemical and rheological properties of asphalt through chemical reactions. At high sulfur/asphalt ratio (> l), sulfur acts as filler and "structuring agent", improving the workability of the sulfur-asphalt aggregate mixture at processing temperatures (130°-160°C) and the mechanical strength of the mixture at service temperatures. (Lee, 1975).

The early study on the use of sulfur in asphalt mixes showed better properties than the conventional asphalt mixes (Benzowitz & Boe, 1938). But due to high prices of sulfur, the product sulfur asphalt was uneconomical. In view of the increase in asphalt price since the beginning of the 1970s, the product was studied again by the US Bureau of Mines and Federal Highways. However, significant problems with storing hot sulfur at asphalt mix plants as well as pre-blending the sulfur with the bitumen were encountered. Sulfur asphalt with high amount of sulfur (≥20) showed poor rutting and cracking resistance.

The effect of commercial PE wax on the rheological properties of bitumen 60/220-grade penetration at high and medium temperature showed a positive influence of sulfur on the rutting resistance of asphalt concrete mixture (Edwards, et al., 2007). A patent was disclosed on the process for preparing storage-stable SBS-modified asphalt by adding sulfur (Planche, 1990). However, due to the high viscosity; the product could not be used in practice. Also, sulfur was added to polymer modified asphalt (PMA) to prepare storage stable binder and applied into practical road paving (Bellomy & McGinnis, 1994).

PE wax is a byproduct from PE industries. Its market value is less than half the cost of polyethylene. The objective of this study is to maximize the utilization of two wastes namely sulfur and PE wax in asphalt modification. Here, we used sulfur in the range 30-40% to produce sulfur asphalt binder while PE wax was used at 2-8%. Sulfur asphalt with such high amounts of sulfur is brittle. Therefore, it was proposed

to add PE wax to sulfur asphalt to improve its rheological properties. No previous work was done to examine the effect of PE wax on the rheological properties of sulfur asphalt binder. In this paper, we will try to explore the use of PE wax to improve sulfur asphalt binder performance and possible correlation between PE wax content and rheological properties of sulfur asphalt binder at medium and high temperatures of application.

4.2.3 Experimental

Materials

Polyethylene wax was collected from Tasnee Petrochemicals Complex, Jubail, Saudi Arabia. It has melting point ~ 70^{o}C. It is a byproduct resulting from incomplete polymerization of polyethylene. Elemental sulfur (99.9% purity) was collected from Saudi Aramco. It is a waste product from oil and gas processing plant. Asphalt cement was purchased from a local refinery. The DSC scans of these samples are presented in Figure 4.2.1.

Sample Preparation

Sulfur and pure asphalt were blended in a high shear blender. Elemental sulfur pellets were grinded to fine powder of size less than 1 mm before feeding to the blender. The blender acts as a batch stirred tank with a constant temperature bath. The bath temperature was maintained at 145^{o}C.Typical mixing procedure was as follows: aluminium cans of approximately 1000 mL were filled with 250–260 g of asphalt and

put in a thermoelectric heater. When asphalt temperature reached 145°C, a high shear mixer was dipped into the can and set to about 2500 rpm. Polyethylene wax was then added gradually, while keeping the temperature within the range of 145 ± 1°C during the addition. After 2 minutes of blending, sulfur powder was added and continued for another 10 minutes to confirm uniform distribution of sulfur and polyethylene wax in the asphalt matrix. Asphalt samples were poured into rubberized molds before being used for rheological testing. The samples specimens were stored in a refrigerator at 5°C. Ten samples of sulfur modified asphalt binders and pure asphalt binder were prepared and tested. Detailed samples information is presented in Table 4.2.1.

DSC measurements

The thermal behaviors of the pure and modified asphalt binder as well as the compositions of the asphalt binder were determined by means of a TA Q1000 DSC. Samples of 7-10 mg were weighed and sealed in aluminum pans. Melting temperature measurements were performed by heating samples from room temperature to 150^{o}C. A heating rate of 5^{o}C/min was applied and nitrogen was used as the purge gas at a flow rate of 50 ml/min.

FTIR Characterization

Fourier transform infrared spectroscopy (FTIR) technique was used to determine the chemical bond changes of pure and modified asphalt binder. FTIR measurement was carried using a Nicolet 6700 spectrometer from Thermo Electron™. All the FTIR spectra were taken in the absorbance mode and in the range 600–4000 cm^{-1} at room

temperature. FTIR spectra were obtained using a spectral resolution of 4 cm^{-1} and 30 co-added scans.

Table 4.2. 1: Composition of sulfur modified asphalt binder used in this study

Sample #	Percentages of different components		
	Sulfur%	Asphalt%	Wax%
1	0	100	0
2	30	70	0
3	30	68	2
4	30	66	4
5	30	64	6
6	30	62	8
7	40	60	0
8	40	58	2
9	40	56	4
10	40	54	6
11	40	52	8

Rolling thin film oven (RTFO) test

Rolling thin film oven test (RTFO) was used to perform ageing of asphalt binders according to ASTM D 2872 procedure. This test simulates the ageing process that takes place during the production and up to the first year of the service life of the pavement. Base asphalt as well as modified asphalt was poured into cylindrical

bottles. 35 grams of asphalt sample was poured in each cylindrical bottle. Then the bottles were placed horizontally in a convection oven, which was rotated at 163^{o}C for 85 min. Air was supplied into the bottle to accelerate ageing. This process created a thin film of asphalt on the inside of the bottles. After completing the run, samples were collected for rheological testing in ARES.

Rheological tests

Dynamic and steady rheological tests were carried out to investigate the effect of polyethylene wax on the rheology of sulfur modified asphalt. The dynamic temperature step measurements for the samples were performed in ARES rheometer. This is a constant strain rheometer equipped with a heavy transducer (range 2-2000 g for normal force; 2-2000 g-cm for torque). All tests were carried out in the range 64°-85°C using a parallel plate set of diameter is 25 mm. With the sample in position, the oven was closed and the sample heated at 64^{o}C for about 5 minutes, thereafter the gap between the plate platen was adjusted to 1.5 mm by lowering the upper platen force transducer assembly at a constant load of 500 g. The melt that extruded beyond the platen rim by this procedure was cleaned off. Strain in the linear viscoelastic range (strain amplitude, γ^{o} of 12.5 %) and frequency of 10 rad/s was used for all the tests. In all the experiments, nitrogen gas was continuously used for heating the samples during testing to avoid oxidation during testing. A holding period of 5 min was allowed before beginning measurements when the temperature reaches steady state. The Orchestrator software was used to calculate the dynamic shear viscosity,

storage modulus, complex modulus and phase angle for all samples. Dynamic frequency sweep tests were conducted at 50^{o}C and frequency ranges of 100-0.1 rad/s and the constant strain of 10%. Different linear viscoelastic variables were calculated using TA Orchestrator software. Dynamic temperature step frequency sweep test was performed to get the master curve for selected asphalt binders. Steady shear rheological tests were conducted at 50^{o}C and shear rate ranges of 0.01-10 s^{-1}.

4.2.4 Results and Discussion

Thermal characterization

Differential scanning calorimetry (DSC) results of pure sulfur, polyethylene wax, pure asphalt and two sulfur modified asphalt binder is shown in Figure 4.2.1. There is no peak in the DSC thermogram for pure asphalt which confirms that asphalt used in this study is pure virgin asphalt. As polyethylene wax results from incomplete polymerization reaction, it doesn't have a sharp melting point; rather it has a broader melting point with a peak ~ 70°C. This melting point of polyethylene wax is higher than the conventional wax which has melting point of ~ 50^{o}C. The high melting point suggested that polyethylene wax could be a potential additive for asphalt modification. The DSC scan of pure elemental sulfur shows that it has two melting peaks. The first melting peak is at 106.12^{o}C which corresponds to rhombic sulfur. The second peak is of 120.4^{o}C and it is corresponded to monoclinic form of sulfur. The literature values are also in the same range (Zupancic & Zumer, 2002).

The modified asphalt binder has three different constituents namely: polyethylene wax, sulfur and asphalt with different weight percentages. One interesting observation in the DSC scan of sulfur modified asphalt binder is that it has only one melting point at ~ 118°C. It ensures that rhombic sulfur has been converted to monoclinic sulfur in the modification process. DSC scan of 40/60 sulfur/asphalt shows that it has a melting point at 118.22^{o}C which is very close the melting point of monoclinic sulfur. The modified asphalt binder with 40% sulfur, 52% asphalt and 8% polyethylene wax has a melting point of 117.78°C.

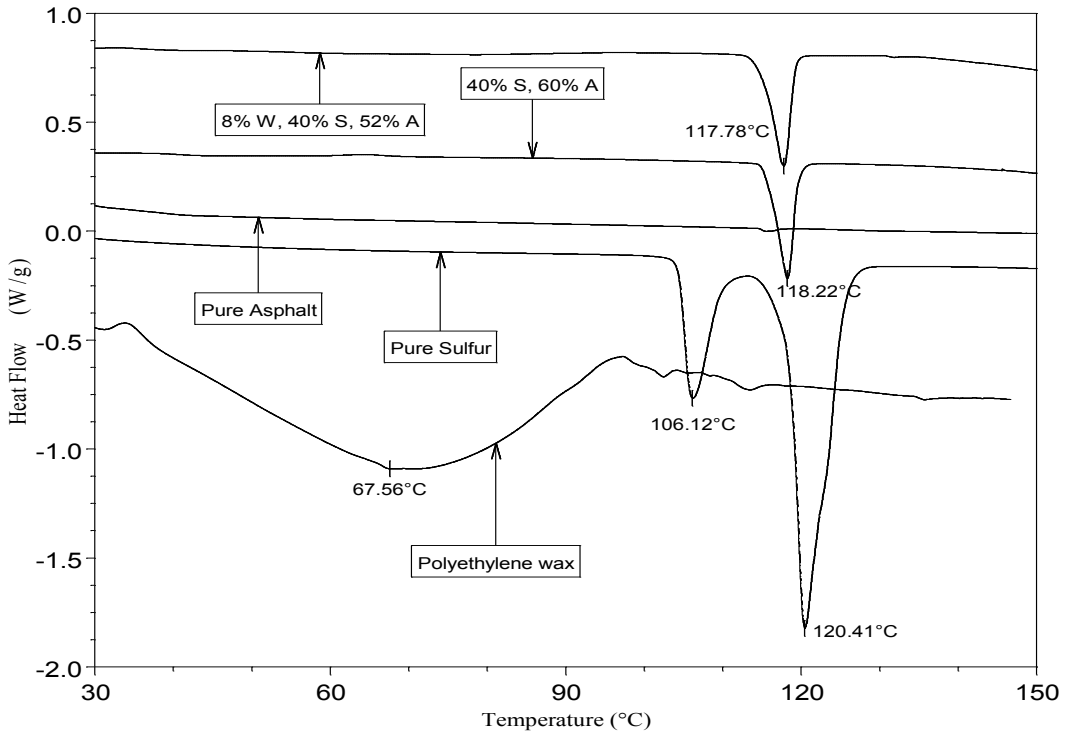

Figure 4.2. 1: DSC scans of the modified asphalt binder and its compositions

FTIR results of asphalt binders

Figure 4.2.2 represents the FTIR spectra of pure asphalt binders. Table 2 listed the main bonds present in asphalt as shown in Figure 4.2.2. Similar results were also mentioned in literature (Larsen, et al., 2009). The bonding of sulfur modified asphalt binders are also similar to the one presented in Figure 4.2.2 but with different intensities. Figure 4.2.3 represents the FTIR spectra 30% sulfur modified asphalt binders. The main differences between pure and sulfur modified asphalt binders are in the range 600-1500 cm^{-1}. The FTIR spectra of other sulfur modified binders are also similar to that presented in Figure 4.2.3. It is noticed that the intensities of the bonds has been changed in modified binders. The relative change of bonding is calculated using the following equations:

$$I_{C\text{-}C} = \frac{\sum \text{Area of the C-C bands for modified asphalt binder}}{\sum \text{Area of the C-C bands for pure asphalt}} \quad (4.2.1)$$

$$I_{C=C} = \frac{\sum \text{Area of the C=C bands for modified asphalt binder}}{\sum \text{Area of the C=C bands for pure asphalt}} \quad (4.2.2)$$

$$I_{S=O} = \frac{\sum \text{Area of the S=O bands for modified asphalt binder}}{\sum \text{Area of the S=O bands for pure asphalt}} \quad (4.2.3)$$

The relative changes of bonding in the modified binders were calculated using the defined in equation 4.2.1-4.2.3. Figure 4.2.4 represents the change in bonding due to chemical modification of the binders. The relative intensity of the C=C and S=O bonds of PE wax modified binders have decreased in comparison with 30/70 sulfur asphalt binders. Moreover the C-C has increased with PE wax concentration. This confirms the chemical cross-linking in PE wax modified asphalt binders. It was also mentioned in the literature that part of the sulfur added reacts chemically with asphalt

to form carbon-sulfur bond and polysulfide bond (Kennepohl & Miller, 1978). Sulfur and PE wax modification of asphalt binder leads to chemical crosslinking. Equation 4 & 5 are two possible cases where PE wax and sulfur can be bonded with unsaturation of asphalt (e.g C=C, S=O) and reduce double bond. In those equations S is sulfur and R is long chain organic molecule which can come from PE wax or asphalt. This chemical bonding is expected to increase the viscoelastic properties of modified asphalt binder which will be explained in the rheological section.

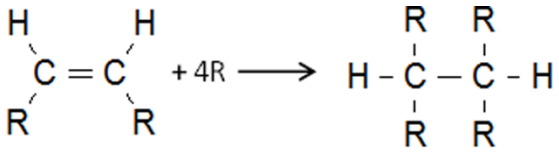

(4.2.4)

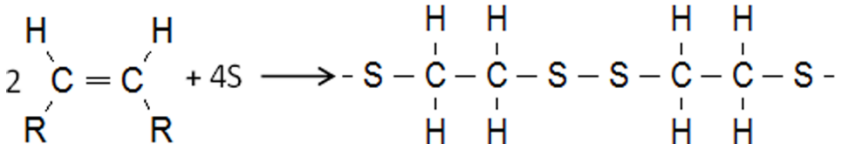

(4.2.5)

Table 4.2. 2: Assignations of the main bands of the FTIR spectra

Webnumbers [cm^{-1}]	Assigned bands
2920, 2850	υC-H aliphatic
1636	υC=C aromatic
1456	δC-H of $-(CH_2)_n-$ (aliphatic index)
1376	δC-H of CH_3 (aliphatic branched)
1031	υS=O sulfoxide
808, 864	υC=C of alkenes
721	δC-H or δC-S

Note: υ = Stretching, and δ = Bending

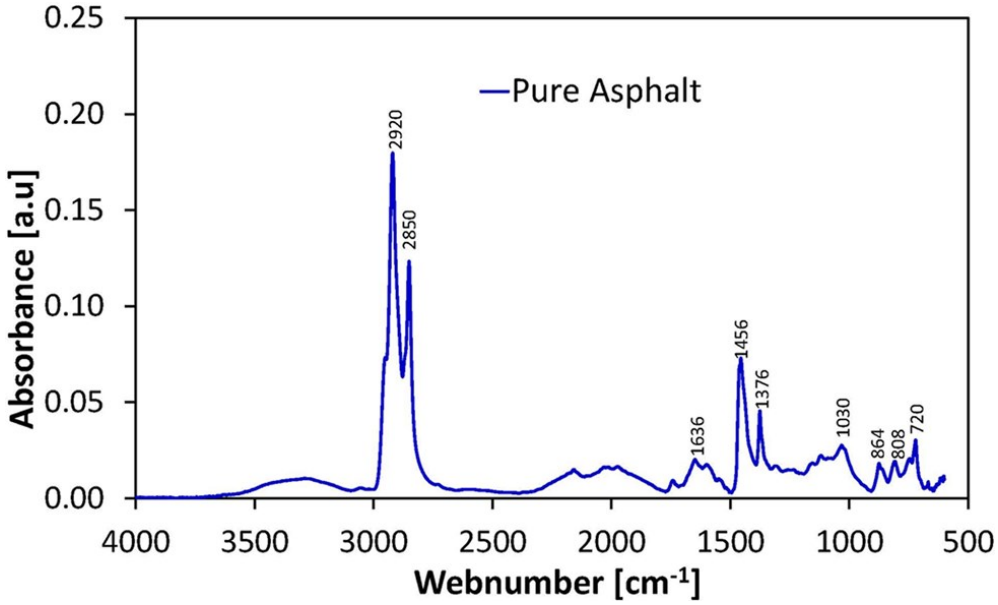

Figure 4.2. 2: FTIR spectra of pure asphalt binder

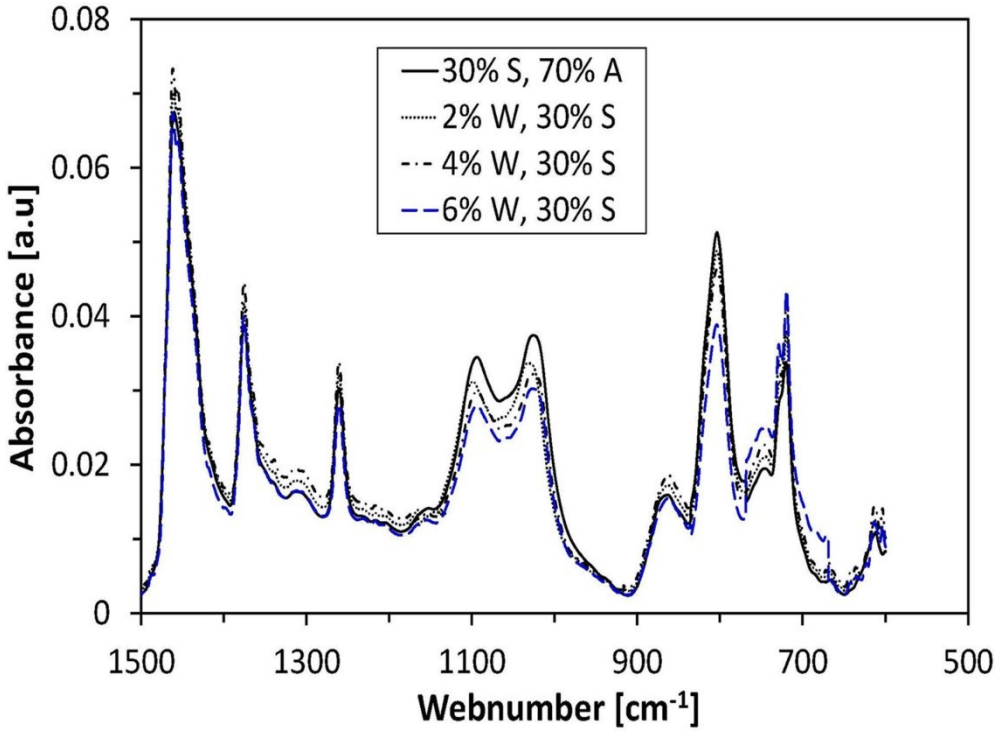

Figure 4.2. 3: FTIR spectra of pure and modified asphalt binders

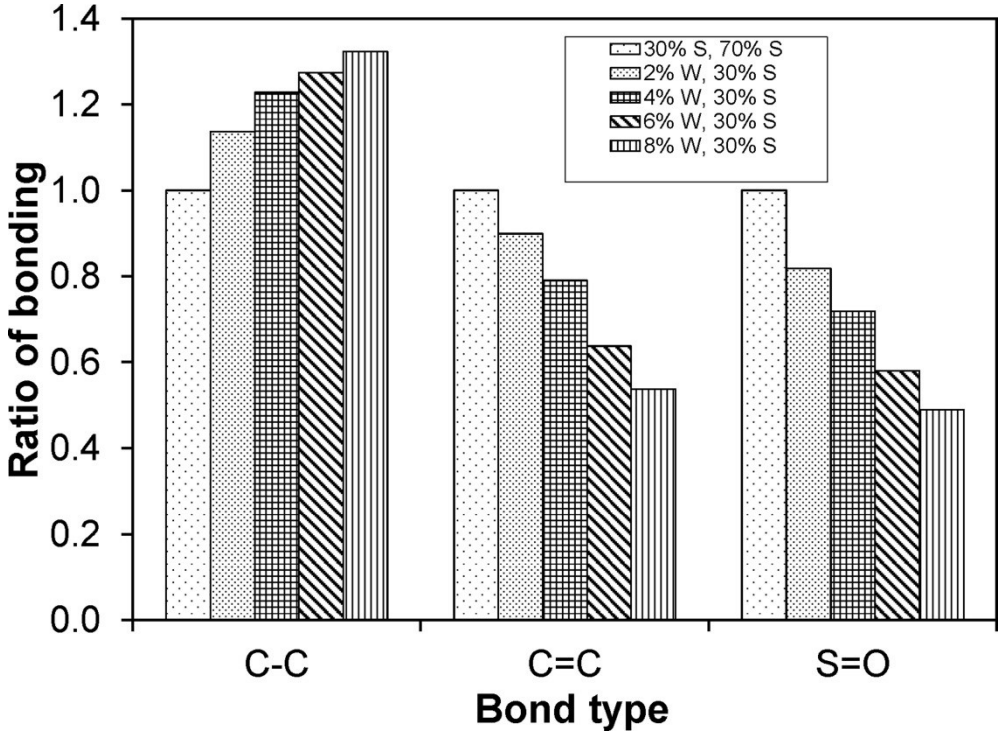

Figure 4.2. 4: The intensity of bonding in pure and modified asphalt binders

Rheological Characterization

Dynamic Shear Rheology

The results of dynamic frequency sweep tests are presented in Figures 4.2.5 for the 30% sulfur modified asphalt binders. The results for the 40% sulfur asphalt are also similar to the one presented in Figure 4.2.5. The results are shown for 0%, 2%, 4%, 6% and 8% polyethylene wax content by weight. Both the 30% and the 40% sulfur modified asphalt binders showed higher storage modulus, G′(ω), and dynamic shear viscosity,η′(ω), compared to base asphalt. The profile of η′(ω) for pure asphalt showed typical Newtonian behavior over almost the entire ω range, but polyethylene

wax modified sulfur/asphalt binder displayed non-Newtonian behavior, which was more pronounced at high polyethylene wax concentrations. Similar behavior was observed for asphalt modification with polymers (Hussein, et al., 2005; Iqbal, et al., 2006). However, sulfur modified asphalt binder without polyethylene wax is very similar to that of pure asphalt with slightly higher values of dynamic viscosity. At low frequency (ω=0.1 rad/s), the value of η′ for 30/70 sulfur/asphalt binder is 5 times higher than that of base asphalt. Addition of 2%, 4%, 6% and 8% polyethylene wax has increased both η′and G′ significantly. To clarify the changes in η′and G′ values due to replacement of asphalt by the same percentage of wax, here we define two modification indices as follows:

$$I_{G'} = \frac{G' \text{of wax modifed binder}}{G' \text{of sulfur asphalt binder}} \tag{4.2.6}$$

$$I_{\eta'} = \frac{\eta' \text{of wax modifed binder}}{\eta' \text{of sulfur asphalt binder}} \tag{4.2.7}$$

Table 4.2.3 represents the calculated values of the two modification indices defined in equations (4.2.6-4.2.7). The values of the two indices showed significant improvement in both G′ and η′. $I_{G'}$ is much more higher than $I_{\eta'}$, meaning that the effect of modification is more pronounced in G′. The 40% sulfur modified asphalt binders showed higher modification indices values compared to that of the 30% sulfur modified asphalt binder. The indices value increases with polyethylene wax content and it is maximum for 8% polyethylene wax content. At high frequency (ω=100 rad) the G′ and η′ values were ~2 to 3 times higher than the sulfur/asphalt binder without polyethylene wax.

Table 4.2. 3: Modification indices for 30% and 40% Sulfur modified asphalt binder

Asphalt binder	Polyethylene wax content [%]	$I_{G'}$ at ω = 0.1 rad/s	$I_{\eta'}$ at ω = 0.1 rad/s
30% Sulfur	2	3.7	1.6
	4	28.2	2.4
	6	76.0	5.3
	8	121.8	7.8
40% Sulfur	2	16.2	1.9
	4	33.1	2.2
	6	44.0	4.2
	8	179.2	9.3

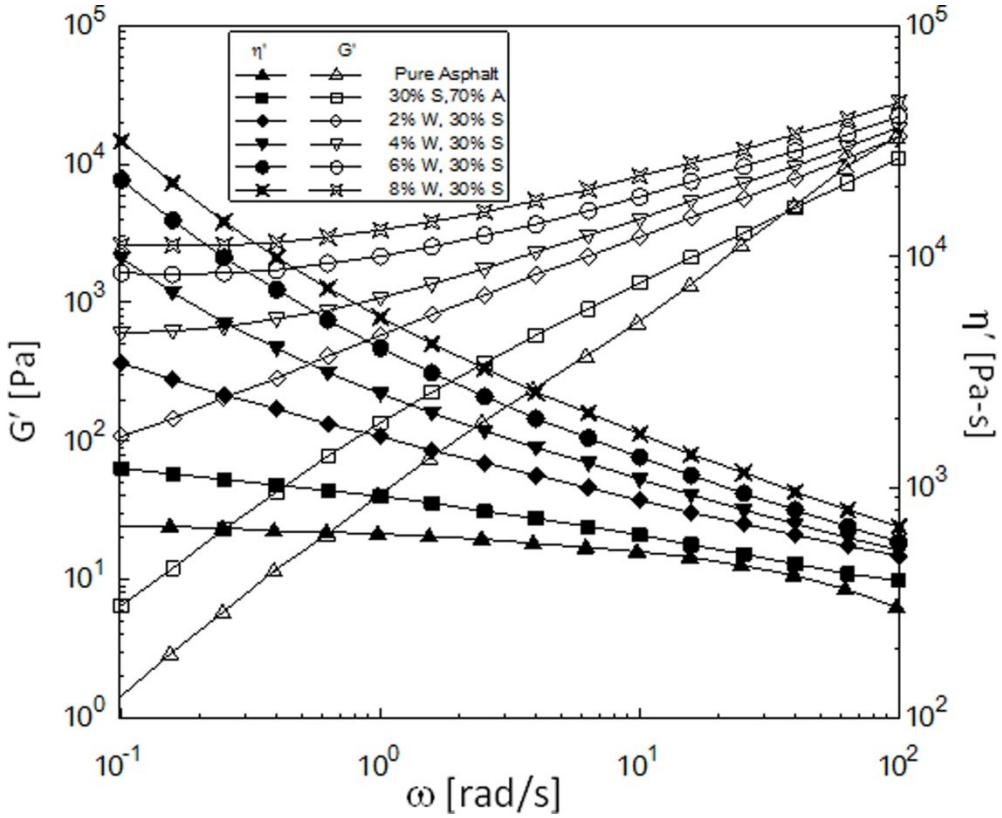

Figure 4.2. 5: Dynamic shear variables G′(ω) and η′(ω) for 30% sulfur modified asphalt binders at 50°C

The high values of G′ suggested having low resistance to low-temperature cracking, because materials become harder at low temperature and crack easily. So, the polyethylene wax content to the sulfur modified asphalt binder should be optimized for cold climate. The increase in G′ with the increase of polyethylene wax concentration is attributed to its high melting point (70^{o}C) since the test was done at 50°C. Similar improvements were observed for polymer modification of asphalt binder (Polacco, et al., 2006). The advantage of high G′ is at high temperature climate. Higher G′ values at lower frequency range suggest better flexibility. According to the principle of time–temperature superposition, this behavior corresponds to long service time or higher temperature, which is needed in hot climate. The slopes of the log G′ versus log ω for low ω range were calculated and its values are 1.49, 1.33, 0.64, 0.58, 0.36, and 0.23 for pure asphalt, 40/60 sulfur/asphalt, 2%, 4%, 6% and 8% polyethylene wax modified sulfur asphalt binder respectively. However, for the percentages of polyethylene wax content the slopes for 30% sulfur modified binders were 0.72, 0.16, 0.044, and 0.029 respectively. So, for same amount of polyethylene wax content, the slopes of the 30% sulfur modified asphalt binders were less than that of 40% sulfur modified asphalt binder. So the melt rheology of sulfur modified asphalt binder suggest that 30% sulfur modified asphalt binders expected to show better deformation resistance at high temperature.

The dynamic shear rheology data were further analyzed by using mechanical spectra to obtain detailed overview of the rheological properties because of

polyethylene wax modification of sulfur/asphalt binder. The mechanical behavior of a viscoelastic material can be modeled by a combination of mechanical elements which represent purely viscous (dashpot) and purely elastic (spring) properties. One of the simplest models is the Maxwell model. A discrete distribution or spectrum of relaxation times may be described by many Maxwell elements combined in series, which is the generalized Maxwell model. The linear viscoelasticity functions in oscillatory shear for a generalized Maxwell model is given by the following relationship (Ferry, 1980):

$$G' = \sum_i \frac{H_i \lambda_i^2 \omega^2}{\left(1 + \lambda_i^2 \omega^2\right)} \tag{4.2.8}$$

Where λ_i and H_i are relaxation time and elastic modulus of i^{th} Maxwell element. The relaxation time and elastic modulus were calculated by TA Orchestrator™ software using non-linear regression analysis of the dynamic shear rheology data. Figure 4.2.6 shows the relaxation spectra of selective sulfur/asphalt binder with different polyethylene wax content. It can be observed that H for base asphalt has rapidly decreased with the increase in λ. It means decrease in elastic properties for pure asphalt is high with time. Similar behavior also noticed for 30/70 sulfur/asphalt as well as 40/60 sulfur/asphalt. However, this decrease is less for sulfur/asphalt binder modified with polyethylene wax. The 30% sulfur/asphalt binder modified using polyethylene wax showed the least decrease compared to that 40% sulfur/asphalt binder. This suggest that 30% sulfur binder with different polyethylene wax content

has maintained higher elastic properties and loses its elasticity at a slower rate in comparison to other sulfur/asphalt binder. These results are consistent with our previous data analysis for G′ in Figure 4.2.5.

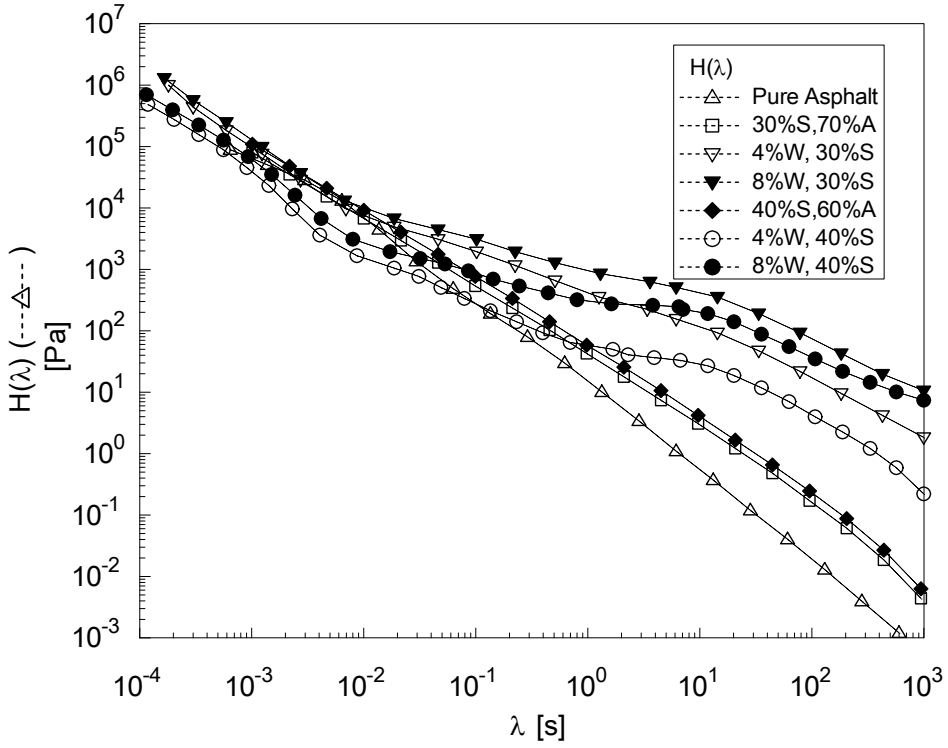

Figure 4.2. 6: Relaxation spectrum of pure asphalt and sulfur modified asphalt with different polyethylene wax content (Ttest = 50°C).

Figures 4.2.7 and 4.2.8 show the results of $\eta^*(T)$ obtained from temperature ramp tests for the 30% and 40% sulfur modified asphalt binder respectively. It is found that η^* increases significantly in case of the binder modified with polyethylene wax. At higher temperature high values of G* ($G^*=\eta^*\omega$) are needed. High values of η^* indicates high rutting resistance at higher temperature. Viscosity- temperature

relationships asphalt binder can be expressed by the well-known Arrhenius equation as follow:

$$\eta^* = Ae^{E_a/RT} \tag{4.2.9}$$

Where E_a is the flow activation energy, A is the pre-exponential term, and R is the universal gas constant. E_a is an important factor that strongly influences the viscosity. The data given in Figure 4.2.7 and 4.2.8 showed good fit to Arrhenius model. E_a was calculated using equation (4.2.6) and the values for different binders are tabulated in Table 4.2.4. Activation energy for pure asphalt is 112.53 kJ/mol. Addition of sulfur to asphalt reduces the activation energy of sulfur asphalt binder. However, addition of polyethylene wax increases activation energies of sulfur modified asphalt. It is evident because of low melting point (70^{o}C) of polyethylene wax compared to that of sulfur melting point (118 ^{o}C). It is observed that the activation energies of 30% sulfur asphalt binders lower than that of 40% sulfur asphalt binder. Therefore, 30% sulfur asphalt binders are better than 40% sulfur asphalt binders.

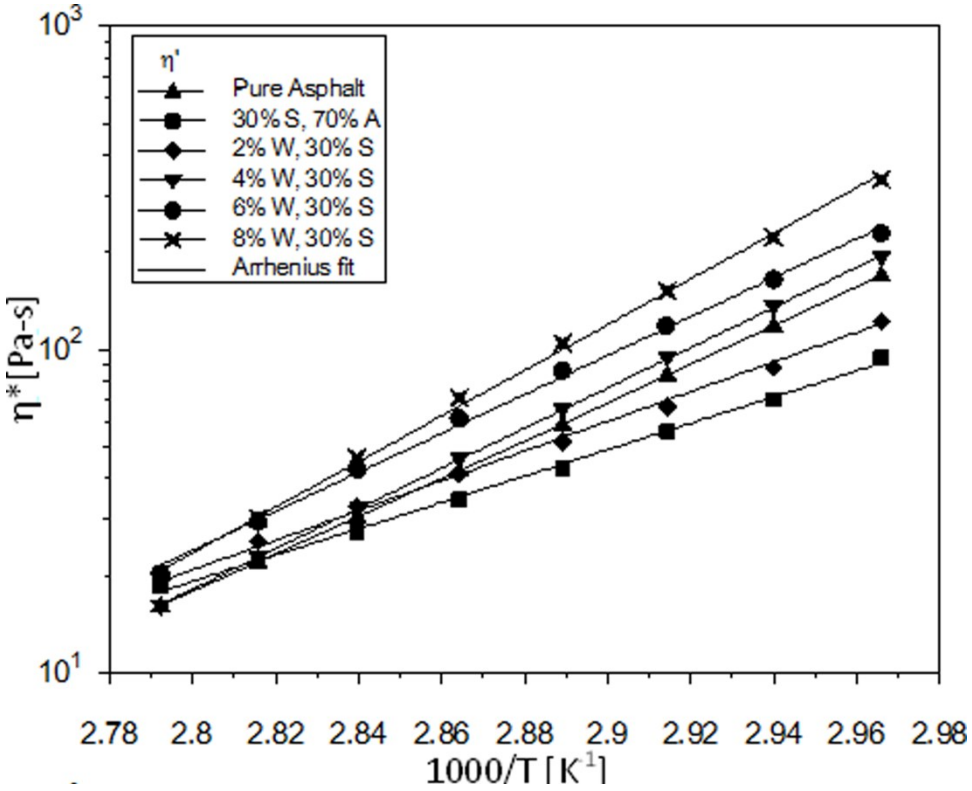

Figure 4.2. 7: *η*(T)* for 30% sulfur modified binder with different percentages of polyethylene wax content

Table 4.2. 4: Activation energy, Ea of pure and modified asphalt binders

Asphalt binder	Polyethylene wax content [%]	E_a (kJ/mol)
Pure Asphalt	0	112.53
30% Sulfur/Asphalt binders	0	77.95
	2	87.91
	4	112.75
	6	121.48
	8	138.29
40% Sulfur/Asphalt binders	0	72.89
	2	117.50
	4	153.61
	6	161.22
	8	163.98

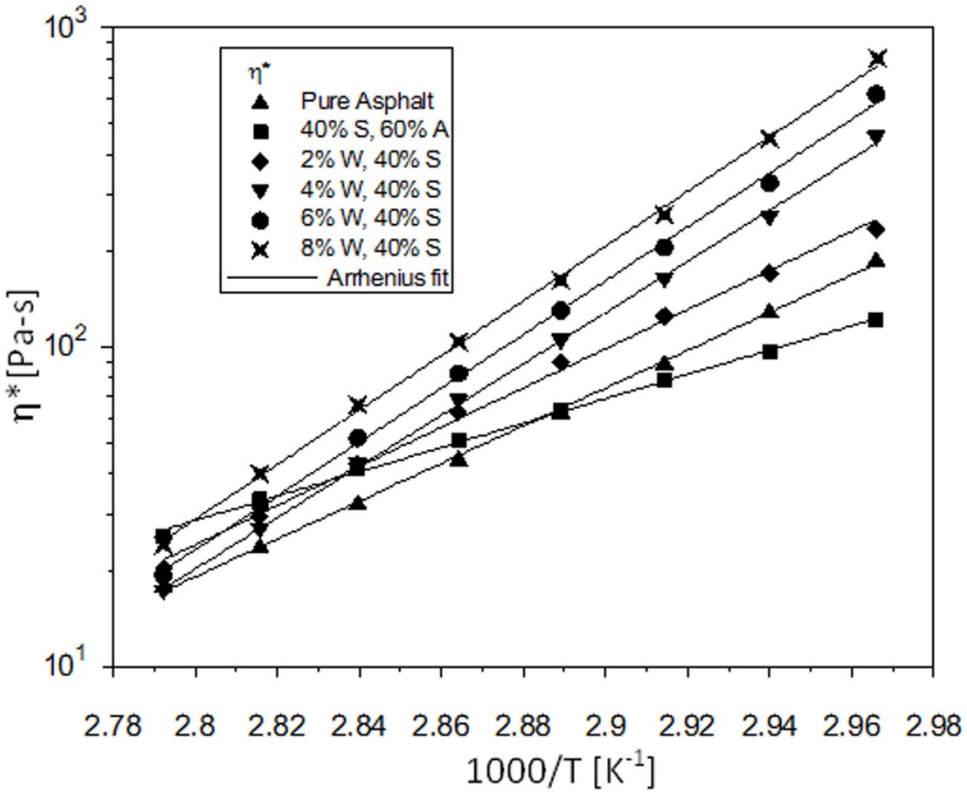

Figure 4.2. 8: *η*(T)* for 40% sulfur modified binder with different percentages of polyethylene wax content

Another way to evaluate the asphalt binder modification is the use of the relative complex viscosity (η_r). It is defined as the ratio of the complex viscosity of modified asphalt to unmodified asphalt (Barnes, 2000). In this paper, we defined η_r as the ratio of polyethylene wax modified asphalt binder to sulfur asphalt binder without polyethylene wax content to see the effect of polyethylene wax modification. In order to examine temperature susceptibility of polyethylene wax modified binders, relative complex viscosity at 10 rad/s in the experimental temperature range were calculated.

Figure 4.2.9 shows the effect of polyethylene wax content on relative complex viscosity at 79°C. η_r increases with polyethylene wax content and it is more than 1.5 for 8% polyethylene wax for both 30% and 40% asphalt binders. In addition, greater thermal susceptibility according to this parameter is observed for 30% sulfur modified binders compared to 40% sulfur modified binders.

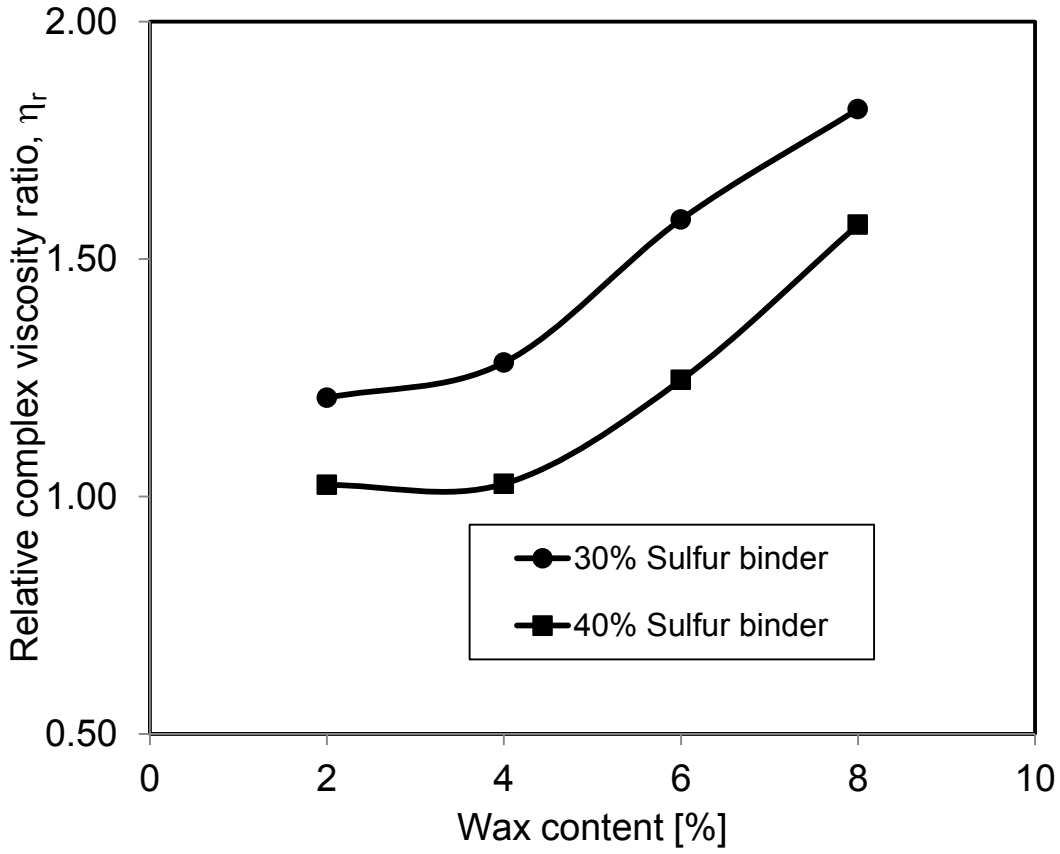

Figure 4.2. 9: Relative complex viscosity ratio as function of polyethylene wax content at high temperature (79°C).

Temperature sweep test was conducted for all binders to extract the values of complex moduli, G^* and phase angle, δ as function of temperature. According to the

strategic highway research program (SHRP), the stiffness parameter $G^*/\sin\delta$ is a factor used to estimate the rutting resistance of asphalt binder. It should be larger than 1 kPa at the maximum pavement design temperature for unaged original asphalt, when measured at 10 rad/s to simulate traffic loading. Higher values of $G^*/\sin\delta$ are expected to give a high resistance to permanent deformation. Figures 4.2.10 and 4.2.11 show $G^*/\sin\delta$ versus temperature for the 30% and 40% sulfur modified asphalt binder respectively. It shows that addition of 30% and 40% sulfur to pure asphalt reduces the values of $G^*/\sin\delta$. So, there is a necessity of modification of these binders to improve rutting resistance. It is also noticeable that addition of polyethylene wax to sulfur asphalt binders increases the values of $G^*/\sin\delta$, which means polyethylene wax improved rutting resistance at high and medium temperatures.

The upper service temperature of pavement structure was calculated and listed in Table 5. As mentioned elsewhere, local asphalt pavement temperatures range -10^{o}C in winter and 76^{o}C for summer (Al-Abdul Wahhab, et al., 1997). According to the above analysis, 10% polyethylene wax for 30% sulfur modified binder satisfied the higher temperature requirement whereas 8% polyethylene wax is needed for 40% sulfur asphalt binder to meet the same criteria.

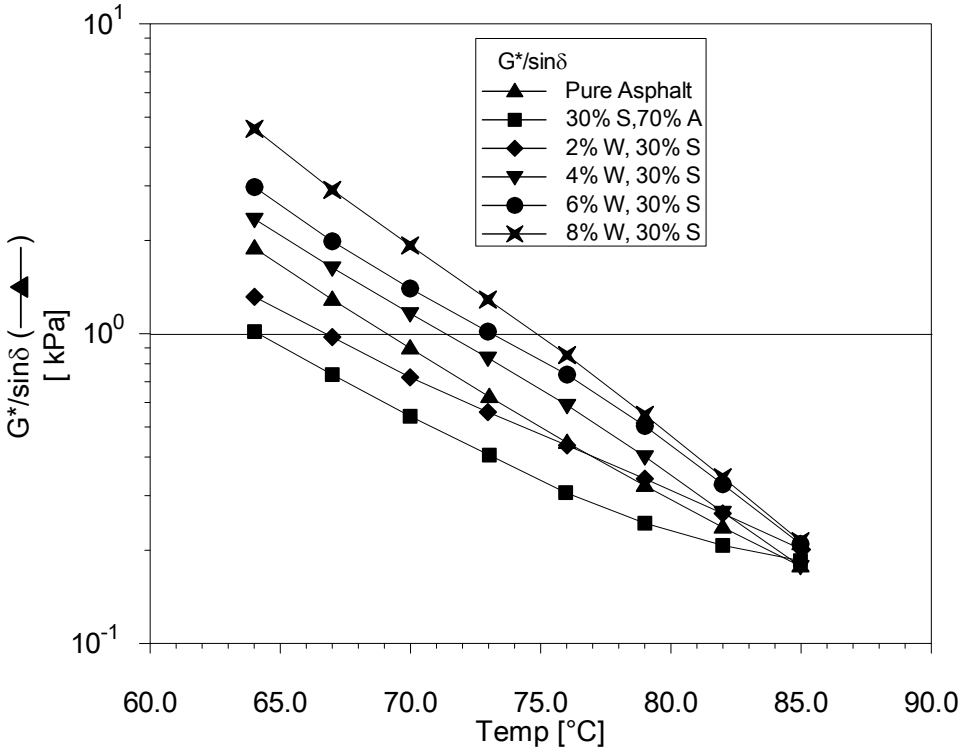

Figure 4.2. 10: *G*/sinδ* versus temperature for 30% sulfur modified asphalt binders with different polyethylene wax content

Table 4.2. 5: Maximum temperature at which G*/sinδ is equal to 1

Asphalt binder	Polyethylene wax content [%]	Max. Temp attained, °C
Pure Asphalt	0	69
30% Sulfur/Asphalt binders	0	65
	2	66.5
	4	69
	6	73
	8	75
40% Sulfur/Asphalt binders	0	67
	2	72.5
	4	74
	6	75
	8	77.5

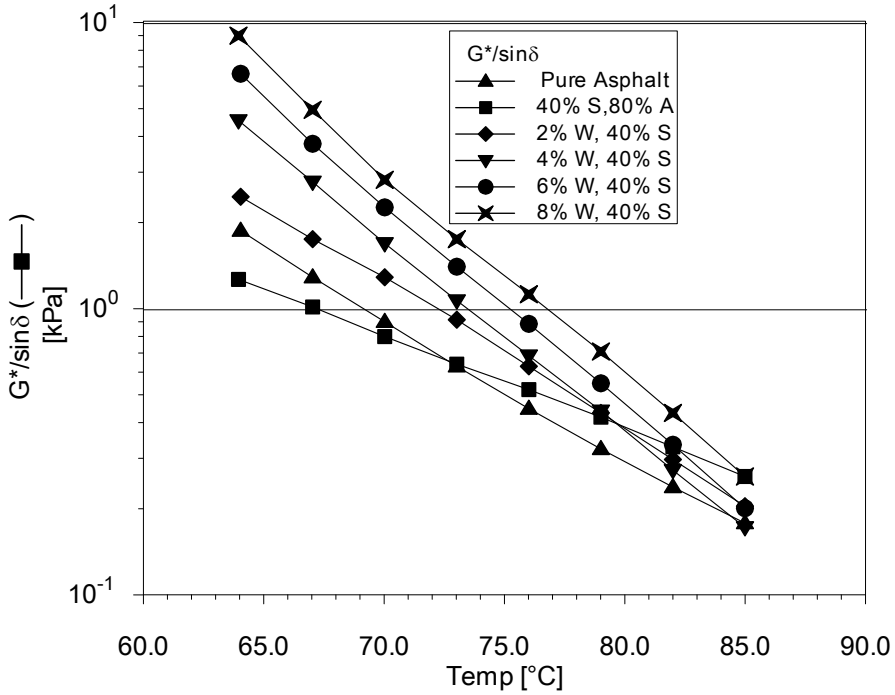

Figure 4.2. 11: G*/ $sin\delta$ versus temperature for 40% sulfur modified asphalt binders with different polyethylene wax content

Dynamic temperature step frequency sweep test was conducted to analyze data using time temperature superposition (TTS) principle. Five different temperatures were used to generate frequency sweep data. The temperature range was 45-85°C with 10°C increments. Frequency range was chosen 100-0.1 rad/s. Data was then shifted using horizontal shifting method. Figure 4.2.12 shows G' master curve for 2%, 6% and 8% polyethylene wax modified sulfur asphalt binders. The reference temperature was 65°C. The temperature dependence of the shift factor a_T is given in Figure 4.2.13. The similar behavior was reported in the literature for polymer modified asphalt (Carreau, et al., 2000; Challa, et al., 1996). It is observed that TTS principle hold for the sulfur asphalt binder studied in this paper. Figure 4.2.12 showed that

polyethylene wax increased G' which means longer pavement life. Actually, this master curve data can converted to relaxation spectra and get the same conclusion that was drawn from Figure 4.2.6.

In the recent years, researchers have observed that the SHRP rutting parameter $G^*/\sin\delta$ is not very effective in predicting the rutting performance of binders, especially in case of modified binders are used (Shenoy, 2002; Bahia, et al., 1999). For such case a new parameter zero shear viscosity, (ZSV) has been suggested by many researchers as a possible measure for the rutting resistance of modified asphalt binders (Binard, et al., 2004; Phillips & Robertus, 1996). ZSV can be calculated from steady shear rate sweep test as well as dynamic frequency sweep test. In the case of steady shear rate test, ZSV is defined as the viscosity exhibits by the sample at very slow rate. At such low shear rates, the binders undergo deformation so slowly, that it can adapt continuously to maintain equilibrium, despite the total amount of shear being large. For the case of dynamic frequency sweep test, ZSV is defined as the viscosity of the sample under very low frequency. The ZSV is said to be an indicator of two rutting related binder characteristics, namely the stiffness of the binder, and the binder's resistance to permanent deformation under long term loading. In this paper, ZSV was calculated based on dynamic frequency sweep test at different temperatures. ZSV extracted by fitting the dynamic viscosity $\eta'(\omega)$ to Ellis model for viscosity. Ellis model for viscosity is given the following relationship:

$$\eta'(\omega) = \frac{\eta_0}{\left(1 + \omega / c_2\right)^{(c_3 - 1)}} \tag{4.2.10}$$

Where, η_0 is the zero shear viscosity, ω is frequency in rad/s and c_2 and c_3 are constants. To get ZSV for different temperature, dynamic temperature step frequency sweep test was conducted for all binders. The temperature range was 50-65^{o}C with 5^{o}C increments. Frequency range was chosen from 100-0.1 rad/s. ZSV were calculated using equation 4.2.8. Temperature dependency of ZSV is plotted in Figures 4.2.12 and 4.2.13 for 30% and 40% sulfur asphalt binders. Generally, the ZSV did follow the same trend for all of the combinations tested. For both 30% and 40% sulfur asphalt binders, there is an increase in ZSV with an increase in polyethylene wax percentages. The statistical results indicate that there were statistically significant differences in the ZSV of polyethylene wax modified binders as a function of polyethylene wax percentages. Also, the values of ZSV for the 30% sulfur/asphalt binders are more than 40% sulfur/asphalt binders especially for polyethylene wax content of 4% or more.

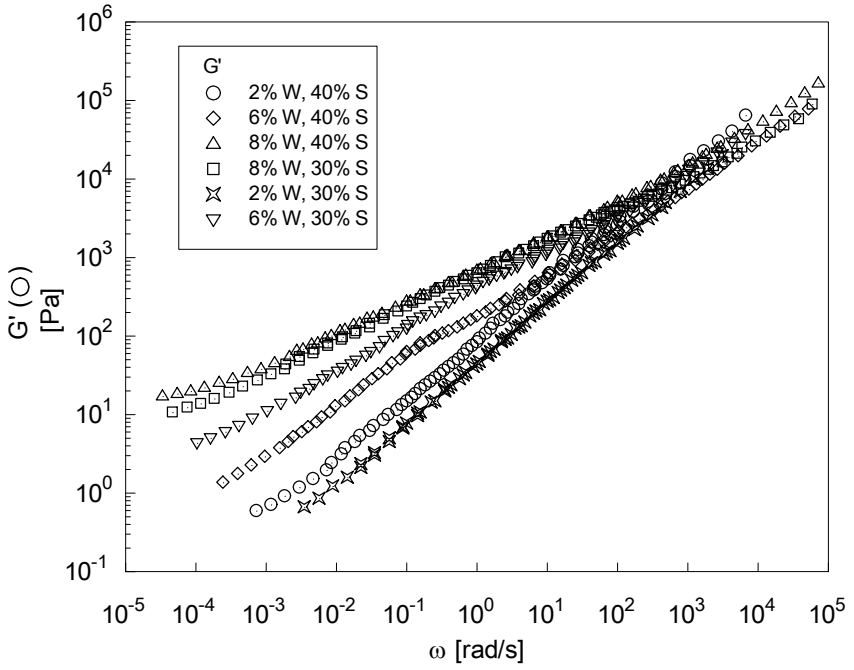

Figure 4.2. 12: *G′(ω)* master curve for selective sulfur/asphalt binders with different polyethylene wax content at T_{ref}=65°C

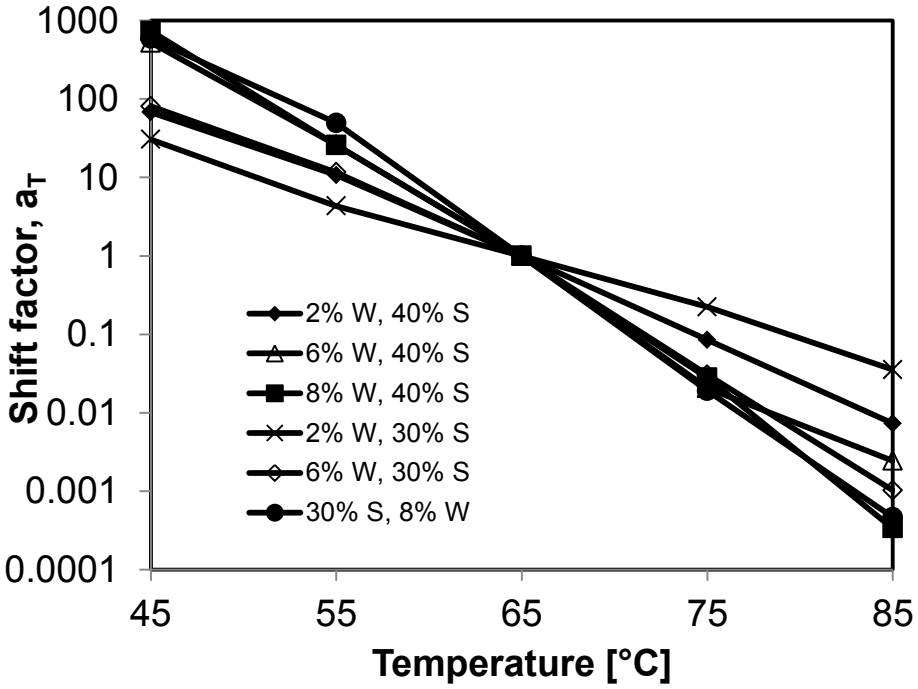

Figure 4.2. 13: Shift factor a_T versus T (T_{ref}=65°C)

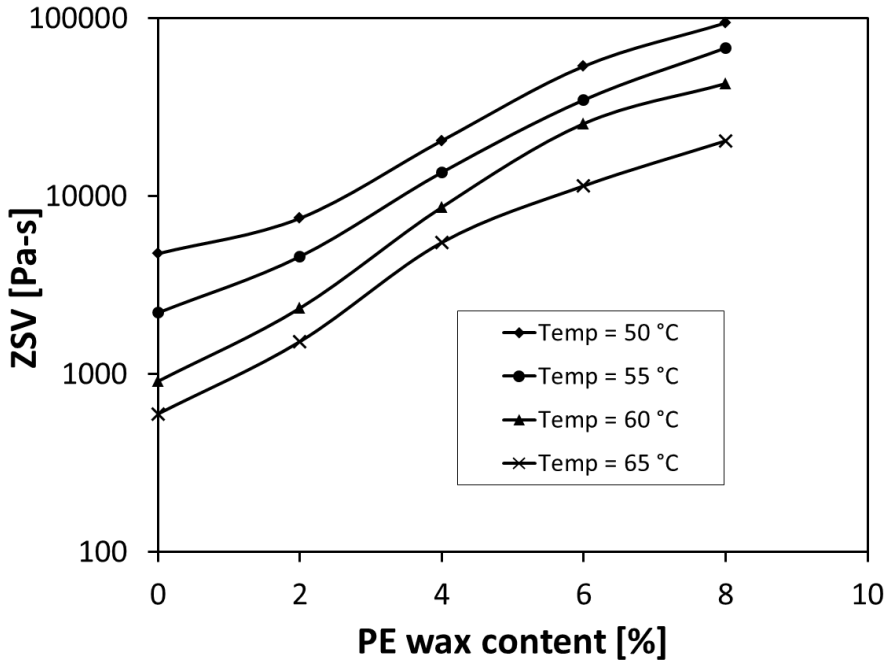

Figure 4.2. 14: Zero shear viscosity as function of polyethylene wax content for 30% Sulfur modified binders

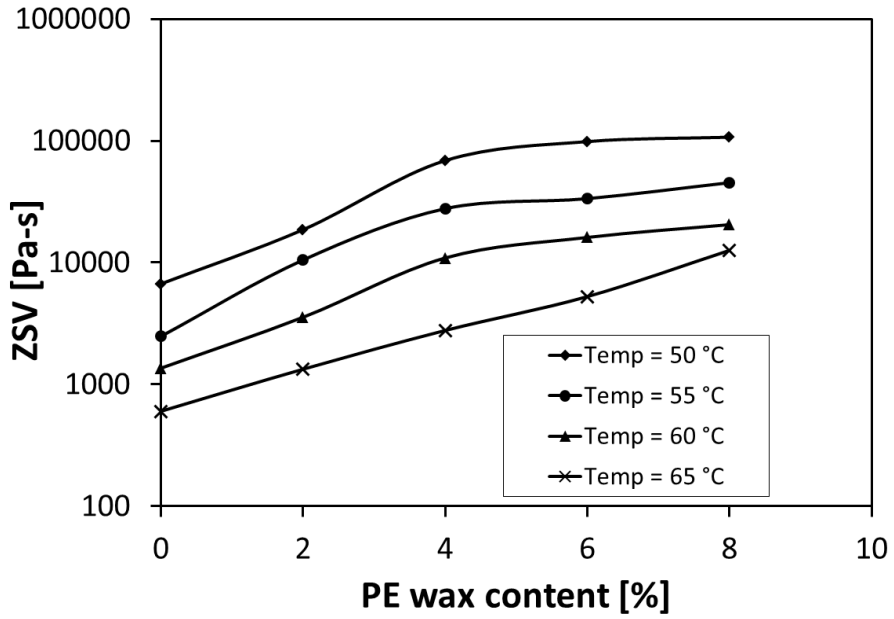

Figure 4.2. 15: Zero shear viscosity as function of polyethylene wax content for 40% Sulfur modified binders

Steady Shear Rheology

Steady rate sweep tests were conducted for all binders at 50^{o}C and shear rate of 0.01-10 s^{-1}. Steady shear viscosity as function of shear rate is plotted in Figure 4.2.15 for the 40% sulfur asphalt binders. Both the 30% and 40% sulfur asphalt binder showed the similar behavior. Pure asphalt and sulfur asphalt binder without polyethylene wax content samples displayed long Newtonian plateau, whereas polyethylene wax modified binders showed power law fluid behavior. It means that polyethylene wax incorporation to the sulfur asphalt binder resulted in shear thinning behavior. The similar results observed in polymer modified asphalt (PMA). This shear thinning behavior can attributed to the crosslinking of polyethylene wax with sulfur and asphalt molecules. As shear rate increases it destroys the crosslinking and thereby reduces viscosity sharply. This behavior is commonly modeled using power law equation which is given as:

$$\eta = c_1 \dot{\gamma} \tag{4.2.11}$$

Where, η is shear rate dependent viscosity and $\dot{\gamma}$ shear rate. The constant c_2 is slope of the line plotted by $\ln\eta$ against $\ln\dot{\gamma}$. The value of the slope shows the degree of shear thinning. It is also called the power law index. The Power law indices for polyethylene wax modified asphalt binder were calculated using the above equation and the values are listed in Table 6 along with the fitting quality r^2. Good fit was observed for all the samples listed in Table 6. It shows that an increase in polyethylene wax content increases shear thinning.

Table 4.2. 6: Power law indices for polyethylene wax modified sulfur/asphalt binders at 50°C

Asphalt binder	Polyethylene wax content [%]	Power law indices	r^2
30% Sulfur/Asphalt binders	2	-0.384	0.997
	4	-0.658	0.983
	6	-0.766	0.996
	8	-0.834	0.996
40% Sulfur/Asphalt binders	2	-0.358	0.967
	4	-0.604	0.991
	6	-0.692	0.993
	8	-0.915	0.999

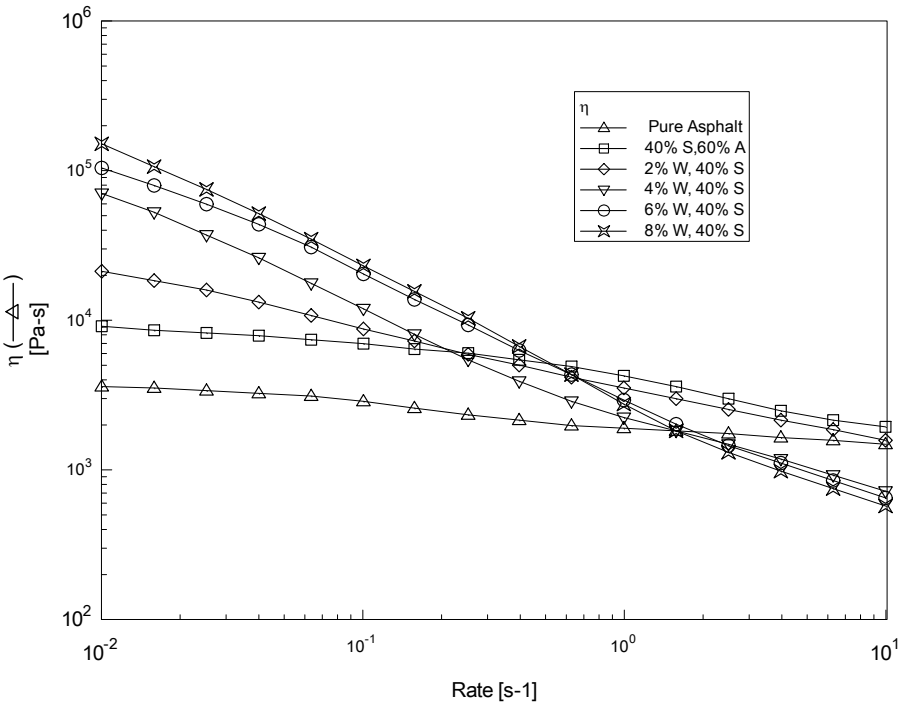

Figure 4.2. 16: Steady shear viscosity of 40% sulfur/asphalt binders at 50°C

Rolling thin film oven test

Figure 4.2.17 shows the effect of short term ageing on selective polyethylene wax modified sulfur/asphalt binders. It is clear that ageing increases η^* with a little bit increase in activation energy. The increase in activation energies for the selective RTFO samples was in the range of 4-7% than that of unaged samples. The viscoelastic properties of aged binders are generally higher than those of unaged ones. The improvement in rheological properties after ageing can be attributed to three major factors. Firstly, ageing has changed chemical compositions of asphalt. A modification of both the quantity and quality of asphaltenes and resins is likely to occur. The increase in asphaltenes and resins contents is a consequence of the effect that ageing has on the elastic properties of asphalt. Secondly, polymerization of sulfur and its crosslink with asphalt composition which is accelerated by high temperature (163^oC) and air oxidation.

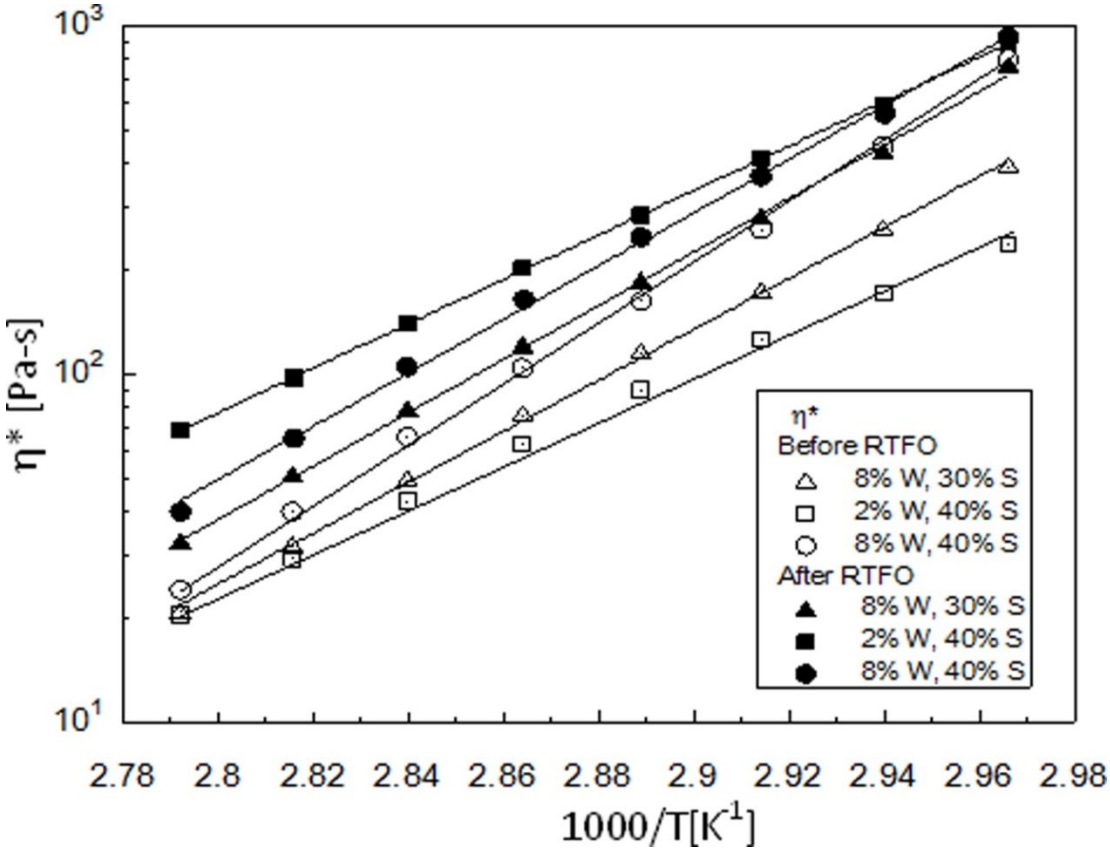

Figure 4.2. 17: Effect of ageing on complex viscosity, η^*

4.2.5 Conclusion

Utilization of waste sulfur and polyethylene wax in asphalt modification was investigated. The influence of polyethylene wax on the rheology of sulfur modified asphalt binders were investigated by FTIR, rheological and thermal characterization techniques. The following conclusions are drawn on the basis of this investigation:

1. FTIR results showed increase in C-S bond due to sulfur incorporation and C=C bond increased due to polyethylene wax addition to sulfur asphalt binder.
2. The addition of polyethylene wax significantly increased the viscoelastic properties ($\eta'$and G') of the modified asphalt binders. The 40% sulfur modified asphalt binders showed slightly higher values of η′and G′ than that of the 30% sulfur modified asphalt binders.
3. Addition of sulfur to pure asphalt reduced the activation energy ~ 30%, but polyethylene wax increases to that of pure asphalt for 4% polyethylene wax in the case of 30% sulfur extended asphalt binder. In the case of 40% sulfur extended asphalt activation energy increases more than that of 30% sulfur extended asphalt.
4. SHRP rutting parameter ($G^*/\sin\delta$) as well as zero shear viscosity (ZSV) increases with the increase in polyethylene for all sulfur asphalt binders, means that polyethylene wax modification increases rutting resistant at high temperature. ZSV analysis showed 30% sulfur extended asphalt binders are superior than that of 40% sulfur extended asphalt binders.
5. Steady shear rheology suggests polyethylene wax modification of sulfur asphalt binders leads to shear thinning behavior.
6. Short term ageing through RTFO improved the rheological properties of the modified binders by crosslinking and entanglement of sulfur and asphalt compositions.

Polyethylene wax modified sulfur asphalt showed better properties compared to the conventional asphalt binder. Utilization of these two industrial wastes in asphalt modification can meet the extra demand for asphalt, reduce the price and improve asphalt pavement life. Application of this process will help to solve the waste disposal problem and keep environment clean.

4.5.6 References

1. Al-Abdul Wahhab, H., Asi, I., Al-Dubabe, I. & Ali, M., 1997. Development of Performance-Based Bitumen Specifications for the Gulf Countries. *Construction and Building Materials ,* 11(1), pp. 15-22.
2. Bahia, H., Zeng, M., Zhai, H. & Khatr, 1999. *Superpave protocols for modified asphalt binders, 15th Quarterly Progess Report for NCHRP Project 9–10.,* Washington: DC: National Cooperative Highway Research Program..
3. Barnes, A., 2000. *A handbook of elementary rheology.* Aberystwyth: University of Wales.
4. Bellomy, R. & McGinnis, E., 1994. *Bitumen composition containing bitumen, polymer and sulfur.* Patent No. US 5371121.
5. Benzowitz, J. & Boe, E., 1938. *Effect of sulfur upon some of the properties of asphalt. Proceedings of ASTM*.
6. Binard, C., Anderson, D., Lapalu, L. & Planche, J., 2004. *Zero shear viscosity of modified and unmodified binders.* Vienna.

7. Carreau, P., Bousmina, M. & Bonniot, F., 2000. 23. Carreau PJ, Bousmina M, Bonniot F (2000), The viscoelastic properties of polymer modified asphalt. *Can J Chem Eng 78(3):495–502.,* 78(3), pp. 495-502.
8. Challa, A., Roy, C. & Ait-kadi, A., Fuel. Rheological properties of bitumen modified with pyrolytic carbon black. *Fuel,* 75(13), pp. 1575-1583.
9. Edwards, Y., Tasdemir, Y. & Isacsson, U., 2007. Rheological effects of commercial waxes and polyphosphoric acid in bitumen 160/220 – high and medium temperature performance. *Constr Build Mater,* 21(10), pp. 1899-1908.
10. Ferry, J., 1980. *Viscoelastic properties of polymers.* New York: Wiley.
11. Hussein, I. A., Iqbal, M. H. & Al-Abdul Wahhab, H. I., 2005. Influence of Mw of LDPE and vinyl acetate content of EVA on the Rheology of Polymer Modified Asphalt. *Rheologica Acta, 45(1), 92-104, 2005,* 45(1), pp. 92-104.
12. Hussein, I. A., Iqbal, M. H. & Wahhab, H. I. A.-A., 2005. Influence of Mw of LDPE and vinyl acetate content of EVA on the Rheology of Polymer Modified Asphalt. *Rheologica Acta,* 45(1), pp. 92-105.
13. Hussein, I. A., Wahhab, H. I. A.-A. & Iqbal, M. H., 2006. Influence of Polymer Type and Structure on Polymer Modified Asphalt Concrete Mix. *Canadian Journal of Chemical Engineering,* 84(4), pp. 480-487.
14. Iqbal, M. H., Hussein, I. A., Al-Abdul Wahhab, H. I. & Amin, B., 2006. Influence of Mw of LDPE and vinyl acetate content of EVA on the rheology of polymer modified asphalt. *Journal of Applied Polymer Science,* 102(4), pp. 3446-3456.

15. Kennepohl, G. & Miller, L., 1978. Sulfur-Asphalt Binder Technology for Pavements-New uses of sulfur II. In: *Advances in Chemistry.* Ontario, Canada: American Chemical society , pp. 113-134.

16. Larsen, D., Alessandrini, J., Bosch, A. & Cortizo, M., 2009. Micro-structural and rheological characteristics of SBS-asphalt blends during their manufacturing. *Constr Build Mater,* 23(8), pp. 2769-2774.

17. Lee, D.Y., 1975. *Ind. Eng. Chem., Prod. Res. Dev,* 14(3).

18. Phillips, M. & Robertus, C., 1996. *Binder rheology and asphalt pavement permanent deformation; the zero shear viscosity.1996.*. Strasbourg.

19. Planche, J., 1990. *18. J.P. Planche, Method for the preparation of bitumen–polymer compositions, 1990.* Patent No. WO 9002776.

20. Polacco, G, Giovanni, Stastna, Jiri, Biondi, Dario, Antonelli, Federico, Vlachovicova, Zora, Zanzotto, Ludovit, 2004. *Journal of Colloid and Interface Science 280 (2004) 366–373.,* Volume 280, pp. 366-373.

21. Polacco, G., Stastna, J., Biondi, D. & Zanzotto, L., 2006. Relation between polymer architecture and nonlinear viscoelastic behavior of modified asphalts. *Current Opinion in Colloid & Interface Science,* Volume 11, pp. 230-245.

22. Shenoy, A., 2002. Model-fitting the master curves of the dynamic shear rheometer data to extract a rut-controlling term for asphalt pavements. *ASTM J Test Eval,* 30(2), pp. 95-102.

23. Zhang, F., Yu, J. & Han, J., 2011. Effects of thermal oxidative ageing on dynamic viscosity, TG/DTG, DTA and FTIR. *Construction and Building Materials,* pp. 129-137.

24. Zhang, F., Yu, J. & Wu, S., 2010. Effect of ageing on rheological properties of storage-stable SBS/sulfur-modified asphalt. *Journal of Hazardous Materials,* Volume 182, pp. 507-517.

25. Zupancic, A. & Zumer, M., 2002. Rheological examination of temperature dependence of conventional and polymer-modified road bitumens. *Can J Chem Eng,* Volume 82, pp. 253-263.

4.3 Asphalt modification using Acid treated waste oil fly ash

4.3.1 Abstract

Oil fly ash (OFA) is generated in large quantities from power generation plants through combustion of fuel oil. Waste OFA contains more than 80% carbon and can be used to improve asphalt performance. H_2SO_4 and HNO_3 acids were used to functionalize the OFA with carboxylic group (-COOH) to improve its dispersion and chemical bonding with asphalt. Differential scanning calorimetry (DSC), FTIR and combined SEM/EDS techniques were used to characterize as-received and treated OFA. Asphalt modification with treated OFA shows better results than that of untreated OFA. The treated OFA were blended with base asphalt and tested for rheological properties of pure and modified asphalt binders. OFA were used at 2-8% by weight of asphalt binder. Melt state rheology was investigated in ARES rheometer using temperature sweep, dynamic shear and steady shear rheological measurements. Both steady and dynamic shear rheology showed that OFA-COOH improved the viscoelastic properties of the modified asphalt binders. OFA-COOH modification reduced temperature susceptibility of modified asphalt binder and increased the upper grading (performance) temperature. The rutting parameter $G^*/\sin\delta$ increased linearly with OFA-COOH content of asphalt binder. Activation energy was found to decrease with OFA-COOH content which indicated better resistance to low temperature cracking of the modified binder. Asphalt modification with treated OFA proved that acid treatment of OFA has enhanced the properties of asphalt mixes.

4.3.1 Introduction

Oil fly ash (OFA) is typically a black powder type waste material that results from the use of crude and residual oil in power generation. OFA is collected in the electrostatic precipitators which are installed on boilers burning residual oil for air pollution control. According to a survey of American Coal Ash Association, 69.30 million tons of coal fly ash produced in 2011 in the United States by coal fired plants and 38% of this quantity was reused in different applications (American Coal Ash Association, 2011). In Saudi Arabia, there are 70 power plants consuming 22 million metric tons of oil and the total amount of disposed OFA in 2008 was about 240,000 cubic meters. This amount is expected to increase to 400,000 cubic meters in 2014. These quantities must be disposed off in an environment friendly way. OFA is mainly used as a replacement of Portland cement; as a filler in polymers, asphalt and cementitious materials; stabilizing agent and also for adsorption of solutes and, solidification for waste and sludge (Sinha, et al., 2010; Shawabkeh & Harahsheh, 2007; Shawabkeh, et al., 2004; Woo-Teck, et al., 2005).

Additive or filler materials can be used in asphalt binders to design against or to repair pavement due to the following problems: surface defects (raveling and stripping), structural defects (rutting, shoving and distortion) and cracking (fatigue and thermal).Many authors have studied the effects of mineral fillers, which are materials passing a sieve size of 0.075mm, on the behavior of asphalt mix (Anani & Al-Abdul Wahhab, 1982; Asi & Assa'ad, 2005; Kandhal, et al., 1998; Karasahin &

Terzi, 2007). Different filler materials may have different mechanical properties in the asphalt mixture.

In a recent patent our research group used untreated OFA (3-10%) in asphalt binder and asphalt concrete mix (Al-Amethel, et al., 2011). Addition of untreated OFA improved rutting resistance, stability and modulus. However, the fatigue properties of the mix were poor due to poor dispersion of ash which is likely due to the inert nature of the OFA surface. Surface modification and grafting are widely used in the polymer literature to improve the bonding between different polymers or between polymers and asphalt. Our group has used functionalized polymers to improve the compatibility of polymers with asphalt (Iqbal, et al., 2006; Hussein, et al., 2005). The use of surface modified or functionalized materials is not new to the pavement industry. OFA contains more than 80% carbon, 7% oxygen, 9% sulfur and the rest are trace metal.

Recently, surface modification of carbon nanotubes (CNT), which resembles OFA in composition, has improved the dispersion in polymers and improved the bonding between the polymer and CNT (Abbasi, et al., 2013). The proven success of surface modification in polymers, polymer nanocomposites and polymer-modified asphalt in improving the interfacial bonding suggests the potential of chemical modification of OFA in improving the dispersion and bonding with asphalt. Therefore, it is suggested to chemically treat the surface of OFA to using the same previous CNT surface modification techniques. The present study focused on the surface modification of

OFA with carboxylic group (-COOH) and characterization of acid treated OFA (OFA-COOH). Then the influence of OFA-COOH on asphalt binder thermo-rheological properties was studied. The authors are not aware of any previous research that attempted to use acid treated waste OFA in asphalt modification.

4.3.2 Experimental

Materials

OFA was collected from Shuaibah power plant of Saudi Electricity Company. The concentrated sulfuric acid (H_2SO_4, 98%) and nitric acid (HNO_3, 68%) were obtained from the Sigma Aldrich Company and they were used as-received without further purification. Asphalt cement of 60/70 penetration grade was obtained from Saudi Aramco Riyadh Refinery.

OFA Functionalization

As-received OFA was washed with water to separate trace oil and some sandy particles. Washed OFA was then dried in the oven at 105^{o}C to evaporate the remaining water. The OFA was then treated with H_2SO_4 and HNO_3 at a volumetric ratio of 3:1. A weight of 200g ash was taken into a 3 liter glass beaker and the acid solution was slowly poured into the ash. After 10 minutes, the ash/acid mixture turned to liquid solution. The beaker with OFA/acid solution was put in hot plate magnetic stirrer assembly. The temperature and speed of rotation of the hot plate were set at 165^{o}C and 100 rpm, respectively. The reaction was allowed to continue

for 12 hours to create the carboxylic acid group on the OFA surface. The reactant mixture was then cooled down to room temperature. The mixture was diluted with deionized water and filtered using vacuum-filter through a 3 μm porosity filter paper to remove unreacted acid. The filtered OFA was then dried in hot chamber at temperature ~ 90^{o}C. The chemically treated OFA following this method is referred to as OFA-COOH.

FTIR Characterization

As-received OFA, modified OFA (OFA-COOH) and OFA/asphalt blend were characterized by FTIR using a Nicolet 6700 spectrometer from Thermo Electron™. A weight of 1-2 mg of OFA was mixed thoroughly with 1.0 g of fine dried powder of KBr. Then, the resulting mixture was hydraulically pressed in a Carver press to obtain a thin transparent disc. The thin disc was placed in an oven at 110^{o}C for 2 h to prevent any interference of any existing water vapor or carbon dioxide molecules. All the FTIR spectra were taken in the transmission mode and in the range 600–4000 cm^{-1} at room temperature. FTIR spectra were obtained using a spectral resolution of 4 cm^{-1} and 30 co-added scans.

Thermal Analysis

The thermal behavior of as-received and treated OFA was determined by means of a TA Q1000 DSC. A Sample of 7-10 mg was weighed and sealed in aluminum hermetic pans. The thermal stability of as-received OFA and OFA-COOH was determined by heating the samples from room temperature to 250^{o}C using at

5^{o}C/min. Pure Nitrogen (99.99%) gas was used to purge the DSC cell a flow rate of 50 ml/min.

SEM and EDX

The scanning electron microscope (JEOL, model JSM 6400) was used to determine the qualitative characteristics and morphology of the fly ash sample. The dried sample was fixed with double side masking tape. In order to make it surface conductive, the fly ash sample was gold coated. It was then viewed on FE-SEM at different magnification to see the surface topography of the sample. Energy dispersive X-ray (EDX) analysis was carried for the analysis of chemical composition of as-received OFA and OFA-COOH.

Sample Preparation for Rheological Testing

OFA and pure asphalt were blended in a high shear blender. The blender acts as a batch stirred tank with a constant temperature bath. Typical mixing procedure was as follows: steel cans of approximately 1000 mL were filled with 250–260 g of asphalt and put in a thermoelectric heater. When the temperature of the asphalt has reached 145°C, a high shear mixer was dipped into the can and set to about 1000 rpm. Calculated amount of OFA was added gradually with base asphalt. The bath temperature was maintained at 145 ± 1°C. Samples were blended for 10 minutes at high shear to confirm uniform distribution of OFA in asphalt matrix. Asphalt sample was poured into silicone molds before being used for rheological testing. The samples specimens were stored in a refrigerator at 5°C.

Rheological Measurements

Dynamic and steady shear rheological tests were carried out to investigate the effect of OFA-COOH on the rheology of modified asphalt binder. The dynamic temperature step measurements were performed in ARES rheometer. This is a constant strain rheometer equipped with a heavy transducer (range 2-2000 g for normal force; 2-2000 g-cm for torque). All tests were carried out in the temperature range 64^{o}C-100^{o}C using a parallel plate set of 25 mm diameter. Then, the sample was heated to 64^{o}C for about 5 minutes; thereafter the gap between the plate platen was adjusted to 1.5 mm by lowering the upper platen force transducer assembly at a constant load of 500 g. The melt that extruded beyond the platen rim by this procedure was cleaned off. Strain in the linear viscoelastic range (strain amplitude, γ^{o} of 12.5 %) and a frequency of 10 rad/s were in the temperature step test. A holding period of 5 min was allowed before beginning measurements when the temperature reaches steady state. The dynamic frequency sweep tests were conducted at 60^{o}C in the range 100-0.1 rad/s at a strain of 10%. Steady shear rheological tests were performed at 50^{o}C and a shear rate in the range of 0.01-10 s^{-1}. In all experiments, nitrogen gas was continuously used for heating the samples during testing to avoid oxidation during testing.

4.3.3 Results and Discussion

OFA surface modification

Surface modification of OFA was done to introduce carboxylic group as described in OFA functionalization section. The carboxylic group (-COOH) was successfully attached to the surface of OFA and it was detected through different characterization technique such as: FTIR spectra, SEM/EDS analysis and DSC analysis.

SEM/EDS Analysis

Evaluation of common and predominant phases within ash samples during treatment was obtained by Energy Dispersive X-ray analysis (EDX) as shown in Table 4.3.1. The surface morphology of ash samples is shown in Figure 4.3.1(a & b). It is apparent that most of the ash particles are spherical in shape with high porosity. The size of these particles is in the range of 10-100 μm. SEM/EDX analysis of OFA particles was performed to determine the ratio of carbon, oxygen and sulfur in these samples. Carbon to oxygen ratio in these samples illustrates the degree of oxidation before and after treatment.

Oxygen to carbon ratio has changed according to the acid treatment method. The ratio of oxygen/carbon in ash before treatment was 0.087 whereas in the treated ash, it was 0.283. This increase in the ratio could be attributed to the addition of -COOH group to OFA surface. Another finding is that, the acid treatment completely removes the trace metals such as vanadium, iron, and nickel from OFA. Acid treatment also

increased the ratio of sulfur/carbon. This could be due to the formation of CO_2 and CO gases as it was visible during the first 30 minutes of reaction. These gases escaped from ash sample, which decreased the amount of carbon and thus increase the relative amount of sulfur.

Table 4.3. 1: Elemental analysis of OFA before and after treatment

SN	Elements	Before treatment		After treatment	
		Weight %	Atomic %	Weight %	Atomic %
1	C	79.99	89.40	67.58	77.75
2	O	7.02	5.89	19.15	16.54
3	S	8.74	3.66	13.16	5.72
4	V	1.83	0.48	0	0
5	Fe	1.07	0.26	0	0
6	Ni	1.36	0.31	0	0
Total		100	100	100	100

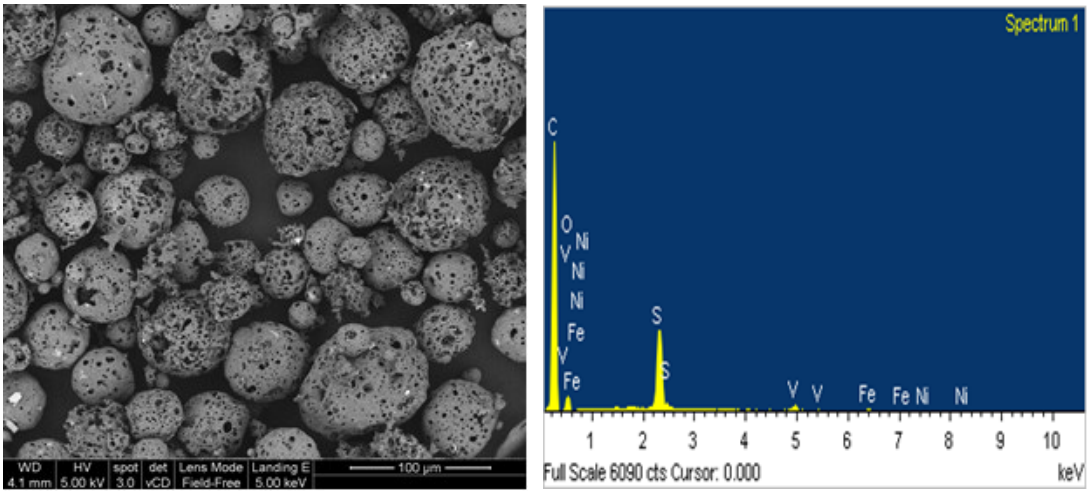

(a) SEM/EDS analysis of as-received OFA

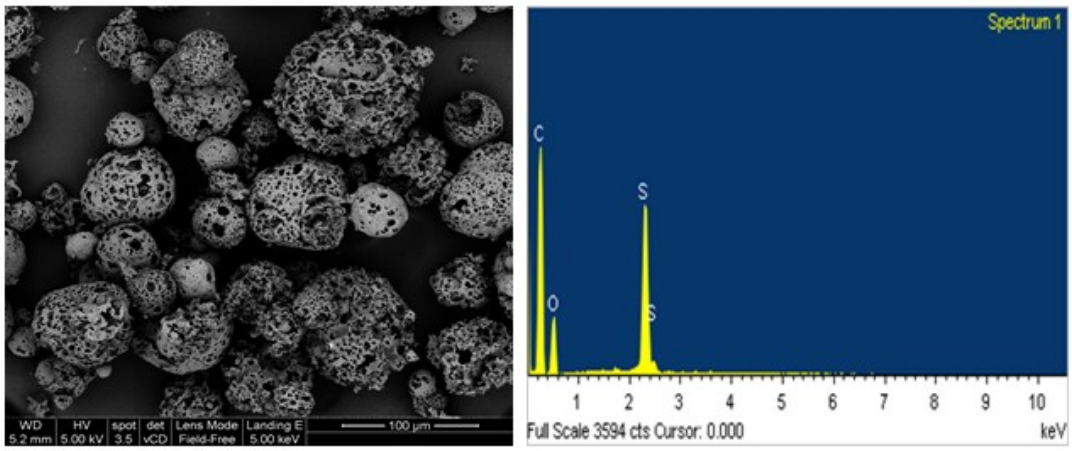

(a) Acid treated OFA sample

Figure 4.3. 1: SEM/EDS analysis of OFA samples

FTIR Analysis

FTIR technique was used to determine whether a new functional group is attached to the fly ash surface after chemical activation. Figure 4.3.2 (a & b) shows the FTIR spectra of as-received and treated OFA over the range of 4000–600 cm^{-1}. The intensity of the peaks for as-received OFA is very small compared to that of treated OFA. An inset of the main portion of as-received sample spectra shows that it has three peaks at 2022, 2162.3 and 2183 cm^{-1}. The peak at 2022 $cm^{-1}$is attributed to transition metal (Fe and Ni) carbonyl compound. The peaks at 2162.3 and 2183cm^{-1} are due to the C≡C stretch of medial alkyne (Coates, 2000).

Figure 4.3.2 (b) shows five major peaks for OFA-COOH at 1216.9, 1365.4, 1742.4, 2849.3 and 2917.3 cm^{-1}, respectively. The peak at 1216.9 cm^{-1} is due to the skeletal vibration of C-C bond whereas the peak at 1742.37cm^{-1} is attributed to the C=O stretching mode of carboxylic acid group (Bikiaris, et al., 2008) indicating the presence of –COOH group on the surface of treated OFA. The peaks around 2849.3 and 2917.3 correspond to the H−C stretch modes of H−C=O in the carboxyl group. The peak at 1365.4 corresponds to the presence of O-H functional group (Shawabkeh, et al., 2011). Therefore, the FTIR study confirmed that carboxylic acid functional group was incorporated on the surface of OFA through acid treatment.

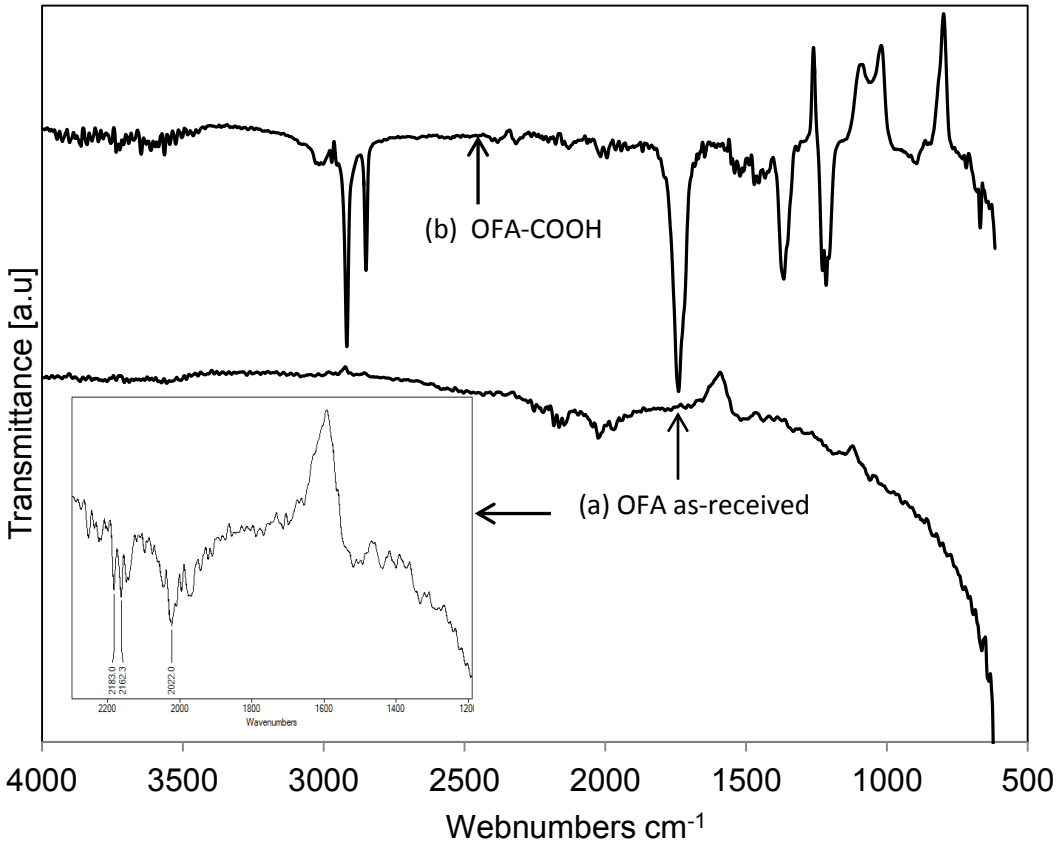

Figure 4.3. 2: FTIR spectrum (a) OFA before treatment (b) OFA after chemical treatment

DSC Analysis

As-received OFA and OFA-COOH were characterized using the differential scanning calorimetry (DSC) in standard mode to detect the presence of any functional group on the OFA surface. The samples were heated from 25^{o}C to 250^{o}C at 5^{o}C/min and the result is shown in Figure 4.3.3. It is known from the thermodynamic principle that the decomposition of chemical bond releases energy which can be detected by

exothermic peak in DSC experiment. The DSC scan of as-received OFA shows that it has no exothermic peak whereas OFA-COOH sample shows an exothermic peak at 165.06^{o}C.This exothermic peak of OFA-COOH sample confirmed the presence of carboxylic group in the acid treated OFA sample which supports our findings through FTIR analysis. The broad endothermic peak at around 100^{o}C is due to the evaporation of moisture from the sample. In addition, the decomposition of the –COOH at ~165°C suggests that at typical blending temperatures of asphalt (140°-160°C) and with high shear the decomposition of OFA-COOH will lead to the formation of OFA-COO^{-} which can react with unsaturated molecules in asphalt and lead to the formation of chemical bonding between asphalt and OFA.

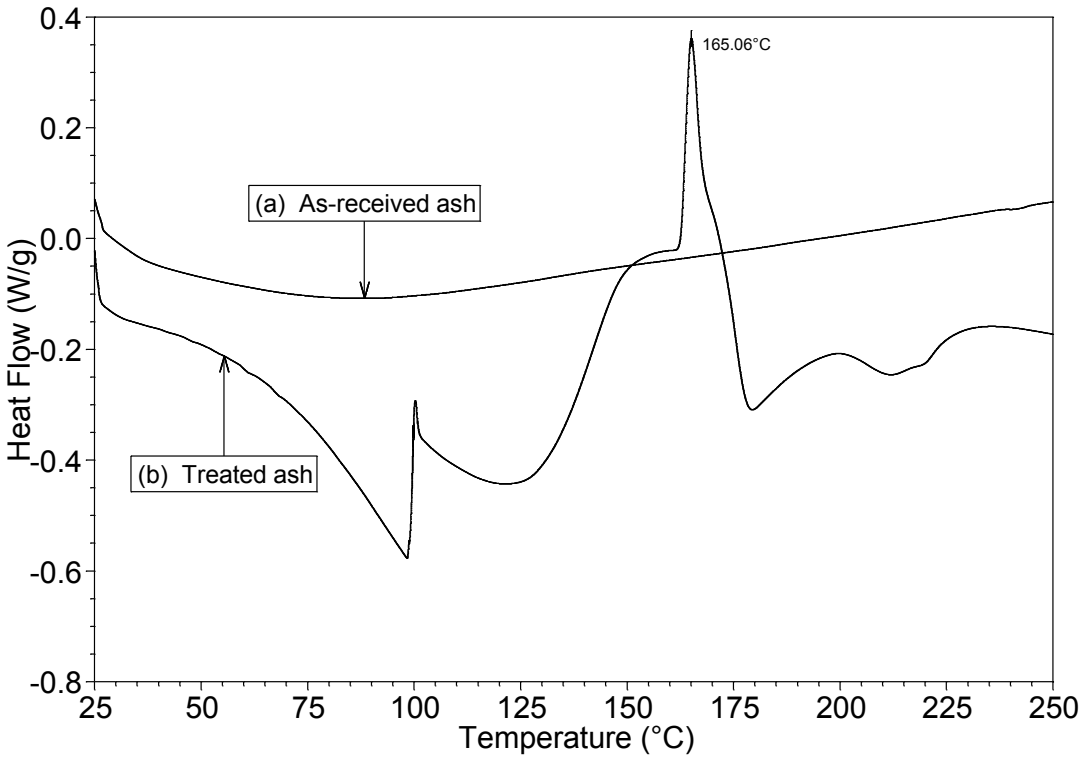

Figure 4.3. 3: DSC scans of as-received OFA and OFA-COOH samples

Rheology of OFA-COOH/asphalt binders

Temperature sweep measurements

Temperature sweep test was conducted for all binders to extract the values of complex moduli, G^* and phase angle, δ, as function of temperature. According to the strategic highway research program (SHRP), the stiffness parameter $G^*/\sin\delta$ is a factor used to estimate the rutting resistance of asphalt binder (The Asphalt Institute, 2003). $G^*/\sin\delta$ should be larger than 1 kPa at the maximum pavement design temperature for unaged original asphalt, when measured at 10 rad/s to simulate traffic

loading. Higher values of $G^*/\sin\delta$ are expected to give a high resistance to permanent deformation.

Figure 4.3.4 shows $G^*/\sin\delta$ versus temperature for pure asphalt, 4% as-received OFA modified asphalt and 4% OFA-COOH modified asphalt binder. The increase in $G^*/\sin\delta$ value for as-received OFA is very small compared to that of treated OFA/asphalt binder. Fig. 4.3.5 shows $G^*/\sin\delta$ versus OFA-COOH content of asphalt binder for different temperatures. It shows the need for chemical treatment of as-received OFA. It shows that the modification of asphalt binder with OFA-COOH increases the rutting resistant significantly and there is a linear relation between OFA-COOH content and $G^*/\sin\delta$. Table 4.3.2 lists the maximum temperature attained at $G^*/\sin\delta \geq 1$kPa. It is mentioned that the maximum local pavement temperature for Saudi Arabia is 76^{o}C for hot summer season (Al-Abdul Wahhab, et al., 1997). Base asphalt cannot fulfill SHRP criteria as the maximum temperature at $G^*/\sin\delta \geq 1$ is 70^{o}C. So, there is a need for modification of pure asphalt binder to increase $G^*/\sin\delta$ to improve rutting resistance. It is noticed that 2% OFA-COOH is needed to upgrade the binder performance from 70^{o}C to 76^{o}C. As the percentage of OFA-COOH increases in the binder, the stiffness of binders goes up. So, the binder modification with treated OFA which is expected to impact the rutting resistance of permanent deformation and increase the temperature range of its application.

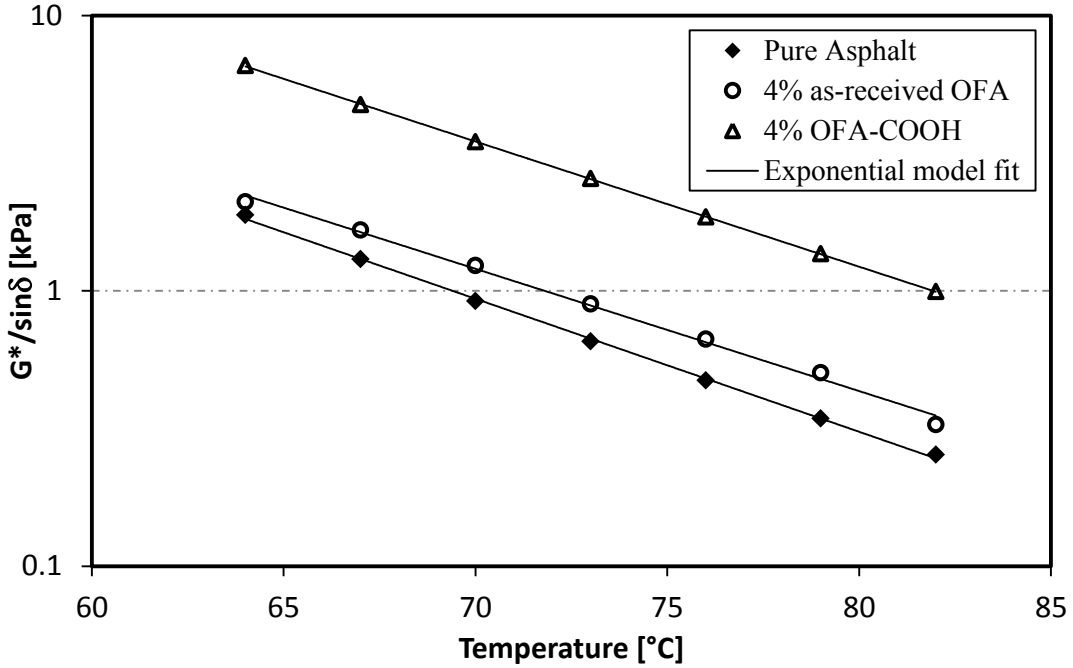

Figure 4.3. 4: $G^*/\sin\delta$ versus temperature for treated and as-received OFA-asphalt binder

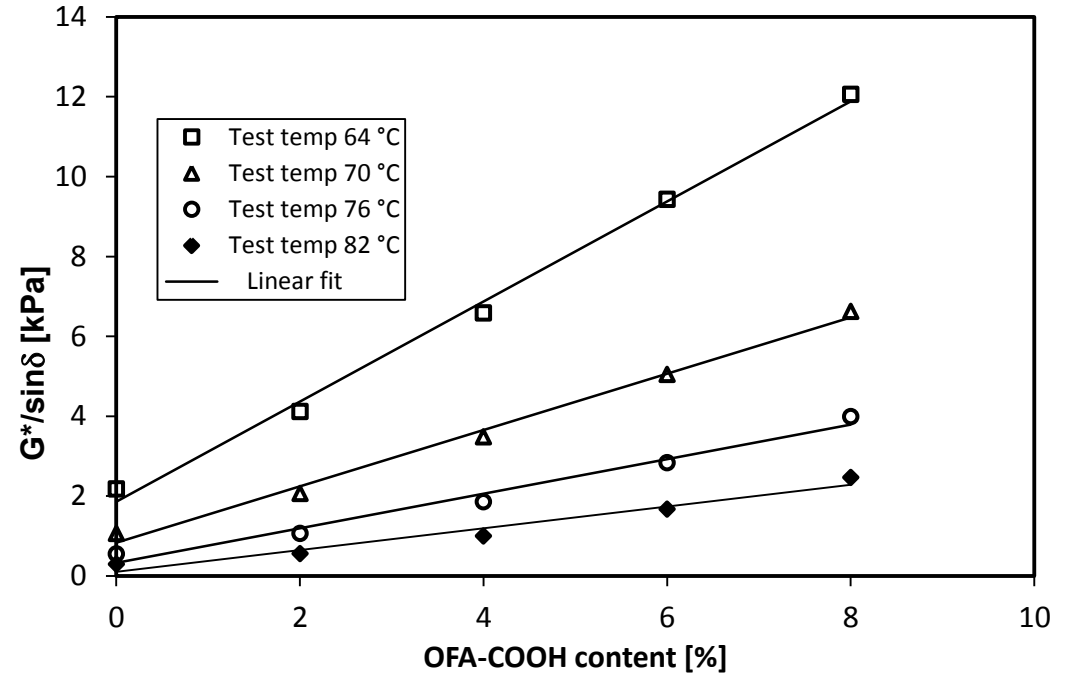

Figure 4.3. 5: $G^*/\sin\delta$ versus OFA-COOH content of asphalt binder for different temperature

Table 4.3. 2: temperature at G*/sinδ = 1kPa for all binders

Binder #	OFA content, %	Max. Temperature attained, °C @ $G^*/\sin\delta$=1 kPa	
		OFA as-received	OFA-COOH
1	0	69.62	69.62
2	2	70.90	76.15
3	4	71.20	81.25
4	6	74.18	85.25
5	8	75.09	88.50

The complex modulus, G* has two components, elastic modulus (G′) and loss modulus (G′′). So, G*/sinδ does not represent the elastic behavior of the binder only. Rheological data of temperature sweep measurement can be quantitatively appreciated by introducing a modification index, I_M. Similar analysis was also used (Airy, 2011)for SBS modified bitumen. To assess the elastic modification of the modified binders we have defined an elastic modification index by the ratio of elastic moduli as:

$$I_M = \frac{\text{Elastic modulus of modified binder}}{\text{Elastic modulus of pure asphalt}} \quad (4.2.1)$$

The calculated modification index from equation (4.3.1) has been plotted against temperature in Figure 4.3.6 in a semi log plot. It shows that the viscoelastic properties of treated OFA modified asphalt binder increases with respect to temperature. If the value of I_M is higher than 1 then the modified binders has more resistance to

temperature deformation. I_M increases with both temperature and OFA-COOH content. I_M versus temperature data are well fitted by exponential equation of the following form:

$$I_M = ae^{bT} \tag{4.2.2}$$

Where, a and b are fitted parameter which are listed in Table 4.3.3. The values of the parameters increases with the increase in amount of OFA-COOH content of the modified binders. It is also interesting to observe that the variation of the modification index within a certain temperature interval is controlled by the material sensitivity to temperature. In this way, the slope of the I_M values, b, is an indirect indicator of the thermal sensitivity and can be used to describe the influence of temperature on the rheological properties. However, higher I_M values also indicate that the corresponding sample will be stiff at lower temperature and can crack easily at low pavement temperature. So, the amount of OFA-COOH content should be optimized to suit both high and low temperature applications. The treated OFA has carboxylic group which was proved earlier by different technique. At the blending condition, high temperature and shear force can cause the decomposition of the carboxylic group which can create crosslink with unsaturated molecules part of the asphalt binder. The improvement of the elastic properties with temperature can be due to the cross-linking of $OFA\text{-}COO^-$ with asphalt.

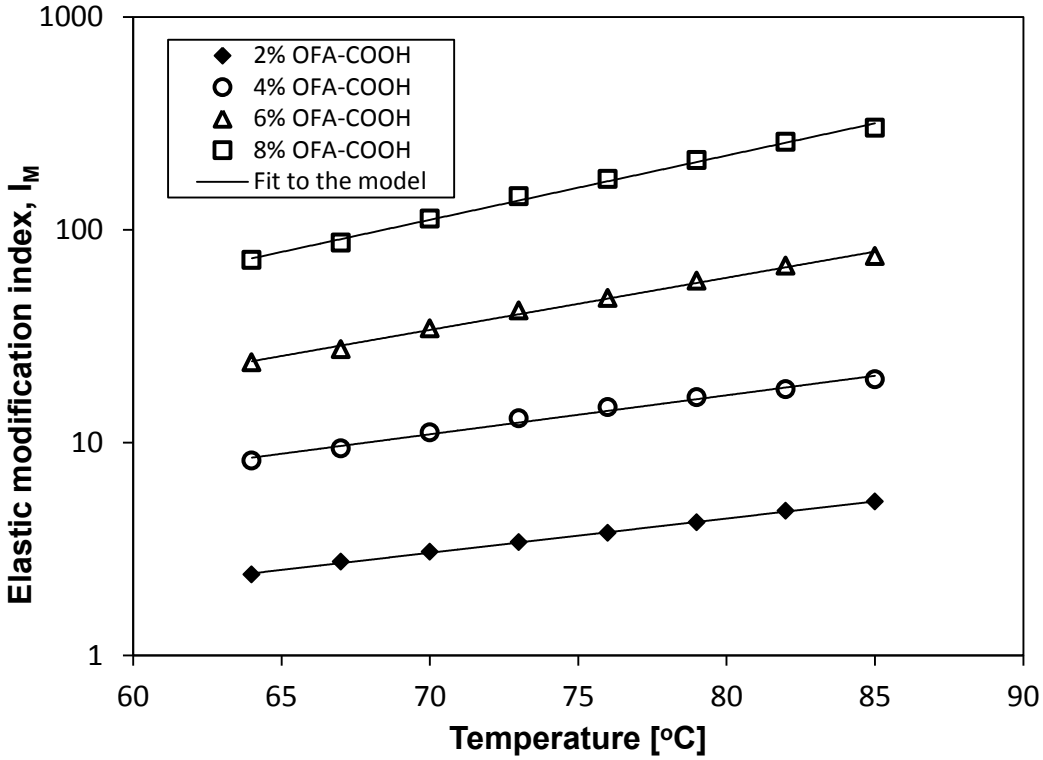

Figure 4.3. 6: Elastic modification index (I_M) as function of temperature for different amount of OFA-COOH content

Table 4.3. 3: Model parameters for equation (4.3.2) for all binders

OFA-COOH content, %	Model parameters		
	a	b	R^2
2	0.23	0.0371	0.999
4	0.57	0.0422	0.988
6	0.65	0.0565	0.994
8	0.86	0.0696	0.996

Temperature sweep data was further analyzed to check the effect of temperature on the asphalt viscosity. Viscosity-temperature relationships of asphalt binder can be expressed by the well-known Arrhenius equation as follow:

$$\frac{G^*}{\omega} = \eta^* = Ae^{\left(E_a/RT\right)} \tag{4.2.3}$$

where, E_a is the flow activation energy, A is the pre-exponential term, and R is the universal gas constant. E_a is an important factor that strongly influences the viscosity. Figure 4.3.7 shows complex viscosity versus 1000/T for pure and modified asphalt binders. The data given in Figure 4.3.7 showed good fit to Arrhenius model. E_a was calculated using equation (4.3.3) and the values for different binders are plotted in Figure 4.3.8. Activation energy for pure asphalt is 113 kJ/mol.

It is observed that addition of OFA-COOH to asphalt reduces the activation energy of the modified asphalt binder as compared to pure asphalt. This reduction of activation follows a linear relationship with OFA-COOH content of the binders which as shown in Figure 4.3.8. Activation energy reduction ranges from 4.6 to 27.95% for 2% to 8% OFA-COOH. The maximum percentage of activation energy reduction is 27.95% for 8% OFA-COOH. Activation energy, E_a has been related to the binder thermal susceptibility (García-Morales, et al., 2004). The lower is activation energy of asphalt binders means lower temperature susceptibility. So, from Figure 4.3.8 it can be concluded that all the modified asphalt binders would be less temperature susceptible than pure asphalt.

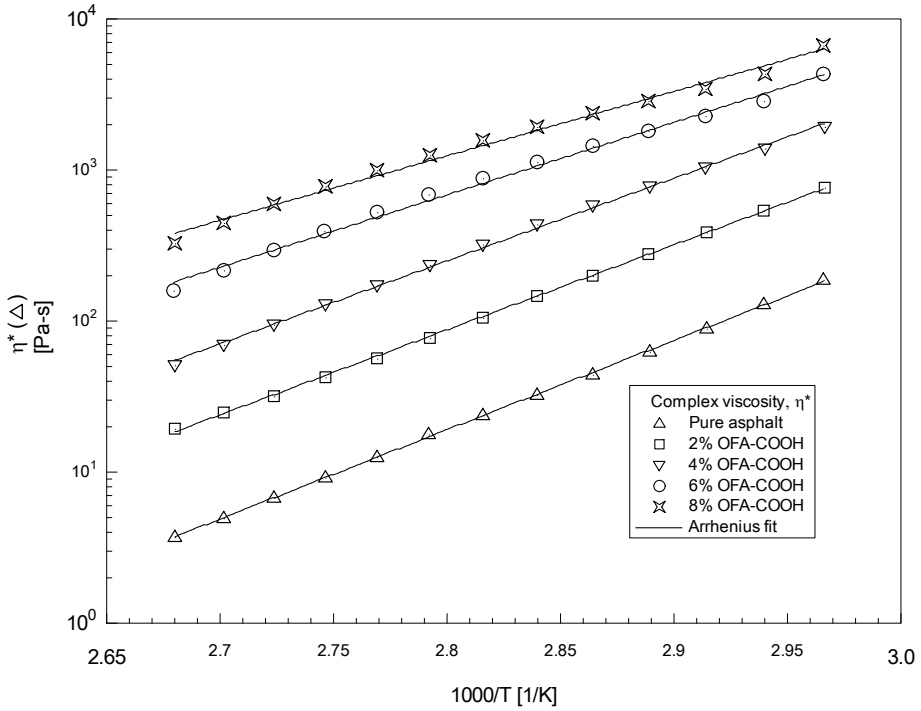

Figure 4.3. 7: Effect of temperature on complex viscosity for all binders

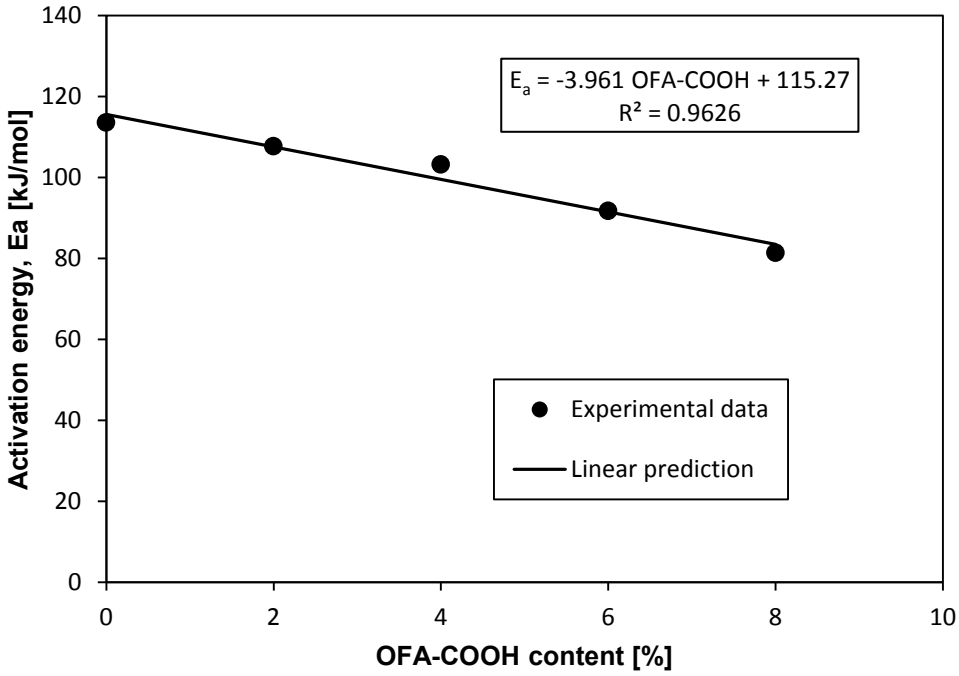

Figure 4.3. 8: Activation energy as function of OFA-COOH content of the asphalt binders

Dynamic frequency sweeps

Dynamic frequency sweep testing for all binders were conducted at 60^{o}C and 100-0.1 rad/s for small deformation (10% strain) in the linear viscoelastic range. Typical linear viscoelastic properties of the OFA-COOH modified asphalt binder are displayed in Figure 4.3.9-4.3.11. G' as function of frequency is shown in Figure 4.3.9 for pure and modified binders at 60°C. The results are shown for 0%, 2%, 4%, 6% and 8% OFA-COOH. The data showed good fit of the five elements Maxwell model. The modified asphalt binder has improved storage modulus, G', as compared to base asphalt for the whole frequency range. The increase in G' values is higher at higher concentration of OFA-COOH. G' is highly sensitive to the morphological state of a heterogeneous system (Cho, et al., 2009). The value of G' is an indication of how much elasticity can be boosted by asphalt modification. The advantage of high G′ is in high temperature climates. Higher G′ values at low frequency range suggest better flexibility. According to the principle of time–temperature superposition, this behavior corresponds to long service time or higher temperature, which is needed in hot climates. The slopes of log G′ versus log ω for low ω were calculated and its values are in the range 0.49-1.43 for modified binder with OFA-COOH content in the range 0-8%. So, the melt rheology of OFA-COOH modified asphalt binder suggests that modified asphalt binders are expected to show better rutting resistance at high temperature.

Figure 4.3.10 shows the dynamic viscosity as function frequency at 60°C. Data showed good fit to Carreau model. The profile of $\eta'(\omega)$ for pure asphalt showed typical Newtonian behavior over almost the entire frequency range, but OFA-COOH modified asphalt binder displayed non-Newtonian behavior, which was more pronounced at high OFA-COOH concentrations. Similar behavior was observed for asphalt modification with polymers (Iqbal, et al., 2006; Hussein, et al., 2005).

Figure4.3.11 represents the well-known Black diagram (phase angle versus G*) representation for pure and modified binders at 60°C. As mentioned by other author (Airey, 2003; Cuadri, et al., 2012) that the reduction of phase angle is related to the presence of elastic networks or entanglements in the modified binder. It is noticed that incorporation of OFA-COOH in asphalt binder decreases the phase angle which means improvement in elastic behavior. This improvement can be due to increase in the degree of crosslinking and/or interfacial bonding between entanglement produced by OFA-COOH and asphalt matrix. The combined effect of shear and heat in the blender could results in several phenomena in the modified asphalt matrix. Some of them can be as: (1) Decomposition of OFA–COOH group into OFA-COO^- and its reaction with asphaltenes and maltenes (2) Increase in compatibility of OFA-COOH and asphalt which could increase the dispersion of OFA in asphalt matrix (3) Change in compositions of asphalt by thermal and mechanical degradation. The combination of these phenomena can lead to cross-linking or improvement in dispersion that will eventually enhance the viscoelastic properties of the modified asphalt binders.

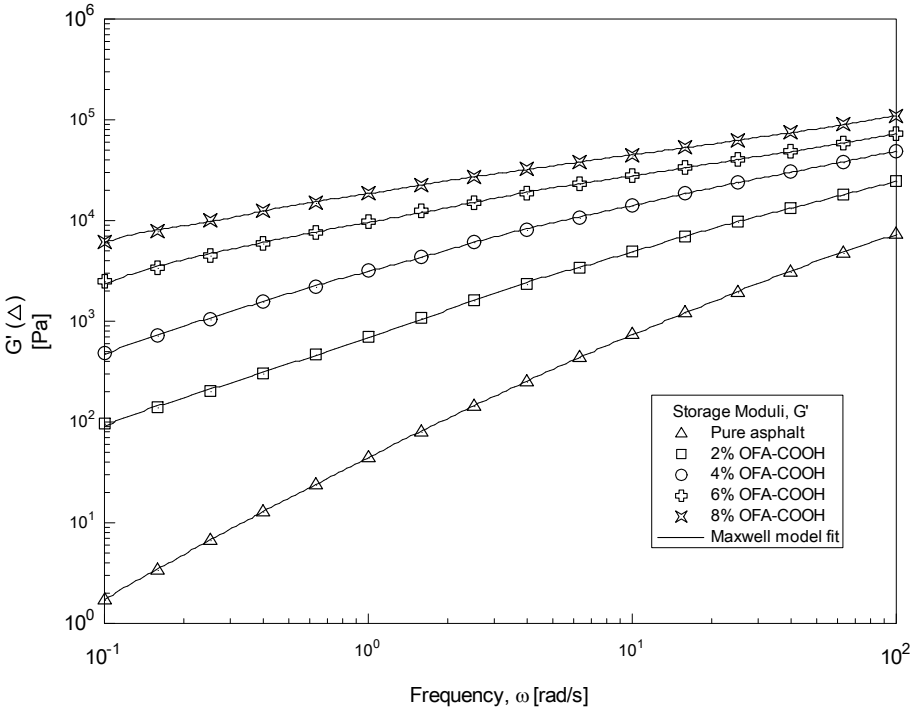

Figure 4.3. 9: Dynamic storage moduli G′as function of frequency at 60°C

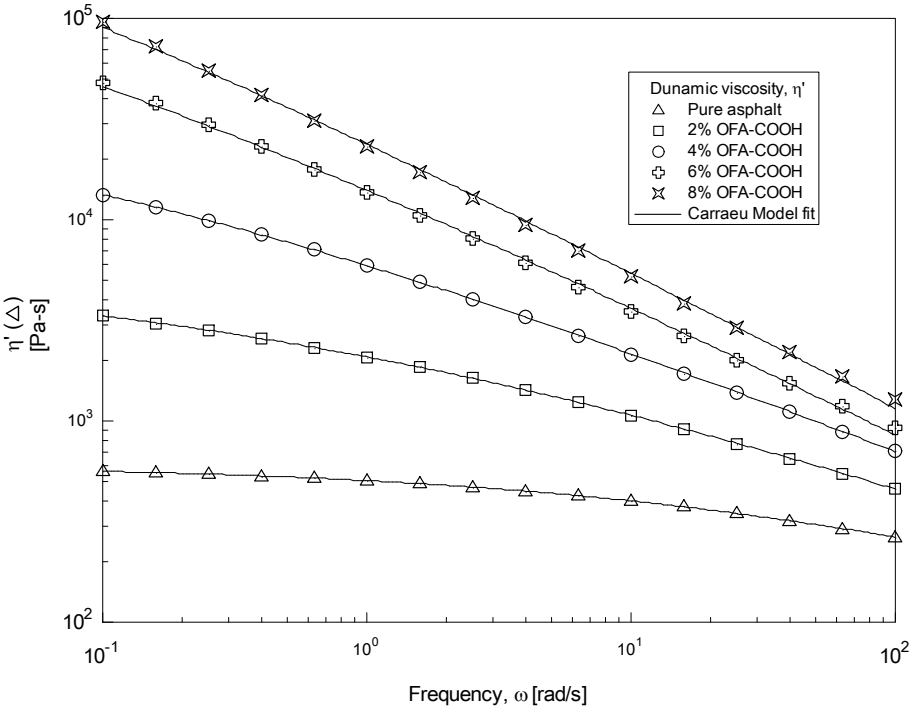

Figure 4.3. 10: Dynamic shear viscosity as function of frequency at 60°C

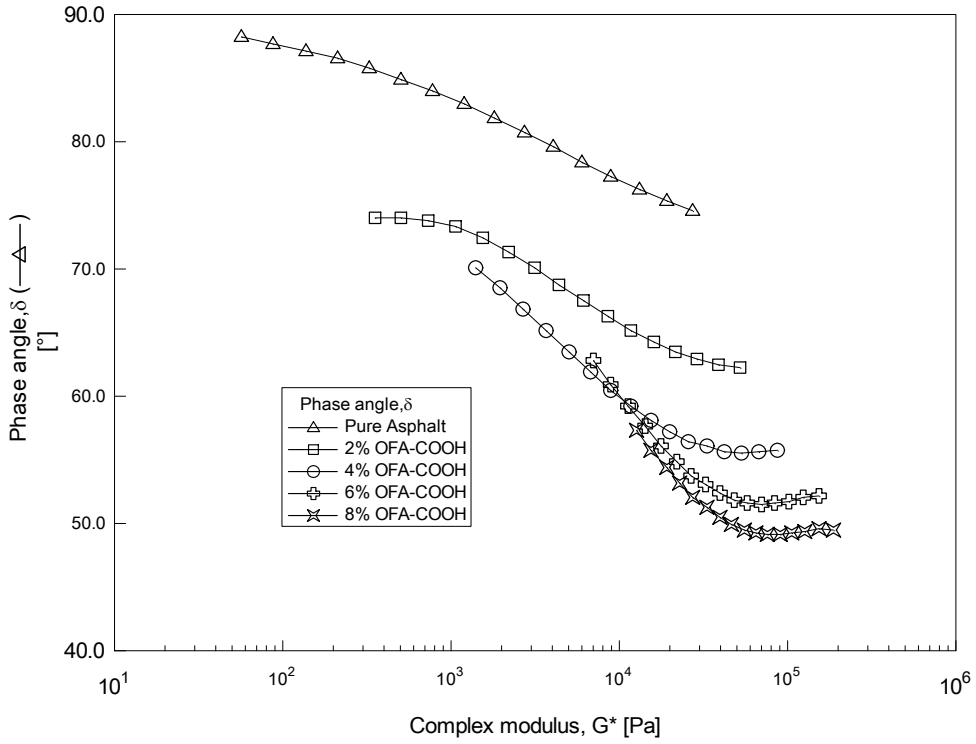

Figure 4.3. 11: Black diagram representation of asphalt binders at 60°C

Steady shear rheology

Steady rate sweep tests were conducted for all binders at 60^{o}C in the range 0.01-4 s^{-1}. Steady shear viscosity as function of shear rate is plotted in Figure4.3.12 for pure and OFA-COOH modified binders. Pure asphalt samples displayed long Newtonian plateau up to the shear rate ~ 2 s^{-1}. The OFA-COOH modified binders showed initial very small width of Newtonian plateau followed by shear thinning behavior at high shear rate. The similar behavior was also reported for polymer modified asphalt binders (Polacco, et al., 2006). These types of shear viscosity data can be well modeled by Carreau model which is given by following equation:

$$\eta = \frac{\eta_0}{\left[1+\left(\quad \right. \right.} \qquad (4.2.4)$$

where, η_0 is the zero shear viscosity, $\dot{\gamma}$ is the critical shear rate for the onset of shear thinning region and a is a parameter related to the slope of the shear thinning region. The shear rate viscosity data were well fitted by the model as can be seen from the Figure 4.3.12. It is noticed that incorporation of OFA-COOH to the asphalt binder increases the viscosity of the binder. As the amount of OFA-COOH is increased in the binder the Newtonian plateau decreases and the shear thinning region increases. This shear thinning behavior can be attributed to the broad molecular weight distribution which results from the size heterogeneity due to the addition of OFA and the possible cross-linking of OFA-COOH and asphalt.

Recently, researchers have observed that the SHRP rutting parameter $G^*/\sin\delta$ is not very effective in predicting the rutting performance of binders, especially in the case of modified binders are used (Shenoy, 2002; Bahia, et al., 1999). For such case a new parameter, zero shear viscosity (η_o) has been suggested by many researchers as a possible measure for the rutting resistance of modified asphalt binders (Binard, et al., 2004; Phillips & Robertus, 1996).η_o was calculated for all binders using equation (4) and the values are shown in Table 4.3.4. It is observed that η_o increases with the increase in OFA-COOH content reported earlier in the analysis of dynamic shear rheology data. The increment in η_o is more pronounce at high OFA-COOH content in

the binders. Also, power law index, n, was obtained and tabulated in Table 4.3.4.The results show enhancement in shear thinning due to the addition of OFA-COOH.

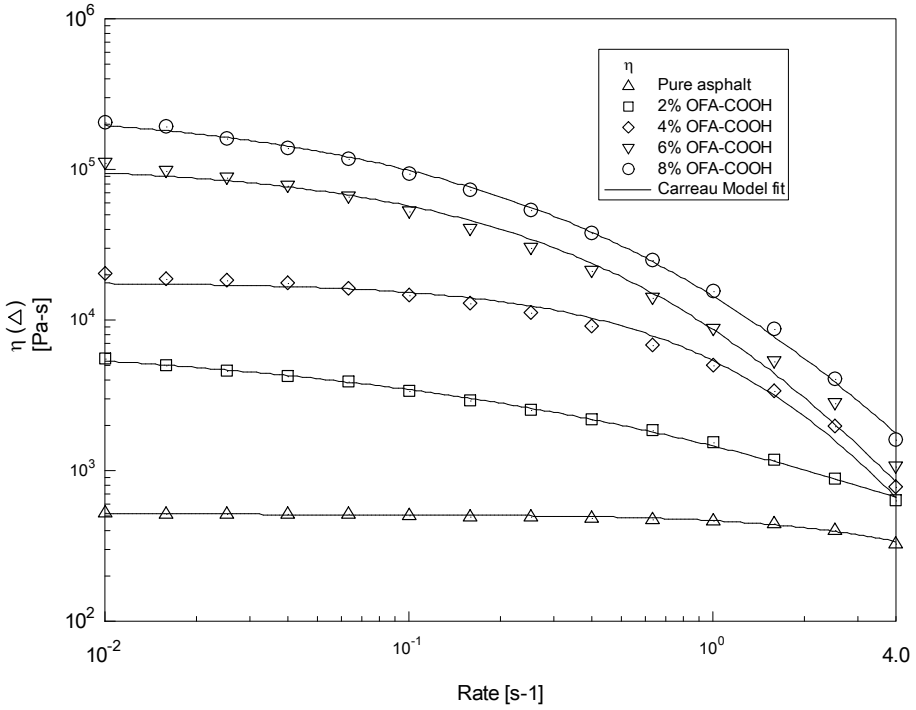

Figure 4.3. 12: Steady shear viscosity function at 60°C

Table 4.3. 4: Carreau model parameters for steady shear data

OFA-COOH Content	Carreau Model Parameters		
	Zero-Shear Viscosity,η_o, (Pa.s)	Power law index, n	Regression coefficient, R^2
0	513	0.68	0.979
2	7491	0.32	0.999
4	17787	-0.60	0.984
6	108800	-0.75	0.991
8	262000	-0.83	0.995

Creep test results

Creep test was conducted for all binders at 60°C to get the rutting behavior of pure and modified asphalt binder. The applied pressure was held constant at 100 Pa and the corresponding strain was measured as function of time. Figure 13 shows the strain response as function of time. The results show that addition of OFA-COOH to asphalt increases the rutting resistance. Figure 4.3.14 represents strain at 10 minutes versus OFA-COOH concentration in the binders. It shows that strain decreases exponentially with the increase in OFA-COOH which support our previous analysis in temperature sweep data analysis section.

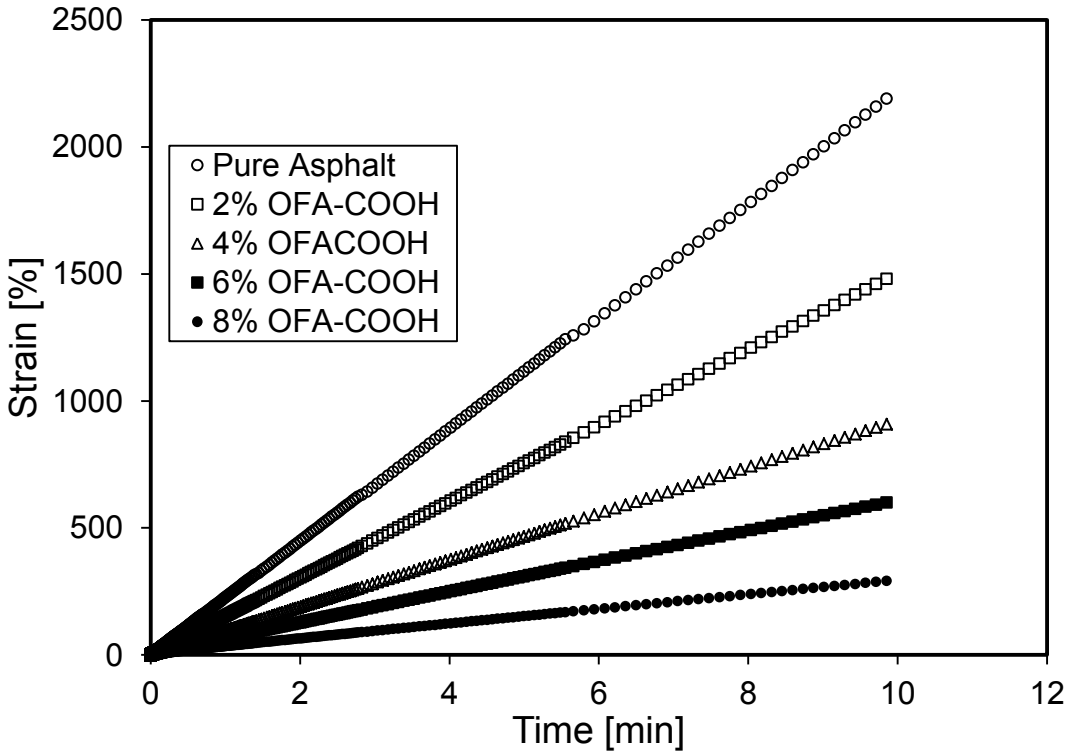

Figure 4.3. 13: Creep test results for pure modified binder at 60°C and 100 Pa

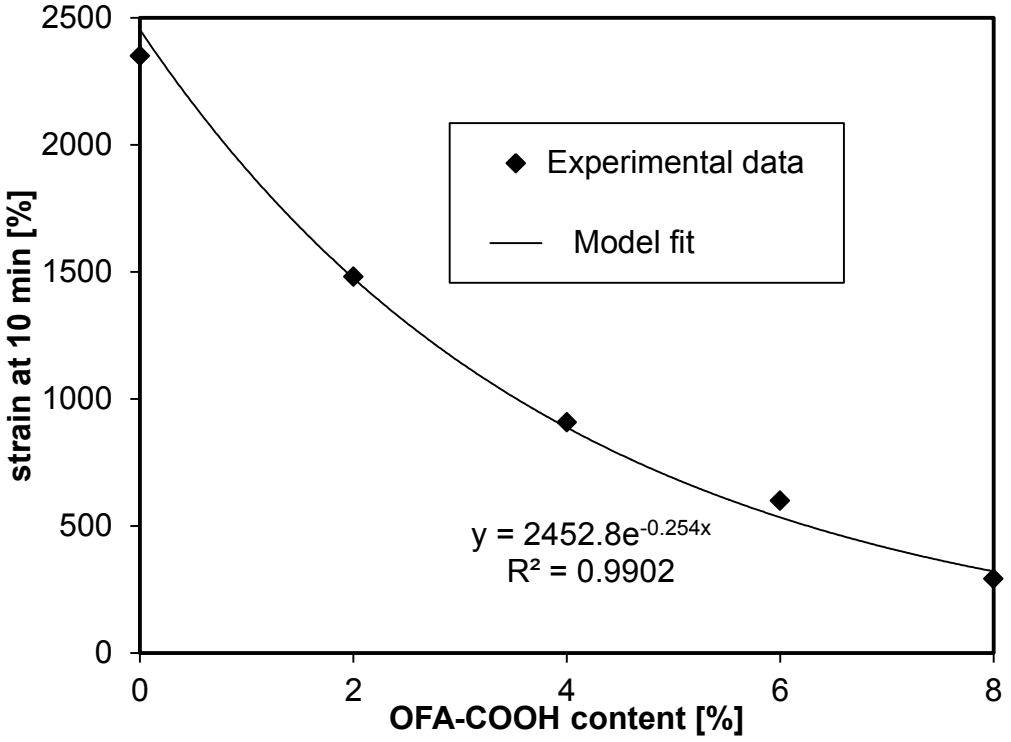

Figure 4.3. 14: Strain at 10 minute versus OFA-COOH content

4.3.5 Conclusion

OFA was treated successfully by acid solution to incorporate carboxylic (-COOH) group to the surface of OFA. The presence of the functional group was detected through different techniques such as: DSC, FTIR and SEM/EDS. Dynamic, steady and temperature sweep rheological measurements of OFA-COOH/asphalt binders were carried out to assess the impact of functionalized OFA on the binder's rheology. The following conclusions are drawn on the basis of this investigation:

1. The addition of OFA-COOH significantly increased the viscoelastic properties of the modified asphalt binders. SHRP rutting parameter $G^*/\sin\delta$

increases with OFA-COOH content and it showed linear relationship with OFA-COOH content. The high temperature performance grading was increased from 70°C to 88°C with the addition of 8% OFA-COOH to pure asphalt.

2. Elastic modification index (I_M) was developed and the modified binders showed less temperature susceptibility. An exponential model was developed to fit the modification index as function of temperature.
3. Addition of OFA-COOH to pure asphalt reduced the activation energy. A linear relationship of E_a and OFA-COOH content showed OFA-COOH modification improved low temperature behavior of the modified asphalt binders.
4. Addition of OFA-COOH increased both G' and η' as suggested by dynamic shear rheology. Black diagram representation of dynamic data proved that an OFA-COOH modification of the asphalt binder leads to enhancement in the viscoelastic properties through chemical bonding.
5. OFA-COOH modification of asphalt binders increased the steady shear viscosity. Addition OFA-COOH to asphalt decreases the Newtonian plateau and increases the shear thinning behavior which indicates ease of processing as suggested by the results of power law index.

Finally the chemically treated waste OFA can be utilized in the modification of asphalt binder. It will solve the waste disposal problem of OFA as well as reduce the amount of asphalt pavement to be used in.

4.3.6 References

1. The Asphalt Institute, 2003. *Performance Graded Asphalt Binder Specification and Testing, SP-1,* Lexington, KY: The Asphalt Institute.
2. Abbasi, S.H.,Adesina, A.A., Atieh, M.A.,Ul-Hamid, A, Hussein, I.A., 2013. Rheology, Mechanical and Thermal Properties of (C18-CNT/LDPE) Nanocomposites. *International Polymer Processing,* pp. 3-13.
3. Abuilaiwi, F. A., Laoui, T., Al-Harthi, M. & Atieh, a. M. A., 2010. Modification and functionalization of multiwalled carbon nanotube (MWCNT) via Fischer esterification. *The Arabian Journal for Science and Engineering,* Volume 35.
4. Airey, G., 2003. Rheological properties of styrene butadiene styrene polymer modified road bitumens. *Fuel,* Volume 82, pp. 1709-1719.
5. Airy, G., 2011. Factors affecting the rheology of polymer modified bitumen. In: T. McNally, ed. *Polymer Modified Bitumen – Properties and Characterization.* s.l.:Woodhead Publishing in Materials..
6. Al-Abdul Wahhab, H., Asi, I. & and Ali, M., 1997. Development of Performance-Based Bitumen Specifications for the Gulf Countries. *Construction and Building Materials Journal,* 11(1), pp. 15-22.
7. Al-Amethel, M., Al Abdul Wahhab, H. I., & Hussein, I. A., 2011. *Utilization of heavy oil fly ash to improve asphalt binder and asphalt concrete performance.* Patent No. US 8062413 B1.
8. American Coal Ash Association, 2011. *Coal Combustion Product (CCP) Production & Use Survey Report, ACCA*.

9. Anani, B. & Al-Abdul Wahhab, H., 1982. Effects of baghouse fines and mineral fillers on properties of asphalt pavements. *Transportation Research Board,* Volume 843, pp. 57-64.
10. Anani, B. & Wahhab, H. A.-A., 1982. Effects of baghouse fines and mineral fillers on properties of asphalt pavements. *Transportation Research Board,* Volume 843, pp. 57-64.
11. Asi, I. & Assa'ad, A., 2005. Effect of Jordanian oil shale fly ash on asphalt mixes. *Journal of Materials in Civil Engineering, 17: 553-559.,* pp. 553-559.
12. Bahia, H., Zeng, M., Zhai, H. & Khatr, 1999. *Superpave protocols for modified asphalt binders, 15th Quarterly Progess Report for NCHRP Project 9–10.,* Washington: DC: National Cooperative Highway Research Program..
13. Binard, C., Anderson, D., Lapalu, L. & Planche, J., 2004. *Zero shear viscosity of modified and unmodified binders.* Vienna, s.n.
14. Cho, Y., Jeong, H. & Kim, B., 2009. *Macromolecular Research,* Volume 17, pp. 879-890.
15. Coates, J., 2000. Interpretation of Infrared Spectra, A Practical Approach. In: *Encyclopedia of Analytical Chemistry.* Chichester: John Wiley & Sons Ltd, p. 10815–10837.
16. Cuadri, A., García-Morales, M., Navarro, F. & Partal, P., 2012. Enhancing the viscoelastic properties of bituminous binders via thiourea-modification. *Fuel,* Volume 97, pp. 862-868.

17. D. Bikiaris, et al., 2008. Effectof acid treatment multi-walled carbon nanotubes on the mechanical, permeability, thermal properties and thermo-oxidative stability of isotactic polypropylene. *Polymer Degradation and Stability,* Volume 93, pp. 952-967.

18. García-Morales, M. et al., 2004. Viscous properties and microstructure of recycled EVA modified bitumen. *Fuel,* 83(1), pp. 31-38.

19. Hussein, I. A., Iqbal, M. H. & Al Abdul Wahhab, H. I., 2005. Influence of Mw of LDPE and vinyl acetate content of EVA on the Rheology of Polymer Modified Asphalt. *Rheologica Acta,* 45(1), pp. 92-105.

20. Iqbal, M. H., Hussein, I. A., Wahhab, H. I. A.-A. & Amin, M. B., 2006. Rheological Investigation of the Influence of Acrylate Polymers on the Modification of Asphalt. *J. Applied Polymer Science,* 102(4), pp. 3446-3456.

21. Kandhal, P., Lynn, C. & Parker, F., 1998. *Characterization tests for mineral fillers related to performance of asphalt paving mixtures,* Auburn.: National Center for Asphalt Technology.

22. Karasahin, M. & Terzi, S., 2007. Evaluation of marble waste dust in the mixture of asphaltic concrete.. *Construction and Building Materials,* Volume 21, pp. 616-620.

23. Larsen, D., Alessandrini, J., Bosch, A. & Cortizo, M., 2009. Micro-structural and rheological characteristics of SBS-asphalt blends during their manufacturing. *Constr Build Mater,* 23(8), pp. 2769-2774.

24. Ouyang, C., Wang, S. & Zhang, Y., 2006. Improving the aging resistance of asphalt by addition of Zinc dialkyldithiophosphate. *Fuel,* Volume 85, pp. 1060-1066.

25. Phillips, M. & Robertus, C., 1996. *Binder rheology and asphalt pavement permanent deformation; the zero shear viscosity.* Strasbourg.

26. Polacco, G., Stastna, J., Biondi, D. & Zanzotto, L., 2006. Relation between polymer architecture and nonlinear rviscoelastic behavior of modified asphalts. *Current Opinion in Colloid & Interface Science,* Volume 11, pp. 230-245.

27. Shawabkeh, R., Al-Harahsheh, A. & Al-Otoom, A., 2004. Copper and zinc sorption by treated oil shale ash. *Separation and Purification Technology,* Volume 40, p. 251.

28. Shawabkeh, R. & Harahsheh, A., 2007. H2S removal from sour liquefied petroleum gas using Jordanian oil shale ash. *Oil Shale,* Volume 24, p. 109.

29. Shawabkeh, Reyad, Khan, Muhammad J, Al-Juhani, Abdulhadi A, Al Abdul Wahhab, Hamad I., Hussein, Ibnelwaleed A., 2011. Enhancement of surface properties of oil fly ash by chemical treatment. *Applied Surface Science 258,* Issue 258, p. 1643– 1650.

30. Shenoy, A., 2002. Model-fitting the master curves of the dynamic shear rheometer data to extract a rut-controlling term for asphalt pavements. *ASTM J Test Eval,* 30(2), pp. 95-102.

31. Sinha, A., Singh, M. & Singh, S., 2010. *Study of use of beneficiated pulverized coal fly-ash as filler and rice straw fibers in manufacturing of paper.* Atlanta, Georgia, USA, Paper Conference and Trade Show , pp. 2237-2253.

32. Woo-Teck, Dong-Hyun, K. K. & Yung-Phil, K., 2005. Characterization of Heavy Oil Fly Ash Generated from a Power Plant. *Journal of Materials.*

4.4 Enhancement of Thermorheological Properties of Asphalt by using C-18 modified Oil Fly Ash

4.4.1 Abstract

Oil fly ash (OFA) is generated in large quantities as a waste from power generation plants and it is used to modify asphalt. Here, waste OFA was acid treated followed by functionalization with 1-Octadecanol (C18) to improve its compatibility with asphalt. Differential scanning calorimetry (DSC), FTIR and SEM/EDS techniques were used to characterize as-received and treated OFA. The treated OFA was blended with base asphalt and rheological properties of pure and modified asphalt binders were measured. The percentage of OFA was varied from 0-8% of asphalt binder. FTIR spectra analysis showed the change in chemical bonding of the modified asphalt binder. Melt state rheology was investigated by temperature sweep, dynamic shear and steady shear rheological measurements in ARES rheometer. Both steady and dynamic shear rheology showed that OFA-C18 improved the viscoelastic properties of the modified asphalt binders. OFA-C18 modification reduced temperature susceptibility of modified asphalt binder, increased the upper grading (performance) temperature. Strategic Highway Research Program rutting parameter ($G^*/\sin\delta$) increased linearly with OFA-C18 content of asphalt binder. Activation energy was found to decrease with OFA-C18 content suggesting reduced temperature

susceptibility of the modified binder. Chemical treatment of waste OFA enhanced its thermorheological properties of modified asphalt.

4.4.2 Introduction

Oil fly ash (OFA) is typically a black powder type waste material that results from the use of crude and residual oil for power generation. OFA is collected in electrostatic precipitators which are installed on boilers burning residual oil for air pollution control. According to a survey of American Coal Ash Association, 69.30 million tons of coal fly ash produced in 2011 in the United States by coal fired plants and 38% of this quantity was reused in different applications (American Coal Ash Association, 2011). In Saudi Arabia, there are 70 power plants consuming 22 million metric tons of diesel fuel, crude oil and heavy fuel oil and total amount of disposed OFA in 2008 was about 240,000 cubic meters. The amount is expected to increase to 400,000 cubic meters by 2014. These quantities must be disposed off in an environment friendly way. OFA is mainly used as a replacement of Portland cement; as a filler in polymers, asphalt and cementitious materials; stabilizing agent and also for adsorption of solutes and, solidification for waste and sludge (Visa, et al., 2010; Shawabkeh & Harahsheh, 2007; Shawabkeh, et al., 2004; Woo-Teck, et al., 2005).

Additive or filler materials can be used in asphalt binders to design against or to repair pavement due to the following problems: surface defects (raveling and stripping), structural defects (rutting, shoving and distortion) and cracking (fatigue and thermal). Many authors have studied the effects of mineral fillers, which are

materials passing a sieve size of 0.075 mm, on the behavior of asphalt mix (Phillips & Robertus, 1996; Asi & Assa'ad, 2005; Kandhal, et al., 1998; Karasahin & Terzi, 2007). Different filler materials may have different mechanical properties in the asphalt mixture.

In a recent patent untreated OFA (3-10%) was used in asphalt binder and asphalt concrete mix (Al-Amethel, et al., 2011). Addition of untreated OFA improved rutting resistance, stability and modulus. However, the fatigue properties of the mix were poor due to poor dispersion of ash. The main reason for this is most likely the fact that the surface of OFA is an inert surface which leads to poor compatibility between OFA and asphalt.

Therefore, it is important to modify the inert surface of OFA to improve its dispersion and chemical bonding with asphalt. Surface modification and grafting are widely used in polymer literature to improve the bonding between different polymers or between polymers and asphalt. Our group has used functionalized polymers to improve the compatibility of polymers with asphalt (Iqbal, et al., 2006; Hussein, et al., 2005). Therefore, the use of surface modified or functionalized materials is not new to the pavement industry. Also, surface modification of carbon nanotubes (CNT), which resemble OFA in composition, has improved the dispersion in polymers and improved the bonding between the polymer and CNT (Abbasi, et al., 2013).

Here, the same surface modification techniques have been implemented on OFA, which contains more than 80% carbon, 7% oxygen, 9% sulfur and the rest are trace metal. The previous success of carbon black and OFA as a filler for asphalt suggests that physical modification of OFA to produce activated OFA is promising. In addition, the proven success of surface modification in polymers, polymer nanocomposites and polymer-modified asphalt in improving the interfacial bonding suggests the potential of chemical modification of OFA in improving the dispersion and bonding with asphalt. The present study focused on the surface modification of OFA with 1-octadecanoate (C18), characterization of OFA-C18 and the effect of OFA-C18 on asphalt binder rheology. The authors are not aware of any previous research that attempted to use treated oil fly ash in asphalt modification.

4.4.3 Experimental

Materials

OFA was collected from Shuaibah power plant of Saudi Electricity Company. The concentrated sulfuric acid (H_2SO_4, 98%) and nitric acid (HNO_3, 68%) were purchased from Sigma Aldrich Company, and they were used as-received. Asphalt cement of 60/70 penetration grade was obtained from Saudi Aramco Riyadh Refinery.

OFA Functionalization

OFA as-received was washed with water to separate trace oil and some sandy particles. Washed OFA was then dried in oven at 105^{o}C to evaporate the remaining water. The OFA was then treated with H_2SO_4 and HNO_3 at a volumetric ratio of 3:1. A weight of 200 g ash was taken into a 3 liter glass beaker and the acid solution was slowly poured into the ash. After 10 minutes, the ash/acid mixture turned to liquid solution. The beaker with OFA/acid solution was put in hot plate magnetic stirrer assembly. The temperature and speed of rotation of the hot plate were set at 165^{o}C and 100 rpm respectively. The reaction was allowed to continue for 12 hours to create the carboxylic acid group on the OFA surface. The reactant mixture was then cooled to room temperature. The mixture was diluted with deionized water and filtered using vacuum-filter through a 3 μm porosity filter paper to remove unreacted acid. The filtered OFA was then dried in hot chamber at temperature ~ 90^{o}C. The treated OFA by this method is referred to as OFA-COOH.

OFA-COOH was then reacted with 1-Octadecanol ($C_{18}H_{38}O$) which is referred to as C_{18}. Its melting point is 59°C, with 95% purity. The Fischer esterification process was followed to substitute the acid group by 1-Octadecanol. This was achieved by heating 1-Octadecanol to its melting point in a reaction flask and maintaining the temperature at 90°C. Acid treated OFA (OFA-COOH) was introduced into the reaction flask containing 1-Octadecanol in a weight ratio of 1:3. The mixture was stirred 10 minutes and then 2ml of

sulfuric acid were added gradually to initiate the following esterification reaction:

$$\text{OFA-COOH} + CH_3(CH_2)_{17}OH \rightleftharpoons \text{OFA-COO}(CH_2)_{17}CH_3 + H_2O \uparrow \qquad (4.4.1)$$

The Fischer Esterification reaction (equation 4.4.1) is an equilibrium reaction. To shift the equilibrium to favor the production of esters, it is customary to use an excess of one of the reactants, either the alcohol or the acid. So, excess amount of 1-Octadecanol was used to favor the OFA-C18 production. Another way to drive a reaction toward its products is to remove one of the products as it forms. Water formed in this reaction was removed by evaporation during the reaction. The reaction was left for 6 hours after which the resulting ash was washed with toluene three times to remove any unreacted 1-Octadecanol and then followed by washing with deionized water to remove any traces of acid. OFA-C18 modified OFA was dried at 60^{o}C under vacuum for 12 hours and was ready to be mixed with asphalt.

FTIR Characterization

The chemical structures of as received OFA and modified OFA (OFA-C18) were characterized by means of FTIR measurement using a Nicolet 6700 spectrometer from Thermo Electron™. A weight of 1-2 mg of the OFA was mixed thoroughly with 1.0 g of fine dried powder of KBr. Then, the resulting mixture was hydraulically

pressed in a Carver press to obtain a thin transparent disc. The thin disc was placed in an oven at 110^{o}C for 2 h to prevent any interference of any existing water vapor or carbon dioxide molecules. All the FTIR spectra were taken in the transmission mode and in the range 600–4000 cm^{-1} at room temperature. FTIR spectra were obtained using a spectral resolution of 4 cm^{-1} and 30 co-added scans.

Thermal Analysis

The thermal behavior of as-received and treated OFA was determined by means of a TA Q1000 DSC. A Sample of 7-10 mg was weighed and sealed in hermetic aluminum pans. As received OFA, OFA-COOH and OFA-C18 were characterized for decomposition of functional group by heating the samples from room temperature to 250^{o}C using a heating rate of 5^{o}C/min. Pure Nitrogen (99.99%) gas was used to purge the DSC cell at a flow rate of 50 ml/min.

SEM and EDS

The scanning electron microscope (JEOL, model JSM 6400) was used to determine the qualitative characteristics and morphology of the fly ash sample. The dried sample was fixed with double side masking tape. In order to make it surface conductive, the fly ash sample was gold coated. It was then viewed on FE-SEM at different magnification to see the surface topography of the sample. Energy dispersive X-ray (EDX) analysis was carried for the analysis of chemical composition of as-received OFA and OFA-C18.

Sample Preparation for Rheological Testing

OFA and pure asphalt were blended in a high shear blender. The blender acts as a batch stirred tank with a constant temperature bath. Typical mixing procedure was as follows: Steel cans of approximately 1000 mL were filled with 250–260 g of asphalt and put in a thermoelectric heater. When the temperature of the asphalt reached 145°C, a high shear mixer was dipped into the can and set to about 1000 rpm. Calculated amount of OFA was added gradually with base asphalt. The bath temperature was maintained at 145 ± 1°C. Samples were blended for 10 minutes at high shear to confirm uniform distribution of OFA in the asphalt matrix. Asphalt sample was poured into silicone molds before being used for rheological testing. The samples specimens were stored in a refrigerator at 5°C.

Rheological tests

Dynamic and steady shear rheological tests were carried out to investigate the effect of OFA-C18 on the rheology of modified asphalt binder. The dynamic temperature step measurements for the samples were performed in ARES rheometer. This is a constant strain rheometer equipped with a heavy transducer (range 2-2000 g for normal force; 2-2000 g-cm for torque). All tests were carried out in range of 64^{o}C-100^{o}C using a parallel plate set of 25 mm diameter. With the sample in position, the oven was closed and the sample heated at 64^{o}C for about 5 minutes, thereafter the gap between the plate platen was adjusted to 1.5 mm by lowering the upper platen force transducer assembly at a constant load of 500 g. The melt that extruded beyond

the platen rim by this procedure was cleaned off. Strain in the linear viscoelastic range (strain amplitude, γ^o of 12.5 %) and frequency of 10 rad/s was used for all the tests. In all the experiments, nitrogen gas was continuously used for heating the samples during testing to avoid oxidation during testing. A holding period of 5 min was allowed before beginning measurements when the temperature reaches steady state. The Orchestrator software was used to calculate the dynamic shear viscosity, storage modulus, complex modulus and phase angle for all samples.Dynamic frequency sweep tests were conducted at 60^{o}C and frequency ranges of 100-0.1 rad/s and the constant strain of 10%. Different linear viscoelastic variables were calculated using TA Orchestrator software. Steady shear rheological tests were conducted at 50^{o}C and a shear rate in the range of 0.01-10 s^{-1}.

4.4.4 Results and Discussion

OFA surface modification

Surface modification of OFA was done according to the procedure described in OFA functionalization section to obtained C18 modified ash (OFA-C18). 1-Octadecanoate group (C18) was successfully attached to the surface of OFA and it was detected through different characterization technique such as: FTIR spectra, SEM/EDS analysis and DSC analysis.

FTIR Analysis

FTIR technique was used to determine whether a new functional group is attached to fly ash surface after chemical activation. Figure 4.4.1 (a & b) shows the FTIR spectra of as-received and treated OFA over the range 4000–600 cm^{-1}. The intensity of the peaks for as-received OFA is very small compared to that of treated OFA. An as-received sample spectrum shows that it has three peaks at 2022, 2162.3 and 2183 cm^{-1}. The peak at 2022 cm^{-1} is attributed to transition metals (Fe and Ni) carbonyl compound whereas the peaks at 2162.3 and 2183 cm^{-1} are due to the C≡C stress of medial alkyne (Coates, 2000).

Figure 4.4.1(a) shows that OFA-C18 has five major peaks at 1186.9, 1469.9, 2849.8 and 2916.8 cm^{-1} respectively. The peak at 1186.9 cm^{-1} is due to tertiary alcohol, C-O stretch whereas the peak at 1469.9 cm^{-1} is attributed to the methyl C-H asymmetric/symmetric bend. The peak at 2849.8 and 2916.8 correspond to C-H stretch of long chain alkyl molecule which is indication of the presence of C18. Similar functional group was also detected by other authors (Abuilaiwi, et al., 2010) for C18 modified CNT. Therefore, the FTIR study confirmed that 1-Octadecanoate (C18) functional group was incorporated on the surface of OFA through Fischer esterification reaction.

DSC Analysis

As-received OFA and OFA-C18 were characterized using differential scanning calorimetry (DSC) in the standard mode to detect the presence of any functional group on the OFA surface. The samples were heated from 25^{o}C to 250^{o}C at 5^{o}C/min and the results are shown in Figure 4.4.2. As-received OFA and OFA-C18 DSC signals are placed in two different axes as the signal of as-received OFA is very small as compared to that of OFA-C18. It is known that the decomposition of chemical bond releases energy which can be detected by exotherms in DSC experiment. The DSC scan of as-received OFA shows that it has no exothermic peak but there is a broad endothermic peak around 90°C which is due to evaporation of moisture from the sample. There are two exothermic peaks in the DSC scan of OFA-C18 at 210.93°C and 222.23°C. These two peaks are due to the decomposition of carboxylic acid and ester (OFA-1-Octadecanoate) groups, respectively. So, the thermal analysis of the as-received OFA and OFA-C18 samples confirmed the presence of 1-Octadecanoate (C18) in the treated OFA which supports our previous analysis using FTIR technique. Also, OFA-C18 decomposes at a temperature higher than 200°C which suggests that it is stable during blending with asphalt which usually takes place at ~145°C. The presence of such organic tails on ash will enhance its compatibility with asphalt.

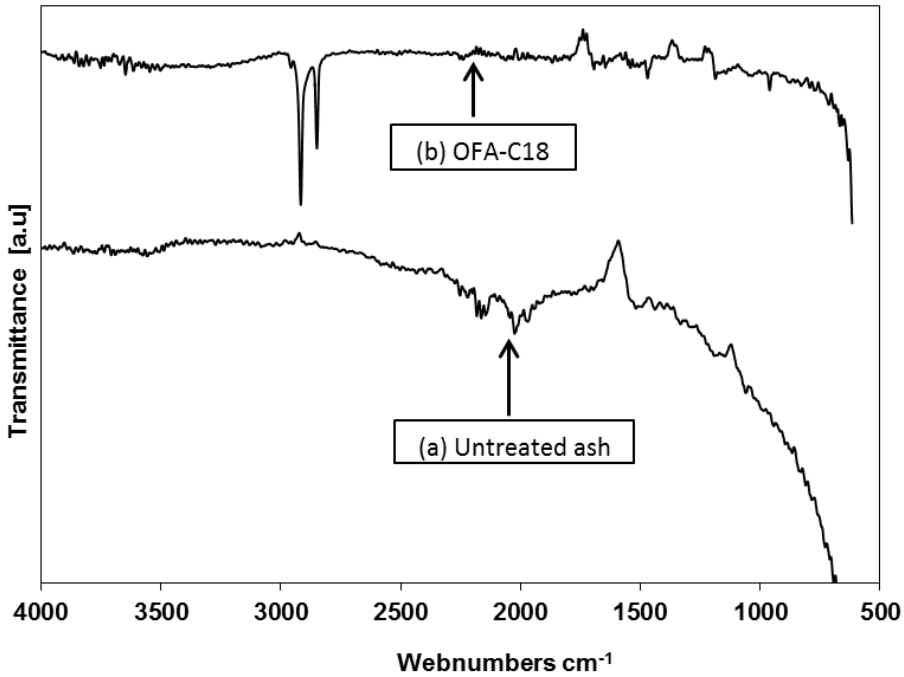

Figure 4.4. 1: FTIR spectrum (a) OFA before treatment (b) OFA after chemical treatment

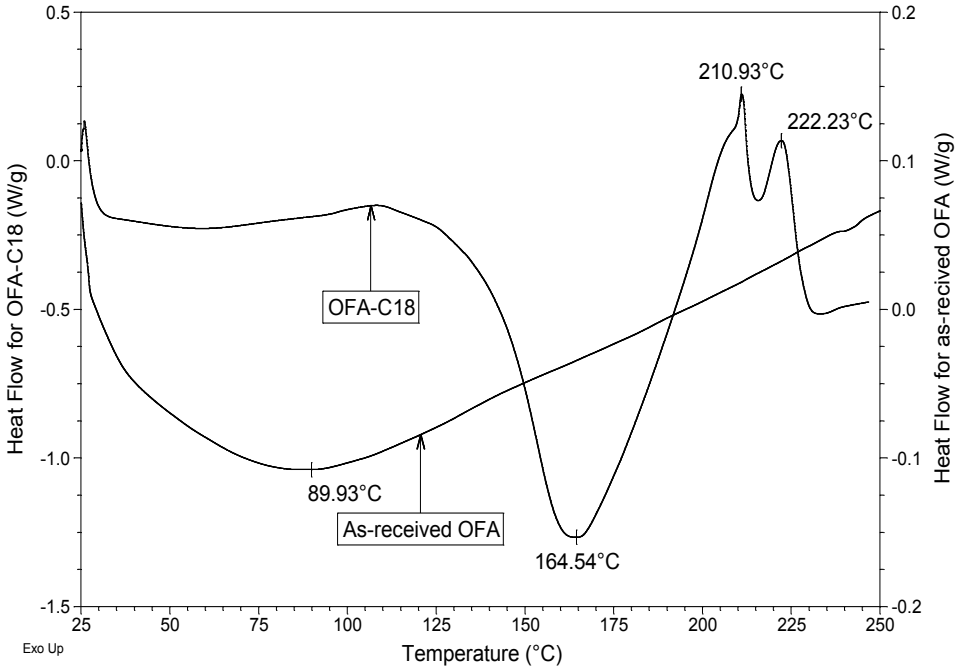

Figure 4.4. 2: DSC scans of as-received OFA and OFA-C18 samples

SEM/EDS Analysis

Evaluation of common and predominant phases within the ash samples during treatment was obtained using Energy Dispersive X-ray analysis (EDS) as shown in Table 4.4.1. The surface morphology of the ash samples is shown in Figure 4.4.3(a & b). It is apparent that most of the ash particles are spherical in shape with high porosity. The size of these particles is in the range of 10-100 μm. However, SEM image of OFA-C18 sample shows some long chain branch attached to OFA surface which is due to C18. Combined SEM/EDS analysis of OFA particles was performed to determine the elemental analysis of the as-received and treated OFA samples. The oxygen to carbon ratio has changed according to the acid treatment method. The ratio of O/C in the ash sample before treatment was 0.087 whereas in the treated ash, it was 0.283. This increase in the ratio could be attributed to the addition of functional group (-COOH) to the OFA surface. Another finding is that, the acid treatment completely removes the trace metals such as vanadium, iron, and nickel from the OFA. Acid treatment also increased the ratio of S/C. This could be due to the formation of CO_2 and CO gases. These gases will escape from ash sample, which will decrease the amount of carbon and thus increase the amount of sulfur (Shawabkeh, et al., 2011). The C18 modification of the OFA-COOH has increased the percentage of carbon from 67.58% to 73.54% due to replacement of –OH group by $CH_3(CH_2)_{17}O$- through Fischer esterification reaction. The other elements (sulfur and oxygen) changed due to the relative change of carbon.

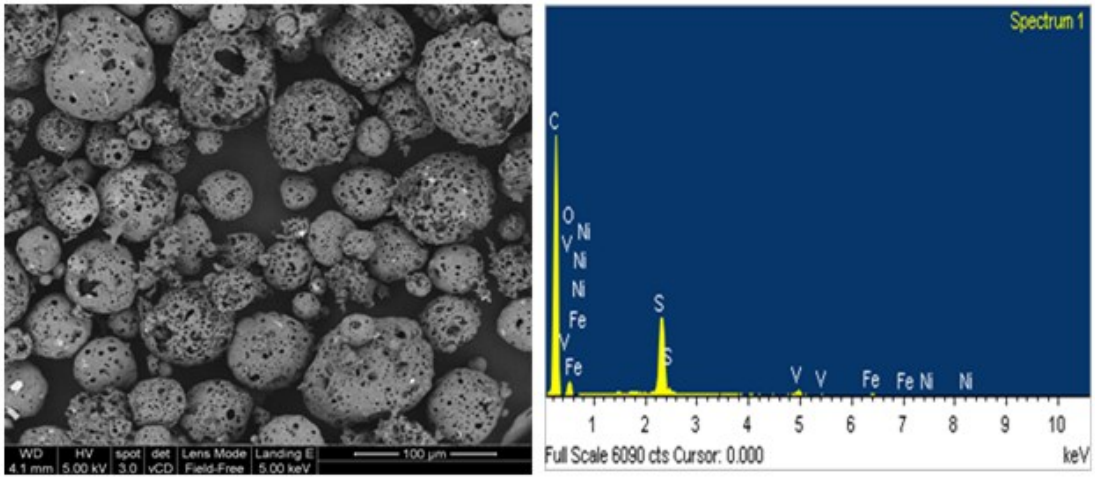

(a) SEM/EDS analysis of as received OFA

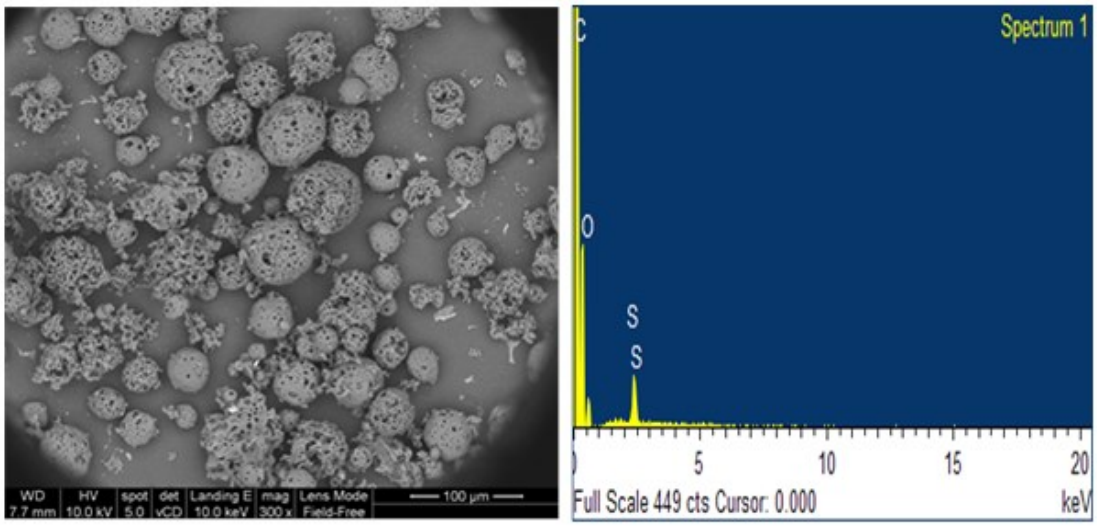

(a) C18 modified OFA sample

Figure 4.4. 3: Combined SEM/EDS analysis of OFA samples

Table 4.4. 1:Elemental analysis of OFA before and after treatment

SN	Elements	As-received OFA		OFA-COOH		OFA-C18	
		Weight %	Atomic %	Weight %	Atomic %	Weight %	Atomic %
1	C	79.99	89.40	67.58	77.75	73.54	79.35
2	O	7.02	5.89	19.15	16.54	24.53	19.87
3	S	8.74	3.66	13.16	5.72	1.93	0.78
4	V	1.83	0.48	0	0	0	0
5	Fe	1.07	0.26	0	0	0	0
6	Ni	1.36	0.31	0	0	0	0
Total		100	100	100	100	100	100

3.2 FTIR results of asphalt binders

Figure 4.4.4 represents the FTIR spectra of pure asphalt binder and Table 4.4.2 lists the main bonds present in the binder. Similar results were also found in the literature (Larsen, et al., 2009). The bonding of the OFA-C18 modified asphalt are also similar to the one presented in Figure 4 but with different intensities.

Figure 4.4.5 represents the FTIR spectra of pure and modified asphalt binders for the range of 600-2000 cm^{-1}. The main differences between pure and modified asphalt binders are appreciated in this range. It is noticed that the intensities of the bonds has been changed for modified asphalt binders. According to the bands of bonding in Table 4.4.2, the ratio changes of chemical bonding has been calculated for the sake of avoiding the samples thickness effect (Ouyang, et al., 2006). The following three

equations are defined to quantify the changes in chemical bonding due to OFA-C18 modification of asphalt binder:

$$I_{S=O} = \frac{\text{Area of the sulfoxide band centered around 1030 cm}^{-1}}{\sum \text{Area of the spectral bands between 600-2000 cm}^{-1}} \quad (4.4.2)$$

$$I_{\text{C-H of CH}_3} = \frac{\text{Area of the aliphatic branched band centered around 1376 cm}^{-1}}{\sum \text{Area of the spectral bands between 600-2000 cm}^{-1}} \quad (4.4.3)$$

$$I_{\text{C-H of -(CH}_2)_n-} = \frac{\text{Area of the aliphatic index band centered around 1456 cm}^{-1}}{\sum \text{Area of the spectral bands between 600-2000 cm}^{-1}} \quad (4.4.4)$$

Based on the above equations (4.4.2-4.4.4) the ratios of the area were calculated and the results are shown in Figure 4.4.6. As the modified ash (OFA-C18) contained both carboxylic (-COOH) and ester (-$COO(CH_2)_{17}CH_3$) bonds it enhances the above bonds defined in equation (4.4.2-4.4.4). The carboxylic functional group contributed to enhance the sulfoxide bond whereas C18 specially contributed to the aliphatic bond index. Figure 4.4.5 showed that the ratio of aliphatic bond index increases with OFA-C18 content up to 4% and then decreases. Similar trend were also observed for other bonds. The decrease of the ratio after certain percentages of OFA-C18 can be due to decrease of intensities for ash particles as it is kwon that carbon particles reduce absorbance spectra (Abuilaiwi, et al., 2010).

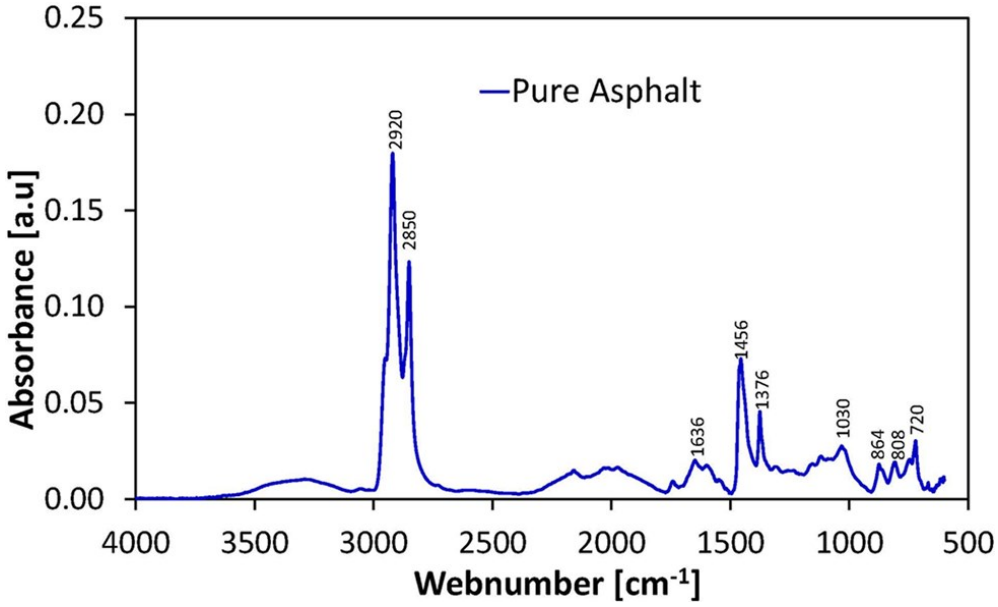

Figure 4.4. 4: FTIR spectra of pure asphalt binder

Table 4.4. 2: Assignations of the main bands of the FTIR spectra

Webnumbers [cm^{-1}]	Assigned bands
2920, 2850	υC-H aliphatic
1636	υC=C aromatic
1456	δC-H of $–(CH_2)_n-$ (aliphatic index)
1376	δC-H of CH_3 (aliphatic branched)
1031	υS=O sulfoxide
808, 864	υC=C of alkenes
721	δC-H of straight chain CH_2

Note: υ = Stretching, and δ = Bending

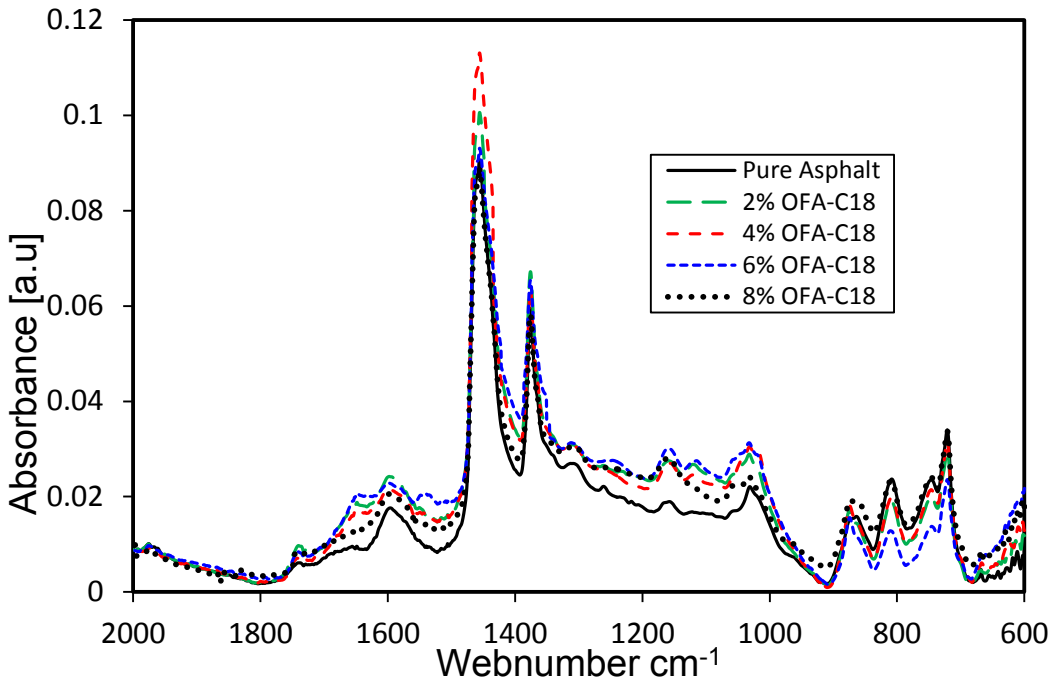

Figure 4.4. 5: FTIR spectra of pure and OFA-C18 modified asphalt binders

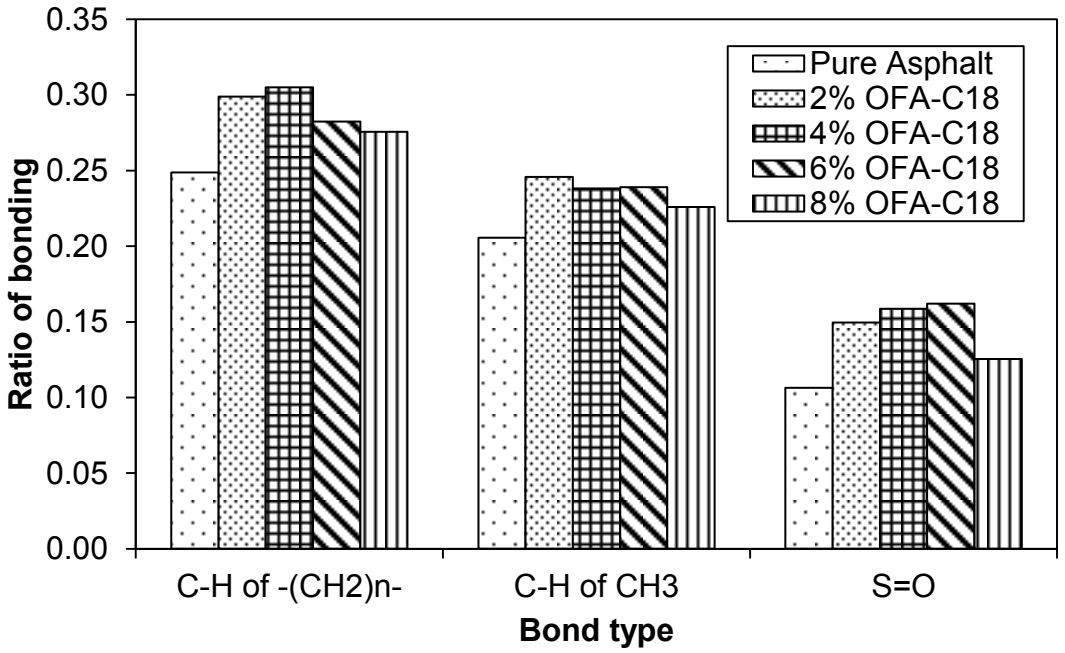

Figure 4.4. 6: Ratio of bonding in pure and OFA-C18 modified asphalt binders

Rheology of OFA-C18/asphalt binders

Steady shear rheology

Steady rate sweep tests were conducted for all binders at 50^{o}C and a shear rate in the range 0.01-10 s^{-1}. Steady shear viscosity as function of shear rate is plotted in Figure 4.4.7 for pure and OFA-C18 modified binders. Pure asphalt sample displayed long Newtonian plateau up to ~ 2 s^{-1}. OFA-C18 modified binders showed a very short Newtonian plateau followed by shear thinning behavior at high shear rate. Similar behavior was also reported for polymer modified asphalt binders (Polacco, et al., 2006). These types of shear viscosity data can be well modeled by Carreau model which is given by following equation:

$$\eta = \frac{\eta_0}{\left[1+\left(\dot{\gamma}\right.\right.} \qquad (4.4.5)$$

where, η_0 is the zero shear viscosity, $\dot{\gamma}$ is the critical shear rate for the onset of shear thinning region and a is a parameter related to the slope of shear thinning region. The viscosity data were well fitted by the model as shown in Figure 4.4.7. It is noticed that incorporation of OFA-C18 in asphalt binder increases the viscosity of the binder. As the amount of OFA-C18 increases in the binder, the Newtonian plateau decreases and the shear thinning region increases. This shear thinning behavior can be attributed to the broad molecular weight distribution which results from the size

heterogeneity due to the addition of OFA and the possible crosslinking of OFA-C18 and asphalt.

Researchers have observed that the SHRP rutting parameter $G^*/\sin\delta$ is not very effective in predicting the rutting performance of binders, especially in the case of modified binders are used (Shenoy, 2002; Bahia, et al., 1999). For such case a new parameter, zero shear viscosity (η_o) has been suggested by many researchers as a possible measure for the rutting resistance of modified asphalt binders (Binard, et al., 2004; Phillips & Robertus, 1996). η_o was calculated for all binders using equation (4.4.5) and the values are shown in Table 4.4.3. It is observed that η_o increases with the increase in OFA-C18 content. The increment in η_o is more pronounce at high OFA-C18 content in the binders. Also, power law index, n, was obtained and tabulated in Table 4.4.3. The results show enhancement in shear thinning due to the addition of OFA-COOH.

Table 4.4. 3: Carreau model parameters for steady shear data

Binder #	OFA-C18 content (%)	Carreau Model Parameters		
		η_o, (Pa.s)	Power law index, n	Regression coefficient, R^2
1	0	1079	0.44	0.998
2	2	3917	0.36	0.999
3	4	7755	0.29	0.998
4	6	15812	0.27	0.999
5	8	29243	0.25	0.999

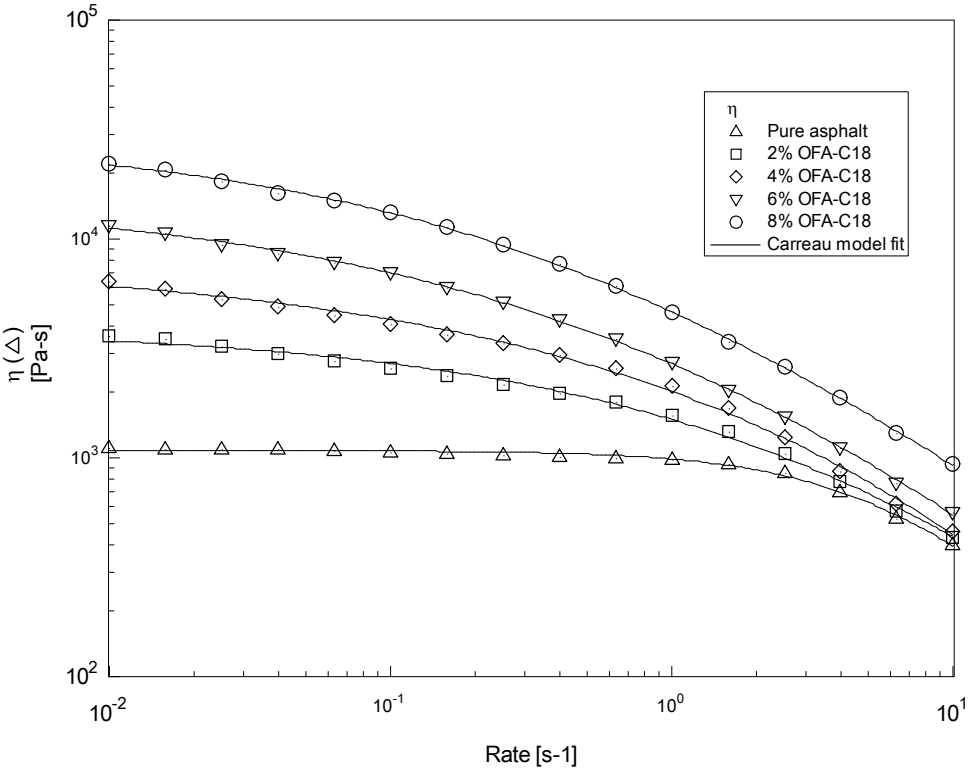

Figure 4.4. 7: Steady shear viscosity function at 50°C

3.3.2 Temperature sweep test

Temperature sweep test was conducted for all binders to extract the values of complex modulus, G^* and phase angle, δ as function of temperature. According to the strategic highway research program (SHRP), the stiffness parameter $G^*/\sin\delta$ is a factor used to estimate the rutting resistance of asphalt binder (The Asphalt Institute, 2003). This factor should be larger than 1 kPa at the maximum pavement design temperature for unaged original asphalt, when measured at 10 rad/s to simulate traffic loading. Higher values of $G^*/\sin\delta$ are expected to give a high resistance to permanent deformation.

Figure 4.4.8 shows $G^*/\sin\delta$ versus temperature for pure asphalt and 4% as-received OFA and 4% OFA-C18 modified binders. It shows that $G^*/\sin\delta$ value for 4% OFA-C18 modified binder is far better than that of 4% as-received OFA modified binder. OFA-C18 has better dispersion in asphalt than as-received OFA. So, it is better to use treated OFA instead of as-received OFA for asphalt modification. The complete PG test results for treated and untreated OFA modified binders are shown in Table 4.4.4. Figure 4.4.9 shows $G^*/\sin\delta$ versus temperature for various amount of OFA-C18 modified asphalt binder. It shows that the modification of asphalt binder with OFA-C18 increases the rutting resistance significantly. The value of $G^*/\sin\delta$ decreases with temperature and there is exponential relationship $G^*/\sin\delta$ and temperature as it shown in Figure 4.4.9. The relationship between $G^*/\sin\delta$ and OFA-C18 content of the binders is linear as shown in Figure 10 for different temperature. Table 4 lists the maximum temperature attained at $G^*/\sin\delta \geq 1$ kPa. It is mentioned that the maximum local pavement temperature for Saudi Arabia is 76^{o}C for hot summer season (Al-Abdul Wahhab, et al., 1997). Base asphalt cannot fulfill SHRP criteria as the maximum temperature at $G^*/\sin\delta \geq 1$is 68^{o}C. So, there is a need for modification of pure asphalt binder to increase $G^*/\sin\delta$ to improve rutting resistance. It is noticed that 4% OFA-C18 is needed to upgrade the binder performance from 70^{o}C to 76^{o}C. As the percentage of OFA-C18 is increased in the binder, the stiffness of binders goes up. So, the binder modification using treated OFA has significantly improved rutting resistance for permanent deformation and increased the range of application.

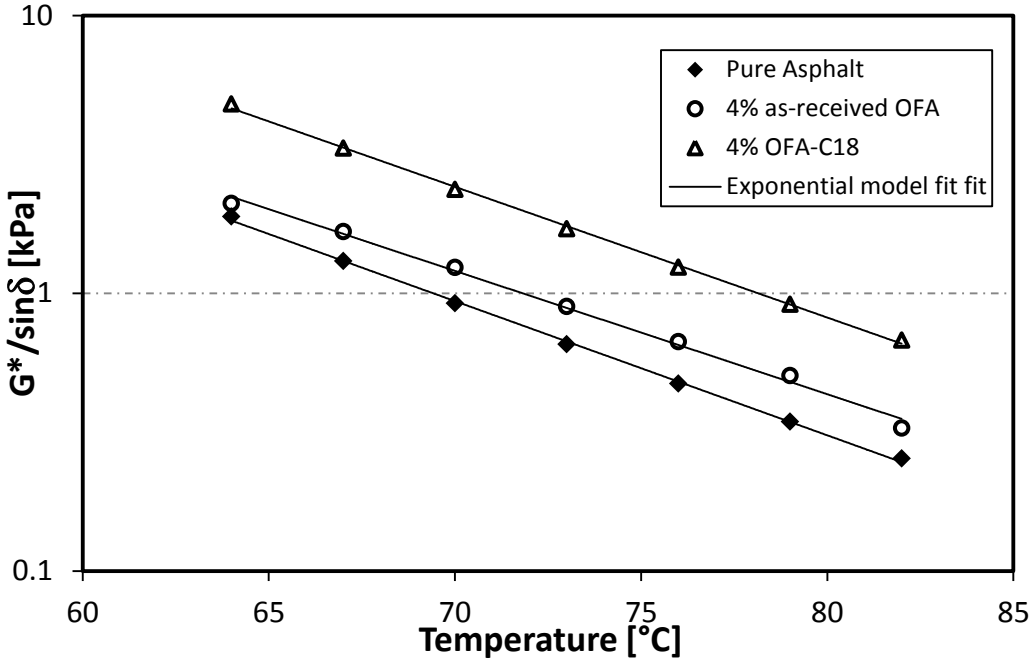

Figure 4.4. 8: *G*/sinδ* versus temperature for treated and as-received OFA-asphalt binder

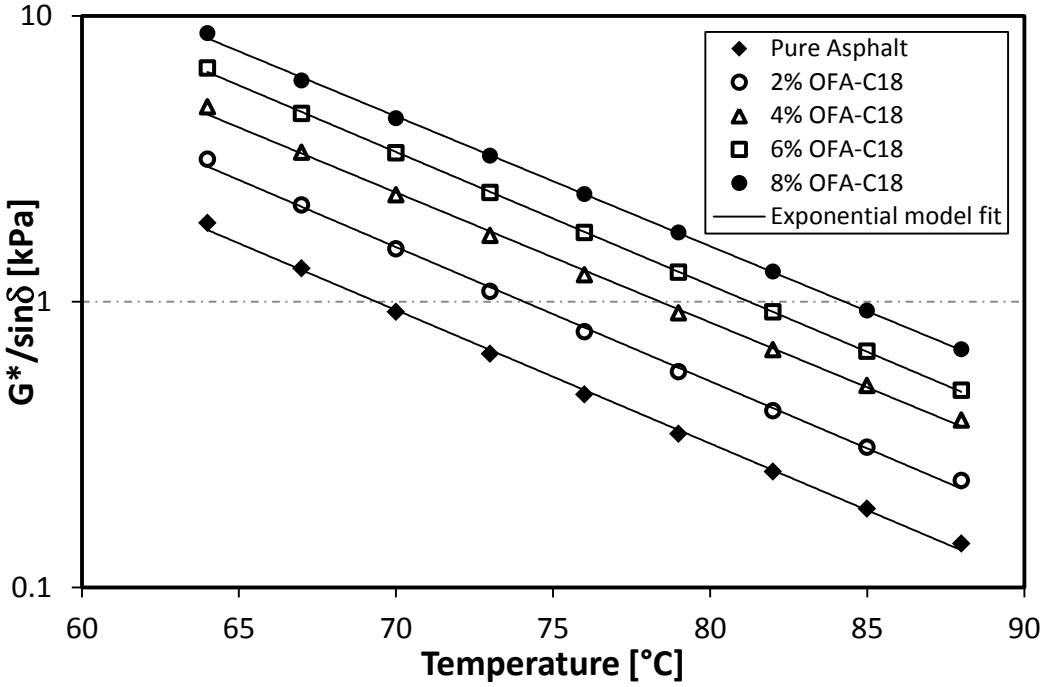

Figure 4.4. 9: *G*/sinδ* versus temperature for different OFA-C18 content

Table 4.4. 4: Maximum temperature at G*/sinδ = 1kPa for all binders

Binder #	OFA content, %	Max. Temperature attained, °C @ $G^*/\sin\delta$=1 kPa	
		OFA-C18	OFA as-received
1	0	68.50	68.50
2	2	74.15	70.91
3	4	77.25	71.20
4	6	81.35	74.18
5	8	84.25	75.09

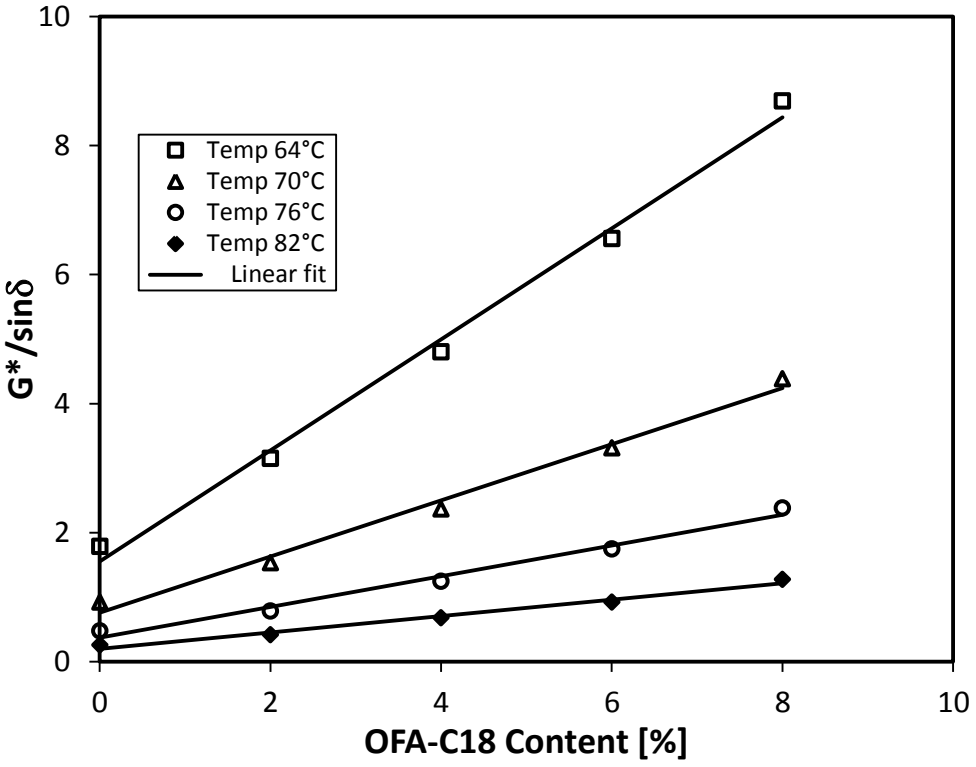

Figure 4.4. 10: $G^*/\sin\delta$ versus OFA-C18 content of asphalt binder for different temperatures

The complex modulus, G* has two components, elastic modulus (G′) and loss modulus (G′′). So, G*/sinδ does not represent the elastic behavior of the binder only. Rheological data of temperature sweep measurement can be quantitatively appreciated by introducing a modification index, I_M. Similar analysis was also used before for SBS modified bitumen (Airy, 2011). To assess the elastic modification of the modified binders an elastic modification index was defined as the ratio of elastic moduli as:

$$I_M = \frac{\text{Elastic modulus of modified binder}}{\text{Elastic modulus of pure asphalt}} \tag{4.4.6}$$

The calculated modification index from equation (4.4.6) is shown against temperature in Figure 4.4.10 in a semi log plot. The results show that the viscoelastic properties of treated OFA modified asphalt binder increases with temperature. If I_M is higher than 1 then the modified binders has more resistance to temperature deformation. The modification index increases with both temperature and OFA-C18 content. I_M versus temperature data are well fitted by exponential equation of the following form:

$$I_M = ae^{bT} \tag{4.4.7}$$

where, a and b are fitted parameters and their values are listed in Table 4.4.5. The values of a and b increase with the increase of OFA-C18 content in the modified binders. Also, the slope of I_M versus temperature curve is an indirect indicator of thermal sensitivity of the binder and can be used to describe the influence of

temperature on the rheological properties. However, high I_M values also indicate that the corresponding sample will be stiff at lower temperature and can crack easily at low pavement temperature. So, an optimum amount of the OFA-C18 should be used to suit both high and low temperature ranges.

Table 4.4. 5: Model parameters for equation (4.4.7) for all binders

OFA-COOH content, %	Model parameters	
	a	b
2	0.23	0.0371
4	0.57	0.0422
6	0.65	0.0565
8	0.86	0.0696

Temperature sweep data was further analyzed to check the effect of temperature on asphalt viscosity. Viscosity-temperature relationships of asphalt binder can be expressed by the well-known Arrhenius equation as follow:

$$\eta^* = Ae^{\left(E_a/RT\right)} \tag{4.4.8}$$

where E_a is the flow activation energy, A is the pre-exponential term, and R is the universal gas constant. E_a is an important factor that strongly influences the viscosity. Figure 4.4.11 shows complex viscosity versus 1000/T for pure and modified asphalt binders. The data given in Figure 4.4.11 showed good fit to Arrhenius model. E_a was calculated using equation (4.4.8) and the values of activation energy along with pre-exponential factor are listed in Table 4.4.6. Activation energy for pure asphalt is 109.29 kJ/mol.

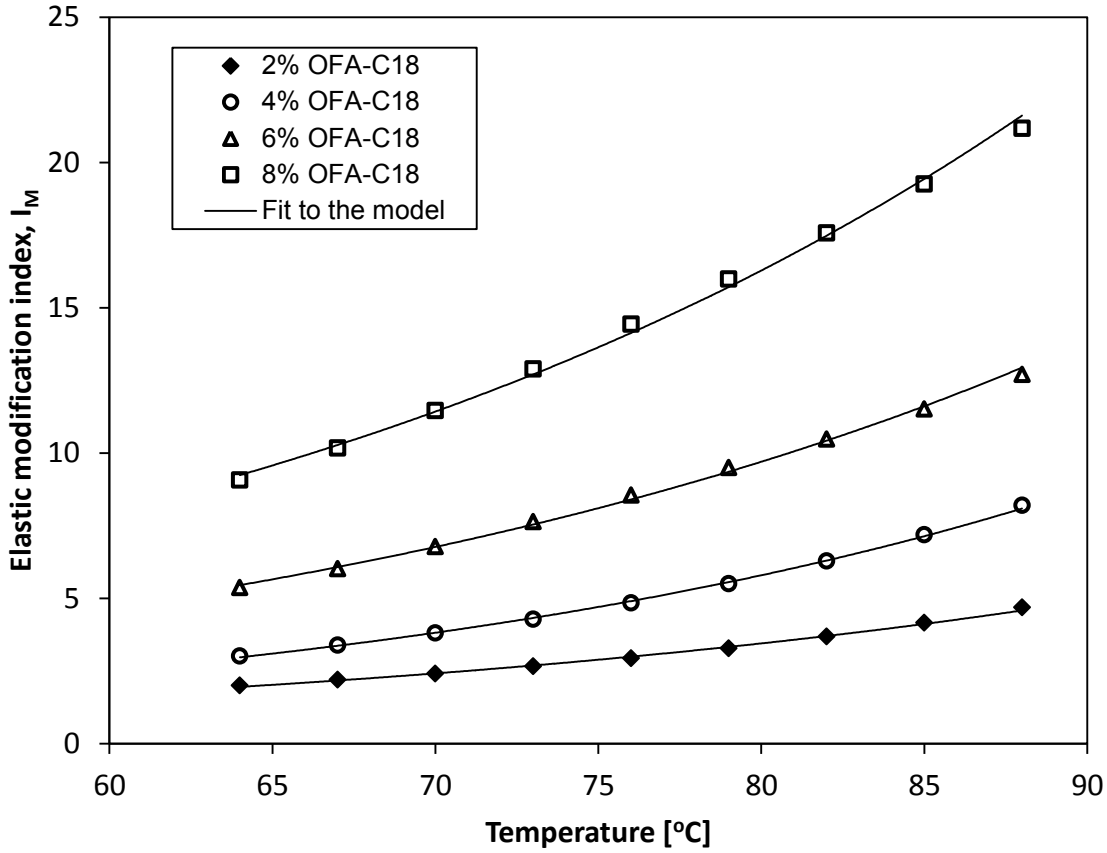

Figure 4.4. 11: Elastic modification index (I_M) as function of temperature for different amount of OFA-C18 content.

It is observed that addition of OFA-C18 to asphalt reduces the activation energy of the modified asphalt binder as compared to pure asphalt. This reduction in activation energy ranges from 2 to 7%. The maximum percentage of activation energy reduction is 7% for 4% OFA-C18. Activation energy, E_a is related to the binder thermal susceptibility (García-Morales, et al., 2004). The low activation energy of asphalt binders suggests low susceptibility to temperature. So, from Table 4.4.4 it can be concluded that all modified asphalt binders would be less temperature susceptible than pure asphalt binder.

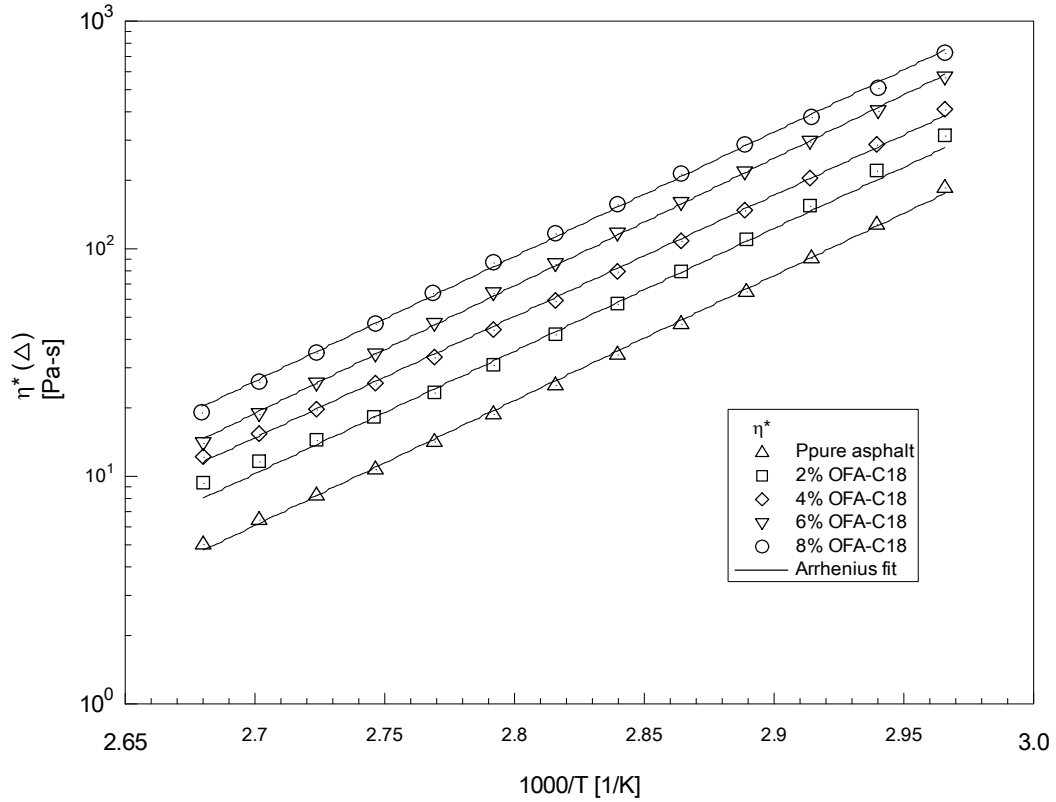

Figure 4.4. 12: Effect of temperature on complex viscosity for all binders

Table 4.4. 6: Arrhenius model parameters for different binders

Binder #	OFA-C18 content (%)	Arrhenius Model Parameters		
		Activation energy, Ea (kJ/mol)	Pre-exponential factor, A(Pa.s)	Fit quality, r^2
1	0	109.29	2.56×10^{-15}	0.9997
2	2	103.17	1.11×10^{-14}	0.9972
3	4	101.92	6.22×10^{-14}	0.9992
4	6	107.21	1.44×10^{-14}	0.9996
5	8	104.78	4.38×10^{-14}	0.9992

Dynamic frequency sweep measurements

Dynamic frequency sweep test for all binders were conducted at 50^{o}C in the range 100-0.1 rad/s at10% strain. Typical linear viscoelastic properties of the OFA-C18 modified asphalt binder are displayed in Figures 4.4.13-4.4.15. Storage modulus, G', as function of frequency is shown in Figure 4.4.13 for pure and modified binders. The results are shown for asphalt with 0%, 2%, 4%, 6% and 8% OFA-C18 content by weight. The data showed good fit of the five elements Maxwell model. For the whole frequency range, the modified asphalt binder has improved G' as compared to base asphalt. The increase in G' is higher at higher concentration of OFA-C18. G' is highly sensitive to the morphological state of a heterogeneous system (Cho, et al., 2009). The value of G' is an indication of how much elasticity can be boosted by the asphalt modification. The advantage of high G′ is at high temperature. High G′ values at low frequency suggest better flexibility. According to the principle of time–temperature superposition, this behavior corresponds to long service time or at tolerance to high temperature, which is needed in hot climate.

The slopes of log G′ versus log ω at low ω range were calculated and their values are 1.71, 1.01, 0.96, 0.94 and 0.92 for pure asphalt, 2%, 4%, 6% and 8% OFA-C18 modified asphalt binder, respectively. So, the melt rheology of OFA-C18 modified asphalt binder suggest that modified asphalt binders expected to show better deformation resistance at high temperature. Figure 4.4.14 shows the dynamic viscosity as function of frequency at 50°C. Data showed good fit to the Carreau

model. The profile of $\eta'(\omega)$ for pure asphalt showed typical Newtonian behavior over almost the entire frequency range, but OFA-C18 modified asphalt binder displayed non-Newtonian behavior, which was more pronounced at high OFA-C18 concentrations. Similar behavior was observed for asphalt modification with polymers (Iqbal, et al., 2006; Hussein, et al., 2005).

Figure 4.4.15 represents the well-known Black diagram (phase angle versus G*) representation for pure and modified binders at 50°C. As mentioned by other authors (Airey, 2003; Cuadri, et al., 2012) that the reduction of phase angle is related to the presence of elastic networks or entanglements in the modified binder. It is noticed that incorporation of OFA-C18 in the binder decreases the phase angle which means improvement in elastic behavior. This improvement is likely due to improved compatibility of OFA-C18 with asphalt. The combined effect of shear and heat in the blender could result in several phenomena in the modified asphalt matrix. Some of them can be as: (1) Formation chemical bonding between C18 and asphalt as shown earlier in the discussion of FTIR section. (2) Increase in compatibility of OFA-C18 and asphalt which could increase the dispersion of OFA in asphalt matrix (3) Change in compositions of asphalt by thermal and mechanical degradation. The combination of these phenomena can lead to improvement in the viscoelastic properties of the modified asphalt binders.

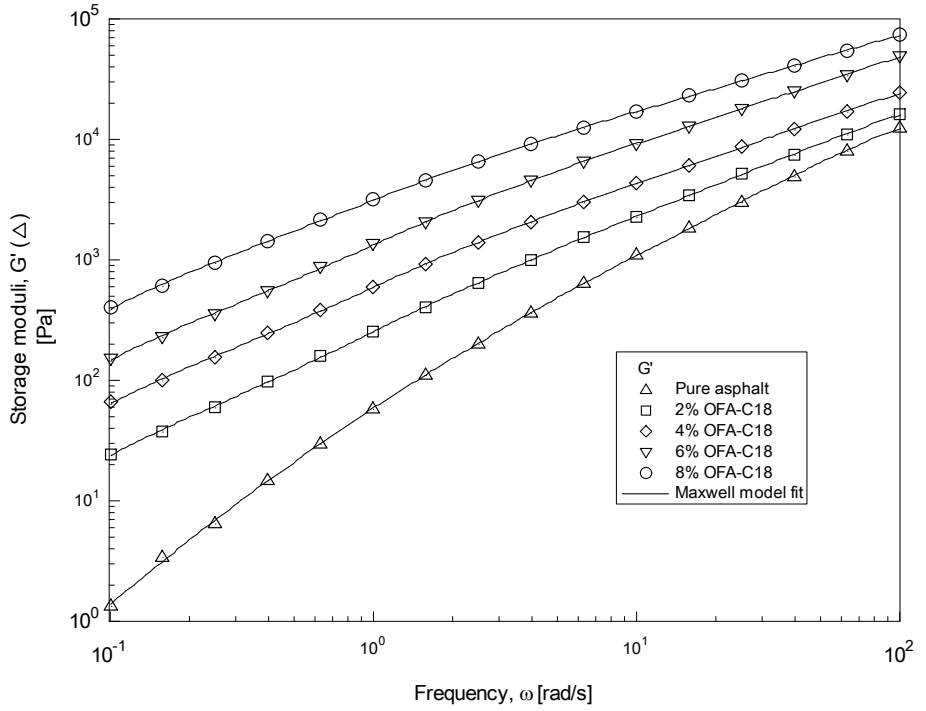

Figure 4.4. 13: Dynamic storage moduli *G´* function of frequency at 50°C

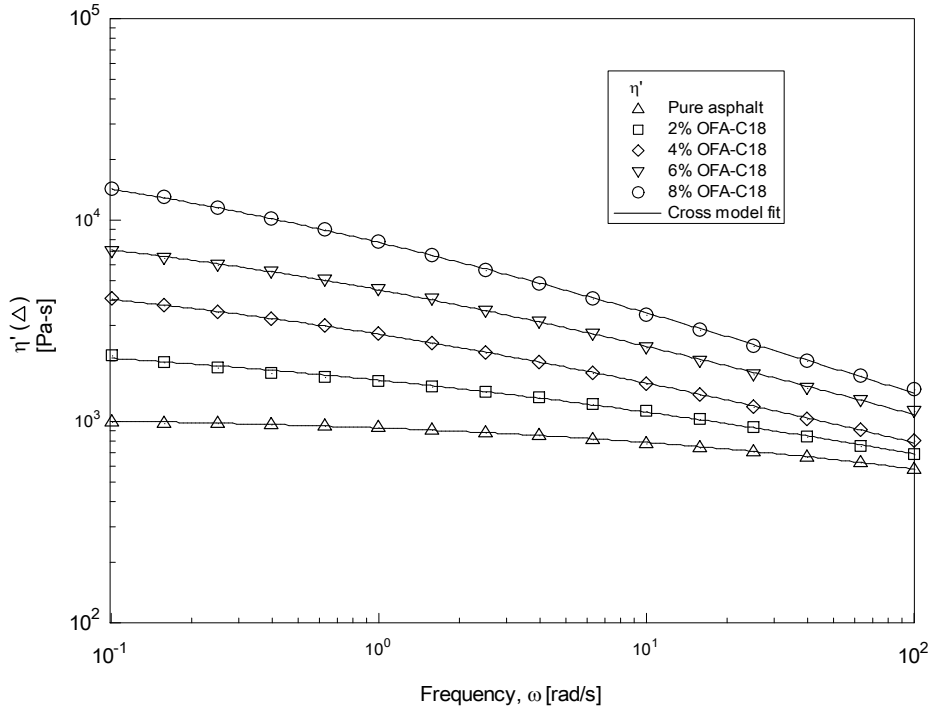

Figure 4.4. 14: Dynamic shear viscosity as function of frequency at 50°C

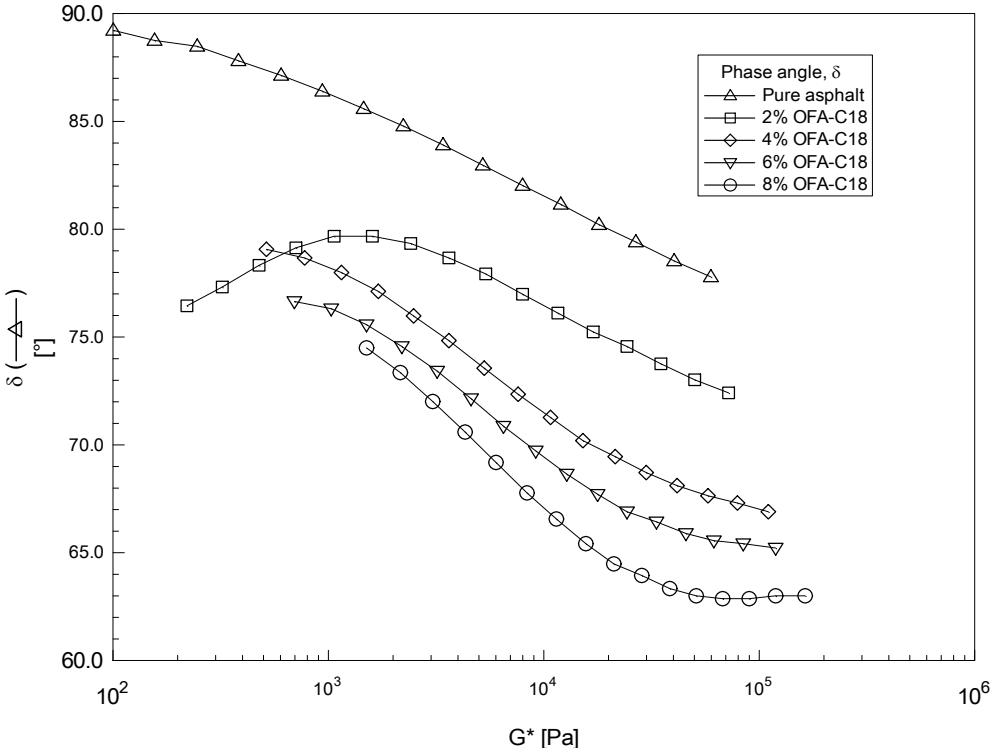

Figure 4.4. 15: Black diagram representation of asphalt binders at 50°C

4.4.5 Conclusion

OFA is treated by H_2SO_4/HNO_3 acid solution and then by 1-Octadecanol (C18) to produce C18 modified OFA. The presence of functional group was detected through different techniques such as: DSC, FTIR and SEM/EDS. Dynamic, steady and temperature sweep rheological measurements of OFA-C18/asphalt binders were performed to assess the impact of functionalization OFA on the binder's rheology. The following conclusions are drawn on the basis of this investigation:

1. The addition of OFA-C18 increased the viscoelastic properties (G^*, G') of the modified asphalt binders. SHRP rutting parameter $G^*/\sin\delta$ increases with OFA-C18 content and it showed linear relationship with OFA-C18 concentration. The high temperature performance grading of modified asphalt has increased from 68°C to 84°C as a result of the addition of 8% OFA-C18.
2. Elastic modification index (I_M) suggests that modified binders are less susceptible to change in temperature. An exponential model was developed to fit the modification index as function of temperature in the form $I_M = ae^{bT}$.
3. Addition of OFA-C18 to pure asphalt reduced the activation energy which suggests that OFA-C18 modification has improved high temperature resistance of modified asphalt binders.
4. Addition of OFA-C18 has increased both G′ and shear viscosity. Black diagram representation of dynamic shear data proved that OFA-C18 modification improves the viscoelastic properties.
5. Addition OFA-C18 to asphalt increases the shear thinning behavior which suggests ease of processing. The power law index decrease from 0.36 to 0.25 when OFA-C18 was increased from 2 to 8%.
6. FTIR analysis of pure and modified asphalt binders showed the change in bonding due to OFA-C18 modification of asphalt binder. The bonding intensities increase with OFA-C18 modification which causes the improvement in binder's properties.

Finally the chemically treated waste OFA can be utilized in the modification of asphalt binder. It will solve the waste disposal problem of OFA as well as reduce the amount of asphalt pavement to be used in.

4.4.6 References

1. The Asphalt Institute, 2003. *Performance Graded Asphalt Binder Specification and Testing, SP-1,* Lexington, KY: The Asphalt Institute.
2. Abbasi, S.H.,Adesina, A.A., Atieh, M.A.,Ul-Hamid, A, Hussein, I.A., 2013. Rheology, Mechanical and Thermal Properties of (C18-CNT/LDPE) Nanocomposites. *International Polymer Processing,* pp. 3-13.
3. Abuilaiwi, F. A., Laoui, T., Al-Harthi, M. & Atieh, a. M. A., 2010. Modification and functionalization of multiwalled carbon nanotube (MWCNT) via Fischer esterification. *The Arabian Journal for Science and Engineering,* Volume 35.
4. Airey, G., 2003. Rheological properties of styrene butadiene styrene polymer modified road bitumens. *Fuel,* Volume 82, pp. 1709-1719.
5. Airy, G., 2011. Factors affecting the rheology of polymer modified bitumen. In: T. McNally, ed. *Polymer Modified Bitumen – Properties and Characterization.* Cambridge: Woodhead Publishing in Materials..
6. Al-Abdul Wahhab, H., Asi, I. & and Ali, M., 1997. Development of Performance-Based Bitumen Specifications for the Gulf Countries. *Construction and Building Materials Journal,* 11(1), pp. 15-22.

7. Al-Amethel, M., Al-Abdul Wahhab, H. I. & Ibnelwaleed A., H., 2011. *Utilization of heavy oil fly ash to improve asphalt binder and asphalt concrete performance.* s.l. Patent No. US 8062413 B1.
8. American Coal Ash Association, 2011. *Coal Combustion Product (CCP) Production & Use Survey Report,* Farmington Hills, MI: AACA.
9. Asi, I. & Assa'ad, A., 2005. Effect of Jordanian oil shale fly ash on asphalt mixes. *Journal of Materials in Civil Engineering,* pp. 553-559.
10. Bahia, H., Zeng, M., Zhai, H. & Khatr, 1999. *Superpave protocols for modified asphalt binders, 15th Quarterly Progess Report for NCHRP Project 9–10.,* Washington: DC: National Cooperative Highway Research Program..
11. Binard, C., Anderson, D., Lapalu, L. & Planche, J., 2004. *Zero shear viscosity of modified and unmodified binders.* Vienna, Eurasphalt & Eurobitume congress.
12. Cho, Y., Jeong, H. & Kim, B., 2009. *Macromolecular Research,* Volume 17, pp. 879-890.
13. Coates, J., 2000. Interpretation of Infrared Spectra, A Practical Approach. In: *Encyclopedia of Analytical Chemistry.* Chichester: John Wiley & Sons Ltd, p. 10815–10837.
14. Cuadri, A., García-Morales, M., Navarro, F. & Partal, P., 2012. Enhancing the viscoelastic properties of bituminous binders via thiourea-modification. *Fuel,* Volume 97, pp. 862-868.
15. García-Morales, M. et al., 2004. Viscous properties and microstructure of recycled EVA modified bitumen. *Fuel,* 83(1), pp. 31-38.

16. Hussein, I. A., Iqbal, M. H. & Al Abdul Wahhab, H. I., 2005. Influence of Mw of LDPE and vinyl acetate content of EVA on the Rheology of Polymer Modified Asphalt. *Rheologica Acta,* 45(1), pp. 92-105.

17. Iqbal, M. H., Hussein, I. A., Wahhab, H. I. A.-A. & Amin, M. B., 2006. Rheological Investigation of the Influence of Acrylate Polymers on the Modification of Asphalt. *J. Applied Polymer Science,* 102(4), pp. 3446-3456.

18. Kandhal, P., Lynn, C. & Parker, F., 1998. *Characterization tests for mineral fillers related to performance of asphalt paving mixtures,* Auburn.: National Center for Asphalt Technology.

19. Karasahin, M. & Terzi, S., 2007. Evaluation of marble waste dust in the mixture of asphaltic concrete.. *Construction and Building Materials,* Volume 21, pp. 616-620.

20. Larsen, D., Alessandrini, J., Bosch, A. & Cortizo, M., 2009. Micro-structural and rheological characteristics of SBS-asphalt blends during their manufacturing. *Constr Build Mater,* 23(8), pp. 2769-2774.

21. Ouyang, C., Wang, S. & Zhang, Y., 2006. Improving the aging resistance of asphalt by addition of Zinc dialkyldithiophosphate. *Fuel,* Volume 85, pp. 1060-1066.

22. Phillips, M. & Robertus, C., 1996. *Binder rheology and asphalt pavement permanent deformation: the zero shear viscosity.* Strasbourg, Eurasphalt & Eurobitume congress, p. 12.

23. Polacco, G., Stastna, J., Biondi, D. & Zanzotto, L., 2006. Relation between polymer architecture and nonlinear rviscoelastic behavior of modified asphalts. *Current Opinion in Colloid & Interface Science,* Volume 11, pp. 230-245.

24. Shawabkeh, R., Al-Harahsheh, A. & Al-Otoom, A., 2004. Copper and zinc sorption by treated oil shale ash. *Separation and Purification Technology,* Volume 40, p. 251.

25. Shawabkeh, R. & Harahsheh, A., 2007. H2S removal from sour liquefied petroleum gas using Jordanian oil shale ash. *Oil Shale,* Volume 24, p. 109.

26. Shawabkeh, Reyad, Khan, Muhammad J, Al-Juhani, Abdulhadi A, Al Abdul Wahhab, Hamad I., Hussein, Ibnelwaleed A., 2011. Enhancement of surface properties of oil fly ash by chemical treatment. *Applied Surface Science 258,* Issue 258, p. 1643– 1650.

27. Shenoy, A., 2002. Model-fitting the master curves of the dynamic shear rheometer data to extract a rut-controlling term for asphalt pavements. *ASTM J Test Eval,* 30(2), pp. 95-102.

28. Visa, M., Bogatu, C. & Duta, A., 2010. Simultaneous adsorption of dyes and heavy metals from multicomponent solutions using fly ash. *Applied Surface Science,* Volume 256, p. 5486.

29. Woo-Teck, Dong-Hyun, K. K. & Yung-Phil, K., 2005. Characterization of Heavy Oil Fly Ash Generated from a Power Plant. *Journal of Materials.*

4.5 Improvement of Asphalt Properties by using Amine modified Oil Fly Ash

4.5.1 Abstract

Oil fly ash (OFA) is generated in large quantities as a waste from power generation plants and it is used to modify asphalt. Here, waste OFA was treated with ammonium hydroxide to get amine functional group to OFA surface to improve its compatibility with asphalt. Differential scanning calorimetry (DSC), FTIR and SEM/EDS techniques were used to characterize as-received and treated OFA. The treated OFA was blended with base asphalt and rheological properties of pure and modified asphalt binders were measured. The percentage of OFA was varied from 0-8% of asphalt binder. Melt state rheology was investigated by temperature sweep, dynamic shear and steady shear rheological measurements in ARES rheometer. Both steady and dynamic shear rheology showed that OFA-Amine improved the viscoelastic properties of the modified asphalt binders. OFA-Amine modification reduced temperature susceptibility of modified asphalt binder, increased the upper grading (performance) temperature. Strategic Highway Research Program rutting parameter ($G^*/\sin\delta$) increased linearly with OFA-Amine content of asphalt binder.

4.5.2 Introduction

Oil fly ash (OFA) is typically a black powder type waste material that results from the use of crude and residual oil for power generation. OFA is collected in electrostatic precipitators which are installed on boilers burning residual oil for air pollution control. According to a survey of American Coal Ash Association, 69.30 million tons of coal fly ash produced in 2011 in the United States by coal fired plants and 38% of this quantity was reused in different applications (American Coal Ash Association, 2011). In Saudi Arabia, there are 70 power plants consuming 22 million metric tons of diesel fuel, crude oil and heavy fuel oil and total amount of disposed OFA in 2008 was about 240,000 cubic meters. The amount is expected to increase to 400,000 cubic meters by 2014. These quantities must be disposed off in an environment friendly way. OFA is mainly used as a replacement of Portland cement; as a filler in polymers, asphalt and cementitious materials; stabilizing agent and also for adsorption of solutes and, solidification for waste and sludge (Visa, et al., 2010; Shawabkeh & Harahsheh, 2007; Shawabkeh, et al., 2004; Woo-Teck, et al., 2005).

Additive or filler materials can be used in asphalt binders to design against or to repair pavement due to the following problems: surface defects (raveling and stripping), structural defects (rutting, shoving and distortion) and cracking (fatigue and thermal). Many authors have studied the effects of mineral fillers, which are materials passing a sieve size of 0.075 mm, on the behavior of asphalt mix (Phillips & Robertus, 1996; Asi & Assa'ad, 2005; Kandhal, et al., 1998; Karasahin & Terzi,

2007). Different filler materials may have different mechanical properties in the asphalt mixture.

In a recent patent untreated OFA (3-10%) was used in asphalt binder and asphalt concrete mix (Al-Amethel, et al., 2011). Addition of untreated OFA improved rutting resistance, stability and modulus. However, the fatigue properties of the mix were poor due to poor dispersion of ash. The main reason for this is most likely the fact that the surface of OFA is an inert surface which leads to poor compatibility between OFA and asphalt.

Therefore, it is important to modify the inert surface of OFA to improve its dispersion and chemical bonding with asphalt. Surface modification and grafting are widely used in polymer literature to improve the bonding between different polymers or between polymers and asphalt. Our group has used functionalized polymers to improve the compatibility of polymers with asphalt (Iqbal, et al., 2006; Hussein, et al., 2005). Therefore, the use of surface modified or functionalized materials is not new to the pavement industry. Also, surface modification of carbon nanotubes (CNT), which resemble OFA in composition, has improved the dispersion in polymers and improved the bonding between the polymer and CNT (Abbasi, et al., 2013).

Here, the same surface modification techniques have been implemented on OFA, which contains more than 80% carbon, 7% oxygen, 9% sulfur and the rest are trace metal. The previous success of carbon black and OFA as a filler for asphalt suggests

that physical modification of OFA to produce activated OFA is promising. In addition, the proven success of surface modification in polymers, polymer nanocomposites and polymer-modified asphalt in improving the interfacial bonding suggests the potential of chemical modification of OFA in improving the dispersion and bonding with asphalt. The present study focused on the surface modification of OFA with ammonium hydroxide, characterization of OFA-amine and the effect of OFA-Amine on asphalt binder rheology. The authors are not aware of any previous research that attempted to use treated oil fly ash in asphalt modification.

4.5.3 Experimental

Materials

OFA was collected from Shuaibah power plant of Saudi Electricity Company. Ammonium hydroxide (NH_4OH, 30%) was purchased from Alpha chemicals. Asphalt cement of 60/70 penetration grade was obtained from Saudi Aramco Riyadh Refinery.

OFA Functionalization

A sample of 100 g OFA was taken in a 500 ml flask and 300 ml NH_4OH was added in the flask. The solution was heated at 120°C and stirred for 24 hours with continuous refluxing by coil condenser equipped with the flask. After 24 hours, another 150 ml NH_4OH was added and cooled down at room temperature. The mixture was then filtered using vacuum-filter through a 3 μm porosity filter paper.

The filtered OFA was dried in a vacuum dryer at 105°C for 1 hour and sealed in a plastic bag for further use.

FTIR Characterization

The chemical structures of as received OFA and modified OFA (OFA-Amine) were characterized by means of FTIR measurement using a Nicolet 6700 spectrometer from Thermo Electron™. A weight of 1-2 mg of the OFA was mixed thoroughly with 1.0 g of fine dried powder of KBr. Then, the resulting mixture was hydraulically pressed in a Carver press to obtain a thin transparent disc. The thin disc was placed in an oven at 110^{o}C for 2 h to prevent any interference of any existing water vapor or carbon dioxide molecules. All the FTIR spectra were taken in the transmission mode and in the range 600–4000 cm^{-1} at room temperature. FTIR spectra were obtained using a spectral resolution of 4 cm^{-1} and 30 co-added scans.

SEM and EDS

The scanning electron microscope (JEOL, model JSM 6400) was used to determine the qualitative characteristics and morphology of the fly ash sample. The dried sample was fixed with double side masking tape. In order to make it surface conductive, the fly ash sample was gold coated. It was then viewed on FE-SEM at different magnification to see the surface topography of the sample. Energy dispersive X-ray (EDX) analysis was carried for the analysis of chemical composition of as-received OFA and OFA-Amine.

Sample Preparation for Rheological Testing

OFA and pure asphalt were blended in a high shear blender. The blender acts as a batch stirred tank with a constant temperature bath. Typical mixing procedure was as follows: Steel cans of approximately 1000 mL were filled with 250–260 g of asphalt and put in a thermoelectric heater. When the temperature of the asphalt reached 145°C, a high shear mixer was dipped into the can and set to about 1000 rpm. Calculated amount of OFA was added gradually with base asphalt. The bath temperature was maintained at 145 ± 1°C. Samples were blended for 10 minutes at high shear to confirm uniform distribution of OFA in the asphalt matrix. Asphalt sample was poured into silicone molds before being used for rheological testing. The samples specimens were stored in a refrigerator at 5°C.

Rheological tests

Dynamic and steady shear rheological tests were carried out to investigate the effect of OFA-Amine on the rheology of modified asphalt binder. The dynamic temperature step measurements for the samples were performed in ARES rheometer. This is a constant strain rheometer equipped with a heavy transducer (range 2-2000 g for normal force; 2-2000 g-cm for torque). All tests were carried out in range of 64^{o}C-100^{o}C using a parallel plate set of 25 mm diameter. With the sample in position, the oven was closed and the sample heated at 64^{o}C for about 5 minutes, thereafter the gap between the plate platen was adjusted to 1.5 mm by lowering the upper platen force transducer assembly at a constant load of 500 g. The melt that extruded beyond

the platen rim by this procedure was cleaned off. Strain in the linear viscoelastic range (strain amplitude, γ^o of 12.5 %) and frequency of 10 rad/s was used for all the tests. In all the experiments, nitrogen gas was continuously used for heating the samples during testing to avoid oxidation during testing. A holding period of 5 min was allowed before beginning measurements when the temperature reaches steady state. The Orchestrator software was used to calculate the dynamic shear viscosity, storage modulus, complex modulus and phase angle for all samples.

Dynamic frequency sweep tests were conducted at 60^{o}C and frequency ranges of 100-0.1 rad/s and the constant strain of 10%. Different linear viscoelastic variables were calculated using TA Orchestrator software. Steady shear rheological tests were conducted at 50^{o}C and a shear rate in the range of 0.01-10 s^{-1}.

4.5.4 Results and Discussion

OFA surface modification

Surface modification of OFA was done according to the procedure described earlier to obtained amine reach OFA (OFA-Amine). Amine group was successfully attached to the surface of OFA and it was detected through FTIR spectra and SEM/EDS analysis.

FTIR Analysis

FTIR technique was used to determine whether a new functional group is attached to fly ash surface after chemical activation. Figure 4.5.1 (a & b) shows the FTIR spectra

of as-received and treated OFA over the range 4000–600 cm^{-1}. The intensity of the peaks for as-received OFA is very small compared to that of treated OFA. An as-received sample spectrum shows that it has three peaks at 2022, 2162.3 and 2183 cm^{-1}. The peak at 2022 cm^{-1} is attributed to transition metals (Fe and Ni) carbonyl compound whereas the peaks at 2162.3 and 2183 cm^{-1} are due to the C≡C stress of medial alkyne (Coates, 2000).

Figure 4.5.1(b) shows that OFA-Amine has three major peaks at 1075, 1434 and 3209 cm^{-1} respectively. The peak at 1075 cm^{-1} is due to primary amine, CN stretch which suggests the presence of amine group on treated OFA. The peak at 1434 cm^{-1} is attributed to the methyl C-H asymmetric/symmetric bend. The peak at 3209 corresponds to hydroxyl group O-H stretch. Similar functional group was also detected by other authors (Yaumi, et al., 2012). Therefore, the FTIR study confirmed that treated OFA has amine functional group on the surface of OFA.

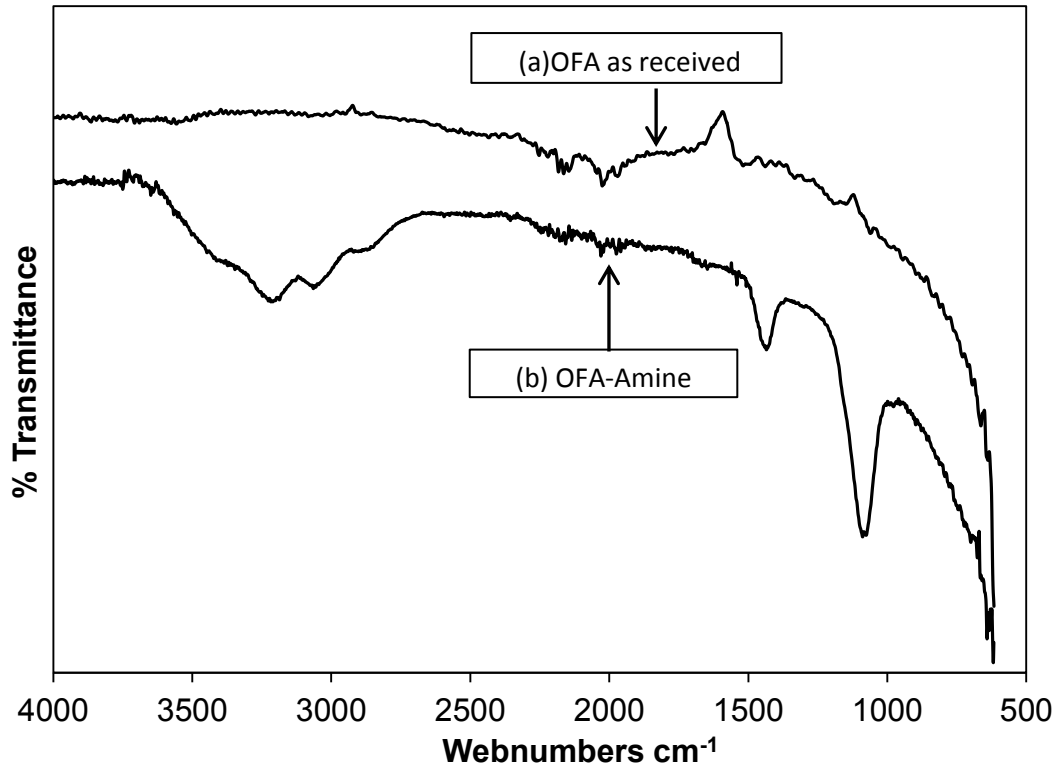

Figure 4.5. 1: FTIR spectrum (a) OFA before treatment (b) OFA after chemical treatment

SEM/EDS Analysis

The modified sample was characterized by the combination of SEM-EDS for elemental analysis. Figure 4.5.2 shows the SEM-EDS results for modified OFA. Table 4.5.1 summarizes the elemental analysis of OFA before and after the modification process. The elemental analysis shows that the treatment process has either removed or reduced the undesired components such as V, Fe, S, and Ni from the OFA sample. The increase in oxygen percentage can be due to the addition of $-OH$ ion into the surface of OFA.

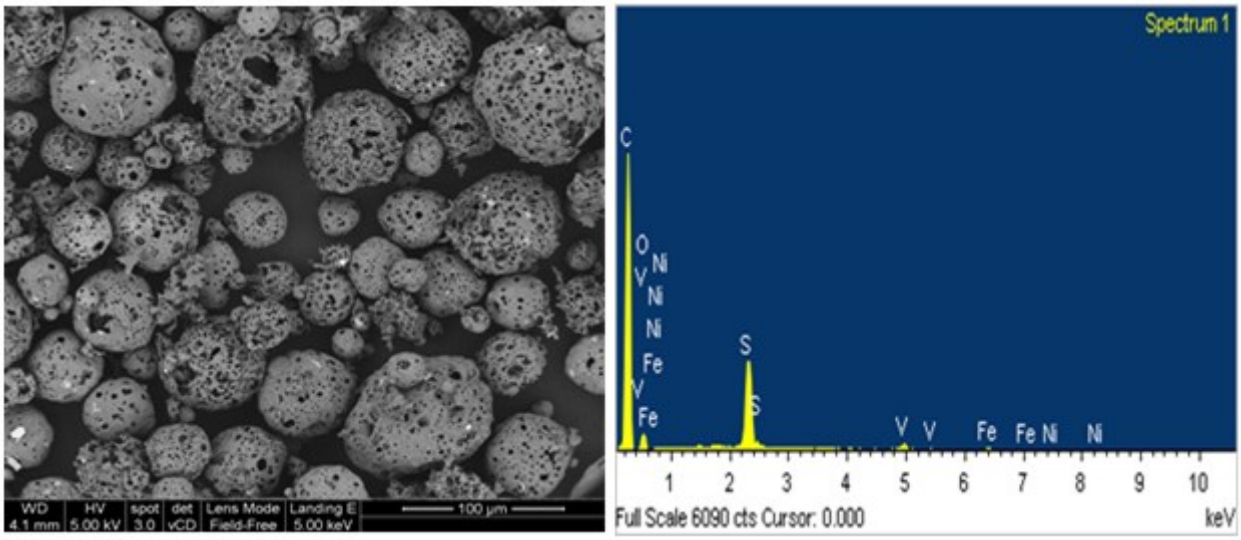

(a) SEM/EDS analysis of as received OFA

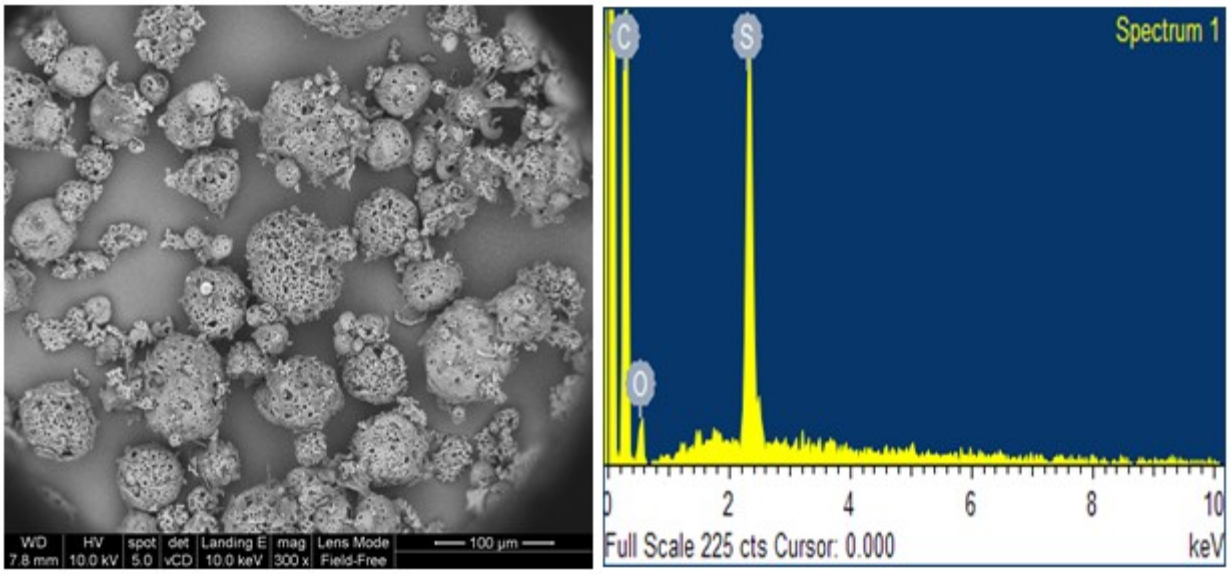

(a) SEM/EDS of OFA-Amine sample

Figure 4.5. 2: Combined SEM/EDS analysis of OFA samples

Table 4.5. 1: Elemental analysis of OFA before and after treatment

Sl #	Elements	Before treatment		After treatment	
		Weight %	Atomic %	Weight %	Atomic %
1	C	79.99	89.40	80.67	87.85
2	O	7.02	5.89	10.40	8.50
3	S	8.74	3.66	8.93	3.64
4	V	1.83	0.48	0	0
5	Fe	1.07	0.26	0	0
6	Ni	1.36	0.31	0	0
Total		100	100	100	100

Rheology of OFA-Amine/asphalt binders

Steady shear rheology

Steady rate sweep tests were conducted for all binders at 50^{o}C and a shear rate in the range 0.01-10 s^{-1}. Steady shear viscosity as function of shear rate is plotted in Figure 4.5.3 for pure and OFA-Amine modified binders. Pure asphalt sample displayed long Newtonian plateau up to ~ 2 s^{-1}. OFA-Amine modified binders showed a short Newtonian plateau followed by shear thinning behavior at high shear rate. Similar behavior was also reported for polymer modified asphalt binders (Polacco, et al., 2006). These types of shear viscosity data can be well modeled by Carreau model which is given by following equation:

$$\eta = \frac{\eta_0}{\left[1+\left(\quad\right.\right.} \qquad (4.5.1)$$

where, η_0 is the zero shear viscosity, $\dot{\gamma}$ is the critical shear rate for the onset of shear thinning region and a is a parameter related to the slope of shear thinning region. The viscosity data were well fitted by the model as shown in Figure 4.5.3. It is noticed that incorporation of OFA-Amine in asphalt binder increases the viscosity of the binder. As the amount of OFA-Amine increases in the binder, the Newtonian plateau decreases and the shear thinning region increases. This shear thinning behavior can be attributed to the broad molecular weight distribution which results from the size heterogeneity due to the addition of OFA and the possible bonding of OFA-Amine and asphalt.

Researchers have observed that the SHRP rutting parameter $G^*/\sin\delta$ is not very effective in predicting the rutting performance of binders, especially in the case of modified binders are used (Shenoy, 2002; Bahia, et al., 1999). For such case a new parameter, zero shear viscosity (η_o) has been suggested by many researchers as a possible measure for the rutting resistance of modified asphalt binders (Binard, et al., 2004; Phillips & Robertus, 1996). η_o was calculated for all binders using equation (5) and the values are shown in Table 4.5.2 It is observed that η_o increases with the increase in OFA-Amine content. The increment in η_o is more pronounce at high OFA-Amine content in the binders. Also, power law index, n, was obtained and tabulated in Table 4.5.2. The critical shear rate decreases with the increase in OFA-

Amine content. The results show enhancement in shear thinning due to the addition of OFA-Amine.

Table 4.5. 2: Carreau model parameters for steady shear data

Binder #	OFA-Amine content (%)	Carreau Model Parameters			
		Zero Shear Viscosity, η_o, (Pa.s)	Critical shear rate, $\dot{\gamma}$ s^{-1}	Power law index	Fit quality, r^2
1	0	1070	2.591	0.178	0.999
2	2	2951	0.758	0.514	0.998
3	4	4362	0.403	0.395	0.999
4	6	6761	0.370	0.358	0.998
5	8	13438	0.105	0.139	0.999

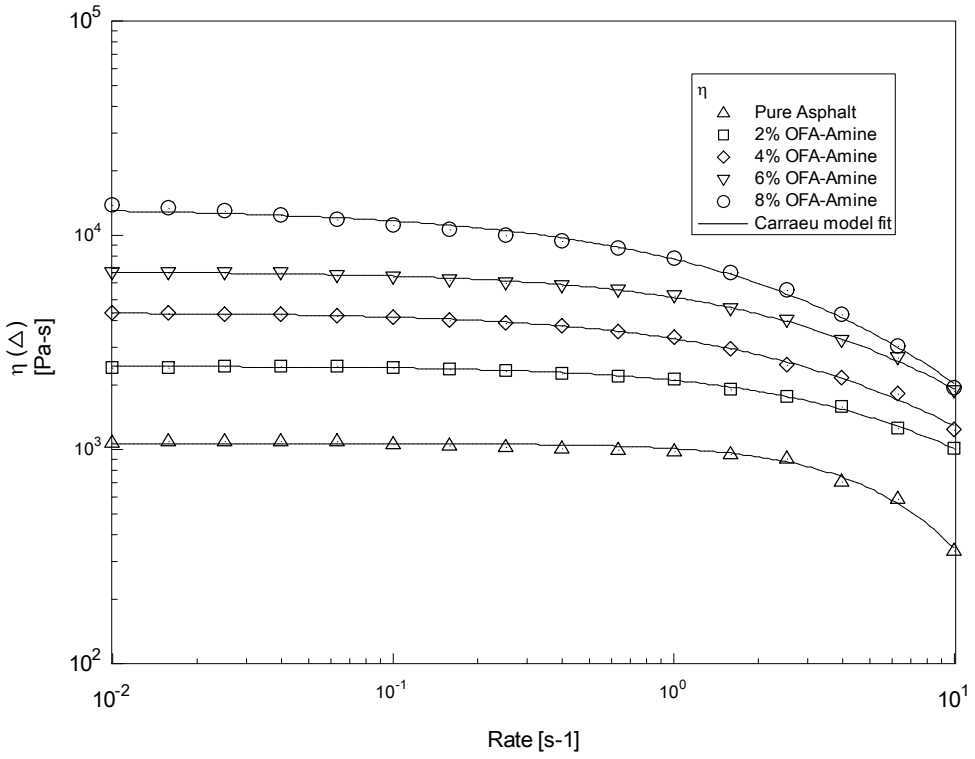

Figure 4.5. 3: Steady shear viscosity function at 50°C

Temperature sweep test

Temperature sweep test was conducted for all binders to extract the values of complex modulus, G^* and phase angle, δ as function of temperature. According to the strategic highway research program (SHRP), the stiffness parameter $G^*/\sin\delta$ is a factor used to estimate the rutting resistance of asphalt binder (The Asphalt Institute, 2003). This factor should be larger than 1 kPa at the maximum pavement design temperature for unaged original asphalt, when measured at 10 rad/s to simulate traffic loading. Higher values of $G^*/\sin\delta$ are expected to give a high resistance to permanent deformation. Figure 4.5.4 shows $G^*/\sin\delta$ versus temperature for pure asphalt and 4% as-received OFA and 4% OFA-Amine modified binders. It shows that $G^*/\sin\delta$ value for 4% OFA-Amine modified binder is far better than that of 4% as-received OFA modified binder. OFA-Amine has better dispersion in asphalt than as-received OFA. So, it is better to use treated OFA instead of as-received OFA for asphalt modification. The complete PG test results for treated and untreated OFA modified binders are shown in Table 4.5.3.

Figure 4.5.5 shows $G^*/\sin\delta$ versus temperature for various amount of OFA-Amine modified asphalt binder. It shows that the modification of asphalt binder with OFA-Amine increases the rutting resistance significantly. The value of $G^*/\sin\delta$ decreases with temperature and there is exponential relationship $G^*/\sin\delta$ and temperature as it shown in Figure 4.5.5. The relationship between $G^*/\sin\delta$ and OFA-Amine content of the binders is linear as shown in Figure 4.5.6 for different temperature. Table 4.5.3

lists the maximum temperature attained at $G^*/\sin\delta \geq 1$ kPa. It is mentioned that the maximum local pavement temperature for Saudi Arabia is 76°C for hot summer season (Al-Abdul Wahhab, et al., 1997). Base asphalt cannot fulfill SHRP criteria as the maximum temperature at $G^*/\sin\delta \geq 1$is 68.5°C. So, there is a need for modification of pure asphalt binder to increase $G^*/\sin\delta$ to improve rutting resistance. It is noticed that 4% OFA-amine is needed to upgrade the binder performance from 70°C to 76°C. As the percentage of OFA-Amine is increased in the binder, the stiffness of binders goes up. So, the binder modification using treated OFA has significantly improved rutting resistance for permanent deformation and increased the range of application of the modified binders.

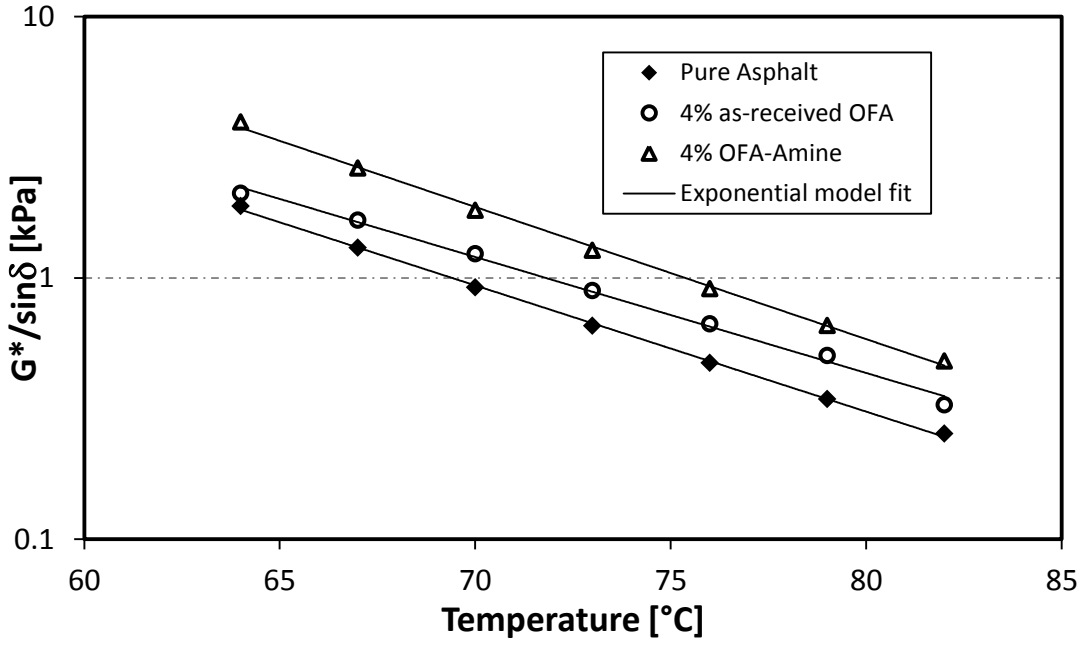

Figure 4.5. 4: $G^*/\sin\delta$ versus temperature for treated and as-received OFA-asphalt binder

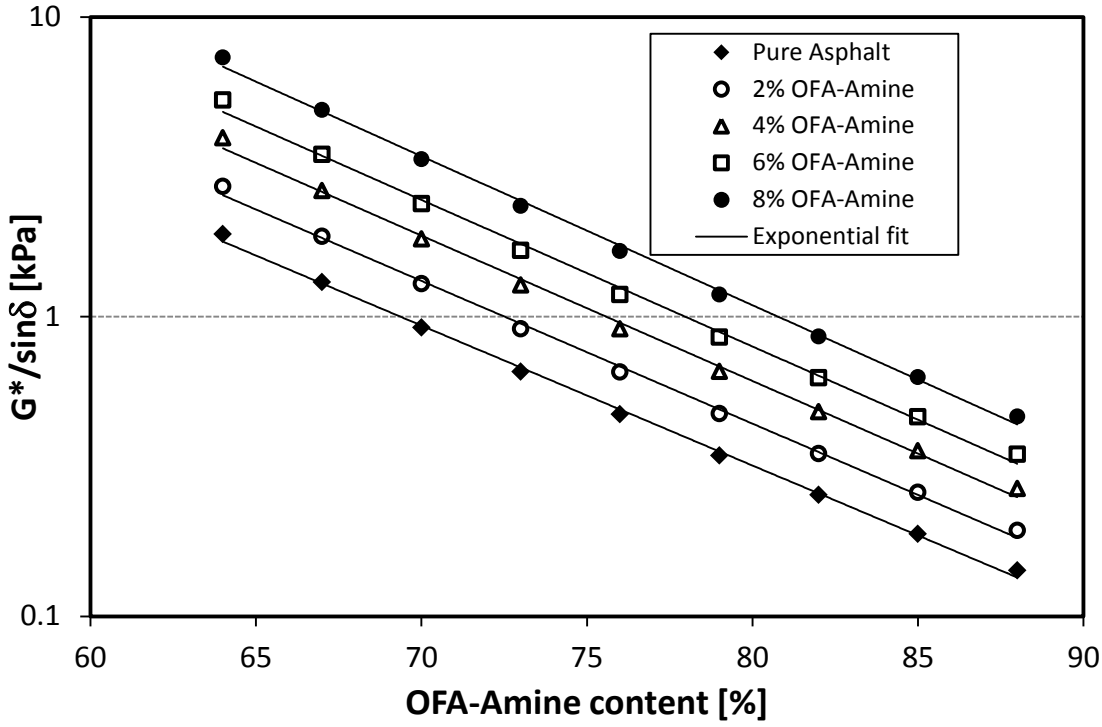

Figure 4.5. 5: *G*/sinδ* versus temperature for different OFA-Amine content

Table 4.5. 3: Maximum temperature at G*/sinδ = 1kPa for all binders

Binder #	OFA content, %	Max. Temperature attained, °C @ *G*/sinδ* =1 kPa	
		OFA-Amine	OFA as-received
1	0	68.50	68.5
2	2	74.30	70.91
3	4	76.15	71.20
4	6	78.50	74.18
5	8	80.25	75.09

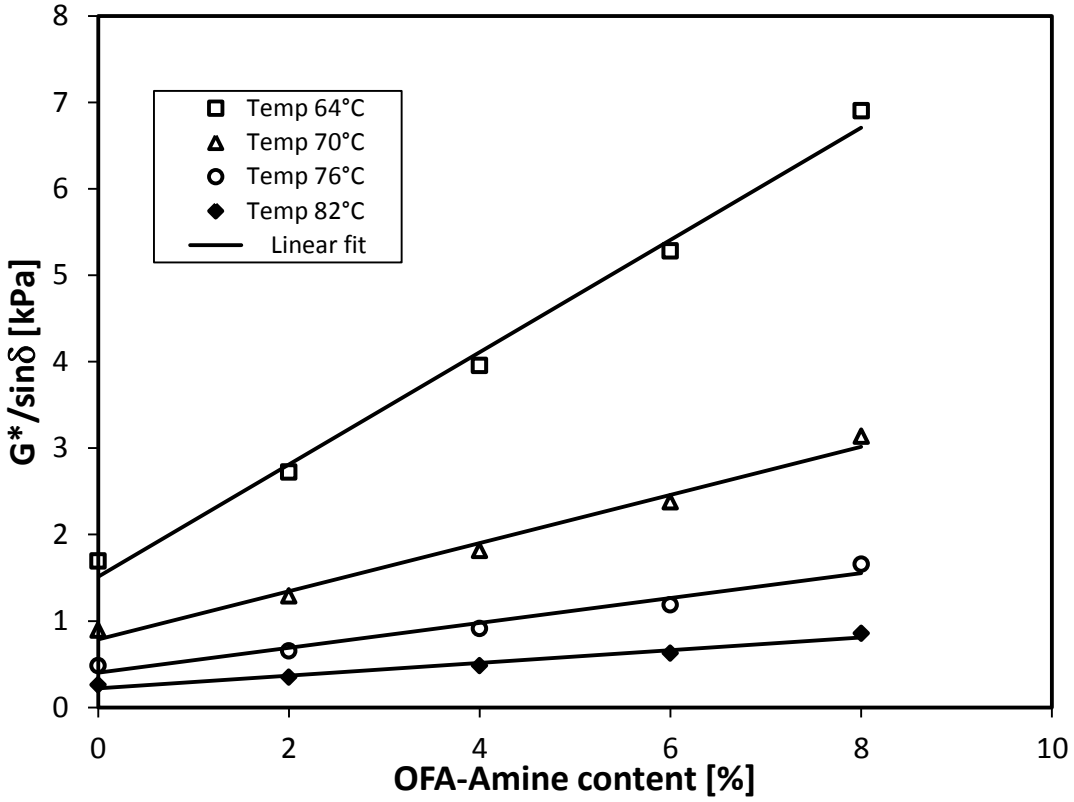

Figure 4.5. 6: $G^*/\sin\delta$ versus OFA-Amine content of asphalt binder for different temperatures

Temperature sweep data was further analyzed to check the effect of temperature on asphalt viscosity. Viscosity-temperature relationships of asphalt binder can be expressed by the well-known Arrhenius equation as follow:

$$\eta^* = Ae^{\left(E_a/RT\right)} \tag{4.5.2}$$

where E_a is the flow activation energy, A is the pre-exponential term, and R is the universal gas constant. E_a is an important factor that strongly influences the viscosity. Figure 4.5.7 shows complex viscosity versus 1000/T for pure and modified asphalt

binders. The data given in Fig. 4.5.7 showed good fit to Arrhenius model. E_a was calculated using equation (4.5.2) and the values of activation energy along with pre-exponential factor are listed in Table 4.5.4. Activation energy for pure asphalt is 109.29 kJ/mol. It is observed that addition of OFA-Amine to asphalt does not change the activation energy of the modified asphalt binders. So, asphalt modification with OFA-Amine has increases the upper performance temperature without changing the thermal susceptibility of asphalt binders.

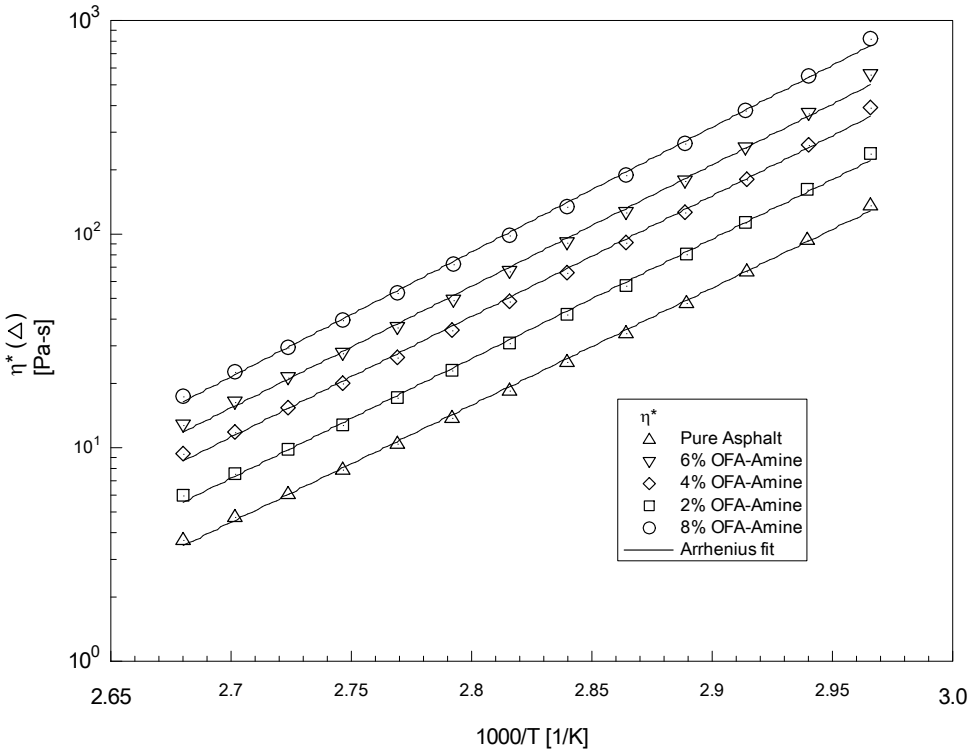

Figure 4.5. 7: Effect of temperature on complex viscosity for all binders

Table 4.5. 4: Arrhenius model parameters for different binders

Binder #	OFA-Amine content (%)	Arrhenius Model Parameters		
		Activation energy, Ea (kJ/mol)	Pre-exponential factor, A(Pa.s)	Fit quality, r^2
1	0	109.29	2.56×10^{-15}	0.9997
2	2	107.10	5.65×10^{-15}	0.9991
3	4	108.06	6.45×10^{-15}	0.9987
4	6	108.89	6.73×10^{-15}	0.9987
5	8	111.77	3.69×10^{-15}	0.9994

Dynamic frequency sweep measurements

Dynamic frequency sweep test for all binders were conducted at 50^{o}C in the range 100-0.1 rad/s at10% strain. Typical linear viscoelastic properties of the OFA-Amine modified asphalt binder are displayed in Figures 4.5.8-4.5.9. Storage modulus, G', as function of frequency is shown in Figure 4.5.8 for pure and modified binders. The results are shown for asphalt with 0%, 2%, 4%, 6% and 8% OFA-Amine content by weight. The data showed good fit of the five elements Maxwell model. For the whole frequency range, the modified asphalt binder has improved G' as compared to base asphalt. The increase in G' is higher at higher concentration of OFA-Amine. G' is highly sensitive to the morphological state of a heterogeneous system (Cho, et al., 2009). The value of G' is an indication of how much elasticity can be boosted by the asphalt modification. The advantage of high G′ is at high temperature. High G′ values at low frequency suggest better flexibility. According to the principle of time–

temperature superposition, this behavior corresponds to long service time or at tolerance to high temperature, which is needed in hot climate.

The slopes of log G′ versus log ω at low ω range were calculated and their values are 1.71, 1.395, 1.33, 1.30 and 1.285 for pure asphalt, 0%, 2%, 4%, 6% and 8% OFA-Amine modified asphalt binder, respectively. So, the melt rheology of OFA-Amine modified asphalt binder suggest that modified asphalt binders expected to show better deformation resistance at high temperature. Figure 4.5.9 shows the dynamic viscosity as function of frequency at 50°C. Data showed good fit to the Carreau model. The profile of η′(ω) for pure asphalt showed typical Newtonian behavior over almost the entire frequency range, but OFA-Amine modified asphalt binder displayed non-Newtonian behavior, which was more pronounced at high OFA-Amine concentrations. Similar behavior was observed for asphalt modification with polymers (Iqbal, et al., 2006; Hussein, et al., 2005).

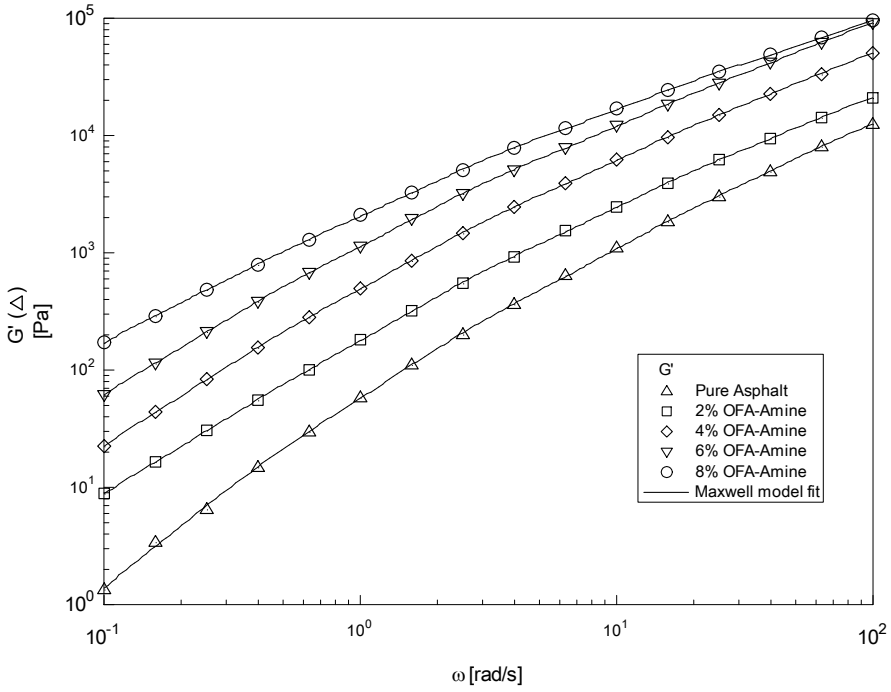

Figure 4.5. 8: Dynamic storage moduli G′ function of frequency at 50°C

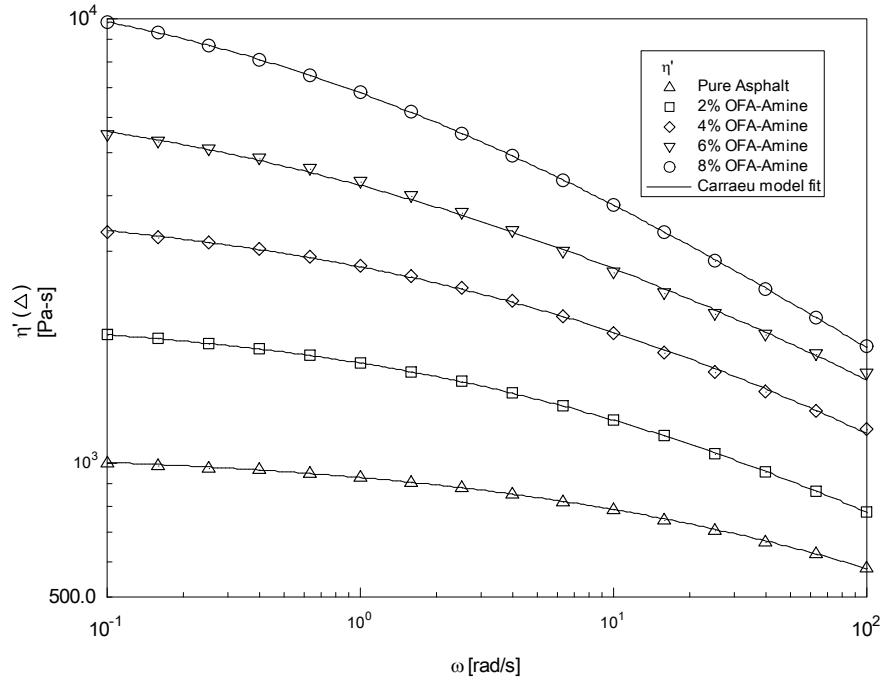

Figure 4.5. 9: Dynamic shear viscosity as function of frequency at 50°C.

4.5.5 Conclusion

OFA is treated by 30% NH_4OH solution to produce amine modified OFA. The presence of functional group was detected through FTIR and SEM/EDS. Dynamic, steady and temperature sweep rheological measurements of OFA-Amine/asphalt binders were performed to assess the impact of functionalization OFA on the binder's rheology. The following conclusions are drawn on the basis of this investigation:

1. The addition of OFA-Amine increased the viscoelastic properties (G^*, G') of the modified asphalt binders. SHRP rutting parameter $G^*/\sin\delta$ increases with OFA-Amine content and it showed linear relationship with OFA-Amine concentration. The high temperature performance grading of modified asphalt has increased from 68.5°C to 80.25 as a result of the addition of 8% OFA-Amine.
2. Addition of OFA-Amine to pure asphalt increases complex viscosity without changing activation energy. Constant activation energy suggests that OFA-Amine modification has maintain temperature resistance of modified asphalt binders.
3. Addition OFA-Amine to asphalt increases the shear thinning behavior which suggests ease of processing. The onset of shear thinning decreases from 2.59 to 0.10 s^{-1} as a result of 8% OFA-Amine addition to pure asphalt.

Finally the chemically treated waste OFA can be utilized in the modification of asphalt binder. It will solve the waste disposal problem of OFA as well as reduce the amount of asphalt pavement to be used in.

4.5.6 References

1. The Asphalt Institute, 2003. *Performance Graded Asphalt Binder Specification and Testing, SP-1,* Lexington, KY: The Asphalt Institute.
2. Abbasi, S.H.,Adesina, A.A., Atieh, M.A.,Ul-Hamid, A, Hussein, I.A., 2013. Rheology, Mechanical and Thermal Properties of (C18-CNT/LDPE) Nanocomposites. *International Polymer Processing,* pp. 3-13.
3. Al-Abdul Wahhab, H., Asi, I. & and Ali, M., 1997. Development of Performance-Based Bitumen Specifications for the Gulf Countries. *Construction and Building Materials Journal,* 11(1), pp. 15-22.
4. Al-Amethel, M., Al-Abdul Wahhab, H. I. & Ibnelwaleed A., H., 2011. *Utilization of heavy oil fly ash to improve asphalt binder and asphalt concrete performance.* Patent No. US 8062413 B1.
5. American Coal Ash Association, 2011. *Coal Combustion Product (CCP) Production & Use Survey Report,* Farmington Hills, MI: AACA.
6. Asi, I. & Assa'ad, A., 2005. Effect of Jordanian oil shale fly ash on asphalt mixes. *Journal of Materials in Civil Engineering,* pp. 553-559.

7. Bahia, H., Zeng, M., Zhai, H. & Khatr, 1999. *Superpave protocols for modified asphalt binders, 15th Quarterly Progess Report for NCHRP Project 9–10.,* Washington: DC: National Cooperative Highway Research Program..
8. Binard, C., Anderson, D., Lapalu, L. & Planche, J., 2004. *Zero shear viscosity of modified and unmodified binders.* Vienna, Eurasphalt & Eurobitume congress.
9. Cho, Y., Jeong, H. & Kim, B., 2009. *Macromolecular Research,* Volume 17, pp. 879-890.
10. Coates, J., 2000. Interpretation of Infrared Spectra, A Practical Approach. In: *Encyclopedia of Analytical Chemistry.* Chichester: John Wiley & Sons Ltd, p. 10815–10837.
11. Hussein, I. A., Iqbal, M. H. & Al Abdul Wahhab, H. I., 2005. Influence of Mw of LDPE and vinyl acetate content of EVA on the Rheology of Polymer Modified Asphalt. *Rheologica Acta,* 45(1), pp. 92-105.
12. Iqbal, M. H., Hussein, I. A., Wahhab, H. I. A.-A. & Amin, M. B., 2006. Rheological Investigation of the Influence of Acrylate Polymers on the Modification of Asphalt. *J. Applied Polymer Science,* 102(4), pp. 3446-3456.
13. Kandhal, P., Lynn, C. & Parker, F., 1998. *Characterization tests for mineral fillers related to performance of asphalt paving mixtures,* Auburn.: National Center for Asphalt Technology.
14. Karasahin, M. & Terzi, S., 2007. Evaluation of marble waste dust in the mixture of asphaltic concrete.. *Construction and Building Materials,* Volume 21, pp. 616-620.

15. Phillips, M. & Robertus, C., 1996. *Binder rheology and asphalt pavement permanent deformation: the zero shear viscosity.* Strasbourg, Eurasphalt & Eurobitume congress, p. 12.

16. Phillips, M. & Robertus, C., 1996. *Binder rheology and asphalt pavement permanent deformation: the zero shear viscosity.* Strasbourg, Eurasphalt & Eurobitume congress, p. 12.

17. Polacco, G., Stastna, J., Biondi, D. & Zanzotto, L., 2006. Relation between polymer architecture and nonlinear rviscoelastic behavior of modified asphalts. *Current Opinion in Colloid & Interface Science,* Volume 11, pp. 230-245.

18. Shawabkeh, R., Al-Harahsheh, A. & Al-Otoom, A., 2004. Copper and zinc sorption by treated oil shale ash. *Separation and Purification Technology,* Volume 40, p. 251.

19. Shawabkeh, R. & Harahsheh, A., 2007. H_2S removal from sour liquefied petroleum gas using Jordanian oil shale ash. *Oil Shale,* Volume 24, p. 109.

20. Shenoy, A., 2002. Model-fitting the master curves of the dynamic shear rheometer data to extract a rut-controlling term for asphalt pavements. *ASTM J Test Eval,* 30(2), pp. 95-102.

21. Visa, M., Bogatu, C. & Duta, A., 2010. Simultaneous adsorption of dyes and heavy metals from multicomponent solutions using fly ash. *Applied Surface Science,* Volume 256, p. 5486.

22. Woo-Teck, Dong-Hyun, K. K. & Yung-Phil, K., 2005. Characterization of Heavy Oil Fly Ash Generated from a Power Plant. *Journal of Materials.*

23. Yaumi, A. L., Hussein, I. A. & Shawabkeh, R. A., 2012. Surface modification of oil fly ash and its application in selective capturing of carbon dioxide. *Applied Surface Science.*

4.6 Mix Design Evaluation of Sulfur Modified Asphalt Concrete Mixes

4.6.1 Mixes code and composition

Based on the rheology results (section 4.1 and 4.2) fourteen asphalt concrete mixes were selected for evaluation using Marshall Stability, Durability and Resilient modulus. Table 4.6.1 represents the detailed information on the selected asphalt mixes.

Table 4.6. 1: Detailed information of the selected mixes

Mixes code #	Percentages of different components				PG
	Sulfur	Asphalt	Wax	Crumb rubber	
S1		100			64-10
S2	20	78	2		64-10
S3	20	76		4	70-10
S4	20	74		6	70-10
S5	30	60	10		76-10
S6	30	66		4	76-10
S7	30	64		6	76-10
S8	40	58	2		70-10
S9	40	52	8		76-10
S10	40	59		1	76-10
S11	40	58		2	76-10
S12	50	49		1	76-10
S13	50	48		2	76-10
S14	50	46		4	76-10

4.6.2 Marshall Stability of the Designed Mixes

Marshall Stability of the designed mixes (listed in Table 4.6.2) was calculated using the setup presented in Figure 4.6.1. Detailed procedure has been discussed in chapter 3. Three specimens for each of the designed mixes were used to get an average stability in kN. Table 4.6.2 represents Marshall Stability results for all the mixes. The results showed that pure asphalt concrete mixes have the highest stability of 20.38 kN. Increases in sulfur content of the mixes decreases the stability of the mixes in general. All other mixes have stability ranging from 15 to 20 kN. Figure 4.6.2 shows a plot of stability versus mixes code for all the designed mixes. Increases in sulfur content of the mixes decreases the stability of the mixes in general. The reason for the decrease in stability with sulfur content can be due the free sulfur content of the mixes. The unbounded sulfur in the mixes will lead to a softening the mix through water penetration during the two hours conditioning in water bath at 60^{o}C. However, this decrease in stability was minimized through polyethylene wax and crumb rubber modification.

Figure 4.6. 1: Marshall Stability and Flow setup

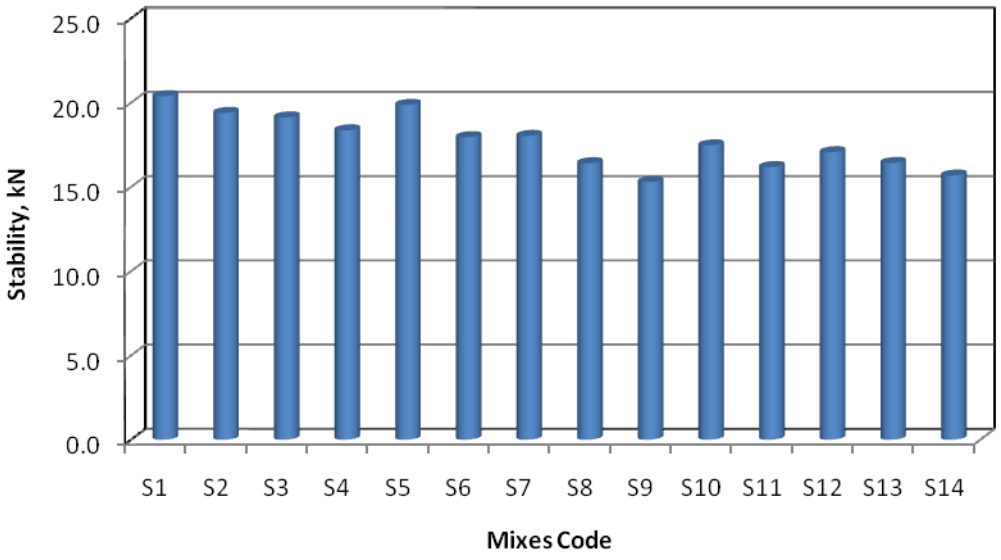

Figure 4.6. 2: Marshall Stability for the designed mixes

Table 4.6. 2: Marshall Stability and Resilient Modulus of the designed mixes

Mixes code #	Sample #	Stability, kN	Average Stability, kN	Resilient Modulus, MPa	Average Resilient Modulus, MPa
S1	1-1	20.24	20.38	5400.25	5342.50
	1-2	22.52		5696.25	
	1-3	18.39		4931.00	
S2	1-1	20.97	19.39	7747.75	7336.17
	1-2	18.70		7327.00	
	1-3	18.51		6933.75	
S3	3-1	19.43	19.13	7173.50	7200.83
	3-2	18.33		7488.00	
	3-3	19.63		6941.00	
S4	4-1	20.02	18.36	8216.75	7341.75
	4-2	17.13		6160.75	
	4-3	17.92		7647.75	
S5	5-1	20.62	19.87	13708.75	12415.33
	5-2	19.57		12809.00	
	5-3	19.40		10728.25	
S6	6-1	19.38	17.95	9218.00	8129.50
	6-2	17.52		8084.50	
	6-3	16.95		7086.00	
S7	7-1	17.53	18.03	9142.25	8635.33
	7-2	18.04		8081.00	
	7-3	18.51		8682.75	
S8	8-1	16.55	16.41	9010.00	7928.67
	8-2	16.27		6774.75	
	8-3	16.40		8001.25	
S9	9-1	15.33	15.29	10112.75	11350.42
	9-2	15.09		12002.75	
	9-3	15.47		12475.75	
S10	10-1	17.64	17.47	8677.00	8547.42
	10-2	17.20		8521.25	
	10-3	17.56		8444.00	
S11	11-1	0.00	16.18	4147.00	6500.75
	11-2	15.38		7320.75	
	11-3	16.99		8034.50	
S12	12-1	14.66	17.06	8021.50	11161.67
	12-2	17.84		13357.25	
	12-3	18.67		12106.25	
S13	13-1	16.87	16.42	7461.75	7526.42
	13-2	16.74		7633.50	
	13-3	15.65		7484.00	
S14	14-1	12.74	15.67	6238.75	7710.67
	14-2	17.79		8467.00	
	14-3	16.49		8426.25	

4.6.3 Resilient Modulus of the Designed Mixes

Resilient modulus (M_R) is an important variable for the mechanistic design approaches of pavement structures. It is the measure of pavement response in terms of dynamic stresses and corresponding resulting strains. Resilient modulus of hot mix asphalt (HMA) is conducted by applying diametral pulse loads. The load is applied in the vertical diametrical plane of a cylindrical specimen of 63.5-mm height by 101.6-mm diameter as shown in Figure 4.6.3. The specimens were prepared using the Superpave compaction method. The resulting horizontal deformation of the specimens is measured and used to calculate the resilient modulus. The test was performed at 25°C and the results are shown in Table 4.6.2. The results for the resilient modulus are shown in Figure 4.6.4. Pure asphalt concrete mix has the least value of M_R. Sulfur modified asphalt concrete has improved resilient modulus of the mixes. The modified mixes are stiffer than the plain mix. Addition of sulfur results in increase in the stiffness and the addition of polyethylene wax increases the elasticity of the mix. Mixes S5 and S9 show very high resilient modulus compared to other mixes. These two mixes have high polyethylene wax content of 10% and 8%, respectively which increases the resilience of the mix to dynamic loads as a result of the improvement in the binder elastic properties at 25°C.

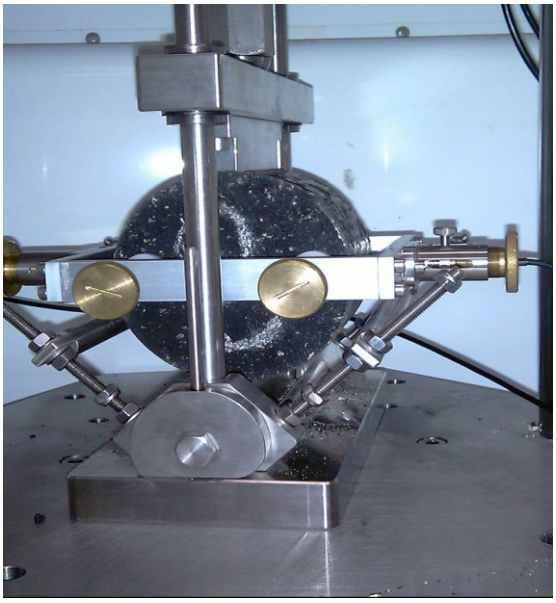

Figure 4.6. 3: Resilient Modulus test setup

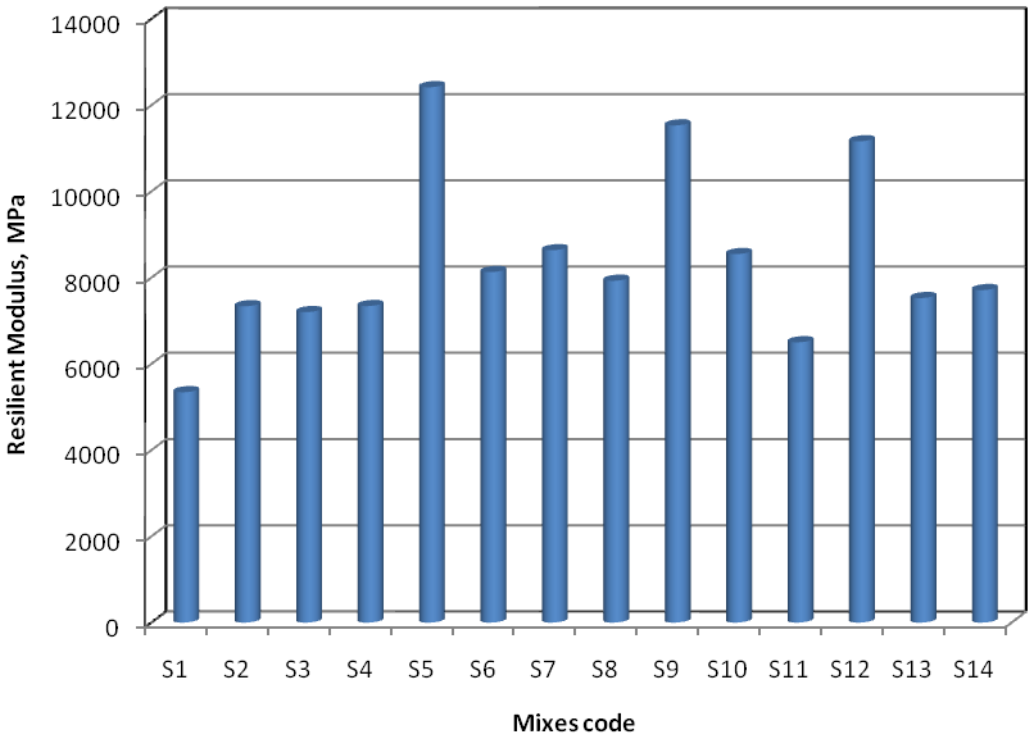

Figure 4.6. 4: Resilient modulus for the designed mixes

4.6.5 Indirect Tensile Strength and Durability of the Designed Mixes

The Indirect Tensile Strength (ITS) test (AASHTO T-245) was used to explore mix resistance to cracks development utilizing ITS as shown in Figure 4.6.5. The ITS test was performed on cylindrical specimens of 63.5-mm height by 101.6-mm diameter. Six specimens were prepared for dry and wet ITS testing following samples compaction. The maximum load the specimen would carry before failure was determined (known as the ITS). The test was carried out at 25°C for dry ITS specimens. Three specimens were conditioned in a water bath of 60^{o}C for 24 hours and then put into a water bath of 25^{o}C for 2 hours. The specimens were then tested for wet ITS. Durability was calculated using the ratio of ITS of the conditioned specimen to ITS of the unconditioned specimen. Results of the ITS test and durability is shown in Table 4.6.3. Figure 4.6.6 represents the durability of the designed mixes. It is noticed that mix # S9 has the highest durability (84.86%), however it has high resilient modulus.

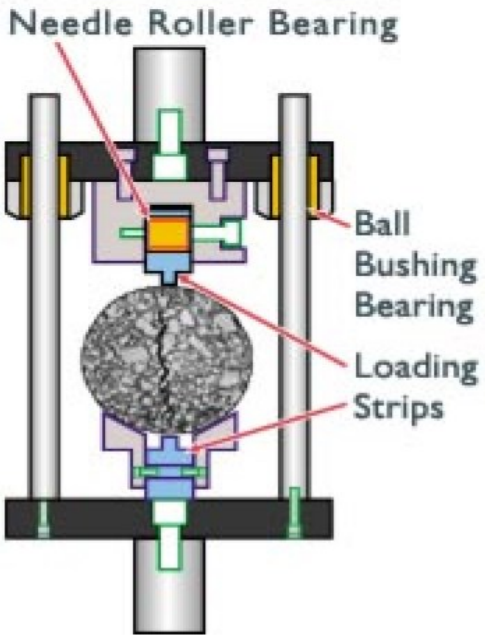

Figure 4.6. 5: ITS test setup

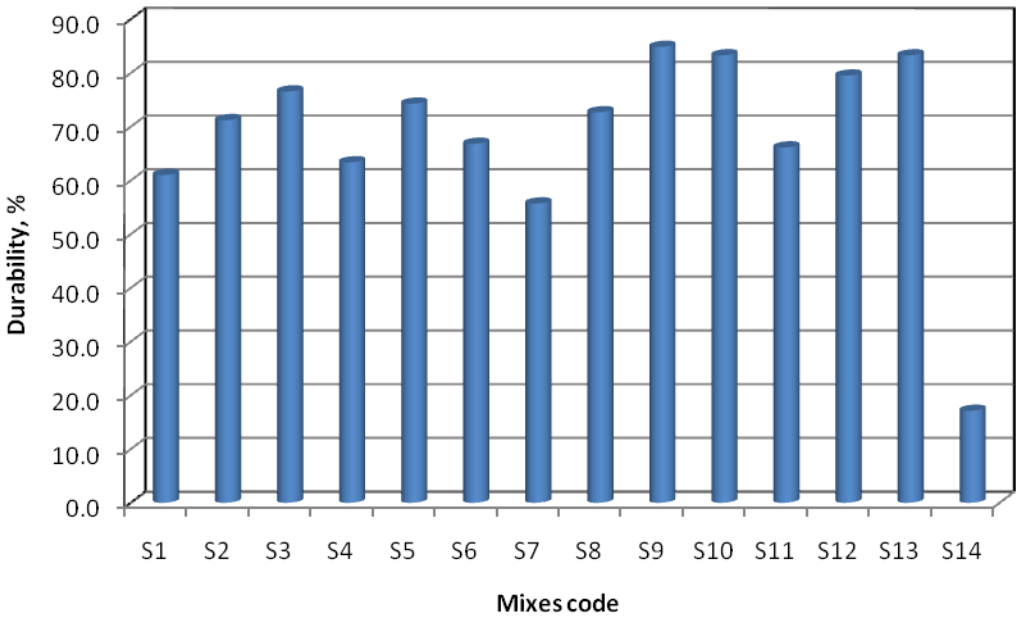

Figure 4.6. 6: Durability of the designed mixes

Table 4.6. 3: ITS and durability of the designed mixes

Mixes code #	Sample #	Dry ITS, kPa	Average Dry ITS, kPa	Wet ITS, kPa	Average Wet ITS,	Durability, %
S1	1-1	1353.04	1260.93	737.33	769.44	61.02
	1-2	1213.88		710.24		
	1-3	1215.87		860.74		
S2	1-1	1568.36	1537.46	1162.04	1095.01	71.22
	1-2	1539.96		1036.55		
	1-3	1504.06		1086.45		
S3	3-1	1470.80	1434.02	1235.37	1097.85	76.56
	3-2	1429.50		988.92		
	3-3	1401.75		1069.26		
S4	4-1	1574.58	1552.43	937.97	983.76	63.37
	4-2	1487.02		773.36		
	4-3	1595.69		1239.95		
S5	5-1	1515.89	1540.66	992.87	1144.50	74.29
	5-2	1472.40		1292.52		
	5-3	1633.70		1148.11		
S6	6-1	1500.06	1402.11	617.55	936.86	66.82
	6-2	1465.49		1200.81		
	6-3	1240.78		992.21		
S7	7-1	1892.99	1783.85	906.58	993.32	55.72
	7-2	1769.24		1462.07		
	7-3	1689.33		613.11		
S8	8-1	1607.65	1583.49	1190.33	1150.99	72.69
	8-2	1630.94		1235.65		
	8-3	1511.88		1026.98		
S9	9-1	1395.10	1444.38	1181.46	1225.72	84.86
	9-2	1457.62		1266.95		
	9-3	1480.42		1228.76		
S10	10-1	1584.36	1389.49	1217.49	1157.31	83.29
	10-2	1354.50		1122.23		
	10-3	1229.60		1132.22		
S11	11-1	1207.78	1315.23	977.98	869.95	66.14
	11-2	1293.03		653.04		
	11-3	1444.88		978.83		
S12	12-1	1467.75	1462.93	1519.64	1163.21	79.51
	12-2	1643.84		1452.36		
	12-3	1277.18		517.62		
S13	13-1	1266.03	1248.50	927.57	1041.48	83.41
	13-2	1217.46		1151.63		
	13-3	1261.99		1045.25		
S14	14-1	1559.43	1443.66	945.56	483.03	33.46
	14-2	1475.83		247.18		
	14-3	1295.70		256.35		

4.6.6 Rutting test (Permanent Deformation)

Four mixes (S1, S3, S5 and S6) were selected for the test of rutting and fatigue resistance. The information of the mixes is shown in Table 4.6.1. Rutting resistance of the selected samples was evaluated using the asphalt pavement analyzer (APA) at 64°C as shown in Figure 4.6.7. Wheel load was set to 45.5 kg (100 lb), and wheel pressure was set to 689.5 kPa (100 psi). 150 mm test samples were compacted using a gyratory compactor to the required density. Test samples were conditioned at test temperature for 4 hours.

Figure 4.6. 7: Asphalt samples after rutting test in APA

Rutting test results are presented in Table 4.6.4 and Figure 4.6.8, which indicate that modified mixes (S3, S5 and S6) has less rutting compared to pure asphalt concrete mix (S1). S5 and S6 mix has similar rutting behavior. Both mixes showed 4.50 and 4.68 mm rutting, respectively, at 8000 load repetitions. Mix S3 has the least rutting of all the tested mixes with 3.82 mm at 8000 load repetitions.

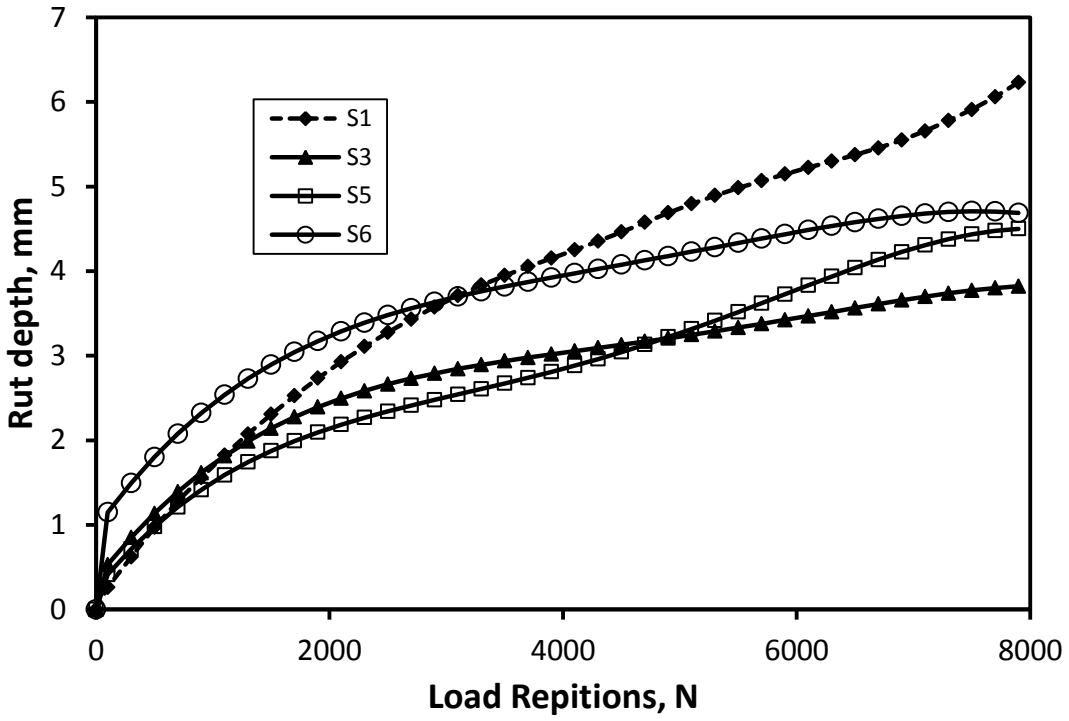

Figure 4.6. 8: Rutting test results of the selected asphalt concrete mixes

Table 4.6. 4: Rutting of the selected asphalt concrete mixes@ 8000 load repetitions

Mix	Rutting (mm) @ 8000 load repetitions
S1(Pure asphalt concrete mix)	6.23
S3(20%S, 4% R, 76% A)	3.82
S5(30%S, 10 W, 60% A)	4.50
S6(30%S, 4% R, 66% A)	4.68

4.6.7 Fatigue Testing

Asphalt concrete slabs (38 cm × 30 cm × 6.6 cm) were compacted to the density of optimum asphalt mixes using slab compactor as shown in Figure 4.6.9.Slabs were cut into beam samples (38 cm × 6.6 cm × 5.0 cm) using masonry saw as shown in Figure 4.6.10. Beam samples were conditioned at test temperature and tested for flexural fatigue (Beam test) following AASHTO T-321 (TP8-94), as shown in Figure 4.6.11.

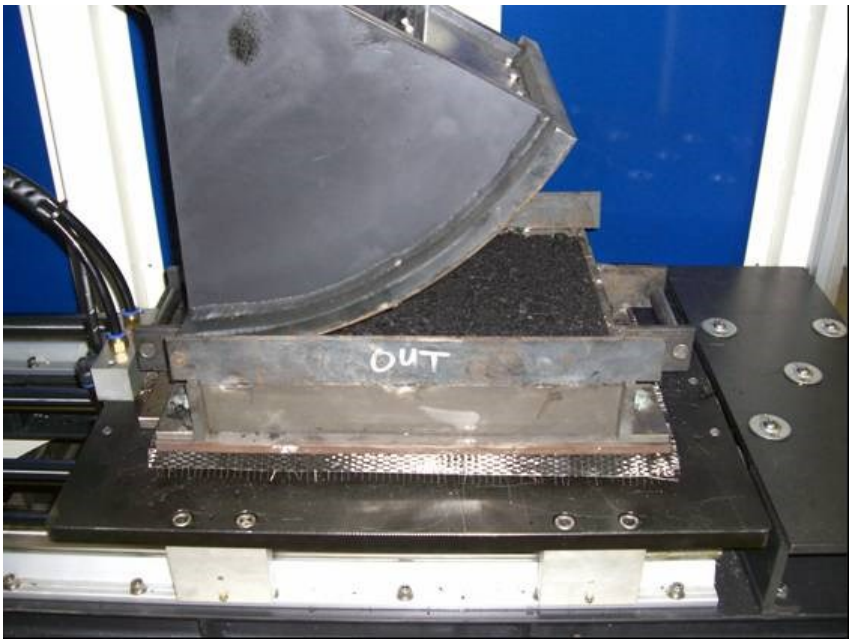

Figure 4.6. 9: Preparation of slab samples

Figure 4.6. 10: Beam samples

Figure 4.6. 11: Beam fatigue test setup

The Flexural Fatigue test, AASHTO T-321 (TP8-94), was used to test the fatigue properties of the prepared asphalt concrete beam samples. The samples were tested in a stress controlled mode to simulate asphalt pavement thick layer construction used by Ministry of Transport (MOT). Five samples were tested under different bending peak to peak stresses (kPa). The corresponding stiffness (MPa), peak to peak strain $\times 10^{-6}$, peak to peak load (kN), deflection (mm), dissipated energy (MJ/m^3), and phase angle (°) were calculated by the software.

As the asphalt concrete beam samples are subjected to load repetitions, stiffness reduces rapidly at the start then reaches a constant slope till failure of the beam, which is defined as 40% of the initial stiffness. Figure 4.6.12 shows the typical trend for asphalt mix tested at peak to peak stress level of 500 kPa. The collected data were analyzed to determine the relations between load repetition to failure (N) and applied peak to peak stress (σ) or initial peak to peak strain (ε). Table 4.6.5 summarizes the fatigue relations developed for all mixes as a function of applied strain or stress. It was established that about 80% of asphalt mixes fatigue will be consumed up to 40% stiffness. The concern is fatigue life to failure where Stiffness = 0. At this point the fatigue life ratio between all mixes will be similar to that up to 40% stiffness. Figure 4.6.13 shows the relation between load repetition (N) and initial strain (ε). Similarly, Figure 4.6.14 shows the relation between load repetition (N) and applied stress (σ). Both Figures show good correlation between applied stress and strain and load repetitions at failure.

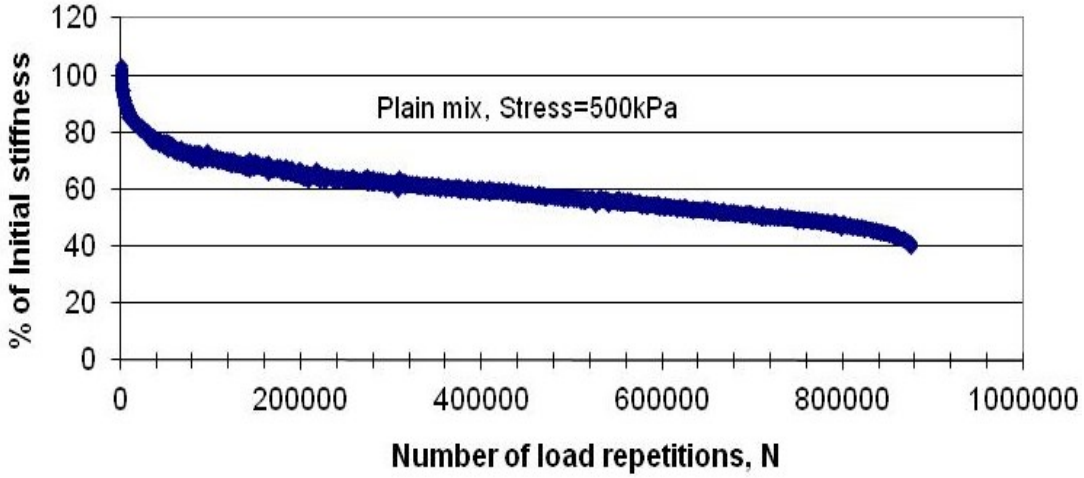

Figure 4.6. 12: Typical trend for asphalt concrete mix at stress level of 500 kPa

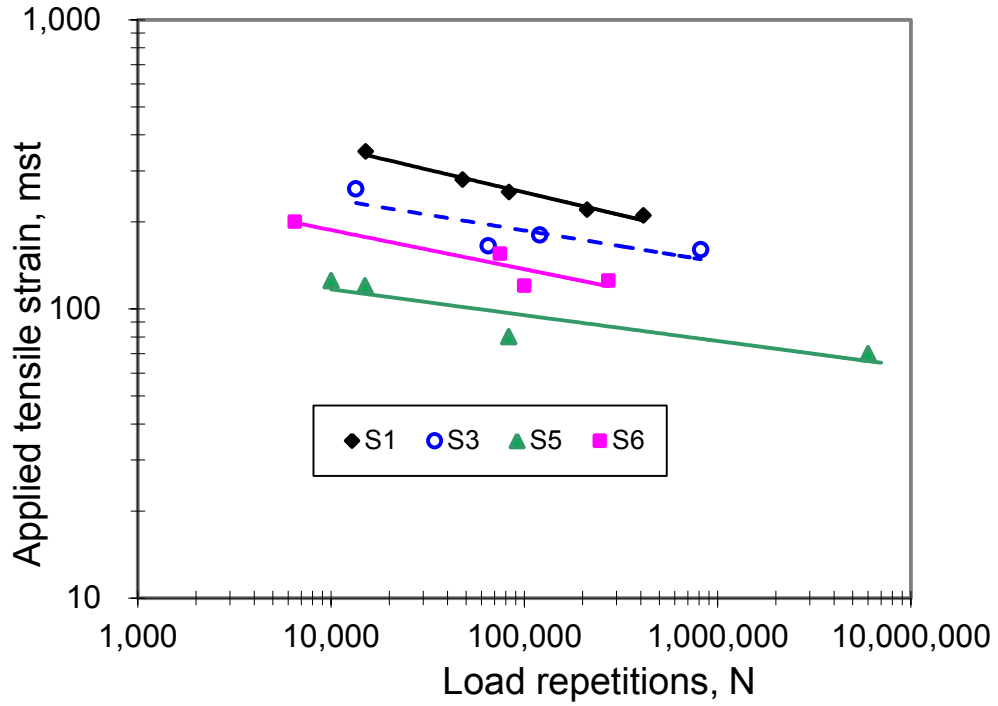

Figure 4.6. 13: Relation between load repetition (N) and applied tensile strain (ε)

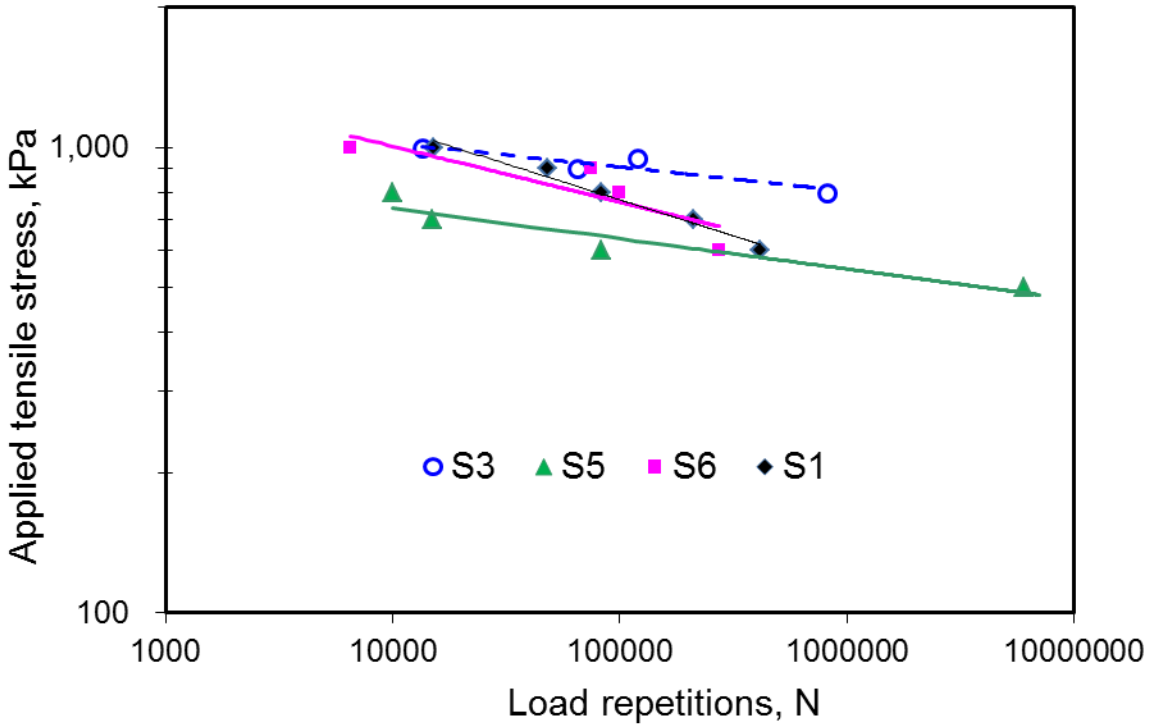

Figure 4.6. 14: Relation between load repetition (N) and applied stress (σ)

Table 4.6. 5: Fatigue vs. applied strain and stress relationships

Mix	Fatigue Equation	
	Function of applied strain	Function of applied stress
S1	$9E+19(\varepsilon^{-6.216})$	$2E+23(\sigma^{-6.297})$
	$R^2 = 0.9783$	$R^2 = 0.9747$
S3	$2E+19(\varepsilon^{-6.276})$	$2E+53(\sigma^{-16.29})$
	$R^2 = 0.6827$	$R^2 = 0.8424$
S5	$9E+22(\varepsilon^{-9.076})$	$2E+43(\sigma^{-13.69})$
	$R^2 = 0.8098$	$R^2 = 0.8967$
S6	$2E+18(\varepsilon^{-6.19})$	$7E+22(\sigma^{-6.217})$
	$R^2 = 0.8381$	$R^2 = 0.7463$

The test mode was, as a controlled stress (σ) and response strain (ε), recorded by the machine. So, the primary fatigue relation is explained by tensile strain (ε) versus fatigue (N). From Figure 4.6.13 and Table 4.6.5 it is noticed that mixes S1, S3 and S6 have slopes of -6.216, -6.276 and -6.19, respectively. The intercepts of the mixes are 9E19, 2E19 and 2E18. These three mixes can be treated as one group. Mix S5 has a slope of -9.076 which is highest among all the mixes. So, S5 is the most sensitive to applied strain and it showed the least fatigue life among the mixes. Pure asphalt mix outperformed all sulfur modified mixes. Rubber modified 30/70 sulfur asphalt mix exhibited better fatigue life than wax modified 30/70 sulfur asphalt mix. This indicates that rubber modification gave more flexibility than wax modification.

Load repetition versus tensile stress is secondary relation for fatigue life. Figure 4.6.14 and Table 4.6.5 shows the fatigue life as function of stress. It shows that mix S1 and S6 has similar fatigue response. At constant stress below 1000, the modified mixes S3 and S5 has higher fatigue resistance than unmodified asphalt concrete mix. But, the relation of stress and fatigue is not the primary function and it cannot be considered for design. The primary function is shown in Figure 4.6.13 which should be used for design.

4.6.8 Analysis of the results

In general, the performances of the sulfur modified asphalt concrete mixes are better than the pure asphalt concrete mixes in respect to ITS, durability, and resilient modulus. With respect to Marshall Stability, pure asphalt concrete is better than all other mixes but it has low resilient modulus and durability. Polyethylene wax-modified asphalt concrete mixes, especially, S5 (30% S, 10% wax) and S9 (40% S, 8% wax) showed higher durability and resilient modulus than others. The PG of these samples is 76-10 (section 4.6.1), suggesting that they will have higher rutting resistance. But, due to high resilient modulus, samples showed lower fatigue life compared to other mixes. Mix S3 has medium resilient modulus (7201 MPa) and good stability (19.1 kN) and durability (76.6%). This mix showed better rutting and fatigue resistance compared to other sulfur stabilized mixes (S5 and S6).

4.7 Mix Design Evaluation of OFA Modified Asphalt Concrete Mixes

4.7.1 Mixes code and composition

Modified and unmodified OFA asphalt binders and mixes were coded for ease of referencing. Table 4.7.1 shows codes and meaning as used in this section, where C stands for OFA, 1 to 3 stands for OFA surface modification treatment method number, and B stands for binder; therefore, C1B is an asphalt binder modified with OFA from treatment-1. Similarly, G stands for OFA when used as a filler; therefore, C3G stands for filler replacemet with modified OFA from method-3. It should be noted that binder codes are also used to identify mixes made with these binders.

Table 4.7. 1: Coding method

SN	Code	Definition
1	B	virgin asphalt binder (0 % OFA)
2	C0	unnmodified OFA
3	C1	modified OFA using treatment-1(OFA-COOH)
4	C2	modified OFA using treatment-2(OFA-Amine)
5	C3	modified OFA using treatment-3(OFA-C18)
6	C0B	asphalt binder modified with unmodified OFA
7	C1B	asphalt binder modified with OFA from treatment-1
8	C2B	asphalt binder modified with OFA from treatment-2
9	C3B	asphalt binder modified with OFA from treatment-3
10	C0G	Filler replacement with unnmodified OFA
11	C1G	Filler replacement with modified OFA from treatment-1
12	C2G	Filler replacement with modified OFA from treatment-2
13	C3G	Filler replacement with modified OFA from treatment-3

4.7.2 Indirect Tensile Strength

The test was done according to the procedure described in section 4.6.5. The results of the tested specimens are presented in Table 4.7.2 as a function of OFA type and mix method. Results indicate that modifying OFA has improved the tensile strength of asphalt mixes and that the optimum ITS values were obtained at 2% for OFA modified binder mixes and at 1% for OFA filler replacement mixes.

Table 4.7. 2: ITS test results for the prepared mixes as function of OFA type and mix method

Mix Type	Percent OFA	Mean ITS, kPa			
		OFA Type			
		As-received OFA	OFA-COOH	OFA-Amine	OFA-C18
Plain Mix (B)	0	897			
OFA with Binder	2	1115	1194	996	968
	4	1010	1070	962	880
	6	1015	1092	860	823
	8	1021	1118	845	785
OFA filler with Aggregate	1	919	1170	715	923
	2	744	886	504	662
	3	440	864	480	628

4.7.3 Resilient Modulus of the Designed Mixes

Resilient modulus of OFA/treated OFA modified asphalt concrete was calculated according to the teat protocol described in section 4.6.3. Results are shown in Table 4.7.3 as function of OFA type and mix method. Similar to ITS test, the results show that modifying OFA has improved the resilient modulus of asphalt mixes, especially OFA modified binder mixes. The optimum M_R values were obtained at 2% for OFA modified binder mixes and at 1% for OFA filler replacement mixes.

Table 4.7. 3: M_R test results for the prepared mixes as function of OFA type and mix method

Mix Type	Percent OFA	Mean M_R, MPa			
		OFA Type			
		As-received OFA	OFA-COOH	OFA-Amine	OFA-C18
Plain Mix(B)	0	3022			
OFA with Binder	2	3454	3800	4564	5436
	4	3363	3500	4395	3786
	6	3225	3434	3873	3547
	8	3280	3461	3362	3274
OFA filler with Aggregate	1	2997	4012	3131	3915
	2	2271	3800	2136	2550
	3	1014	3233	1850	2305

4.7.3 Rutting test

Optimized plain and modified asphalt mixes were evaluated for rutting resistance using the asphalt pavement analyzer (APA) at 64°C according to test procedure described in section 4.6.6. Rutting test results are presented in Table 4.7.4 and Figure 4.7.1, which indicate that asphalt mix with 1% OFA filler replacement (C0G) has rutting behavior similar to plain asphalt concrete mix (B). Both mixes had 5.12 and 5.01 mm rutting, respectively, at 8000 load repetition. Modifying asphalt cement with 2% plain OFA prior to blending with aggregate reduced the rutting of C0G mix to 3.32 mm. Asphalt mix with 1% modified OFA filler replacement (C1G) has rutting of 3.11 mm. Asphalt mix with 2% modified OFA with binder (C1B) gave the least rutting of 2.2 mm.

OFA resulting from the second modification treatment gave the highest rutting among the three treatment methods. C2B and C2G mixes gave 4.8 and 4.2 mm rutting, respectively. OFA resulting from the first and third treatments were effective in reducing rutting by about 50%. Binder modification with OFA is more effective in reducing rutting than filler replacement. Rutting for C1B and C3B mixes are 2.23 and 2.6 mm, respectively, as compared to 3.11 and 3.19 mm for C1G and C3G, respectively.

Table 4.7. 4: Asphalt concrete mixes coding and rutting test results

SN	Mix Code	Mix definition	Rutting, mm
1	B	Plain Mix (0 % OFA)	5.01
2	C0B	Asphalt binder modified with 2% unmodified OFA	3.32
3	C0G	1% filler replacement with unmodified OFA	5.12
4	C1B	Asphalt binder modified with 2% OFA from treatment-1	2.23
5	C1G	1% Filler replacement with modified OFA from treatment-1	3.11
6	C2B	asphalt binder modified with 2% OFA from treatment-2	4.80
7	C2G	1% Filler replacement with modified OFA from treatment-2	4.20
8	C3B	asphalt binder modified with 2% OFA from treatment-3	2.60
9	C3G	1% Filler replacement with modified OFA from treatment-3	3.19

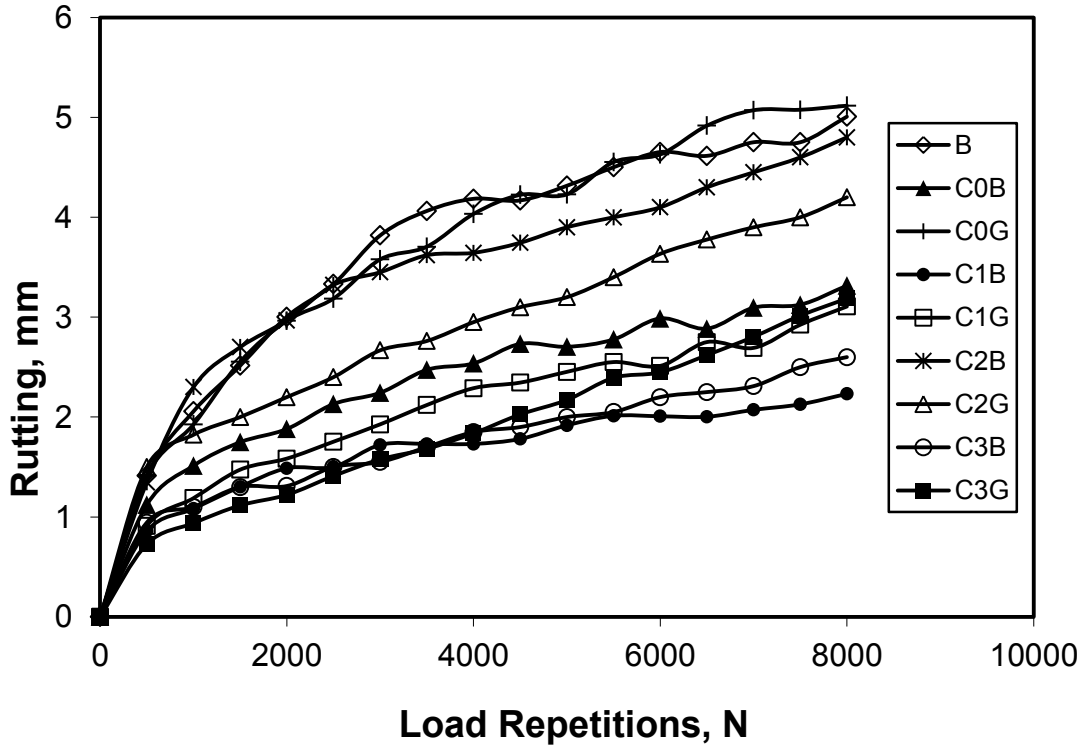

Figure 4.7. 1: Rutting test results

4.7.4 Fatigue Testing

Flexural Fatigue test was used to test the fatigue properties of the prepared asphalt concrete beam samples according to the procedure described in section 4.6.7. Figure 4.7.2 shows the relation between load repetition (N) and initial strain (ε). Similarly, Figure 4.7.3 shows the relation between load repetition (N) and applied stress (σ). Both Figures show good correlation between applied stress and strain and load repetitions at failure. Table 4.7.5 summarizes the fatigue relations developed so far for all mixes as a function of applied strain or stress.

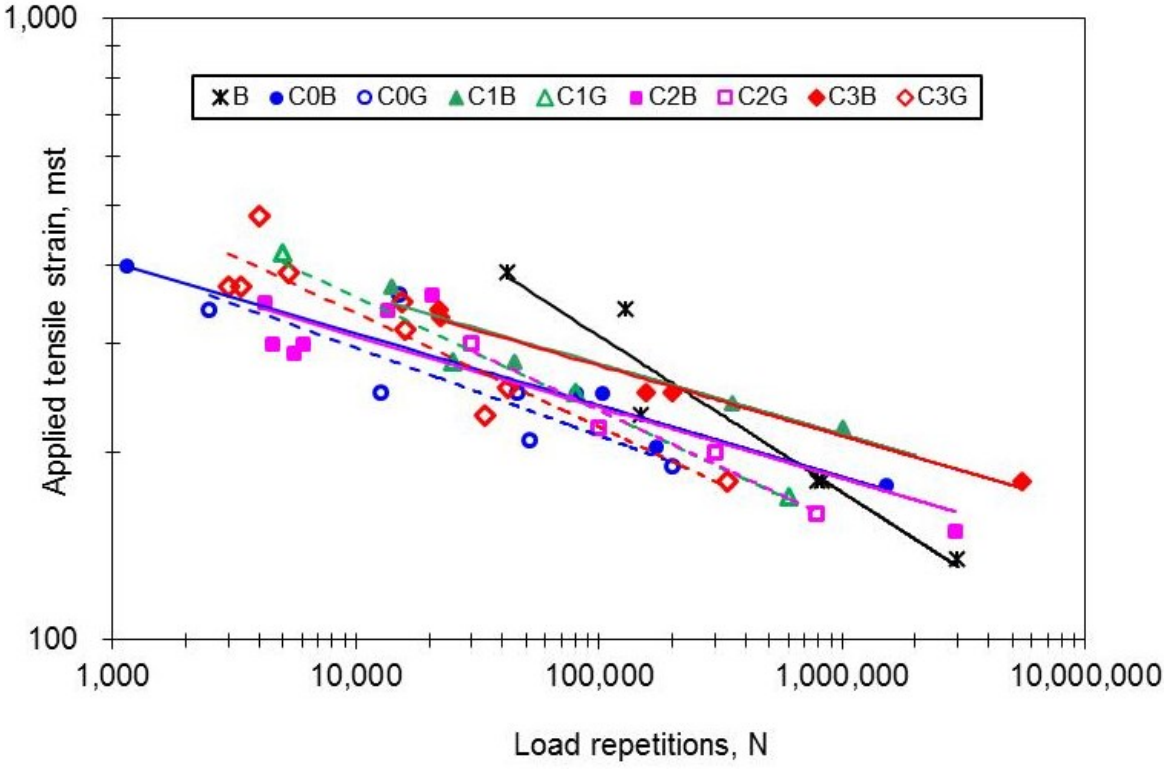

Figure 4.7. 2: Relation between load repetition (N) and applied strain (ε)

Since the test mode was a controlled stress, the primary fatigue relation is explained by tensile strain (ε)–fatigue (N) relationship. A careful inspection of Table 4.7.5 and Figure 4.7.2 indicates that the tested mixes can be divided into three major groups as follows:

- Plain asphalt mix (mix B) has the highest slope of all mixes (–3.984), which indicates low sensitivity to applied strains (or deflection in the field) as compared to other mixes. The mix has the least intercept of all mixes (8E+14).
- C3G, C1G and C2G mixes exhibited slopes of –5.464 to –5.495. The intercepts of these mixes were 1E18, 9E17 and 6E17, respectively. In addition, mix C0G, which has a slope of –7.092 and an intercept of 3E21, can be added to this group. These mixes have the least performance of all tested mixes.
- C1B, C3B, C2B and C0B mixes exhibited the least slope of all mixes (–8.696 to –8.85), which indicates the highest sensitivity to applied strains as compared to other mixes. The intercepts of mixes C1B and C3B (3E26 and 4E26) are the highest of all mixes followed by the intercepts of C2B and C0B mixes (7E25 and 5E25). The performance of C1B and C3B mixes is the best of all tested mixes.

Based on these trends, the following observations can be made:

- At strain level greater than 300 mst, plain asphalt outperformed all other mixes.

- At strain levels less than 300 mst, C1B and C3B mixes outperformed all other mixes followed by C2B and C0B mixes.

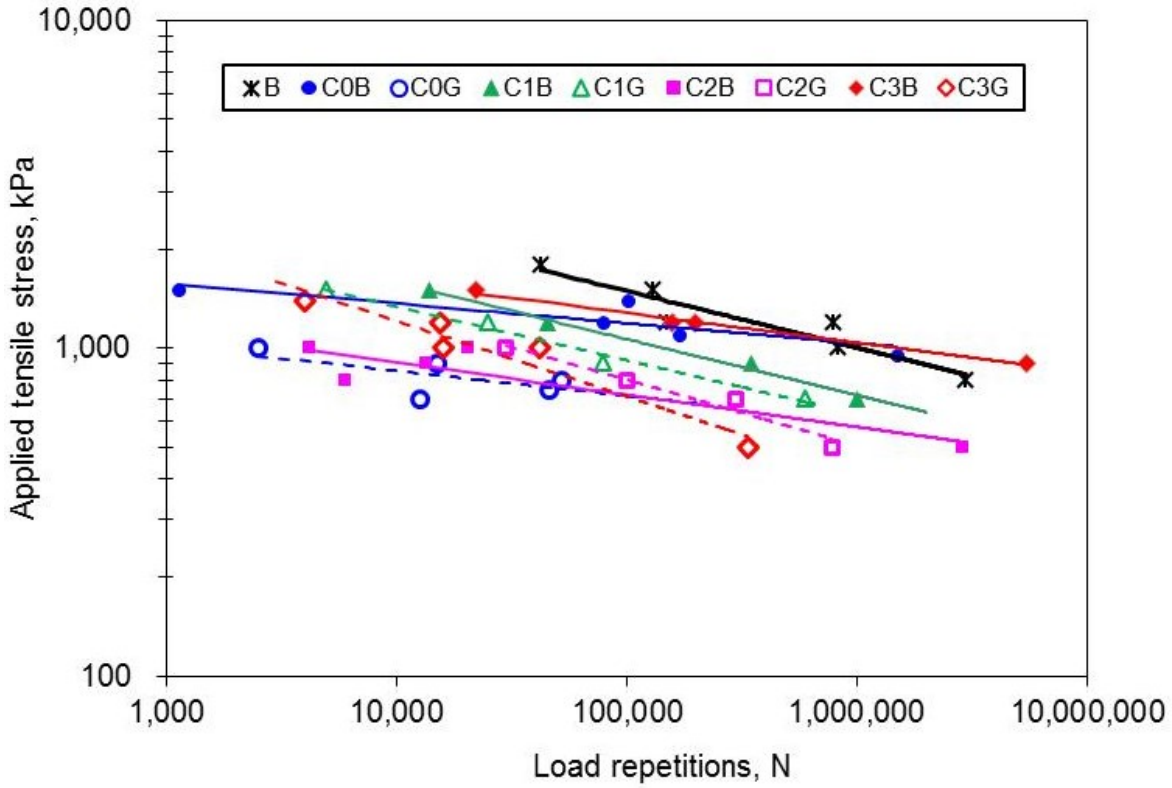

Figure 4.7. 3: Relation between load repetition (N) and applied stress (σ)

Figure 4.7.3 and Table 4.7.5 present tensile stress (σ)–fatigue (N) relationship which is not the primary relation for the test mode and indicates that the tested mixes can be divided into two major groups as follows:

- C0B, C3B, C2B and C0G mixes exhibited the least slope of all mixes (−10.2 to −16.4), which indicates the highest sensitivity to applied stress as compared to other mixes. The intercepts of mixes C0B and C3B (3E55 and 1E39) are

the highest of all mixes followed by the intercepts of C2B and C0G mixes (2E34 and 1E24). The performance of C0B and C3B mixes is the best of all tested mixes.

- B, C1B, C1G, C2G and C3G mixes exhibited slopes of –4.329 to –5.6.098. The intercepts of these mixes ranged between 2E17 and 2E32. B mix has the highest intercept and performance among these mixes.

Based on these trends, the following observations can be made:

- At stress level greater than 1100 kPa, plain asphalt mix outperformed all other mixes.
- At stress level less than 1100 kPa, C0B and C3B mixes outperformed all other mixes followed by plain asphalt mix then C1B mix.

Adding OFA (plain or modified) to the asphalt binder increased the endurance of asphalt concrete mixes at strain levels less than 300 mst. Highway pavements normally operate at strain levels around 130 to 150 mst.

Table 4.7. 5: Fatigue vs. applied strain and stress relationships

Mix	Fatigue Equation	
	Function of applied strain	Function of applied stress
B (Plain Asphalt)	$8E+14(\varepsilon^{-3.984})$	$2E+23(\sigma^{-5.78})$
	$R^2 = 0.9221$	$R^2 = 0.883$
C0B	$5E+25(\varepsilon^{-8.696})$	$3E+55(\sigma^{-16.43})$
	$R^2 = 0.9604$	$R^2 = 0.6313$
C0G	$3E+21(\varepsilon^{-7.092})$	$1E+42(\sigma^{-12.99})$
	$R^2 = 0.6908$	$R^2 = 0.96$
C1B	$3E+26(\varepsilon^{-8.772})$	$5E+22(\sigma^{-5.848})$
	$R^2 = 0.9253$	$R^2 = 0.9907$
C1G	$9E+17(\varepsilon^{-5.464})$	$1E+23(\sigma^{-6.098})$
	$R^2 = 0.9818$	$R^2 = 0.984$
C2B	$7E+25(\varepsilon^{-8.772})$	$2E+34(\sigma^{-10.2})$
	$R^2 = 0.7834$	$R^2 = 0.8159$
C2G	$1E+18(\varepsilon^{-5.495})$	$2E+19(\sigma^{-4.95})$
	$R^2 = 0.9679$	$R^2 = 0.9557$
C3B	$4E+26(\varepsilon^{-8.85})$	$1E+39(\sigma^{-10.99})$
	$R^2 = 0.9853$	$R^2 = 0.9912$
C3G	$6E+17(\varepsilon^{-5.464})$	$2E+17(\sigma^{-4.329})$
	$R^2 = 0.8617$	$R^2 = 0.9276$

4.7.5 Analysis of the results

Careful inspection of the PG grading results (section 4.6.1) showed that treatment method-1 and method-3 has similar performance (see Table 4.3.2and Table 4.4.4) and they are better than method-2. In the case of rutting, method-1and method-3 are same and they showed rutting of 2.23 mm and 2.60 mm respectively at 8000 load repetitions. So, the effect of treatment method on PG grading and rutting can be described as method-1≥ method-3 > method-2. The reason behind this observation can be explained from the chemistry point of view. Method-1 introduced carboxylic group (-COOH) to the surface of OFA and its presence was detected by FTIR spectra. Method-2 derived from method-1 by partial replacement of –COOH group by introducing C-18 to the OFA surface. So, method-1 and method-3 have common functional group –COOH and C-18 is extra in method-3. Method-2 has incorporated amine group to the surface of OFA. The standard bond energy of carboxylic acid group (111 kJ/mol) and C-C18 (179 kJ/mol) are lower than that of amine group (213 kJ/mol). So, modified ash from method-1and method-3 would be more reactive as they decompose easily and bonded to asphalt when blended OFA with asphalt. Whereas, ash from method-2 does not decompose easily due to high bond energy (213 kJ/mol) and so the reactivity is lower with asphalt binder.

Another observation is that the fatigue performance of method-1 and method-3 are very similar at low strain level and it is better than method-2 as it was shown in

section 4.7.4. So, Fatigue performance also suggested the same relationship (method-1≥ method-3 > method-2) which was drawn in the case of rutting and PG grading.

Although the increase in ash content in asphalt binder increases PG grading of the ash modified binder, the optimum mechanical properties of the asphalt concrete mixes was obtained for 2% ash. Why the mechanical properties not increasing with ash content increasing? The answer is that at higher concentration of ash in the asphalt matrix will result in agglomeration of ash particles. This was proved for CNT-C18/LDPE Nano composites CNT (Abbasi, et al., 2013).

4.8 Environment Impact Evaluation

Sulfur is a hazardous chemical and can create enviroment pollution though immisssion from sulfur asphalt concrete mixes. Environment impact evaluation study was conducted to the slected sulfur asphalt concrete mixes to ensure the safety standard is maintained. Asphalt was heated first and mixed with Sulfur at the required percentages by weight of asphalt. The resulting blend was added to the hot aggregates (1200 gm) and mixed thoroughly at 140^{o}C. Four different asphalt concrete mixtures were prepared as follows: Plain asphalt mixture as control mix; S3; S5; S6 (section 4.6.6).

The prepared mixtures were immediately placed in a 4-litre can with interior bottom and sides lined with cardboard, of 5 mm thickness and the mix was stirred with a spoon. The meter probe was placed 5-10 mm from the mix surface. The

measurements were made with removed cover to determine ambient gases emission in open airspace. The gaseous concentrations of sulfur dioxide and hydrogen sulfide were measured using H_2S/SO_2 analyzer, Model 450i, manufactured by Thermo Electron Corporation, USA, as shown in Figure 4.8.1. The results of gaseous measurements are tabulated in Table 4.8.1. The Threshold Limit Values of Chemical Substances and Physical Agents in the Workroom Environment as per American Conference of Governmental Industrial Hygienists are provided in Table 4.8.2 for ready reference.

Figure 4.8. 1:Thermo Electron Corporation 450i H_2S/SO_2 gases analyzer

Table 4.8. 1: Summary of environmental pollution test results

Blend Type	Temperature °C	Ambient Gas Emission in ppm	
		H_2S	SO_2
Control Mix	minimum	0.02	0.04
	average	0.11	0.03
	maximum	0.21	0.11
S3	minimum	0.37	0.14
	average	0.9	0.54
	maximum	1.85	0.95
S5	minimum	0.41	0.13
	average	1.66	0.72
	maximum	1.93	1.05
S6	minimum	0.43	0.125
	average	1.41	0.68
	maximum	1.81	1.07

It was found that in the plain asphalt concrete blend (Control mix) at 140°C the gaseous emission was not noticeable as indicated in Table 4.8.1. In the asphalt concrete mixtures prepared using sulfur modified asphalt binders (mix S3, S5 and S6), it was found that in an open space and at 140°C, the average concentration of SO_2 (sulfur dioxide) was in the order of 0.54 to 0.72 ppm, which does not exceeds the permissible limit of sulfur dioxide (2.0 ppm) as per Table 4.8.2. Similarly, the emission of H_2S gas was in the order of 0.9 to 1.66 ppm, which does not exceed the permissible limits. It may be noted that although the sample and experiment is limited in size compared to the actual field construction, it still does not completely

simulate the conditions in actual practice, where the mixing will be carried out in an open space with much easy dilution of the emission gases from the source into nearby environment.

Table 4.8. 2: Industrial hygiene standards

Pollutant	Average Threshold Concentration	Maximum Short-Term Limit Value
H_2S	10 ppm (8 hours)	15 ppm
SO_2	2 ppm (8 hours)	5 ppm
Sulfur	No Specification	
Particulates (insoluble)	10 mg/m³	

CHAPTER 5

CONCLUSIONS AND RECOMMENDATIONS

5.1 Conclusions

Primary aim of this research was to use several industrial waste materials to improve performance of asphalt. Four industrial wastes namely: elemental sulfur, oil fly ash (OFA), crumb rubber and polyethylene wax were used to modify asphalt. Two types of modified asphalt binder: (1) sulfur modified asphalt binder and (2) OFA modified asphalt binder were prepared using these industrial wastes. Pure and modified asphalt binder was investigated for viscoelastic properties through rheological tools. Mechanical performance properties of selected asphalt concrete mixes were also evaluated and compared. Section 5.1.1 and 5.1.2 presents the most important conclusions based on the investigation of sulfur modified and OFA modified asphalt binders.

5.1.1 Sulfur modified asphalt binder

Elemental sulfur is a byproduct comes from oil and gas processing industries. Due to environmental restriction a huge amount of sulfur is being produced through gas sweetening processes and its abundance has reduced its price worldwide. Also, the storage of the sulfur poses an environmental hazard. Sulfur modification of asphalt

was studied to explore new outlet for sulfur as well as to reduce the price asphalt. Elemental sulfur pellet was grounded to powder form and blended with hot asphalt at ~145°C in high shear blender. Sulfur was used in the range 20-50% by weight of asphalt binder. Sulfur asphalt with such high amount of sulfur showed poor rheological properties. Polyethylene wax and crumb rubber as rheology modifiers, were used with sulfur asphalt to enhance its rheological properties. The effect of polyethylene wax was studied by modifying sulfur asphalt with four different concentrations (2, 4, 6 and 8%). Similarly, four level of crumb rubber (1, 2, 4 and 6%) were used to investigate the effect of crumb rubber on sulfur asphalt. The following conclusions are drawn on the basis of polyethylene wax and crumb rubber modification of asphalt:

- The addition of crumb rubber and polyethylene wax have significantly increased the viscoelastic properties (G′,η* etc) of the sulfur modified asphalt binders. The linear relationship was obtained for the low frequency (ω = 1 rad/s) dynamic shear data. This improvement in viscoelastic properties was due to the increase in C-S bond and S=O bond in modified asphalt as it was proved through FTIR results.
- SHRP rutting parameter ($G^*/\sin\delta$) as well as zero shear viscosity increases with increase in crumb rubber and polyethylene wax percentages for all sulfur asphalt binders, which suggests that crumb rubber modification increases rutting resistant at high temperature.

- A modification index (I_M) was defined to quantify the improvement of elastic properties of modified binders. It shows that elastic properties of modified binder increases exponentially with temperature ($I_M = ae^{bT}$) which suggests that crumb rubber and polyethylene wax improved the high temperature viscoelastic properties.
- Short term ageing through RTFO improved the rheological properties of the modified binders by crosslinking and entanglement of sulfur and additives with asphalt compositions.
- Mechanical analysis of sulfur asphalt concrete mixes shows that crumb rubber and polyethylene wax modification increases resilient modulus, indirect tensile strength, and durability. Modified mixes showed lower rutting compared to plain asphalt concrete mixes. However, the fatigue life of some modified asphalt (especially high sulfur, 30%) concrete mixes was less than the plain mix. Crumb rubber modified sulfur asphalt concrete showed better rutting and fatigue performance.

5.1.2 OFA modified asphalt binder

OFA is a zero value waste that generated from coal and residual oil fired power plant. Its production is increasing day by day. It is an environmentally hazardous waste that needs to landfill which consumed large area. Research is going on to find new ways of recycling/reuse of this waste to save environment and to manufacture value added products. Use of as-received OFA in asphaltic mixture is not new. It was

used in several countries in the world to make asphalt pavement. Asphalt modification by untreated OFA showed poor rheological properties was well poor rutting resistance and fatigue life due to poor compatibility of OFA and asphalt. OFA was treated physically and chemically to improve its surface properties to increase compatibility and reactivity of OFA and asphalt. OFA treatment incorporated three functional groups (carboxyl, C18 and anime) to OFA surface. OFA modified asphalt binder was prepared by blending OFA/treated OFA with asphalt at high shear rate and at 145°C in a blender. Effect of treated OFA type and concentration on asphalt modification was studied by modifying asphalt with four different concentrations (2, 4, 6, 8%). The following conclusions are drawn on the basis of investigation:

- The addition of treated OFA (especially OFA-COOH and OFA-C18) significantly increased the viscoelastic properties of the modified asphalt binders. SHRP rutting parameter $G^*/\sin\delta$ increases with treated OFA content and it showed linear relationship. The high temperature performance grading was increased from 69°C to 88°C, 84°C and 80°C for the addition of 8% OFA-COOH, 8% OFA-C18 and OFA-Amine respectively to pure asphalt.
- Elastic modification index (I_M) was developed and the modified binders showed less temperature susceptibility. An exponential model was developed to fit the modification index as function of temperature.
- Addition of OFA-COOH to pure asphalt reduced the activation energy, whereas E_a remains constant for OFA-C18 and OFA-Amine modified binders.

- Addition of treated OFA increased both G′ and η′ as suggested by dynamic shear rheology. Black diagram representation of dynamic data proved that OFA-COOH and OFA-C18 modification of the asphalt binder leads to enhancement in the viscoelastic properties through chemical bonding. Increase of chemical bonding was proved through FTIR spectra of pure and modified asphalt binders.
- Treated OFA modification of asphalt binders increased the steady shear viscosity. Addition OFA to asphalt decreases the Newtonian plateau and increases the shear thinning behavior which indicates ease of processing as suggested by the results of power law index.
- Pure and modified asphalt concrete mixes results showed that treated OFA modified asphalt concrete mixes has superior mechanical properties. Resilient modulus, indirect tensile strength and Marshall Stability of the modified OFA asphalt concrete mixes were better than that of pure asphalt concrete mix. Optimum OFA concentration was found to be 2% for all OFA types.
- Rutting resistance and fatigue life of treated OFA modified asphalt concrete mixes were better than that of untreated modified asphalt concrete and plain asphalt concrete mixes.

Finally the chemically treated waste OFA can be utilized in the modification of asphalt binder. It will solve the waste disposal problem of OFA as well as reduce the amount of asphalt pavement to be used in.

5.2 Recommendations for Future Work

Despite several conclusions being drawn from this research project, a lot is still to be done on the modification of asphalt using these industrial wastes. A list of recommendations is summarized in the following paragraphs:

- Sulfur asphalt concrete usually stiff in nature. Use of crumb rubber increases toughness of sulfur asphalt concrete mixes. However, the fatigue life of the modified sulfur asphalt concrete was lower than that of pure asphalt concrete mix. Future research should be focused on to find a liquid rheology modifier which will increase the fatigue life of sulfur asphalt concrete mixes.
- Several road sections should be constructed in different whether and locations to monitor the actual performance of the modified asphalt concrete mixes.
- OFA modification was done in small laboratory scale. A pilot scale reactor should be design and operate for possible large scale treatment of OFA.
- Spent chemicals from the OFA treatment should be recovered and reuse to reduce treatment cost.

References

1. Abbasi, S.H.,Adesina, A.A., Atieh, M.A.,Ul-Hamid, A, Hussein, I.A., 2013. Rheology, Mechanical and Thermal Properties of (C18-CNT/LDPE) Nanocomposites. *International Polymer Processing,* pp. 3-13.
2. Abdelrahman, M.A., and S.H. Carpenter 1999. Mechanism of Interaction of Asphalt Cement with Crumb Rubber Modifier. *Transportation Research Record 1661*, Transportation Research Board, National Research Council, Washington, D.C.
3. Abuilaiwi, F. A., Laoui, T., Al-Harthi, M. & Atieh, a. M. A., 2010. Modification and functionalization of multiwalled carbon nanotube (MWCNT) via Fischer esterification. *The Arabian Journal for Science and Engineering,* Volume 35.
4. Abu-Rizaiza, A.S. 2004. Characteristics of Fly Ash from Residual Oil Combustion at Rabigh Electric Power Plant. Journal of Environmental Science, Volume 8, No. 2..
5. Airey, G., 2003. Rheological properties of styrene butadiene styrene polymer modified road bitumens. *Fuel,* Volume 82, pp. 1709-1719.
6. Airy, G., 2011. *Factors affecting the rheology of polymer modified bitumen. In: Polymer Modified Bitumen – Properties and Characterization.*Tony McNally Editor. Woodhead Publishing in Materials.

7. Al-Abdul Wahhab, H., Asi, I. & and Ali, M., 1997. Development of Performance-Based Bitumen Specifications for the Gulf Countries. *Construction and Building Materials Journal,* 11(1), pp. 15-22.
8. Al-Amethel, M., Al-Abdul Wahhab, H. I. & Ibnelwaleed A., H., 2011. *Utilization of heavy oil fly ash to improve asphalt binder and asphalt concrete performance.* Patent No. US 8062413 B1.
9. Al-Suhaibani, A.R.S.,1986. Use of Fly Ash as an Asphalt Extender in Asphalt Concrete Mixes. Ph.D. Thesis, Michigan Univ., Ann Arbor (USA).
10. American Association of State Highway and Transportation Officials (AASHTO) 2002.*Standard Specifications for Transportation Materials and Methods of Sampling and Testing*, 22nd Edition, AASHTO, Washington D.C
11. American Coal Ash Association, 2011. *Coal Combustion Product (CCP) Production & Use Survey Report,* Farmington Hills, MI: AACA.
12. Amirkhanian, S. N. 2003. Establishment of an Asphalt-Rubber Technology Service (ARTS).*Proceedings of the Asphalt Rubber 2003 Conference*, Brasilia, Brazil.
13. Amirkhanian**,** S. N. and B. Williams 1993. Recyclablity of Moisture Damaged Flexible Pavements, *J. Mat. Civil Eng*. Volume 5, pp. 510–530**.**
14. Anani, B. & Al-Abdul Wahhab, H., 1982. Effects of baghouse fines and mineral fillers on properties of asphalt pavements. *Transportation Research Board,* Volume 843, pp. 57-64.

15. Asi, I. & Assa'ad, A., 2005. Effect of Jordanian oil shale fly ash on asphalt mixes. *Journal of Materials in Civil Engineering,* pp. 553-559.

16. Bacci, P., M. Del Monte, A. Longhetto, A. Piano, F. Prodi, P. Redaelli, C. Sabbioni, and A. Ventura, 1983. Characterization of the Particulate Emission by a Large Oil Fuel Fired Power Plant," *Journal of Aerosol Science*, Volume 14, pp. 557-572.

17. Baek, J. and S. Lee, 2007. Utilization of Chemically Modified Heavy Oil Fly Ash as a Novel Sorbent for the Removal of Vapor-phase Mercury from Coal-fired Flue Gas CCT, CCT 2007, Cagliari, Sardinia, Italy, 15-17 May.

18. Bahia, H., Zeng, M., Zhai, H. & Khatr, 1999. *Superpave protocols for modified asphalt binders, 15th Quarterly Progess Report for NCHRP Project 9–10.,* Washington: DC: National Cooperative Highway Research Program.

19. Barnes, A., 2000. *A handbook of elementary rheology.* Aberystwyth: University of Wales.

20. Bellayer, S., J.W. Gilman, N. Eidelman, S. Bourbigot, X. Flambard, D.M. Fox, H.C.D. Long, and P.C. Trulove, 2005. Preparation of Homogeneously Dispersed Multiwalled Carbon Nanotube/Polystyrene Nanocomposites via Melt Extrusion Using Trialkyl Imidazolium Compatibilizer," *Adv. Funct. Mater*., Volume 15, pp. 910-916.

21. Bellomy, R. & McGinnis, E., 1994. *Bitumen composition containing bitumen, polymer and sulfur.* Patent No. US 5371121.

22. Benko, 2002. USA, Patent No. US 6387965B1.

23. Benzowitz, J. & Boe, E., 1938. *Effect of sulfur upon some of the properties of asphalt. Proceedings of ASTM.*

24. Bernard, 1999. USA, Patent No. US 5936015.

25. Berthelot,C. F., D.H. Allen and C.R. Searcy 2003. Method for Performing Accelerated Characterization of Viscoelastic Constitutive Behavior of Asphalt Concrete*,J. Mat. Civil Eng.* Volume 15, pp. 496–505.

26. Bikiaris, D. et al., 2008. Effectof acid treatment multi-walled carbon nanotubes on the mechanical, permeability, thermal properties and thermo-oxidative stability of isotactic polypropylene. *Polymer Degradation and Stability,* Volume 93, pp. 952-967.

27. Binard, C., Anderson, D., Lapalu, L. & Planche, J., 2004. *Zero shear viscosity of modified and unmodified binders.* Vienna, Eurasphalt & Eurobitume congress.

28. Branca, C., Frusteri, F., Magazu, V., and Mangione, A., 2004. Characterization of Carbon Nanotubes by TEM and Infrared Spectroscopy, *J. Phys. Chem. B*, Volume 108, pp. 3469-3473.

29. Carreau, P., Bousmina, M. & Bonniot, F., 2000. The viscoelastic properties of polymer modified asphalt. *Can J Chem Eng ,* 78(3), pp. 495-502.

30. Challa, A., Roy, C. & Ait-kadi, A., 1996. Rheological properties of bitumen modified with pyrolytic carbon black. *Fuel,* 75(13), pp. 1575-1583.

31. Cho, Y., Jeong, H. & Kim, B., 2009. *Macromolecular Research,* Volume 17, pp. 879-890.

32. Coates, J., 2000. Interpretation of Infrared Spectra, A Practical Approach. In: *Encyclopedia of Analytical Chemistry.* Chichester: John Wiley & Sons Ltd, pp. 10815–10837.

33. Cuadri, A., García-Morales, M., Navarro, F. & Partal, P., 2012. Enhancing the viscoelastic properties of bituminous binders via thiourea-modification. *Fuel,* Volume 97, pp. 862-868.

34. Daous, M.A., 2004. Utilization of Cement Kiln Dust and Fly Ash in Cement Blends in Saudi Arabia *Journal of King Abdulaziz University: Engineering Sciences*, Volume 15, No. 1, pp. 33-45.

35. Dermatas, D. and X. Meng, 2003. Utilization of Fly Ash for Stabilization/Solidification of Heavy Metal Contaminated Soils, *Engineering Geology*, Volume 70, pp. 377-394.

36. Edwards, Y., Tasdemir, Y. & Isacsson, U., 2007. Rheological effects of commercial waxes and polyphosphoric acid in bitumen 160/220 – high and medium temperature performance. *Constr Build Mater,* 21(10), pp. 1899-1908.

37. Edwards, Y., Y. Tasdemir and U. Isacsson 2006. Effect of commercial waxes on asphalt concrete mixtures performance. *J.Cold region Science and Technology,* Volume 45, pp. 32-41.

38. Edwards, Y., Y. Tasdemir and U. Isacsson 2006. Rheological effects of commercial waxes and phosporic acid in bitumen 160/220. High and Medium Temperature Performance. *J. of Const. and Buildg. Mat*., Volume 21, pp. 1899-1908.

39. Feldman, N.,1982. Control of Residual Fuel Oil Particulate Emissions by Additives, *19th Symposium (International) on Combustion*, The Combustion Institute, Pittsburgh, pp. 1387-1393.

40. Ferry, J., 1980. *Viscoelastic properties of polymers.* New York: Wiley.

41. García-Morales, M. et al., 2004. Viscous properties and microstructure of recycled EVA modified bitumen. *Fuel,* 83(1), pp. 31-38.

42. Gregg, S. and L. Sing, 1982. *Adsorption, Surface Area and Porosity*, 2nd ed., Academic Press, London.

43. Guo, P., X. Guo, and C. Zheng 2010. Roles of Gamma-Fe_2O_3 in Fly Ash for Mercury Removal: Results of Density Functional Theory Study, *Applied Surface Science*, Volume 256, p. 6991.

44. Hussein, I. A., Iqbal, M. H. & Al Abdul Wahhab, H. I., 2005. Influence of Mw of LDPE and vinyl acetate content of EVA on the Rheology of Polymer Modified Asphalt. *Rheologica Acta,* 45(1), pp. 92-105.

45. Hussein, I. A., Wahhab, H. I. A.-A. & Iqbal, M. H., 2006. Influence of Polymer Type and Structure on Polymer Modified Asphalt Concrete Mix. *Canadian Journal of Chemical Engineering,* 84(4), pp. 480-487.

46. Iqbal, M. H., Hussein, I. A., Al-Abdul Wahhab, H. I. & Amin, B., 2006. Influence of Mw of LDPE and vinyl acetate content of EVA on the rheology of polymer modified asphalt. *Journal of Applied Polymer Science,* 102(4), pp. 3446-3456.

47. Kandhal, P., Lynn, C. & Parker, F., 1998. *Characterization tests for mineral fillers related to performance of asphalt paving mixtures,* Auburn.: National Center for Asphalt Technology.

48. Kanitpong, K., K. Nam, W. Martono and H. Bahia, 2008. Evaluation of a warm mix asphalt additive. *Proceedings of the Institution of Civil Engineers Construction Materials*, Volume 161, pp.1-8.

49. Karasahin, M. & Terzi, S., 2007. Evaluation of marble waste dust in the mixture of asphaltic concrete.. *Construction and Building Materials,* Volume 21, pp. 616-620.

50. Kennepohl, G. & Miller, L., 1978. Sulfur-Asphalt Binder Technology for Pavements-New uses of sulfur II. In: Advances in Chemistry. Ontario, Canada: American Chemical society , pp. 113-134.

51. Kishore, S.M., D.S. Kulkarni, and S. Sharathchandra 2002. Effect of Surface Treatment on the Impact Behavior of Fly-ash Filled Polymer Composites, Polym. Int., Volume 51, pp. 1378-1384.

52. Krishnan, J. M. and C.L. Rao 2001. Permeability and Blending of Asphalt Mixture using Theory, *Int. J. Eng. Sci.* Volume 39, pp. 611–627.

53. Kwon, W.T., D.H. Kim, and Y.P. Kim, 2005. Characterization of Heavy Oil Fuel Fly Ash Generated from a Power Plant, The Azo Journal of Materials Online

54. Larsen, D., Alessandrini, J., Bosch, A. & Cortizo, M., 2009. Micro-structural and rheological characteristics of SBS-asphalt blends during their manufacturing. *Constr Build Mater,* 23(8), pp. 2769-2774.

55. Lee, D.Y., 1975. *Ind. Eng. Chem., Prod. Res. Dev,* 14(3).

56. Li Zhang, Zhenhua Li, Xianghui Du, and Xijun Chang, 2011. Activated Carbon Functionalized with 1-amino-2-naphthol-4-sulfonate as a Selective Solid-phase Sorbent for the Extraction of Gold (III), *Microchim Acta*, Volume. 174, pp. 391-398.

57. Liang, 1998. Canada, Patent No. US 5719215.

58. Lim, Y.T. and Park O.O., 2000. Rheological Evidence for the Microstructure of Intercalated Polymer/Layered Silicate Nanocomposites," *Macromol. Rapid Commun*., Volume 21, pp. 231-235.

59. Lin, K.F., C.Y. Hsu, T.S. Huang, W.Y. Chiu, Y.H. Lee, and T.H. Young, 2005. A Novel Method to Prepare Chitosan/Montmorillonite Nanocomposites, *Journal of Applied Polymer Science*, Volume 98, pp. 2042-2047.

60. Liu, X. and Q. Wu 2002. Polyamide 66/Clay Nanocomposites via Melt Intercalation, *Macromol. Mater. Eng.*, Volume 287, pp. 180-186.

61. Lu, X. & Isacsson, U., 1997. Rheological characterization of styrene–butadiene-styrine copolymer modified bitumines. *Contruction and Building Materials,* 11(23).

62. Mathias Leite, L. F., P. Almeida da Silva, G. Edel, L. Goretti da Motta, and L.A.Herrmann do Nascimento, 2003. Asphalt Rubber in Brazil: Pavement Performance and Laboratory Study. *Proceedings of the Asphalt Rubber 2003 Conference*, Brasilia, Brazil.

63. McCrum, N.G., C.P. Buckley and C.B. Bucknall, 1999. *Principles of Polymer Engineering*, 2nd Ed., Oxford Science Publications, Oxford

64. Miguel Rodrıguez, V. et al., 2006. Degradation and stabilisation of poly(ethylene-stat-vinyl acetate): Spectroscopic and rheological examination of thermal and thermo-oxidative degradation mechanisms. *Polymer Degradation and Stability,* Volume 91, pp. 154-164.

65. Miknis, F.P. and L.C. Michon 1998. Some Application of Nuclear Magnetic Response Imaging to Crumb Rubber Modified Asphalts. *Fuel*, Volume 77, No. 5.

66. NCASI, 2003. Beneficial Use of Industrial By-Products, Identification and Review of Material Specifications, Performance Standards, and Technical Guidance

67. Ouyang, C., Wang, S. & Zhang, Y., 2006. Improving the aging resistance of asphalt by addition of Zinc dialkyldithiophosphate. *Fuel,* Volume 85, pp. 1060-1066.

68. Panda, M. and M. Mazumdar, 2002.Utilization of reclaimed polyethylene in bituminous paving mixes. *J Mater Civil Eng*, Volume14, No. 6, pp. 527–30.

69. Phillips, M. & Robertus, C., 1996. *Binder rheology and asphalt pavement permanent deformation: the zero shear viscosity*. Strasbourg, Eurasphalt & Eurobitume congress, p. 12.

70. Planche, J., 1990. *18. J.P. Planche, Method for the preparation of bitumen–polymer compositions, PCT WO 9002776, 1990.* Patent No. WO 9002776.

71. Polacco, G, Giovanni, Stastna, Jiri, Biondi, Dario, Antonelli, Federico, Vlachovicova, Zora, Zanzotto, Ludovit, 2004. *Journal of Colloid and Interface Science 280 (2004) 366–373.,* Volume 280, pp. 366-373.

72. Polacco, G., Stastna, J., Biondi, D. & Zanzotto, L., 2006. Relation between polymer architecture and nonlinea rviscoelastic behavior of modified asphalts. *Current Opinion in Colloid & Interface Science,* Volume 11, pp. 230-245.

73. Prabakar, J., N. Dendorkar, and R.K. Morchhale 2004. Influence of Fly Ash on Strength Behavior of Typical Soils, *Construction and Building Materials*, Volume 18, pp. 263-267

74. Putman, B. J. 2005. *Quantification of the Effects of Crumb Rubber in CRM Binders*, Dissertation, Clemson University, Clemson, SC.

75. Qingxi, Y., 2010. The recycling and reuse of waste tire worldwide. *World Rubber Ind,* 37(2).

76. Riu, Y.T., B.G. Kim, Y.Y. Choi, S.Y. Hong, S.K. Hwang, and J.H. Park, 1996. Properties and Combustion Characteristics of Heavy Oil Fly Ash, *J. Korea Solid Wastes Engineering Society*, Volume 13, pp. 236-246.

77. Seggiani, M., S. Vitolo, M. Pastorelli, and P. Ghetti, 2007. Combustion Reactivity of Different Oil-Fired Fly Ashes as Received and Leached, *Fuel*, Volume 86, pp. 1885-1891.

78. Shawabkeh, R. & Harahsheh, A., 2007. H2S removal from sour liquefied petroleum gas using Jordanian oil shale ash. *Oil Shale,* Volume 24, p. 109.

79. Shawabkeh, R., Al-Harahsheh, A. & Al-Otoom, A., 2004. Copper and zinc sorption by treated oil shale ash. *Separation and Purification Technology,* Volume 40, p. 251.

80. Shawabkeh, Reyad, Khan, Muhammad J, Al-Juhani, Abdulhadi A, Al Abdul Wahhab, Hamad I., Hussein, Ibnelwaleed A., 2011. Enhancement of surface properties of oil fly ash by chemical treatment. *Applied Surface Science 258,* Issue 258, p. 1643– 1650.

81. Shenoy, A., 2002. Model-fitting the master curves of the dynamic shear rheometer data to extract a rut-controlling term for asphalt pavements. *ASTM J Test Eval,* 30(2), pp. 95-102.

82. Sinha, A., Singh, M. & Singh, S., 2010. *Study of use of beneficiated pulverized coal fly-ash as filler and rice straw fibers in manufacturing of paper.* Atlanta, Georgia, USA, Paper Conference and Trade Show , pp. 2237-2253.

83. Sombatsompop, N., S. Thongsang, T. Markpin, and E. Wimolmala, 2004. Fly Ash Particles and Precipitated Silica as Fillers in Rubbers. I. Untreated Fillers in Natural Rubber and Styrene-Butadiene Rubber Compounds, *J. Appl. Polym. Sci*., Volume 93, pp. 2119-2130.

84. Syvester, 2006. USA, Patent No. US 7074846B2.

85. The Asphalt Institute, 2003. Performance Graded Asphalt Binder Specification and Testing, SP-1, Lexington, KY: The Asphalt Institute.

86. U.S. Environmental Protection Agency, 2007. Human and Ecological Risk Assessment of Coal Combustion Wastes, RTI, Research Triangle Park, August 6.

87. Visa, M., Bogatu, C. & Duta, A., 2010. Simultaneous adsorption of dyes and heavy metals from multicomponent solutions using fly ash. *Applied Surface Science,* Volume 256, p. 5486.

88. Walsh, P.M., G. Wei and J. Xie, 1991, Metal Oxide and Coke Particulates Formed During Combustion of Residual Fuel Oil," *Proceedings of the 10th Annual Meeting of the American Association for Aerosol Research*, Paper 7P.36, Traverse City, MI.

89. Woo-Teck, Dong-Hyun, K. K. & Yung-Phil, K., 2005. Characterization of Heavy Oil Fly Ash Generated from a Power Plant. *Journal of Materials.*

90. Yamaguchi, K., I. Sasakit, I. Nishizaki, S. Meiarashit, and A. Moriyoshi, 2005. Reinforcing Effects of Carbon Black on Asphalt Binder for Pavement, *Journal of The Japan Petroleum Institute*, Volume 48, No. 6, pp. 373-379.

91. Yang Yu-Fen, Gai Guo-Sheng, Cai Zhen-Fang, and Chen Qing-Ru, 2006. Surface Modification of Purified Fly Ash and Application in Polymer, *Journal of Hazardous Materials*, Volume 133, pp. 276-282.

92. Yaumi, A. L., Hussein, I. A. & Shawabkeh, R. A., 2012. Surface modification of oil fly ash and its application in selective capturing of carbon dioxide. *Applied Surface Science.*

93. Zhang, F., Yu, J. & Han, J., 2011. Effects of thermal oxidative ageing on dynamic viscosity, TG/DTG, DTA and FTIR. *Construction and Building Materials,* pp. 129-137.

94. Zhang, F., Yu, J. & Wu, S., 2010. Effect of ageing on rheological properties of storage-stable SBS/sulfur-modified asphalt. *Journal of Hazardous Materials,* Volume 182, pp. 507-517.

95. Zupancic, A. & Zumer, M., 2002. Rheological examination of temperature dependence of conventional and polymer-modified road bitumens. *Can J Chem Eng,* Volume 82, pp. 253-263.

Vitae

Name : Mohammad Anwar Parvez

Nationality : Bangladeshi

Date of Birth : 11th December, 1979

Email : maparvez2003@yahoo.com; maparvez2003@gmail.com

Present Address : House # 1912, New Shabab Place, KFUPM. Dhahran, Saudi Arabia, Telephone # +966038605822, Mobile # +966553935483

Permanent Address : Village: Mazukhan, Post office: Ratanpur, P.S: Kaliakair, District: Gazipur, Bangladesh, Mobile # +8801817537789

Academic Background:

2008 to 2013: PhD in Chemical Engineering

King Fahd University of Petroleum & Minerals, Saudi Arabia.

Dissertation title: "Improvement of Asphalt Performance Using Industrial Wastes"

2006 to 2008: M. Sc. in Chemical Engineering

King Fahd University of Petroleum & Minerals, Saudi Arabia.

Thesis title: "Rheological, Thermal and Mechanical Characterization of Metallocene Polyethylene with Controlled Long Chain Branching".

1999-2004: B.Sc. in Chemical Engineering

Bangladesh University of Engineering & Technology (BUET), Bangladesh.